

Molecular Mechanisms of Meiotic Segregation Errors during Female Reproductive Ageing

Lisa Martine Lister

**Supervisors: Professor Mary Herbert & Professor David Elliott
Institute of Ageing and Health, Newcastle Fertility Centre, International
Centre for Life**

***Institute for
Ageing and
Health***



**A thesis submitted for the degree of Doctor of Philosophy
December 2012**

Abstract

In humans, the frequency of meiotic segregation errors increases dramatically during female ageing. The impact of this on human reproductive health is amplified by the growing trend for women to postpone childbearing. It has long been known that the majority of meiotic segregation errors occur during the first meiotic division (MI). MI is a unique cell division involving dissolution of bivalent chromosomes formed when maternal and paternal homologs undergo reciprocal exchange of DNA and remain physically linked at chiasmata at the sites of crossover formation. Dissolution of bivalents results in dyad chromosomes consisting of two chromatids linked by centromeric cohesion. Dyads are either lost to the polar body or remain in the oocyte and realign on the metaphase II spindle, where they remain until fertilisation. My work is part of a collaborative project focussed on elucidating the molecular link between female age and chromosome segregation errors during MI. Using an aged mouse model to monitor oocyte chromosome segregation we discovered a dramatically increased incidence of anaphase defects during MI in oocytes from aged mice. This was preceded by depletion of chromosomal cohesin, which is required for cohesion between sister chromatids, thereby stabilising bivalent chromosomes. Consistent with this, single chiasmate bivalents become destabilised during female ageing. Depletion of cohesin was also associated with loss of the unified structure of sister centromeres, which is required for accurate segregation during MI. In addition, cohesin loss was associated with reduced recruitment of its protector, Sgo2. On the basis of these data, I propose that a gradual decline in chromosomal cohesin during female ageing impedes recruitment of Sgo2, which in turn may further amplify cohesin loss during prometaphase resulting in depletion of cohesin below the threshold required to maintain bivalent architecture. According to this hypothesis, cohesin depletion is sufficient to explain the age-related increase in MI errors and provides a plausible molecular mechanism for the association between female age and germ cell genomic instability.

Acknowledgements

I would like to say a huge thank you to my friends and family for all their support and for keeping me positive. Thank you especially to Dimitri, Louise and Sarah, for working with me on this project over the years; Daniel, Irina and Randy for your amazing proof reading skills; my Nan for asking at least once a week how it was going; my Mum for understanding why everything had to be just right; and my Dad for just being himself.

Special thanks must go to Mary Herbert, for encouraging me to register to do my PhD, and for her continued support throughout the duration.

Last, but not least, a thank you to my husband Stu, for always being there for me, and for constantly giving me good reasons to get it finished.

Contents

Abstract.....	I
Acknowledgements.....	II
Contents.....	III
List of Figures.....	VII
List of Tables.....	XI
Publications.....	XI
Chapter 1. Introduction.....	1
1.1. Meiosis and Aneuploidy.....	1
1.2. Oogenesis: a protracted process.....	4
1.3. Formation of bivalent chromosomes – Homologous chromosome cohesion.....	10
1.4. Mechanisms of Chromosome Segregation.....	12
1.5. Cohesin – The Chromosome Glue.....	23
1.5.1. <i>The Mitotic Cohesin Complex</i>	23
1.5.2. <i>Cohesin Associated Proteins</i>	25
1.5.3. <i>Meiotic Cohesin</i>	27
1.5.4. <i>Cohesin Dissociation</i>	28
1.6. Shugoshin – the ‘guardian’ protector.....	30
1.7. Cell cycle regulation of chromosome segregation during meiosis.....	34
1.7.1. <i>Cyclin Dependent Kinases</i>	34
1.7.2. <i>The Anaphase Promoting Complex</i>	36
1.8. Regulation of the APC/C by the spindle checkpoint.....	40
Chapter 2. Aims.....	42
Chapter 3. Methods.....	43
3.1. Mouse Strains.....	43

3.2. Oocyte Harvest	43
3.3. Oocyte Culture	44
3.4. Microinjection	44
3.5. Fluorescent Construct Cloning.....	46
3.6. Message RNA Construction.....	48
3.7. Small Interfering RNA	49
3.8. Chromosome Spreads	49
3.9. Chromosome Spread Immunofluorescence.....	51
3.10. Whole Oocyte Immunofluorescence	52
3.11. Wax Embedding Ovaries	53
3.12. Sectioning.....	53
3.13. Haematoxylin and Eosin Staining	54
3.14. Microscopy	54
3.15. Timelapse Imaging	55
3.16. Metamorph analysis of live cell microscopy.....	55
3.17. Metamorph analysis of chromosome spreads	56
3.18. Statistical Analysis.....	57
3.19. Stocks and Solutions	57
Chapter 4. Results I – Reproductive Ageing and Fertility.....	59
4.1. Depletion of the human female germ cell pool with advancing female age	64
4.2. Is the competence to complete MI affected by advancing female age?	68
4.3. Decline in clinical pregnancy rates with advancing female age	69
4.4. Decline in implantation rates with advancing female age.....	73
4.5. Use of a mouse model for female reproductive ageing.....	77
4.6. Dimensions of the C57BL/ <i>Icrfa</i> ^t mouse breeding data	80
4.7. Fertility of the C57BL/ <i>Icrfa</i> ^t mouse	81

4.8. Depletion of the germ cell pool with advancing female age in the C57BL/1crfa ^f mouse	86
4.9. What is the equivalence between human and mouse female ageing? 91	
Chapter 5. Results II - Maternal-age related segregation errors	95
5.1. Imaging of oocyte chromosome dynamics by timelapse fluorescence imaging.....	97
5.2. Age-dependence of defective chromosome dynamics during progression through MI	103
5.3. Classification and incidence of age-related chromosome defects	105
5.4. Timing of key events during progression through meiotic M phases .	109
5.5 Is the interval from GVBD to anaphase linked to segregation defects, and how does this fit with spindle checkpoint function?	113
5.6. The spindle checkpoint can be satisfied in the absence of correct monopolar attachments in meiosis I.....	115
5.7. Are lagging chromosomes and a delayed anaphase due to the presence of univalent chromosomes in oocytes from aged mice?	120
Chapter 6. Results III – Mechanisms underlying anaphase defects	123
6.1. Is cohesin depleted during maternal ageing?	125
6.2. Is depletion of cohesin during maternal ageing associated with individualisation of sister centromeres?.....	127
6.3. Sister centromere splitting occurs gradually during female ageing....	131
6.4. Is cohesin lost during prophase arrest in oocytes?	133
6.5. Cohesin loss from oocyte chromosomes during female ageing.....	134
6.6. Is there a separase-independent mechanism of cohesin removal in meiosis?	137
6.7. Is recruitment of the cohesin protector Sgo2 compromised during female ageing?.....	139
6.8. Does depletion of Sgo2 result in loss of chromosomal cohesin during progression through M phase of meiosis I?.....	144
6.8.1 <i>Optimisation of siRNA techniques</i>	144

6.8.2	<i>Injection of Sgo2 siRNA induces premature separation of sister centromeres</i>	151
6.9.	What is the effect of Sgo knock down on chromosomal cohesin?	152
6.10.	Do reduced levels of cohesin influence the recruitment of Shugoshin?	155
Chapter 7.	Discussion	158
7.1.	The mouse provides a promising model for female reproductive ageing	158
7.2.	The effect of female age on chromosome dynamics	160
7.3.	The structural integrity of the bivalent, and cohesin depletion during female ageing.....	161
7.4.	Chromosomal association of Sgo2 is impaired in cohesin deficient mice	167
7.5.	Proposed model for cohesin depletion and chromosome segregation errors during female ageing.....	168
7.6.	What might be the mechanisms of cohesin depletion?	169
7.7.	Is it possible that cohesin depletion reflects a problem with its replenishment during ageing?	171
7.8.	How do the meiotic defects of mouse oocytes fit with what we know about reproductive ageing in humans?	172
7.9.	What can we conclude?.....	173
7.10.	What are the next steps for this research?	174

List of Figures

Figure 1.1 - A diagrammatic representation showing chromosome segregation in mitosis and meiosis.....	2
Figure 1.2 - The incidence of trisomy increases with maternal age	3
Figure 1.3 - There is an increasing trend for women to postpone childbearing...4	
Figure 1.4 - The human meiotic timeline.....	5
Figure 1.5 - The protracted prophase of human oocytes.. ..	8
Figure 1.6 - The process of oocyte maturation.....	8
Figure 1.7 - Models of follicular decline in human ovaries.	9
Figure 1.8 - Chiasmata must form during prophase, and be maintained until anaphase I for accurate homologous chromosome segregation.	10
Figure 1.9 - Mitotic chromosome segregation.....	13
Figure 1.10 - Chromosome segregation errors in mitosis.	15
Figure 1.11 - Meiotic chromosome segregation.....	18
Figure 1.12 - A schematic for kinetochore-microtubule attachments during mitosis and meiosis I.....	20
Figure 1.13 - Monopolar attachments are essential for biorientation and accurate homologous chromosome segregation.	21
Figure 1.14 - The cohesin complex.....	25
Figure 1.15 - A schematic for cohesin dissociation.....	31
Figure 1.16 - Sgo2 is required to protect centromeric cohesin for correct segregation to occur in mammalian oocytes.....	33
Figure 1.17 - The proposed roles of Cdk-cyclin complexes in the mammalian cell cycle.	35
Figure 1.18 - Schematic for securin APC/C activity and associated substrate protein levels in mitosis.....	37
Figure 1.19 - Schematic of securin and cyclin B1 degradation and separase activation in mitosis and meiosis.....	39
Figure 3.1 - Plasmid map for constructs based on a pRN3 plasmid backbone.	48
Figure 3.2 - Metamorph analysis functions.	57
Figure 4.1 - The incidence of trisomy increases with maternal age.	60
Figure 4.2 - The average age of women undergoing fertility treatment has greatly increased since 1991.	61

Figure 4.3 - Models of follicular decline in human ovaries.	62
Figure 4.4 - A range of different ages of women attended the Newcastle Fertility Centre for treatment.....	65
Figure 4.5 - Oocyte numbers decline as a function of female age in humans...66	
Figure 4.6 - Inclusion of cancelled treatment cycles does not change the pattern of decline in the yield of human oocytes.	67
Figure 4.7 - Maturation to MII was not inhibited by female age in humans..	69
Figure 4.8 - Pregnancy rates decline as a function of female age	71
Figure 4.9 - Fertility rates decline as a function of female age during natural and assisted conception.	72
Figure 4.10 - Birth rates are rescued when using donor oocytes.....	74
Figure 4.11 - Implantation rates decline as a function of female age.....	75
Figure 4.12 - Implantation rates decline at a faster rate than the decline in the mean oocyte number as a function of female age	76
Figure 4.13 - C57BL/1crfa ^f strain female in its enriched environment.....	78
Figure 4.14 - Linear extrapolation model to determine the corresponding ages of mouse and human females.....	79
Figure 4.15 - Litter frequency and size decrease gradually with advancing maternal age.....	82
Figure 4.16 - There is an increased incidence of neonatal death with advancing maternal age.....	83
Figure 4.17 - The interval between litters increases with advancing maternal age.....	85
Figure 4.18 - Oocyte numbers decline as a function of female age	87
Figure 4.19 - GVBD was not influenced by increased female age, but PB formation was increased in oocytes from older mice	88
Figure 4.20 - Oocyte numbers and litter size decline at different rates as a function of female age.....	90
Figure 4.21 - Linear extrapolation model of reproductive trends in humans and mice	91
Figure 4.22 - Oocyte numbers and fertility decline at different rates in mice and humans as a function of female age	92
Figure 4.23 - Non-linear extrapolation model of the reproductive lifespan in humans and mice.....	93
Figure 5.1 - H2B-RFP Plasmid Map.....	98
Figure 5.2 - Oocyte micro-injection and translation of histone H2B-RFP.	99

Figure 5.3 - A representative example of chromosome behaviour in an oocyte from a 2 month old mouse.	101
Figure 5.4 - Meiotic progression of an oocyte from a 2 month old mouse.....	102
Figure 5.5 - Meiotic progression of oocytes from a 14 month old mouse.....	104
Figure 5.6 - Aberrant chromosome dynamics are more prevalent in oocytes from 14 month old mice..	106
Figure 5.7 - MII misalignment increases progressively after anaphase I in oocytes from 14 month old mice	107
Figure 5.8 - Single sisters are observed in MII oocytes from 14 month old mice	107
Figure 5.9 - The interval from GVBD to chromosome congression.....	110
Figure 5.10 - The interval from GVBD to chromosome alignment.....	110
Figure 5.11 - The interval from GVBD to anaphase.	111
Figure 5.12 - The interval from anaphase of MI to MII alignment.....	112
Figure 5.13 - Meiotic progression was delayed in oocytes from 14 month old mice.	113
Figure 5.14 - Timeline depicting the incidence of defects.	114
Figure 5.15 - Schematic illustrating segregation patterns for univalent chromosomes	116
Figure 5.16 - Chromosomes in <i>Sycp3</i> ^{-/-} mice achieve alignment before undergoing an error prone anaphase.....	117
Figure 5.17 - Anaphase is delayed in <i>Sycp3</i> ^{-/-} oocytes which display lagging chromosomes at anaphase.....	119
Figure 5.18 - Distally associated chiasmata are prevalent in oocytes from 14 month old mice.....	121
Figure 6.1 - Distally associated chiasmata are prevalent in oocytes from <i>SMC1β</i> knockout mice.....	124
Figure 6.2 - The cohesin complex.....	124
Figure 6.3 - Chromosome associated cohesin is reduced in the oocytes of aged mice.	126
Figure 6.4 - Centromeric cohesin is reduced in the oocytes of aged mice.....	127
Figure 6.5 - Splitting of sister centromeres occurs in oocytes of aged mice ...	128
Figure 6.6 - Reduced cohesin is associated with centromere splitting in aged mice	129
Figure 6.7 - Errors leading to abnormal chromosome segregation at anaphase I.	130

Figure 6.8 - The distance between sister centromeres increases with advancing maternal age.....	132
Figure 6.9 - Stages of oocyte growth.	133
Figure 6.10 - Separase is expressed in fully grown GV, preantral, and primordial stage oocytes.....	136
Figure 6.11 - Sgo2 levels are reduced in oocytes of aged mice	140
Figure 6.12 - Sister centromere splitting with advanced female age is associated with Sgo2 mislocalisation.....	141
Figure 6.13 - Time course staining of Sgo2 and PP2A in prometaphase oocytes.	142
Figure 6.14 - Sgo2 is recruited to chromosomes at the prophase to metaphase transition in oocytes.	143
Figure 6.15 - Maturation after siRNA injection.	146
Figure 6.16 - Sgo2 siRNA knockdown.	147
Figure 6.17 - PP2A localisation disrupted in Sgo2 knockdown oocytes.....	148
Figure 6.18 - Prolonged incubation in media supplemented with IBMX+cAMP and translation of Histone H2B compromises asymmetric division during MI.	149
Figure 6.19 - Single sister chromatids are observed at MII in Sgo2 knockdown chromosome spreads..	152
Figure 6.20 - Rec8 and CREST are reduced in Sgo2 knockdown oocytes.....	154
Figure 6.21 - Sgo2 knockdown is associated with increased sister centromere splitting.....	155
Figure 6.22 - Sgo2 levels are reduced in oocytes of Smc1 β deficient mice... ..	156
Figure 7.1 - Errors associated with cohesin loss at MI.....	165
Figure 7.2 - Schematic representing the hypothesised processes contributing to MI segregation errors.....	168

List of Tables

Table 1.1 - Cohesin subunits and associated proteins.	28
Table 3.1 - Plasmids designed for mRNA synthesis.	48
Table 3.2 - Antibody dilutions.....	52

Publications

Kouznetsova, A., **Lister, L.**, Nordenskjold, M., Herbert, M. and Hoog, C. (2007) 'Bi-orientation of achiasmatic chromosomes in meiosis I oocytes contributes to aneuploidy in mice', *Nat Genet*, 39(8), pp. 966-8.

Lister, L.M., Kouznetsova, A., Hyslop, L.A., Kalleas, D., Pace, S.L., Barel, J.C., Nathan, A., Floros, V., Adelfalk, C., Watanabe, Y., Jessberger, R., Kirkwood, T.B., Hoog, C. and Herbert, M. (2010) 'Age-related meiotic segregation errors in mammalian oocytes are preceded by depletion of cohesin and Sgo2', *Curr Biol*, 20(17), pp. 1511-21.

Touati, S.A., Cladiere, D., **Lister, L.M.**, Leontiou, I., Chambon, J.P., Rattani, A., Bottger, F., Stemmann, O., Nasmyth, K., Herbert, M. and Wassmann, K. (2012) 'Cyclin A2 is required for sister chromatid segregation, but not separase control, in mouse oocyte meiosis', *Cell Rep*, 2(5), pp. 1077-87.

Chapter 1. Introduction

1.1. Meiosis and Aneuploidy

Meiosis is a specialised form of cell division in which diploid progenitors form haploid gametes by undergoing two rounds of chromosome segregation without an intervening round of DNA synthesis. The first meiotic division (MI) is a reductional division whereby the number of chromosomes is halved following segregation of recombinant maternal and paternal homologous chromosomes. The second meiotic division (MII) is an equational division, in which sister chromatids segregate, as in mitosis (Figure 1.1).

Both divisions need to be tightly regulated to avoid chromosome missegregation which can ultimately lead to infertility, miscarriage or birth defects. When errors do occur, the majority arise during female MI (Hassold and Hunt, 2001), when homologous chromosomes segregate either to the oocyte or to the polar body (PB) (Figure 1.1 and Figure 1.6). Failure of the homologous chromosomes to segregate evenly results in aberrant numbers of chromosomes being retained, giving rise to an aneuploid oocyte. Aneuploidy arising from MI errors in female germ cells is the foremost genetic cause of developmental and intellectual disabilities. In humans, the frequency of female MI segregation errors increases dramatically with advancing maternal age (Hassold and Hunt, 2001; Hunt and Hassold, 2010).

Female reproductive ageing is characterised by depletion of the ovarian pool of germ cells, eventually resulting in menopause at 45-55 years. However, for reasons that have remained unclear, the preceding decade is marked by a dramatic increase in the incidence of oocyte aneuploidy (Hassold and Hunt, 2001). The age-related increase in oocyte aneuploidy has a major impact on human reproductive health. Approximately 2–3% of clinically recognised pregnancies among women in their twenties involve trisomic fetuses. However, this shoots up to over 35% among women in their forties (Figure 1.2) (Hassold and Hunt, 2001; Hunt and Hassold, 2010). One such trisomy is Down's syndrome (trisomy 21).

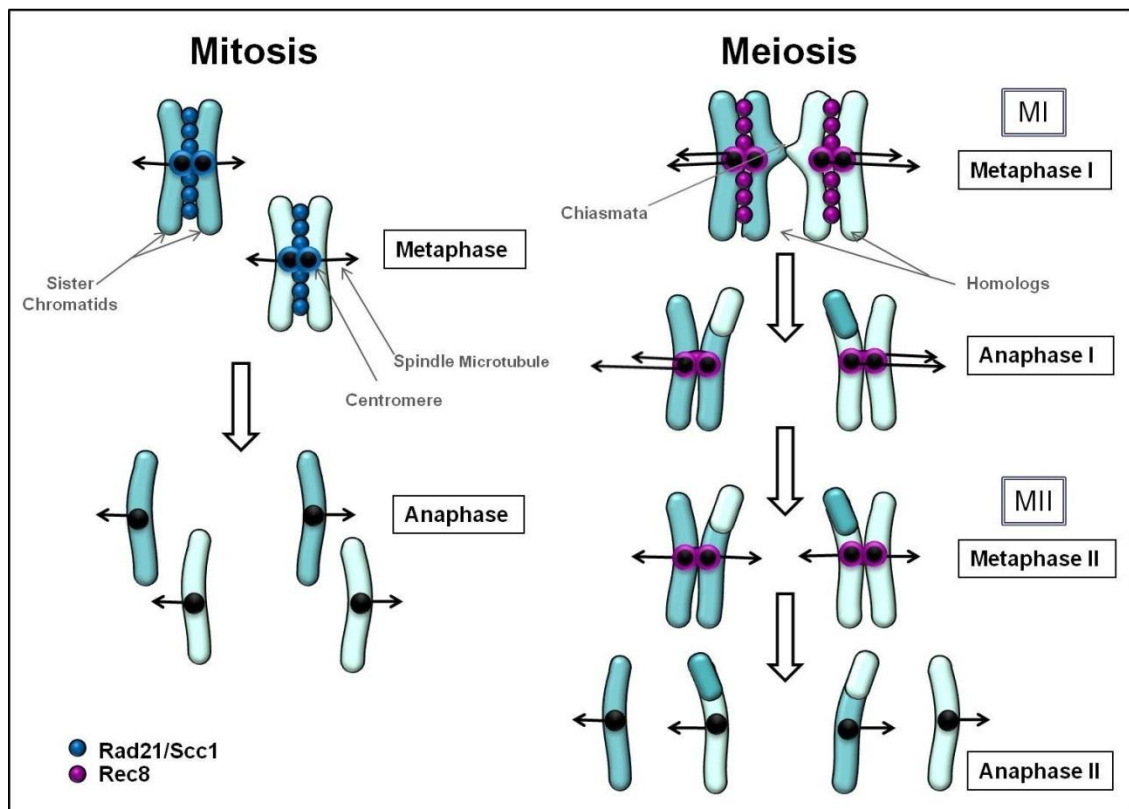


Figure 1.1 - A diagrammatic representation showing chromosome segregation in mitosis and meiosis. In mitosis, each round of DNA replication is followed by a round of equational segregation of replicated sister chromatids, which are held together by a cohesin from the time of replication until anaphase. In meiosis, there is only one round of DNA replication followed by two rounds of chromosome segregation. The first meiotic division (MI) is reductional, involving the segregation of recombinant homologous chromosomes (chromosomes which share the same genes, but not necessarily the same alleles). The second division (MII) is more similar to mitosis as it is equational, involving the segregation of sister chromatids. Homologous recombination results in genetic variation between parents and offspring and in the establishment of physical linkages (chiasmata) between homologues, which is essential for their correct segregation during anaphase of MI. These linked homologous chromosomes can also be referred to as a bivalent. As in mitosis, sister chromatids are held together at the centromeres and down the chromosome arms by cohesin, which stabilises chiasmata until the onset of anaphase. In mitosis all cohesin is resolved for mitotic segregation. However in meiosis this happens as a stepwise process, with arm cohesin being lost during anaphase of MI, and the centromeric cohesion is maintained until anaphase of MII. The chromosomes are separated by the pulling forces of the spindle microtubules (black arrows). The blue circles represent the mitotic cohesin containing Rad21/Scc1, and the purple circles represent the meiotic cohesin counterpart containing Rec8 (recombination and chiasmata are further described in section 1.3; cohesin is further explained in section 1.5).

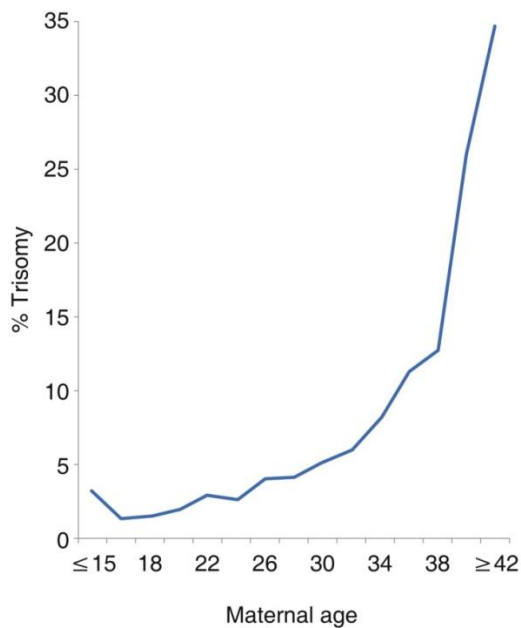


Figure 1.2 - The incidence of trisomy increases with maternal age. A graphical representation showing the correlation between the occurrence of trisomic pregnancies and maternal age. The risk of trisomy rapidly increases after the age of 35. (Hunt and Hassold, 2010).

Over the last 20 years the incidence of a Down's syndrome pregnancy has increased by 71% in association with increased maternal age (Morris and Alberman, 2009). More serious abnormalities would most likely not be compatible with embryo development to a stage where they would be capable of implanting. These would manifest themselves as infertility in older women. With the growing trend for women to wait until later in their lives to start a family (Figure 1.3), unravelling the underlying causes of age-related oocyte chromosome segregation errors becomes a pressing concern. While it is known that errors arising during MI account for >80% of trisomies involving chromosome 21 (Down syndrome) and chromosome 16 (the most common cause of miscarriage) (Hassold and Hunt, 2001), the underlying mechanisms and the biological basis of the association with female age is a major unsolved problem in reproductive biology.

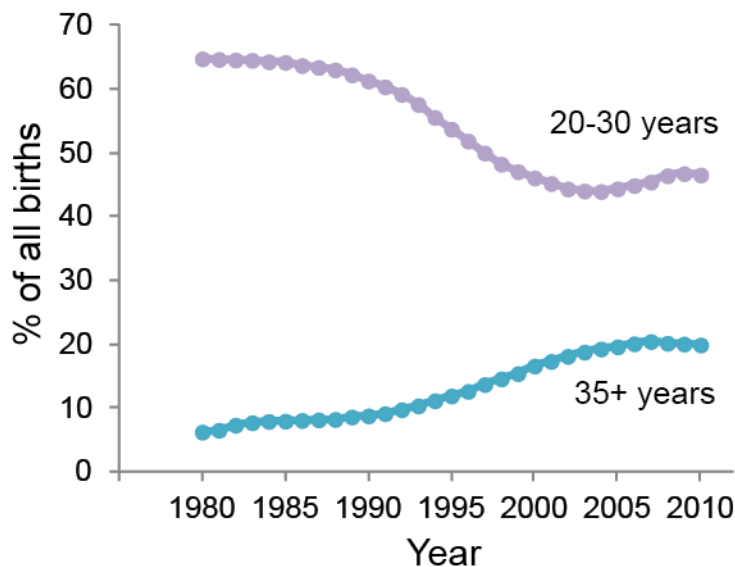


Figure 1.3 - There is an increasing trend for women to postpone childbearing. Graphical representation of data from the national statistics office (<http://www.statistics.gov.uk>) reflecting the decrease in the percentage of births to women under 30 years of age, and the increase in births to women 35 years of age and older.

1.2. Oogenesis: a protracted process

Why might MI be so error prone? Ovaries of most mammalian species acquire their lifetime quota of oocytes during foetal life. It is here that meiosis I commences, but it is not completed until after puberty. In other cells of the body this first stage, prophase, would be completed within hours, but in mammalian oocytes it can last weeks, months, or in the case of humans, decades. With the growing trend for women to delay childbearing this could be up to five decades later (Figure 1.4 and Figure 1.5). By contrast, sperm production occurs continuously from puberty, throughout the male lifespan (Figure 1.4) (Hassold and Hunt, 2001).

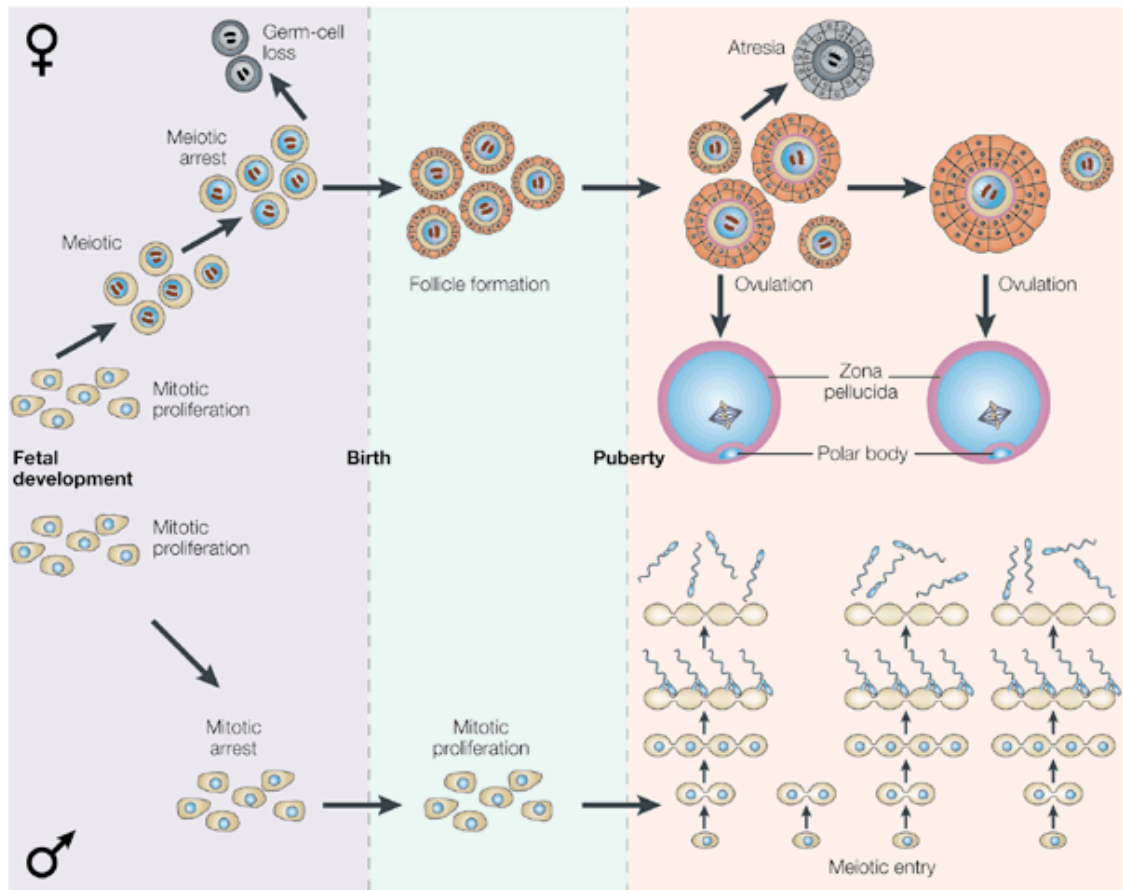


Figure 1.4 - The human meiotic timeline. Females: In the foetal ovary mitotic proliferation occurs briefly before the cells enter an extended meiotic prophase and arrest before birth. At this time the pool of oocytes is substantially reduced by apoptotic death. By the time of birth, pregranulosa cells surround the surviving oocytes forming primordial follicles. These follicles are stimulated to grow throughout the reproductive lifespan, with typically one fully grown oocyte being ovulated each month and several growing oocytes become atretic (apoptotic death of follicles). This continues depleting the oocyte pool until menopause occurs.

Males: In the foetal testis proliferation occurs briefly then the cells enter an extended mitotic arrest before birth. After birth, these spermatogonia resume proliferation, and once puberty has been reached they are stimulated to undergo meiosis and become sperm. Sperm production continues throughout the male lifetime as spermatogonia continue to proliferate and daughter cells enter into meiosis. (Hassold and Hunt, 2001).

Oogenesis is the term used to describe the formation of fully grown oocytes from primordial germ cells (PGCs), which migrate to the genital ridge during foetal development (Gomperts *et al.*, 1994; McLaren, 2000; Molyneaux *et al.*, 2001). PGCs undergo several rounds of mitotic division, giving rise to several million oogonia, which enter meiosis in an asynchronous fashion giving rise to primordial oocytes.

Entry into meiosis begins from 14-16 days gestation in mice, and from around 9 weeks gestation in humans (Peters, 1970; Picton, 2001). It is marked by the pairing of maternal and paternal chromosomes which then undergo homologous recombination, also known as crossover formation. Cytologically distinct structures known as chiasmata form at the sites of crossovers thereby maintaining the physical linkages between homologues to form a bivalent chromosome structure (described in more detail in section 1.3). Oocytes become surrounded by a layer of pregranulosa cells creating primordial follicles. The oocyte then arrests in prophase, which is also known as the dictyate stage. At this point the oocyte has a large, clearly visible nucleus called the germinal vesicle (GV) (Figure 1.6). Mouse oocytes reach this stage within the first couple of days of birth, and humans at around 15-22 weeks of gestation (Picton, 2001; Maheshwari and Fowler, 2008; Adhikari and Liu, 2009).

Oocyte loss due to atresia is prevalent during the early stages of oocyte development. In humans, germ cell numbers decrease from approximately 7 million, to only ~2 million remaining at birth (Peters, 1970; Gosden, 1987; Picton, 2001). This reduction in oocyte number continues through life, with acceleration in the rate of decline from around the mid 30's (Figure 1.7) (Faddy *et al.*, 1992; Faddy, 2000; Hansen *et al.*, 2008).

The generally accepted understanding of female reproductive ageing is based on the widely believed dogma that the lifetime stock of oocytes is formed before, or shortly after birth (Zuckerman, 1951). However, some controversial reports have challenged this accepted theory, with findings of mitotically active so-called germline stem cells (GSC), or oogonial stem cells (OSC), in juvenile and adult mouse ovaries, that are thought to sustain oocyte production in the postnatal ovary (Johnson *et al.*, 2004; Johnson *et al.*, 2005; Zou *et al.*, 2009). More recently, it has been reported that OSCs have been isolated from human ovarian tissue (White *et al.*, 2012). These were engineered to express GFP, and injected into human ovarian cortical biopsies, which were xenografted into immunodeficient female mice. When the grafts were collected 7-14 days later, it was reported that they formed immature follicles containing GFP-positive oocytes (White *et al.*, 2012). However, much controversy still exists around this work. It is still undetermined what role any such de novo oocyte production has

in the normal reproductive lifespan, and whether it would have any impact on the field of reproductive technology.

Throughout life, primordial follicles recruited to the growing pool either succumb to atresia due to the apoptotic death of granulosa cells (Hurst *et al.*, 2006; Tingen *et al.*, 2009), or after puberty can grow to a stage where they are ovulated (Picton, 2001). The follicle forms an antrum in response to follicle stimulating hormone (FSH), released from the pituitary gland under the control of the gonadotrophin releasing hormone produced by the hypothalamus (Conn *et al.*, 1987; Kumar *et al.*, 1997). Fully grown oocytes exit prophase and undergo the first meiotic division following the preovulatory surge of luteinising hormone (LH) from the pituitary gland (Mehlmann, 2005). In humans, and other monoovulatory species, one oocyte is ovulated each month until the onset of menopause at around 50 years of age (Faddy *et al.*, 1992; Hassold and Hunt, 2001). Shortly before ovulation meiosis resumes and the oocyte exits prophase arrest and enters into M phase of MI. The resumption of meiosis is marked by germinal vesicle breakdown (GVBD), which is followed by the assembly of the MI spindle (discussed in more detail in section 1.4). Completion of M phase of MI, which lasts for 6-10 hr in mice and 10-20 hr in humans, is marked by anaphase and PB formation. The oocyte then arrests again at the metaphase of MII until it is fertilised or otherwise activated (Figure 1.5 and Figure 1.6).

During the protracted prophase and M phase of MI, oocyte chromosomes are maintained in a precarious configuration whereby the bivalent structure of linked homologues is dependent of the maintenance of chiasmata (Figure 1.5).

Failure to stabilise chiasmata until the onset of anaphase would greatly increase the risk of missegregation during MI. Thus, the question of how chiasmata are stabilised is fundamental to our understanding of the underlying causes of MI errors in the female germline.

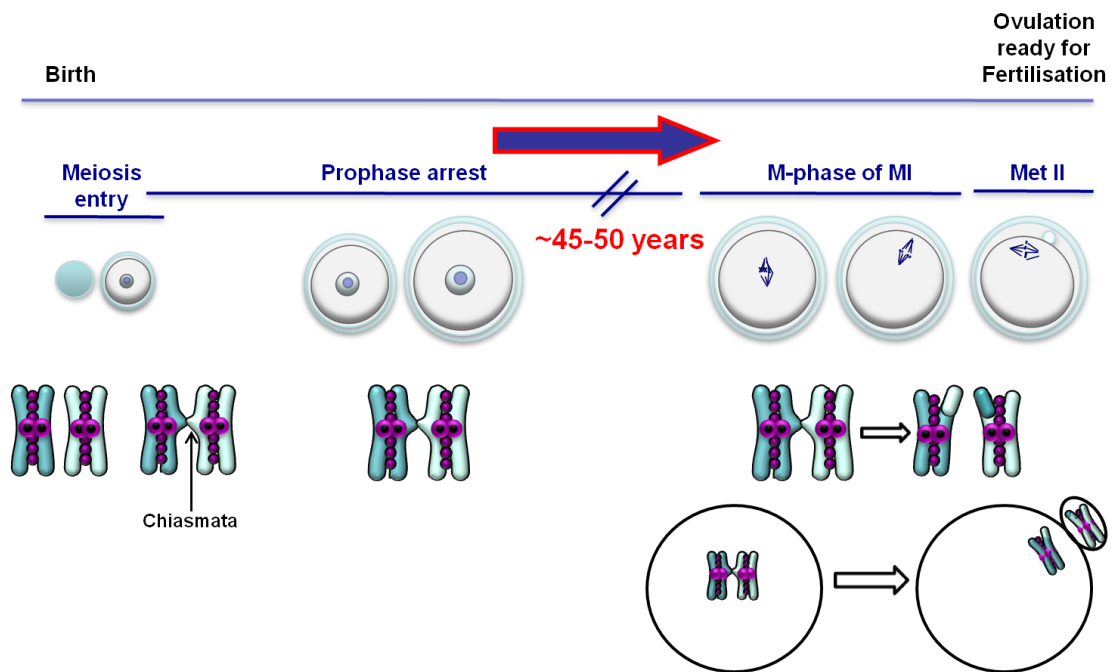


Figure 1.5 - The protracted prophase of human oocytes. The human oocyte begins meiosis during foetal life, and then arrests in prophase until recruited for growth before ovulation. This arrest can be up to 50 years in human oocytes.

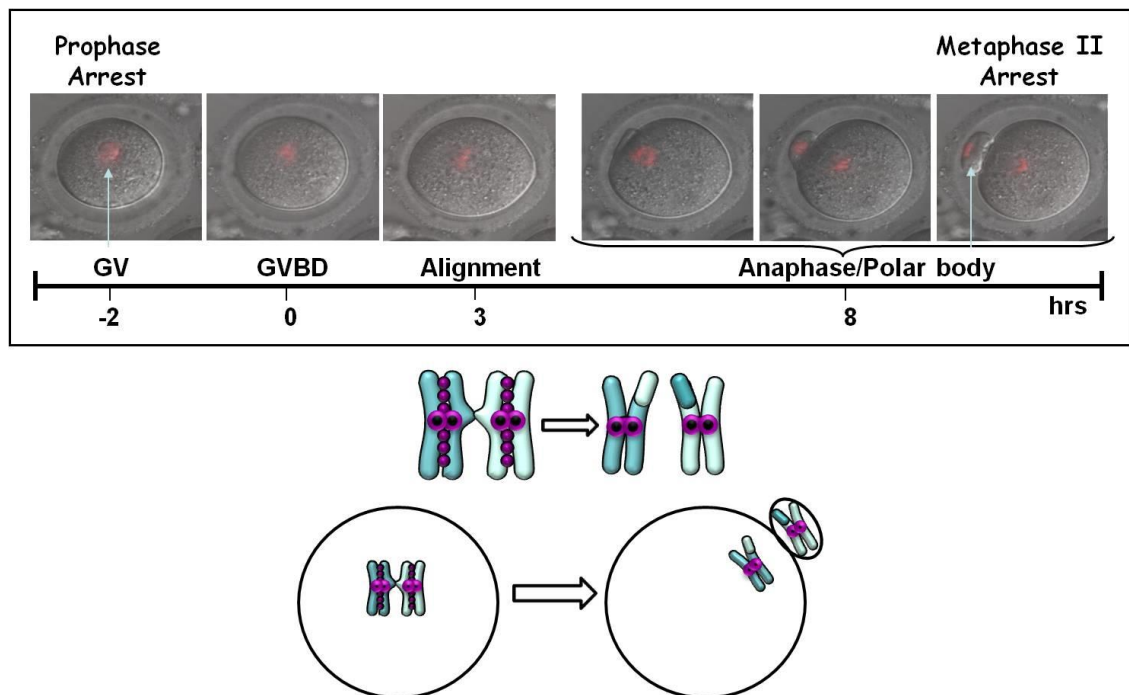


Figure 1.6 - The process of oocyte maturation. Images depicting mouse oocyte maturation after the end of the protracted prophase arrest. Arrows show the germinal vesicle (GV) and the polar body (PB). The chromosomes are shown in red. The illustration beneath depicts the metaphase to anaphase transition, shown in relation to PB formation.

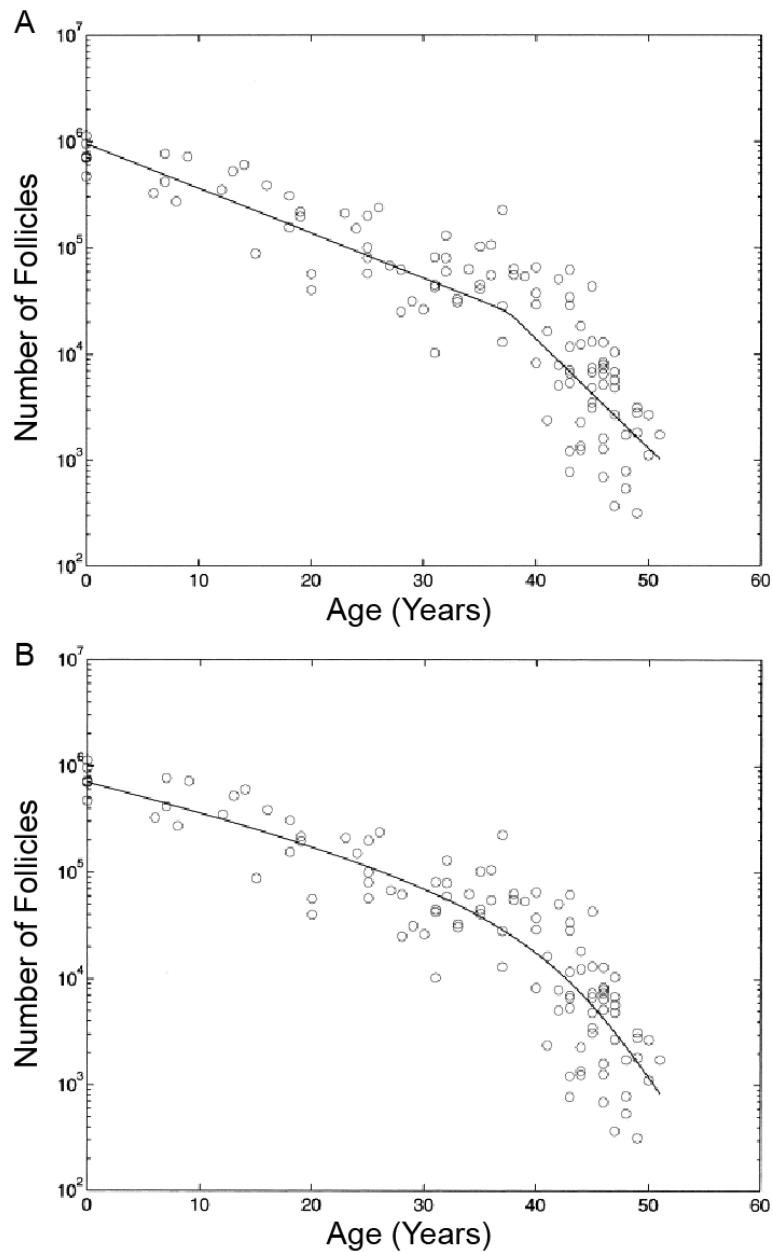


Figure 1.7 - Models of follicular decline in human ovaries. Data from pairs of human ovaries from neonatal age to 51 years of age ($n=110$ from 4 different data sets (Block, 1952; Block, 1953; Richardson *et al.*, 1987; Gougeon *et al.*, 1994) used in (Faddy *et al.*, 1992; Faddy and Gosden, 1996; Faddy, 2000)). (A) Biphasic exponential model of decline showing an increased loss of follicles, and hence oocytes, after 37.5 years of age (Faddy *et al.*, 1992). (B) Revised model, the decay curve a result of performing a differential equation on the data, illustrating a gradual increase in the rate of follicular decline with increasing female age (Faddy, 2000).

1.3. Formation of bivalent chromosomes – Homologous chromosome cohesion

In most organisms, accurate segregation of homologous chromosomes during the reductional division of MI requires that the homologues become physically linked. This happens early during prophase, which occurs after the pre-meiotic S phase. Maternal and paternal homologs undergo reciprocal recombination between non-sister chromatids to generate crossovers (Kleckner, 2006). In the resulting structures, known as bivalent chromosomes, recombined homologs are linked by chiasmata, which correspond to the site of crossovers (Figure 1.8).

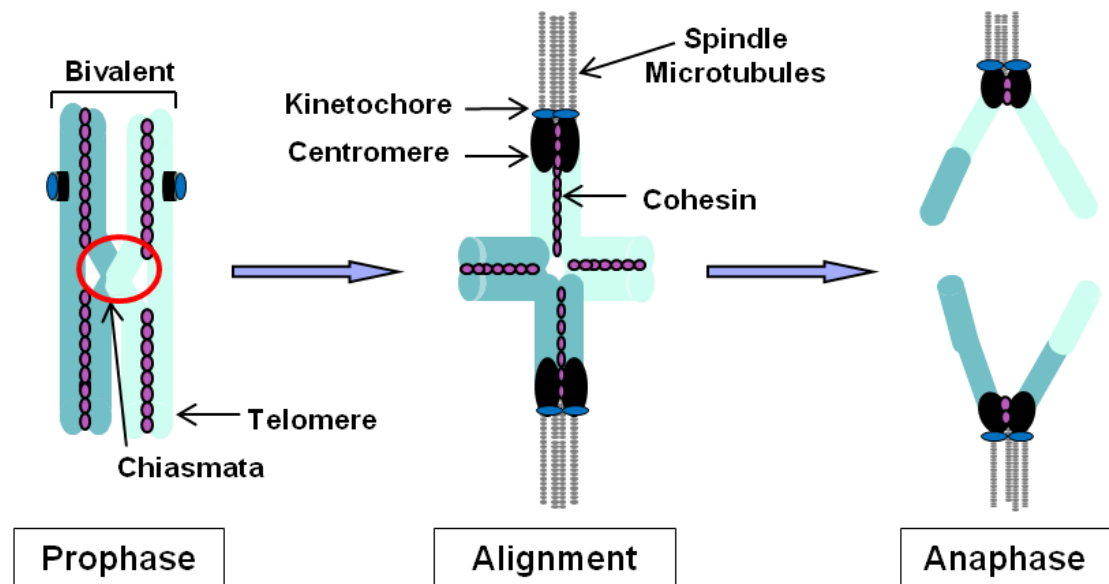


Figure 1.8 - Chiasmata must form during prophase, and be maintained until anaphase I for accurate homologous chromosome segregation. Diagrammatic representation of the linkage and reciprocal exchange between homologous chromosomes (chiasmata, red circle). Chiasmata are necessary for correct alignment on the spindle, and must be maintained until the onset of anaphase I for correct segregation to occur.

There are four key stages to the meiotic prophase: leptotene, zygotene, pachytene and diplotene. In leptotene the chromosomes are visible under the microscope as long thin strands. This tangle of chromosomes then begins to condense and individualise, homologous chromosome pair during leptotene, then synapse with the formation of the synaptonemal complex (SC) during zygotene (Page and Hawley, 2004; Kleckner, 2006). Homologous chromosome

recombination is initiated by the formation of double strand breaks (DSBs) by proteins homologous to the evolutionarily conserved *Saccharomyces cerevisiae* endonuclease Spo11 (Keeney *et al.*, 1997; Keeney and Neale, 2006).

According to our current understanding, DSBs are formed during leptotene and are repaired by the recombinase Dmc1 (Neale and Keeney, 2006) and other proteins during pachytene. At pachytene SC assembly is completed and recombination events are resolved either as crossovers or non-crossovers (Kleckner, 1996). At diplotene the chromosomes decondense, the SC gradually disassembles and the homologous chromosomes remained linked at chiasmata, which form at the site of crossovers and are transiently visible as Mlh1 foci (Svetlanov and Cohen, 2004). The chromosomes continue to be held together as they condense and enter prophase arrest of MI (Page and Hawley, 2004).

Without the physical linkage at chiasmata, the homologous chromosomes would not orientate themselves correctly on the spindle to be able to faithfully segregate during anaphase of MI (Figure 1.8). Therefore it is essential that the homologues are linked, and that these linkages are not placed in regions susceptible to premature resolution during MI. This would lead to the presence of univalent chromosomes, single chromosomes which are unpaired with their homologous chromosomes. If crossovers are formed in the sub-telomeric, or pericentromeric regions, the homologues are more susceptible to non-disjunction (Lamb *et al.*, 1997; Hodges *et al.*, 2005; Hassold and Hunt, 2007). Genetic mapping studies of the frequency and placement of recombinations in Down's syndrome chromosome 21 populations, indicate that approximately 45% of non-disjunction tetrads failed to undergo an exchange, and 41% have only a single exchange, with more than 80% of those being at the distal end of the chromosome (Lamb *et al.*, 1997). In view of the increased incidence of Down's syndrome with advancing maternal age, it is interesting to note that a decrease in chiasmata frequency and an increase in the incidence of univalent chromosomes at MI have also been observed with increasing female age in a number of mouse strains (Henderson and Edwards, 1968; Polani and Jagiello, 1976; Speed, 1977). The association between the risk of trisomy and the number and position of crossovers (Lamb *et al.*, 1997) gave rise to the 'two-hit' model for chromosome missegregation during MI. It was proposed that the first

hit, which occurs during foetal life, involves the establishment of bivalents with susceptible chiasmata configurations. The second hit occurs in the sexually mature female, when the recombined homologues segregate during anaphase of MI, just before ovulation. This was attributed either to an age-related 'degradation of a meiotic process' preceding chromosome segregation during MI, or to a decline in the oocyte's ability to recognise and respond to these failures, thereby allowing missegregation to occur (Lamb *et al.*, 1997). While these findings provided the first solid basis for a mechanistic understanding of susceptibility to errors during MI, it was later established that the association between trisomy and the incidence of univalent chromosomes or sub-telomeric exchanges was lost with advancing female age (Lamb *et al.*, 2005; Oliver *et al.*, 2008). However, aneuploidy resulting from a single pericentromeric exchange has been reported to increase with maternal age (Oliver *et al.*, 2008). These findings indicate that the causes of aneuploidy in oocytes of older women are complex, and appear to be due to events occurring subsequent to crossover formation.

1.4. Mechanisms of Chromosome Segregation

Accurate chromosome segregation is critical to ensure that cells are duplicated without any loss or damage to the genome. This relies on the correct attachment of chromosomes to the segregation machinery (the spindle), and correct control via the surveillance mechanisms of the spindle-assembly checkpoint (SAC), to ensure that the chromosomes are correctly aligned before segregation occurs.

The spindle consists of two spindle poles (centrosomes in animal cells), and the microtubules which connect the chromosomes to these poles. At the onset of mitosis a single centrosome (consisting of two centrioles and associated pericentriolar material) duplicates, and migrates to opposite sides of the nucleus, establishing bipolarity (Figure 1.9A). After nuclear envelope breakdown, the chromosomes make initial attachments via their kinetochores to the lateral surface of growing microtubules from opposite poles by a "search

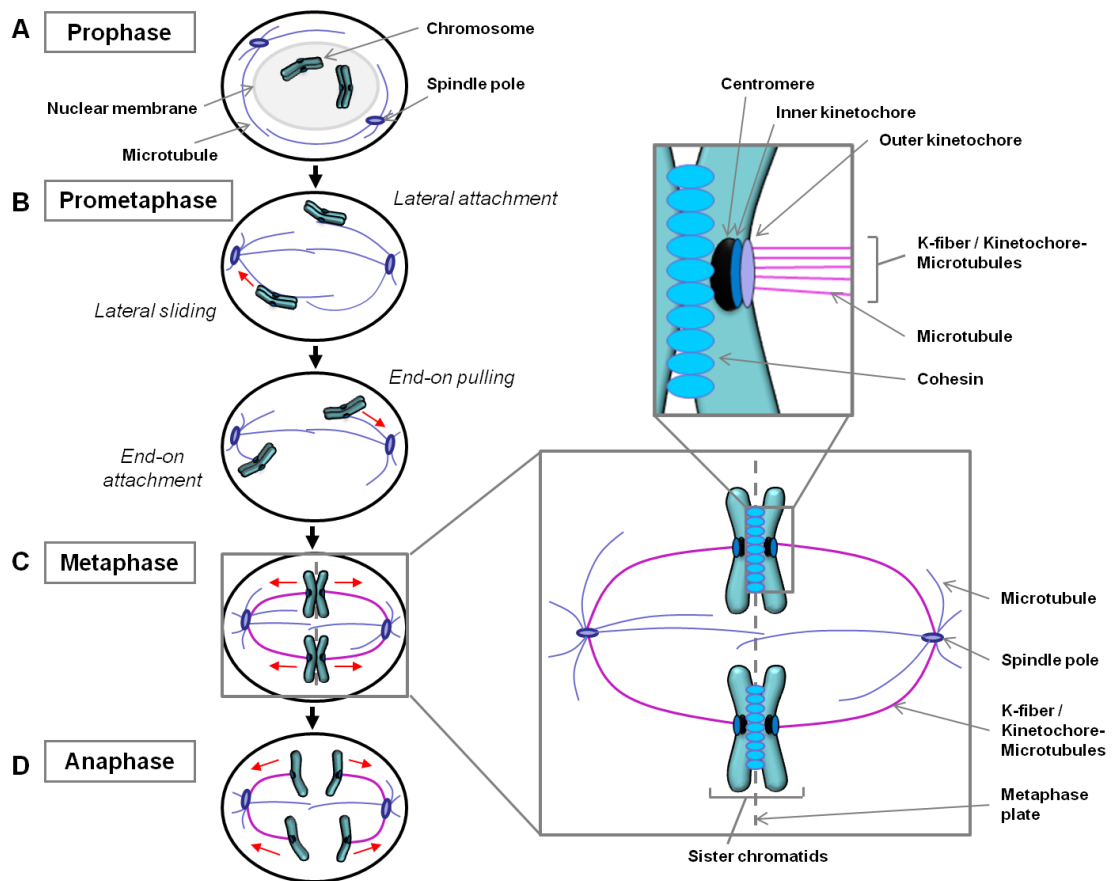


Figure 1.9 - Mitotic chromosome segregation. Schematic illustrating normal chromosome segregation in vertebrate somatic cells. (A) During prophase the chromosomes are enclosed in a nuclear envelope. (B) Nuclear envelope breakdown indicates entry into prometaphase. Kinetochores form lateral attachments with microtubules, and slide towards the spindle poles. These are then changed to end-on attachments, with the formation of kinetochore-microtubules (K-fibers). (C) The opposite pulling forces promote biorientation of sister chromatids and the chromosomes align on the metaphase plate. (D) Cohesin cleavage occurs at anaphase upon satisfaction of the SAC, and microtubule depolymerisation allows sisters to segregate to opposite spindle poles. Red arrows indicate the direction of movement, or tension on the kinetochores. (Adapted from (Tanaka, 2013)).

and capture” mechanism (Figure 1.9B) (Kirschner and Mitchison, 1986; Petronczki *et al.*, 2003; Hauf and Watanabe, 2004; Tanaka, 2013).

Interactions between the spindle microtubules and kinetochores are integral to alignment and chromosome segregation. Kinetochores (from the Greek words ‘kineto’ meaning ‘move’, and ‘chore’, meaning ‘means for distribution’) are made up of multiple conserved protein complexes, which assemble on the centromeres (from ‘centro’, meaning ‘central’, and ‘mere’, meaning ‘part’) of chromosomes, linking centromeric DNA to spindle microtubules. During prometaphase the initial lateral attachments are converted to end-on

attachments. Kinetochore-microtubules, also known as K-fibers, are formed by the end-on attachment of multiple microtubules to the kinetochore. When the kinetochores of each pair of sister chromatids form end-on attachments with microtubules from opposite spindle poles, biorientation occurs, with the chromosomes aligned on the metaphase plate (Figure 1.9C) (Petronczki *et al.*, 2003; Hauf and Watanabe, 2004; Tanaka, 2013). Tension is generated at the sister kinetochores by the pulling forces of the kinetochore-microtubules, and the resisting forces of the cohesin linking the sisters. It is this tension which allows the SAC to sense whether the chromatids are correctly attached to the spindle, or even whether they are attached at all. Sister chromatids with incorrect orientation or attachments are at risk of missegregation, so the SAC will delay cell cycle progression until correct attachments can be achieved by generating the so-called “wait anaphase” signal (the spindle checkpoint is further explained in section 1.7). Once the SAC is satisfied, the cohesin complexes responsible for cohesion between sisters are cleaved (cohesin cleavage is further explained in section 1.5). Following cohesin cleavage, sisters segregate to their opposite spindle poles by end-on pulling of the shrinking kinetochore-microtubules (Anaphase A) (Figure 1.9D and Figure 1.10A) (Petronczki *et al.*, 2003; Hauf and Watanabe, 2004; Tanaka, 2013). Anaphase A is then followed by Anaphase B, where spindle elongation then separates the chromosomes further (Maiato and Lince-Faria, 2010).

A faulty SAC can give rise to aneuploid daughter cells, due to inaccurate segregation of unattached or incorrectly attached chromosomes (Figure 1.10B) (Musacchio and Salmon, 2007; Foley and Kapoor, 2013). Where the SAC is not functional, cohesin can be prematurely cleaved, and cells exit mitosis irrespective of their attachments. Defects in sister chromatid cohesion itself can give rise to aneuploidy as the sister chromatids can segregate randomly as they attach to microtubules (Figure 1.10C) (Peters *et al.*, 2008; Nasmyth and Haering, 2009). Although during mitosis in most eukaryotes, the kinetochores of sister chromatids can attach to spindle microtubules via multiple attachment sites, it is crucial for a correct chromosome segregation event that sister kinetochores attach to microtubules from opposite spindle poles (amphitelic attachment) (Petronczki *et al.*, 2003; Hauf and Watanabe, 2004; Tanaka, 2013).

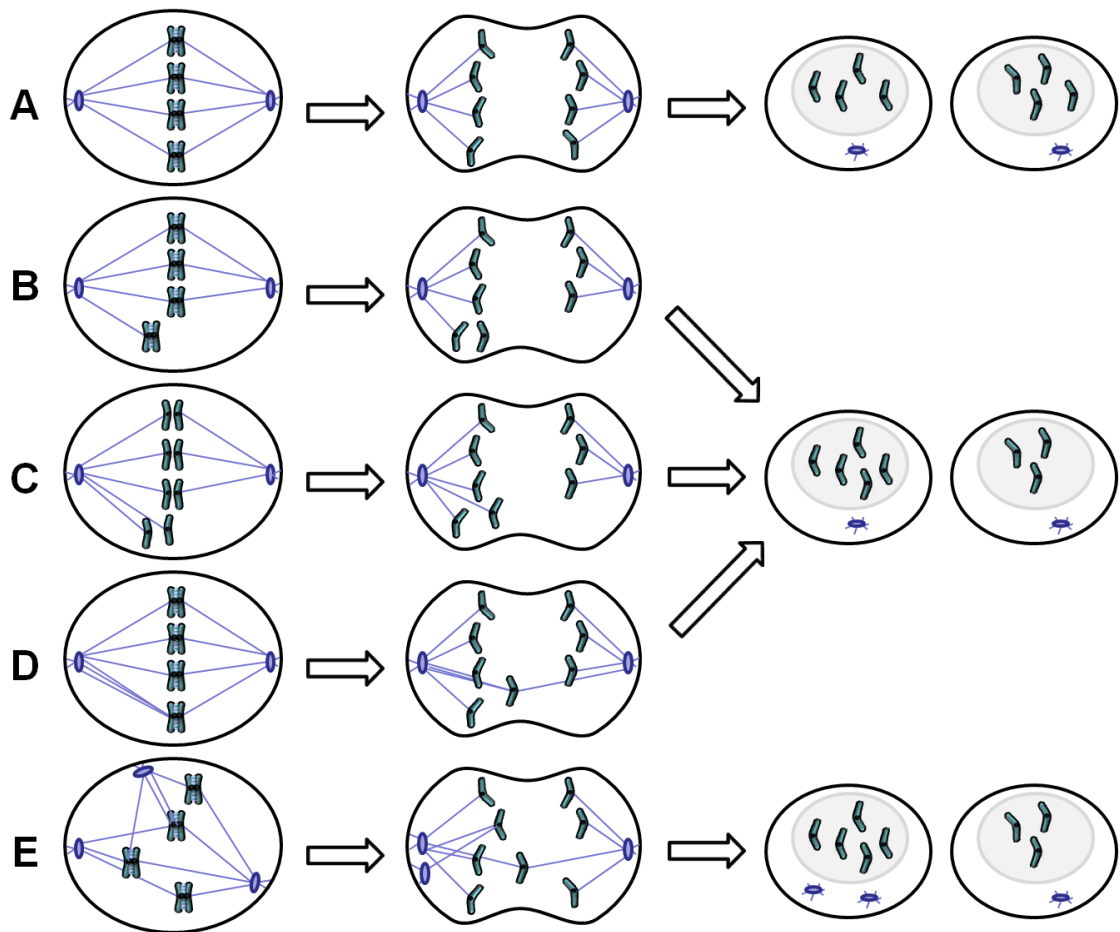


Figure 1.10 - Chromosome segregation errors in mitosis. A) Normal chromosome segregation pattern. The chromosomes align at the metaphase plate, with sister chromatids attaching to spindles from opposite poles. The SAC is satisfied, cohesion between the sisters is resolved, and the sisters segregate equally, forming two identical daughter cells. (B) Mis-segregation due to incorrect function of the SAC. Aberrantly attached chromosomes do not signal cell cycle arrest, leading to aneuploid cells. (C) Mis-segregation due to premature loss of sister chromatid cohesion. Single sisters attach to microtubules and are segregated randomly leading to aneuploid cells. (D) Mis-segregation due to uncorrected mis-attachment. A sister kinetochore attaches to microtubules from opposite centrosomes (merotelic attachment), leading to lagging chromosomes and aneuploid cells. (E) Mis-segregation due to uncorrected mis-attachment and a multipolar spindle. Kinetochores attach to microtubules from several centrosomes, resulting merotelic and syntelic attachments, leading to aneuploid cells. (Adapted from (Siegel and Amon, 2012)).

However it is possible for one kinetochore to attach to microtubules emanating from opposite spindle poles (merotelic attachments, Figure 1.10D and E), or for both sister kinetochores to attach to microtubules from one pole (syntelic attachments) (Petronczki *et al.*, 2003; Hauf and Watanabe, 2004; Tanaka, 2013). Mis-attachments frequently occur in early mitosis, however they are usually corrected before the onset of anaphase (Cimini *et al.*, 2001; Petronczki *et al.*, 2003).

Failure to correct erroneous attachments often results in lagging chromosomes, which occur when chromosomes segregate asynchronously during anaphase (Figure 1.10D and E) (Cimini *et al.*, 2001; Cimini *et al.*, 2003). This is thought to be predominantly caused by incorrect kinetochore-microtubule attachments. Merotelic attachments are particularly precarious, as kinetochores effectively have the appropriate number of microtubule attachments, making it possible for them to satisfy the SAC, thereby allowing anaphase to occur (albeit an erroneous one). In some cases, the cell may possess more than two centrosomes, or have fractured centrosomes. This can give rise to a multipolar spindle, and consequently aberrant kinetochore attachments and lagging chromosomes (Figure 1.10E) (Ganem *et al.*, 2009).

Aneuploidy resulting from errors in chromosome segregation has been strongly linked to cancer. A study examining the incidence of somatic copy number alterations in cancer cells have shown that one-quarter of the genome of a typical cancer cell is affected by either whole-arm or whole-chromosome aneuploidy (Beroukhim *et al.*, 2010). There is a preferential gain or loss of whole chromosomes, frequently occurring in many different types of cancer (Gordon *et al.*, 2012), with merotelic attachments being the primary mechanism of aneuploidy and chromosomal instability (Gregan *et al.*, 2011). To help resolve this, the cell has a variety of proteins and mechanisms in place to help correct or prevent merotelic attachments (Thompson *et al.*, 2010; Gregan *et al.*, 2011). Aneuploid tumour cells have been shown to have defects in these mechanisms (Gordon *et al.*, 2012).

Aside from cancer, chromosome instability is also common during early human embryogenesis. Approximately 80% of human embryos have aneuploid blastomeres (Vanneste *et al.*, 2009; Vanneste *et al.*, 2012). Aneuploidy has further been found in normal tissues such as the brain (Kingsbury *et al.*, 2005; Rehen *et al.*, 2005).

Chromosome missegregation in meiosis is the leading cause of infertility, miscarriage and birth defects (Hassold and Hunt, 2001). Approximately one third of miscarriages, and 10-30% of fertilised human oocytes are aneuploid (Hassold and Hunt, 2001). In contrast to mitosis where spindle bipolarity is predefined, oocyte spindles lack centrosomes. The mammalian meiotic spindle

is instead structured by multiple microtubule organising centres (MTOCs) (Figure 1.11A). After GVBD the many MTOCs scattered in the cytoplasm attract each other and congress at the centre of the oocyte where they form the spindle poles and contribute to an increase in the number of microtubules, and to the individualisation of chromosomes (Figure 1.11B). This forms an apolar microtubule ball (Schuh and Ellenberg, 2007). The randomly orientated growing microtubules are organised into a bipolar array around the chromosomes, which then elongates to a barrel-shaped spindle, and establishes chromosome biorientation as the chromosomes invade the spindle centre to form the metaphase plate (Figure 1.11C) (Schuh and Ellenberg, 2007). In contrast to mitosis, this bipolar spindle is formed in the absence of kinetochore fibers, which are instead acquired at the end MI, allowing the final alignment and anaphase to occur (Figure 1.11D) (Brunet *et al.*, 1999).

Another fundamental difference of meiosis in oocytes is the asymmetric division. This is essential as it enables the oocyte to retain most of the cytoplasm by producing a much smaller PB, the genetic dustbin of the oocyte. Thus, the oocyte retains the maternal stores accumulated during oogenesis and is the only viable product of female meiosis.

Spindle microtubules and actin microfilaments control the asymmetry of the MI division. It is achieved by the migration of the spindle from the centre of the oocyte where it is formed, to the closest part of the oocyte cortex for PB extrusion. Chromosome segregation in vertebrate oocytes is driven by spindle elongation (Anaphase B), followed by a shortening of kinetochore-microtubules (Anaphase A) (FitzHarris, 2012). This early spindle elongation stage determines the extent of chromosome segregation and the size of the resulting PB (FitzHarris, 2012).

As well as oocytes lacking centrosomes, their spindles lack the astral microtubules which connect the spindle poles to the cell cortex. In mouse oocytes the migration and anchoring of the spindle involves an interaction between the chromosomes and actin microfilaments, not microtubules (Longo and Chen, 1985; Maro *et al.*, 1986; Maro and Verlhac, 2002; Schuh and Ellenberg, 2008). Clusters of chromosomes are able to recruit MTOCs to organise the tubulin polymerised in their vicinity into spindles and induce an

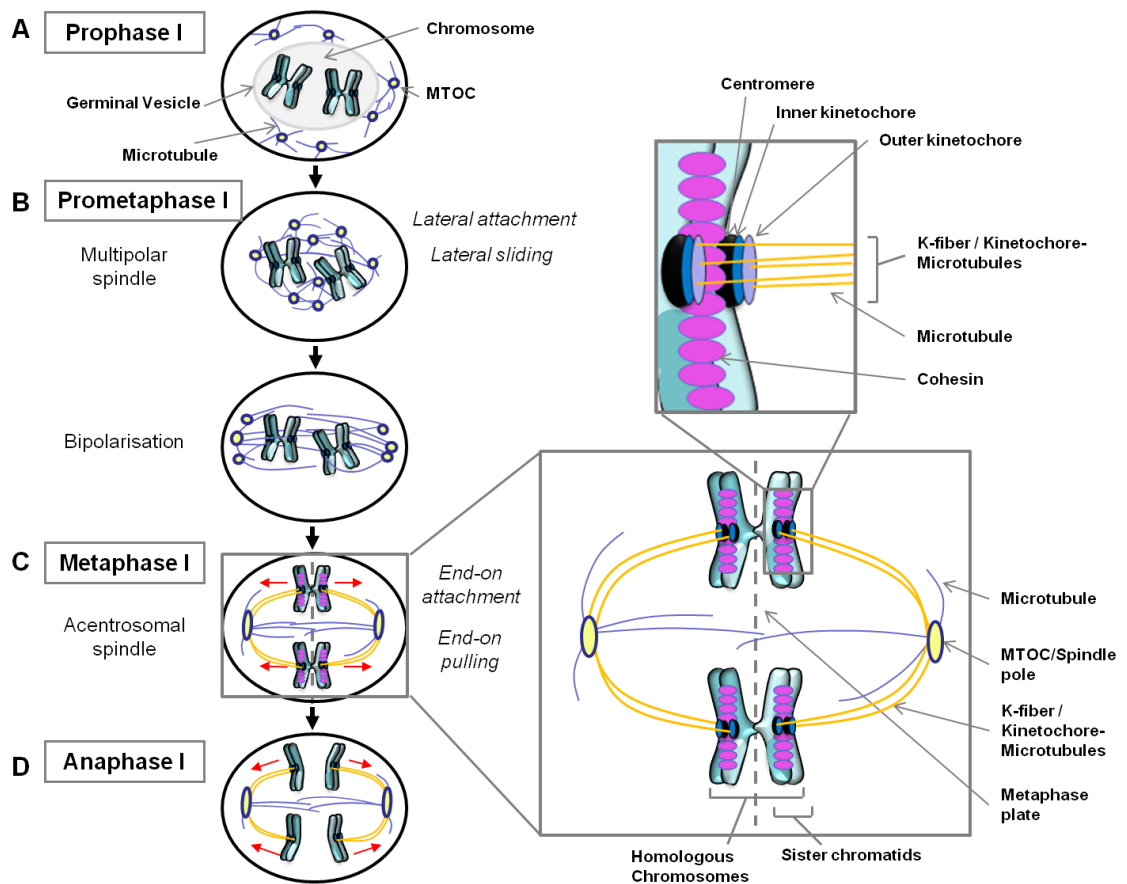


Figure 1.11 - Meiotic chromosome segregation. Schematic illustrating normal chromosome segregation in mammalian oocytes. (A) During prophase the chromosomes (recombinant maternal and paternal homologous chromosomes) are enclosed in the GV. (B) GVBD indicates entry into prometaphase. Microtubule organising centres (MTOCs) congress at the centre of the oocyte where they form spindle poles. This then elongates to form a barrel-shaped spindle. Kinetochore-microtubule attachments form lateral attachments with microtubules establishing chromosome biorientation as the chromosomes invade the spindle centre to form the metaphase plate. (C) End on attachment and K-fibers occur at the end of MI. (D) If the SAC is satisfied cohesin cleavage occurs down the chromosome arms, but not between sister centromeres, and microtubule depolymerisation allows homologous pairs to segregate to opposite spindle poles at anaphase. Red arrows indicate the direction of movement, or tension on the kinetochores. For ease of illustration only 2 homologous pairs are shown, with no spindle migration to the oocyte cortex before anaphase. (Adapted from (Schuh and Ellenberg, 2007; Tanaka, 2013)).

actin-rich, microvillus-free domain in the adjacent cortical region (Maro *et al.*, 1984; Longo and Chen, 1985; Maro *et al.*, 1986). Spindle migration requires a continuously reorganising cytoplasmic actin network, organised by the actin-filament nucleators Formin-2 (Azoury *et al.*, 2008; Schuh and Ellenberg, 2008) and Spire1/2 (Pfender *et al.*, 2011) which pull and/or push on the microtubule spindle. The spindle is surrounded by a cage of actin, and both migrate to the closest part of the oocyte cortex (Verlhac *et al.*, 2000; Schuh and Ellenberg,

2008). The oocyte cortex is covered with microvilli and a dense layer of actin, and underneath the cortex is an even distribution of cortical granules (Longo and Chen, 1985). Spindle migration promotes cortical differentiation, resulting in an area absent of microvilli and rich in actin (the actin cap) (Longo and Chen, 1985). This is the first sign of oocyte polarisation and defines the site of PB formation.

In contrast to mitotic cell division, which requires biorientation of sisters, meiosis requires biorientation of bivalent chromosomes on the first meiotic spindle. This requires that sister kinetochores form attachments with microtubules emanating from the same spindle pole (syntelic attachment) (Petronczki *et al.*, 2003; Watanabe, 2012). Thus, bipolar attachment of bivalents requires monopolar attachment of sisters, facilitated by sister kinetochores being juxtaposed side by side (Figure 1.11) instead of the back-to-back configuration of mitotic sister chromosomes (Östergren, 1951; Watanabe, 2012). Whereas the mechanisms responsible for monopolar attachment in yeast are well documented, very little has been established in higher organisms.

Budding yeast mono-orientation requires the protein complex monopolin (Toth *et al.*, 2000; Rabitsch *et al.*, 2003; Yokobayashi and Watanabe, 2005; Petronczki *et al.*, 2006; Watanabe, 2012), which is stabilised at the centromeres by sporulation-specific protein 13 (Spo13) and cell division control protein 5 (Cdc5) (Katis *et al.*, 2004; Lee *et al.*, 2004; Matos *et al.*, 2008). In fission yeast meiosis, monopolar attachment protein 1 (Moa1) interacts with Rec8 to maintain centromeric cohesion and mono-orientation (Yokobayashi and Watanabe, 2005; Sakuno *et al.*, 2009). Similarly, in higher organisms, Rec8 has been shown to play an essential role in mono-orientation in plants and nematodes, and inactivation of Rec8 at the kinetochore in mouse oocytes leads to bi-orientation of univalent chromosomes (Watanabe, 2012). This illustrates a conserved function of Rec8 in sister chromatid mono-orientation.

As one kinetochore can be bound by multiple microtubules, homologue pairs can, and frequently do, become attached with an incorrect orientation. However, these attachments do not generate tension at the kinetochore and are therefore not stabilised (Petronczki *et al.*, 2003; Marston and Amon, 2004) (Figure 1.12 and Figure 1.13).

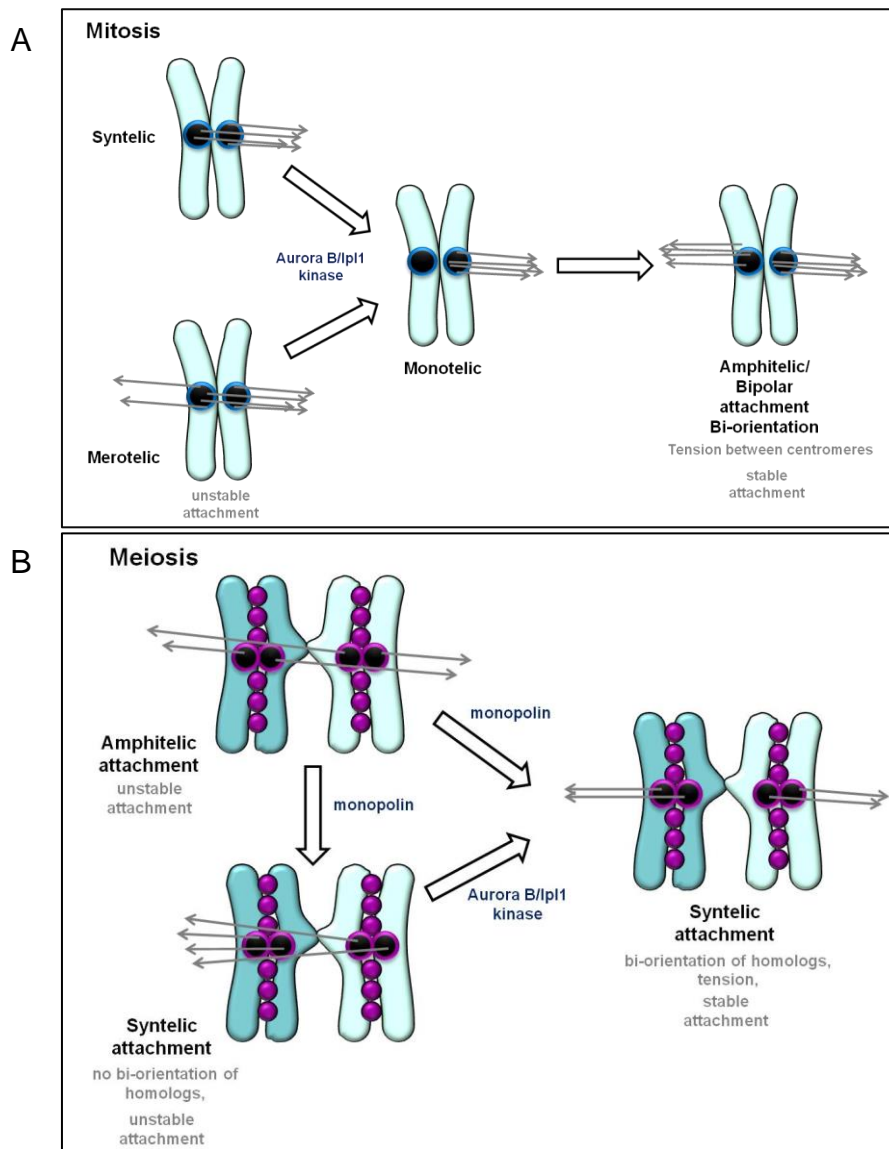


Figure 1.12 - A schematic for kinetochore-microtubule attachments during mitosis and meiosis I. A schematic for kinetochore-microtubule attachments during mitosis and meiosis I. (A) Mitosis: The microtubules can attach to the kinetochores in a multitude of manners, but in mitosis (and similarly in meiosis II) only amphitelic attachments generate the tension between the sister centromeres, necessary for accurate segregation. The Aurora B/lp1 kinase with mitotic-centromere-associated kinesin (MCAK) (Andrews *et al.*, 2004; Kline-Smith *et al.*, 2004; Lan *et al.*, 2004; Knowlton *et al.*, 2006) is believed to destabilise and eliminate incorrect syntelic and merotelic attachments to transiently create monotelic attachments, which can then become reattached in the correct manner. (B) Meiosis I: Proper segregation of homologues during MI requires that sisters co-segregate to the same spindle pole. This requires the formation of syntelic rather than amphitelic attachment of sisters. In yeast this is orchestrated by a protein complex known as monoplin (Toth *et al.*, 2000) and by cohesin at the core centromere. The mechanisms governing monopolar attachment in vertebrates have not yet been established. Aurora B/lp1 and monopolins acting together eventually produce the stable, tension generating syntelic attachments, with bi-orientated homologues with the centromere pairs attached to opposite poles. MCAK contributes to chromosome alignment in MI, but is not necessary for preventing chromosome segregation errors (Illingworth *et al.*, 2010). Figure adapted from (Petronczki *et al.*, 2003).

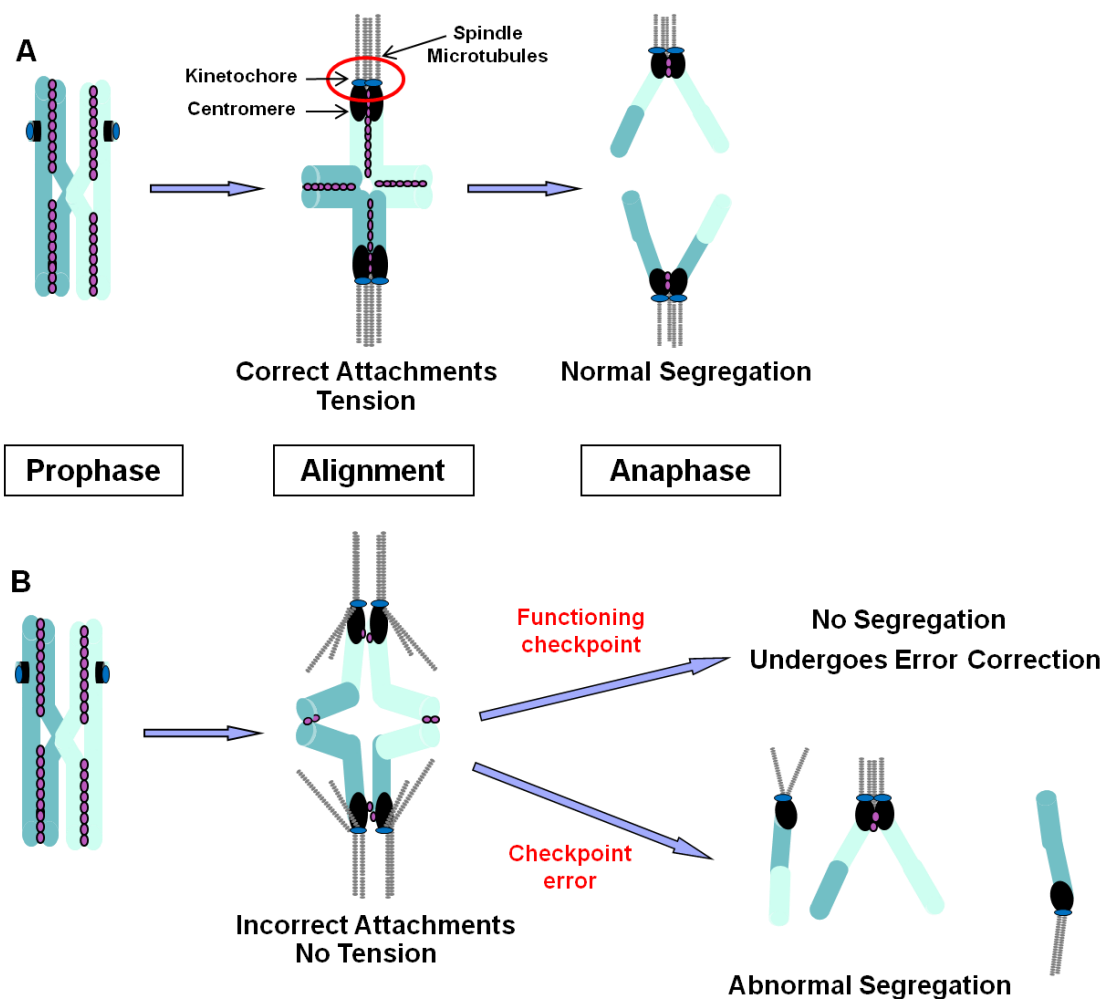


Figure 1.13 - Monopolar attachments are essential for biorientation and accurate homologous chromosome segregation. (A) Diagrammatic representation of monopolar kinetochore-microtubule attachments (red circle). Correct attachments are necessary for the establishment of chromosome biorientation, tension, and normal segregation of homologous chromosomes. (B) Incorrect attachments should be recognised by the spindle checkpoint, and not proceed through meiosis until corrected. If the spindle checkpoint is not functioning, abnormal segregation may occur.

Approximately 90% of oocyte chromosomes undergo at least one round of error correction of kinetochore-microtubule attachments before achieving correct biorientation (Kitajima *et al.*, 2011). This is striking when compared to the estimated 10% of mis-attachments which occur during prometaphase in somatic cells (Salmon *et al.*, 2005).

That biorientation is so error prone may go some way to explaining the frequency of MI segregation errors (Hassold and Hunt, 2001). Once error correction has efficiently occurred, and chromosome attachments satisfy the SAC, cohesin cleavage is triggered down the chromosome arms, but not at the

centromeres (cohesin cleavage is further explained in section 1.5) to allow separation of homologous chromosomes at anaphase (Brunet *et al.*, 1999).

In an ideal system, any incorrect attachments would be sensed by the SAC, and the oocyte arrested at MI until such a time as the erroneous attachments could be corrected. A single unattached chromosome in mitosis is sufficient to elicit such a response from the SAC (Musacchio and Salmon, 2007). However, although the case in spermatocytes (Kot and Handel, 1990), reports have shown that oocytes have ways of bypassing the SAC. The evidence suggests that the presence of one, or even several univalent chromosomes is accepted, but if there are too many, the oocyte will arrest in MI (LeMaire-Adkins *et al.*, 1997; Yuan *et al.*, 2002; Hodges *et al.*, 2005). The classic example is the XO mouse, which is univalent for chromosome X, and is able to evade the SAC and contribute to aneuploidy (LeMaire-Adkins *et al.*, 1997). Univalent chromosomes are also evident in a mouse strain lacking a structural component of the synaptonemal complex (*Sycp3*) (Kouznetsova *et al.*, 2007). By forming bipolar attachments the univalents can satisfy the requirements of the SAC and progress to anaphase, producing an aneuploid MII oocyte (Kouznetsova *et al.*, 2007). Consistent with findings in oocytes of XO females, univalent segregation during anaphase results in an extra whole chromosome (an intact univalent), two single sisters, or one single sister in the MII oocyte (LeMaire-Adkins and Hunt, 2000; Kouznetsova *et al.*, 2007). However, studies in the XO mouse indicate that the background strain can influence the segregation pattern of the X chromosome, with one background favouring its intact segregation (C57BL/6J), and another, its bipolar attachment resulting in equational segregation (C3H/HeJ) (LeMaire-Adkins *et al.*, 1997; LeMaire-Adkins and Hunt, 2000). This was also found to be the case in oocytes deficient in the DNA mismatch repair gene, *Mlh1*. In these oocytes recombination is drastically reduced, resulting in the majority of chromosomes segregating as unpaired univalents at MI. On one background (C57BL/6J) the oocytes arrest at MI (Woods *et al.*, 1999), presumably unable to form bipolar attachments, but on the same background that enabled the XO mouse to segregate equationally (C3H/HeJ) the *Mlh1* mouse was also able to undergo anaphase of MI, despite still showing a prevalence of univalents due to reduced recombination (Nagaoka *et al.*, 2011). In this case the SAC is evaded by the bipolar attachment of a

'critical mass' of chromosomes, but not all of them (Nagaoka *et al.*, 2011).

Together these studies indicate that (i) the oocyte SAC is not capable of distinguishing between monopolar and bipolar attachment of sisters (ii) that the oocyte SAC may be "leaky" (iii) that there is variation between mouse strains with respect to SAC function.

Recent reports indicate that the oocyte SAC may indeed be "leaky". Using a combination of live cell imaging and immunofluorescence of fixed oocytes, it was reported that the onset of APC/C mediated proteolysis during exit from MI is not sensitive to the presence of misaligned bivalents (Lane *et al.*, 2012). Moreover, it has been reported that the staining of the checkpoint protein mitotic arrest deficient 2 (Mad2) is lost from kinetochores, even in the absence of stable kinetochore-microtubule attachments (Gui and Homer, 2012). Thus, the balance of currently available evidence indicates that SAC function in oocytes is different from that in somatic cells.

This 'leaky' SAC may explain the prevalence of segregation errors in MI oocytes. However, current evidence indicates that the increase in segregation errors observed with advancing maternal age can't be explained by a deterioration of SAC function (Duncan *et al.*, 2009; Lister *et al.*, 2010).

1.5. Cohesin – The Chromosome Glue

Chiasma can only link the homologous chromosomes because the sister chromatids are already attached in the first instance. Without sister chromatid cohesion, the sisters would begin to separate before they even had a chance to become aligned on the spindle poles. Cohesin at the arms is essential for the stabilisation of the chiasmata, and cohesion at the centromeres is essential for mono-orientation of sister kinetochores (Peters, 2006; Nasmyth and Haering, 2009).

1.5.1. The Mitotic Cohesin Complex

During DNA replication the sister chromatids become extensively intertwined when two adjacent replication forks collide. This is termed DNA catenation

(Sundin and Varshavsky, 1980) and is resolved by the enzyme topoisomerase II before anaphase can occur (DiNardo *et al.*, 1984; Steck and Drlica, 1984; Baxter *et al.*, 2011). However, proteins not involved in DNA catenation but essential for cohesion were discovered. Indeed it was found that catenation is not even required for proper segregation in yeast circular minichromosomes (Koshland and Hartwell, 1987). This indicated that catenation alone is not sufficient to hold sister chromatids together.

It was later discovered that a protein complex called cohesin links the sister chromatids together as they are replicated. The main components of cohesin were discovered by genetic screens for mutants that gave rise to precocious sister chromatid separation during mitosis in the budding yeast *Saccharomyces cerevisiae* (Guacci *et al.*, 1997; Michaelis *et al.*, 1997; Toth *et al.*, 1999). There were found to be four core proteins of the cohesin complex, two from the structural maintenance of chromosomes family (Smc), Smc1 (also known as SMC1 α in vertebrates) and Smc3, and two sister chromatid cohesion proteins, Scc1 (also known as Mcd1 or Rad21) and Scc3 (also known as SA1 and SA2 in mammalian cells) (Peters *et al.*, 2008; Nasmyth and Haering, 2009). The amino acid structures and cohesive function of these components has been highly conserved through evolution from yeast to man (Table 1.1) (Losada *et al.*, 1998; Sumara *et al.*, 2000; Peters *et al.*, 2008; Nasmyth and Haering, 2009). The SMC family are composed of an antiparallel coiled coil 'hinge' domain at one end, with a globular ATP nuclear binding domain (NBD) domain at the other. The hinge domains of Smc1 and Smc3 bind together forming a V-shaped heterodimer, with the Smc1 NBD at one end and the Smc3 NBD at the other, both physically linked by the Scc1 kleisin (meaning 'Bridge' in Greek) protein to make a large tripartite ring (Gruber *et al.*, 2003; Peters *et al.*, 2008; Nasmyth and Haering, 2009; Nasmyth, 2011). Interestingly, Scc1's N terminus binds only to Smc3, and its C terminus to Smc1. This interaction depends on the prior binding of Scc1's C terminus to Smc1 before the N terminus can bind to Smc3. This ensures that only one Scc1 molecule can bind to the heterodimer at any one time (Figure 1.14) (Peters *et al.*, 2008; Nasmyth and Haering, 2009).

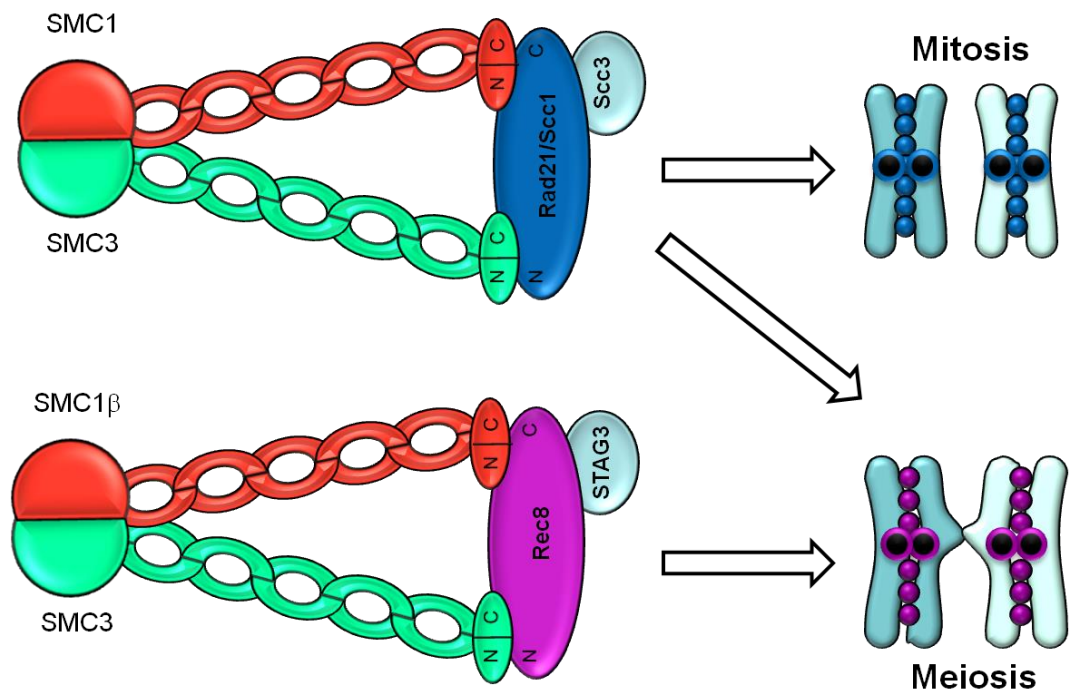


Figure 1.14 - The cohesin complex. A diagrammatic representation of the architecture of the cohesin complex. Scc1 (also known as Rad21, or the meiotic variant Rec8) connects the nuclear binding domains of the Smc1 and Smc3 heterodimer forming a ring like structure. Scc1 then recruits Scc3. Meiotic cohesin complexes can contain either Rec8 or Scc1, but it is only the Rec8 containing cohesin that is necessary for cohesion during MI. Mammalian meiotic cohesin complexes also consist of SMC1 β , and STAG3.

Scc1 is further associated with the fourth member of this core complex of proteins, Scc3 (Peters *et al.*, 2008; Nasmyth and Haering, 2009). These essential proteins are associated with the chromosomes from DNA replication, and the most accepted theory is that the sister chromatids become entrapped within the ring like structure, between the Smc proteins with the Scc1 closing the gate behind them.

1.5.2. Cohesin Associated Proteins

Aside from these core components, other proteins have been discovered that play a role in the efficiency of cohesin, which are highly conserved in most eukaryotes. Precocious dissociation of sisters protein 5 (Pds5) is less tightly bound than the other four subunits, but can be found at similar locations on the genome. Where depletion of Pds5 only has a minimal effect on cohesin in frogs

(Losada *et al.*, 2005), and no effect on cohesion in mice (Zhang *et al.*, 2007), it is essential in both budding (Hartman *et al.*, 2000; Panizza *et al.*, 2000) and fission yeast (Tanaka *et al.*, 2001), flies (Dorsett *et al.*, 2005) and worms (Wang *et al.*, 2003).

The binding of cohesin to DNA is integral to its function, and sister chromatids must be linked before the onset of DNA replication (Uhlmann and Nasmyth, 1998). The 'sister chromatid cohesion' proteins Scc2 (known as Nipbl in mammalian cells) and Scc4, and the 'establishment of cohesin' protein Eco1 (Eso1 and -2 in mammalian cells) are essential for, as the names imply, the establishment of cohesion. The Scc2-Scc4 cohesin loader complex is required for the initial loading of cohesin onto the chromosomes, but is dispensable during S phase (Ciosk *et al.*, 2000). Scc2 has a further role in yeast meiosis in regulating gene expression by recruiting cohesin to the chromosome as a transcriptional activator (Lin *et al.*, 2011). It is the acetyl-transferase Eco1 which is required for the establishment of cohesin during S phase, but not maintaining it during G2 or M phase (Toth *et al.*, 1999). Eco1 acetylates a pair of lysines (K112 and K113) within Smc3's NBD close to the ATP-binding pocket. This acetylation is a conserved mechanism in regulating sister chromatid cohesion (Rolef Ben-Shahar *et al.*, 2008; Unal *et al.*, 2008; Zhang *et al.*, 2008). Interestingly, it was discovered that the fission yeast ortholog of Eco1, Eso1, helps to establish cohesion by suppressing the Pds5 inhibition of cohesion formation. In this case Eso1 is dispensable when Pds5 is deleted. Pds5 seems to have a dual role in the establishment and maintenance of sister chromatid cohesion (Tanaka *et al.*, 2001). Subsequent studies in budding yeast showed that the lethal phenotype of an Eco1 deletion can also be suppressed by an inactivation of Pds5, Scc3 or Rad61/Wapl. Rad61/Wapl forms a complex with Pds5 and Scc3 and co-localises with cohesin on the chromosomes, where they inhibit the entrapment of sister chromatids by a mechanism involving the K112 and K113 lysines on Smc3. Eco1 therefore promotes sister chromatid cohesion by inhibiting these 'anti establishment' properties (Rolef Ben-Shahar *et al.*, 2008; Rowland *et al.*, 2009; Sutani *et al.*, 2009). The vertebrate protein sororin is also essential for sister chromatid cohesion (Rankin *et al.*, 2005). It is recruited to cohesin in a manner which depends on Smc3 acetylation and DNA replication. Sororin displaces Wapl from Pds5 thereby neutralising the effects

of Wapl and stabilising cohesin (Lafont *et al.*, 2010; Nishiyama *et al.*, 2010).

1.5.3. Meiotic Cohesin

The complexities of meiosis require similar, yet distinct mechanisms of cohesion. The core cohesin complex is mostly conserved between meiosis and mitosis, yet with subtle distinctions in their makeup. As already discussed, meiosis first involves the segregation of homologous chromosomes at MI, followed by the separation of the sister chromatids in MII. This requires that cohesion is removed in a stepwise manner, with arm cohesion being resolved during MI, but centromeric cohesion being tightly maintained, ensuring the sisters stay together until anaphase of MII. In some meiotic cohesin complexes, the Scc1 kleisin subunit is replaced by the meiosis specific paralog, Rec8 (Klein *et al.*, 1999; Watanabe and Nurse, 1999), which is conserved from yeast to man (Peters *et al.*, 2008; Nasmyth and Haering, 2009). Rec8-containing cohesin is necessary for cohesion during MI (Watanabe and Nurse, 1999) and for recombination (Klein *et al.*, 1999). Scc1-containing cohesin still exists in meiosis, but does not appear to be required for cohesion during MI or MII (Tachibana-Konwalski *et al.*, 2010). However, it is necessary for cohesion between sister chromatids in the first mitotic division after fertilisation (Tachibana-Konwalski *et al.*, 2010). Meiosis specific isoforms also exist for other key members of the core cohesin complex (Table 1.1). For example, in mammalian cells, the Smc1 can be replaced by Smc1 β (Revenkova *et al.*, 2001; Revenkova *et al.*, 2004), and SA1 and SA2 by STAG3 (Pezzi *et al.*, 2000; Prieto *et al.*, 2001). Also, in fission yeast the cohesin's Scc3 like subunit Psc3 is replaced by Rec11 along the chromosome arms, but not at the centromeres (Kitajima *et al.*, 2003b).

Species		Cohesin Core Subunits			
		SMC	SMC	Kleisin WHD	HEAT Repeat
<i>Saccharomyces cerevisiae</i>	mitosis	SMC1	SMC3	SCC1/MCD1	SCC3/IRR1
	meiosis			REC8	
<i>Schizosaccharomyces pombe</i>	mitosis	psm1	psm3	rad21	psc3
	meiosis			rec8	rec11
<i>Caenorhabditis elegans</i>	mitosis	him-1	smc-3	scc-1 coh-1	scc-3
	meiosis			rec-8 coh-3	
<i>Drosophila melanogaster</i>	mitosis	SMC1	Cap	Rad21	SA SA-2
	meiosis			c(2)M	
<i>Xenopus laevis</i>	mitosis	smc1a	smc3	rad21	stag1 stag2
	meiosis	smc1b		rec8	
<i>Homo sapiens</i>	mitosis	SMC1A	SMC3	RAD21	STAG1 STAG2
	meiosis	SMC1B		REC8	STAG3

	Accessory Proteins				
	HEAT Repeat Associated	Cohesin Loading		Establishment/ Release of Cohesion	
<i>Saccharomyces cerevisiae</i>	PDS5	SCC2	SCC4	ECO1	RAD61/WPL1
<i>Schizosaccharomyces pombe</i>	pds5	mis4	ssl3	eso1	wapl1
<i>Caenorhabditis elegans</i>	evl-14	pqn-85	mau-2	F08F8.4	wapl-1
<i>Drosophila melanogaster</i>	pds5	Nipped-B	CG4203	san eco	wapl1
<i>Xenopus laevis</i>	pds5a pds5b	nipbl	kiaa0892	esco1	wapal1
<i>Homo sapiens</i>	PDS5A PDS5B	NIPBL	KIAA0892	ESCO1 ESCO2	WAPAL1

	Other Associated Proteins		
	Separase	Securin	Shugoshin
<i>Saccharomyces cerevisiae</i>	ESP1	PDS1	SGO1
<i>Schizosaccharomyces pombe</i>	cut1	cut2	sgo1 sgo2
<i>Caenorhabditis elegans</i>	sep-1	ify-1	C33H5.15
<i>Drosophila melanogaster</i>	Sse thr	pim	Mei-S332
<i>Xenopus laevis</i>	espl1	LOC398156	sgo1
<i>Homo sapiens</i>	ESPL1	PTTG1	SGO1 SGO2

Table 1.1 - Cohesin subunits and associated proteins. The gene names of the mitosis and meiosis specific subunits of cohesin and their associated proteins. (Nasmyth and Haering, 2009).

1.5.4. Cohesin Dissociation

In somatic cells, cohesin dissociation from the chromosomes involves two distinct mechanisms, and these differ between mitosis and meiosis, and indeed between species. During mitosis in most eukaryotic cells the first stage is known as the prophase pathway, and takes place during prophase and prometaphase. The prophase pathway involves removal of the majority of cohesin from chromosome arms, but not centromeres (Losada *et al.*, 1998; Sumara *et al.*, 2000; Waizenegger *et al.*, 2000). The second stage takes place

at the onset of anaphase and involves the cleavage of the remaining Scc1 kleisin subunit by a thiol protease named separase (Esp1 and Cut1 in budding and fission yeast respectively) (Uhlmann and Nasmyth, 1998; Uhlmann *et al.*, 1999; Hauf *et al.*, 2001), breaking open the cohesin ring and allowing the sister chromatids to come apart (Figure 1.15). Separase is kept inactive through most of the cell cycle by an inhibitory binding partner known as securin (Pds1 and Cut2 in budding and fission yeast respectively), and by the inhibitory phosphorylation of Cyclin B-Cdk (Shirayama *et al.*, 1999; Stemmann *et al.*, 2001). Securin and cyclin B are ubiquitinated by the anaphase promoting complex/cyclosome (APC/C) and targeted for destruction by the proteasome (Cohen-Fix *et al.*, 1996; Funabiki *et al.*, 1996; Ciosk *et al.*, 1998; Stemmann *et al.*, 2001). This APC/C dependent process is regulated by the spindle assembly checkpoint (SAC), which ensures that securin release and hence anaphase onset is not initiated until all the chromosomes are properly aligned (discussed in more detail in section 1.7).

The prophase pathway is independent of the APC, and instead depends on the enzyme Polo-like kinase 1 (Plk1) (Losada *et al.*, 2002; Sumara *et al.*, 2002; Gimenez-Abian *et al.*, 2004). Plk1 contributes by the phosphorylation of the C terminal domain of cohesin's Scc3/SA subunits (Hauf *et al.*, 2005; McGuinness *et al.*, 2005), which is mediated by another mitotic kinase, Aurora B (Losada *et al.*, 2002; Gimenez-Abian *et al.*, 2004). These phosphorylations decrease the binding efficiency of cohesin (Sumara *et al.*, 2002). In budding yeast and vertebrates, Wpl1/Wapl is also required for the removal of cohesin complexes from the DNA. If Wapl is depleted from mammalian cells, cohesin dissociation is reduced in prophase to a larger extent than after the inactivation of Plk1 or Aurora B. Similarly, Wapl has also been found to interact with the SA2 subunit (Gandhi *et al.*, 2006; Kueng *et al.*, 2006) whose phosphorylation is required for cohesin removal in mitosis. Despite progress in understanding the mechanism, the significance of the prophase pathway remains unclear.

It is not known whether the prophase pathway is active in meiosis. According to our current understanding, the two stages of meiotic cohesin dissociation involve the APC/C dependent cleavage of the kleisin subunit by separase. However, removal of cohesin is confined to chromosome arms during the first meiotic division, with centromeric cohesin tightly holding the sister chromatids

together until the second meiotic division (Buonomo *et al.*, 2000; Kitajima *et al.*, 2003a; Kudo *et al.*, 2006) (Figure 1.1). Interestingly, the mechanism responsible for protecting centromeric cohesin from separase-mediated cleavage during anaphase of MI, is similar to that responsible for protecting centromeric cohesin from Plk1-mediated prophase pathway in somatic cells (Figure 1.15 and section 1.6)

Given that cohesion between sisters is required to stabilise chiasmata, the maintenance of cohesin during prophase and prometaphase is essential for proper segregation of homologous chromosomes during anaphase of MI. Thus, if the prophase pathway is functional during prophase or prometaphase of MI, it would need to be very tightly regulated to ensure that sufficient arm cohesin is maintained to stabilise chiasmata. In addition, evidence in yeast indicates that protection of cohesin at the centromeres is essential for monopolar orientation of sister kinetochores (Watanabe and Nurse, 1999). Centromeric cohesin is also essential for correct segregation during MII. In conclusion, the regulation of cohesin is essential for the establishment of haploid gametes during meiosis.

1.6. Shugoshin – the ‘guardian’ protector

The Japanese translation of Shugoshin is ‘guardian spirit’, and that is just what it is. Shugoshin (Sgo) is a guardian, or protector of centromeric cohesin, without which faithful chromosome segregation would be impossible.

Through functional screening in fission yeast, searching for a gene that yielded mitotic toxicity when co-expressed with Rec8 (which was shown to be cleaved by separase in mitosis, so would not be a problem unless a protector was also expressed), Sgo1 was identified as a meiotic cohesion protein (Kitajima *et al.*, 2004). Sgo1 localises to pericentromeric chromosome regions at MI, but disappears from the chromosomes for anaphase to occur. Sgo1 depleted cells were able to undergo a seemingly normal meiosis I, showing that monopolar attachments were still established, however chromosomes were unable to segregate properly at meiosis II. They showed that the cells were already lacking the Rec8 cohesin, normally enriched at the centromeric regions during

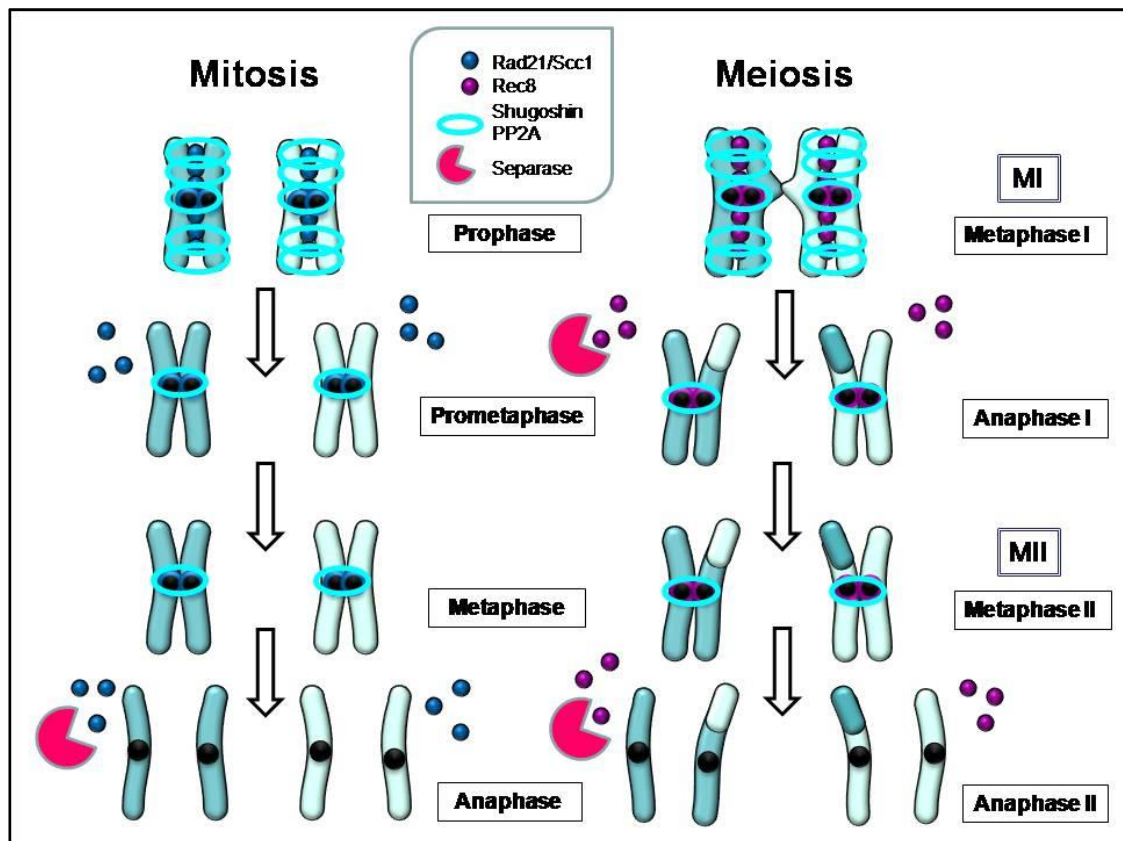


Figure 1.15 - A schematic for cohesin dissociation. A diagrammatic representation of cohesin dissociation from the chromosomes. In mitosis all cohesin is resolved for mitotic segregation. Arm cohesion is removed by the prophase pathway, and centromeric cohesion is removed through cleavage by separase. In meiosis cohesin is lost in a stepwise manner, but both steps require cleavage by separase. Arm cohesin is lost for anaphase I to occur at MI, but the centromeric cohesion is maintained until anaphase at MII. The dark blue circles represent the mitotic cohesion component Rad21/Scc1, and the purple circles the meiotic counterpart Rec8. The light blue rings represent the cohesin protector shugoshin. The pink pies illustrate separase.

anaphase I (Kitajima *et al.*, 2003b). This resulted in the precocious separation of sister kinetochores, and random segregation of sister chromatids at MII. In yeast, Sgo1 is believed to protect the centromeric Rec8 from separase at anaphase I by recruiting protein phosphatase 2A (PP2A) to the centromeres, which counteracts the phosphorylation of Rec8 required for its cleavage by separase (Kitajima *et al.*, 2006; Riedel *et al.*, 2006; Katis *et al.*, 2010). Kitajima *et al.* also found a second fission yeast shugoshin homologue, Sgo2 (Kitajima *et al.*, 2004). Despite their sequences being different lengths (Sgo1 319aa and Sgo2 647aa) they have a similar sequence architecture (both with an N-terminal coiled coil motif and comparable central and C-terminal segments). Where in yeast Sgo1 is only required for protection in meiosis I, Sgo2 is expressed in both meiotic and mitotic cells. Sgo2 plays a central role in proper chromosome

segregation, though it is dispensable for the protection of centromeric cohesion (Kitajima *et al.*, 2004). Fission yeast Sgo2 instead promotes Aurora B localisation to the centromeres where it can correct erroneous kinetochore attachments (Kawashima *et al.*, 2007).

There was found to be some conservation between fission yeast shugoshin and the *Drosophila* protein MEI-S332, which was previously identified as being essential for protecting centromeric cohesion in *Drosophila* meiosis (Kerrebrock *et al.*, 1995). Using a fission yeast knockout screen, another group were also able to isolate *sgo1* and *sgo2* as genes similar in function to MEI-S332 (Rabitsch *et al.*, 2004). Budding yeast was only found to have the one homologue (Sgo1), indicating that Sgo1 must be able to perform the same functions as Sgo1 and Sgo2 in fission yeast.

Mouse Sgo1 and Sgo2 are universally expressed in proliferating cells, with Sgo2 being notably stronger in germ cells (Lee *et al.*, 2008). Mice deficient for Sgo2 do not have any defects in sister chromatid cohesion in embryonic cultured fibroblasts or adult somatic tissue. The mutant mice develop normally, but are, however, infertile. This indicates that Sgo2 is essential for meiosis, but is dispensable for mitosis (Llano *et al.*, 2008). Sgo1 and Sgo2 are both localised to the inner kinetochore region in MI and MII (Lee *et al.*, 2008). In mitosis and meiosis cohesin is only protected when the kinetochores are not under tension by the pulling spindle forces. Therefore, protection is released at the end of metaphase in mitosis, but only by the end of metaphase II in meiosis (Lee *et al.*, 2008).

Deletion of Sgo2 in mammalian oocytes results in a loss of centromeric cohesion and premature sister chromatid separation, resulting in precociously separated single chromatids being observed at MII (with no observed defect at MI). By contrast depletion of Sgo1 results in failure of ~10% of homologous pairs to disjoin. Thus, in mouse oocytes Sgo2 appears to act alone in protecting centromeric cohesion (Figure 1.16), while the precise role and action of Sgo1 remains unclear. PP2A co-localises with Sgo2 indicating that Sgo2 rather than Sgo1 interacts with PP2A to protect centromeric cohesin in mouse oocytes (Lee *et al.*, 2008).

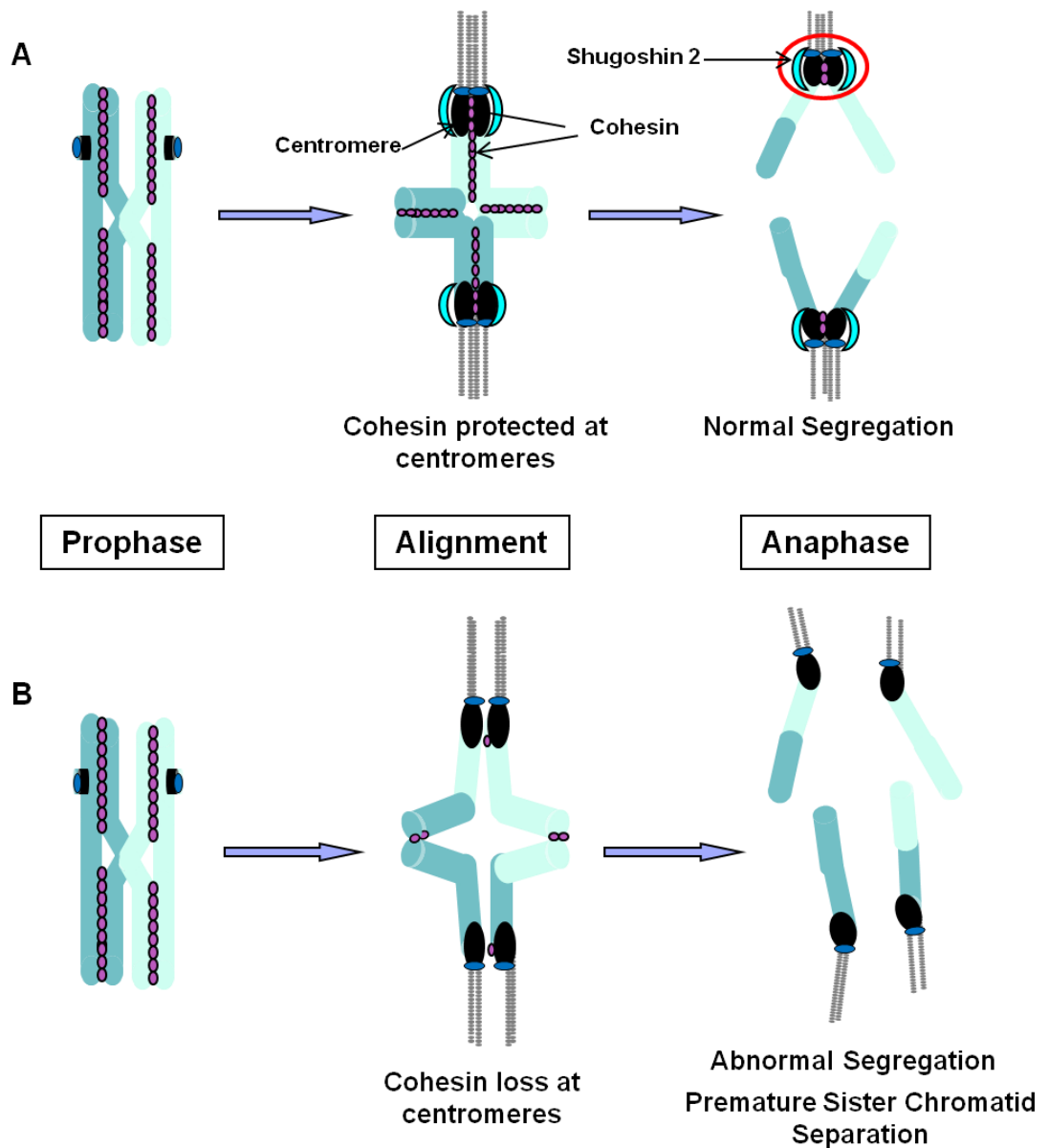


Figure 1.16 - Sgo2 is required to protect centromeric cohesin for correct segregation to occur in mammalian oocytes. (A) Diagrammatic representation of the protection of centromeric cohesin by Shugoshin 2 (red circle; Shugoshin 2 in light blue) in mammalian oocytes. Cohesin is lost from the chromosome arms by separate cleavage for anaphase I to occur, segregating homologous chromosomes. It is however essential that the centromeric cohesin is protected from separate until the onset of anaphase II. (B) If cohesin is lost from the centromeres before anaphase I, premature sister chromatid separation will occur.

In somatic cells and yeast, the localisation of Shugoshin requires the conserved spindle checkpoint kinase Bub1 (Kitajima *et al.*, 2004). In fact, centromeric Rec8 cannot be detected after MI in fission yeast deficient for Bub1. It has also been found that Bub1 phosphorylates Histone H2A in fission yeast, and a mutant of this conserved phosphorylation site (serine 121) is unable to localise

Shugoshin to the centromeres (Kawashima *et al.*, 2010). By contrast, oocytes deficient in Bub1 largely maintain cohesin between sisters during MI (McGuinness *et al.*, 2009), indicating that the interaction between Sgo2 and Bub1 is not essential for protection of centromeric cohesin in mammalian oocytes.

In human mitosis, Sgo2 was found to interact with another checkpoint protein, Mad2, in a manner resembling the interactions of Mad2 with Cdc20 and Mad1 (Orth *et al.*, 2011). This binding is important for the proper location of Sgo2 to centromeres. Mad2 binding was conserved in *Xenopus* Sgo (the sole Shugoshin protein in this organism), with interactions in oocytes suggesting that this also has a meiotic function (Orth *et al.*, 2011). Mad2 may play a role in regulating Sgo2 localization and sister-chromatid cohesion in meiosis I.

1.7. Cell cycle regulation of chromosome segregation during meiosis

The Cell Cycle can be defined as the series of events that lead to the reproduction of a cell. A complex network of proteins is needed to control the cell cycle events leading to cellular division. Various checkpoints exist to monitor and regulate the progression through the cell cycle. A cell cannot progress through the checkpoints until all the demands of the specific checkpoints are met, thereby ensuring the faithful replication of the cell.

1.7.1. Cyclin Dependent Kinases

The eukaryotic cell cycle is regulated by Cyclin Dependent Kinases (CDKs), a family of serine/threonine protein kinases whose activation is dependent on the binding of a regulatory cyclin subunit (Figure 1.17). The formation of distinct cyclin/CDK complexes controls the progression through the various cell cycle stages.

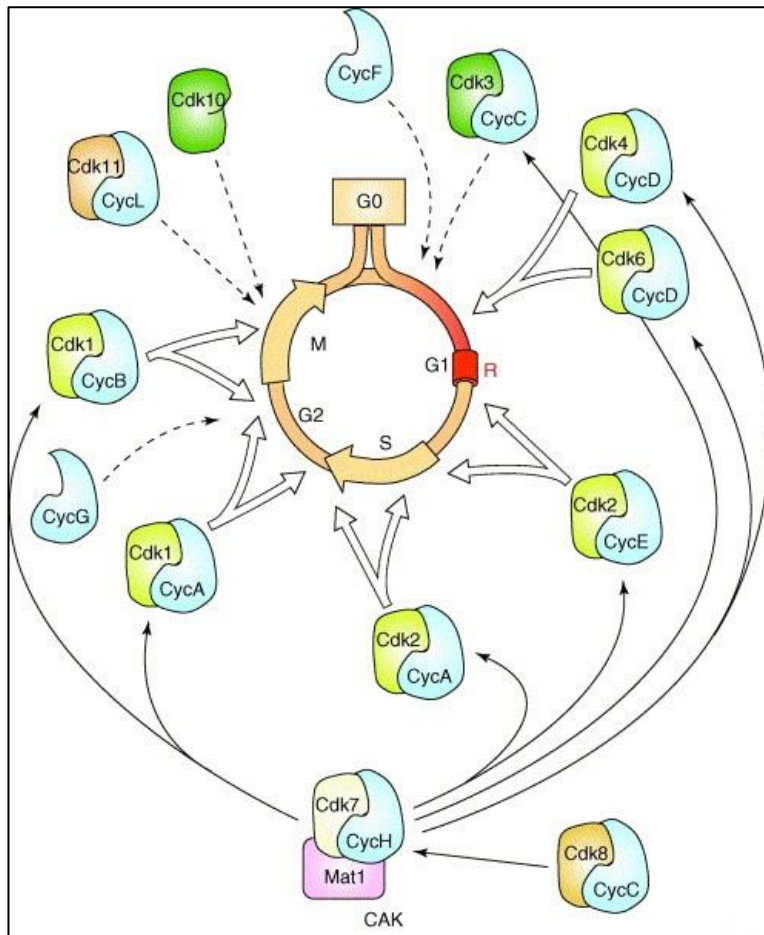


Figure 1.17 - The proposed roles of Cdk-cyclin complexes in the mammalian cell cycle. Open arrows depict widely accepted roles. Dashed arrows represent preliminary data. The filled arrows represent the interactions of Cdk activating kinase (CAK) which phosphorylates and activates all cell cycle Cdks. Taken from (Malumbres and Barbacid, 2005).

The Cyclins are members of a diverse family of proteins involved in the progression of cells through their cell cycle. Their concentrations oscillate in a cyclic manner, produced by gene expression, and degraded by proteolysis as needed, in order to drive the cells through the different stages of the cycle. At least 11 different cyclins are known, many of which have different isoforms (Figure 1.17). Cyclins are expressed in different tissues, cell types and stages. Cyclin B-Cdk1 is the main player in orchestrating progression through M phase, and its importance in both mitosis and meiosis have been well documented (Malumbres and Barbacid, 2005; Polanski *et al.*, 2012).

Cyclin A-Cdk complexes regulate the initiation of mitosis and progression through prometaphase in mammalian cells (Pagano *et al.*, 1992). *Drosophila* has just the one cyclin A, which activates Cdk1 and is essential for entry into

mitosis. *Xenopus* (Minshull *et al.*, 1990; Howe *et al.*, 1995), mice (Sweeney *et al.*, 1996) and humans (Yang *et al.*, 1997) have two cyclin A's, both of which can bind to Cdk1 or Cdk2. Cyclin A2 activates Cdk1 on entry into mitosis, and Cdk2 at the G1/S transition. Cyclin A2 is ubiquitously expressed but cyclin A1 expression is confined to germ cells and early embryos (Sweeney *et al.*, 1996). Overexpressing cyclin A delays anaphase in human and *Drosophila* cells, and has also been observed to inhibit the formation of a stable metaphase plate (Sigrist *et al.*, 1995; den Elzen and Pines, 2001; Geley *et al.*, 2001). In this regard it is interesting that mammalian oocytes, which express Cyclin A2 and A1, do not form stable kinetochore-microtubule attachments until shortly before anaphase (Brunet *et al.*, 1999). This raises the possibility that cyclin A might function to prolong the M phase of MI until the spindle has sufficient time to migrate to the oocyte cortex in order to form a PB.

Findings from our lab and others (Touati *et al.*, 2012) indicate that Cyclin A2 is required for deprotection of cohesin during anaphase. Functional disruption of cyclin A inhibits sister chromatid separation during anaphase of MII.

Intriguingly, we found that non-degradable cyclin A resulted in premature separation of sisters during MI (Touati *et al.*, 2012). Together these data indicate that cyclin A may play a key role in the step wise removal of cohesin in mammalian oocytes.

1.7.2. The Anaphase Promoting Complex

The transition from metaphase to anaphase requires the inactivation of cyclin B-Cdk1. This is achieved through the degradation of its cyclin binding partner, cyclin B1 by the proteasome after it has been ubiquitinated by the APC/C (Zachariae and Nasmyth, 1999; Acquaviva and Pines, 2006; Peters, 2006). Cdk1 is then thought to undergo a conformational change that prevents ATP hydrolysis and the access of protein substrates to the active site, thereby resulting in its inactivation (Jeffrey *et al.*, 1995). The APC also targets securin for degradation thereby releasing the cohesin cleaver separase (Nasmyth, 2001). APC/C substrate specificity is mediated by co-activator proteins that associate with it during specific periods of the cell cycle. The best studied are Cdc20 and Cdh1 (Zachariae and Nasmyth, 1999; Acquaviva and Pines, 2006;

Peters, 2006). The transient associations with these co-activators are tightly regulated to determine when in the cell cycle the APC/C is active. Motifs important for substrate recognition by the APC/C are the Destruction box (D-box) and the KEN-box. The D-box drives ubiquitination by APC/C^{Cdc20} in substrates such as cyclin B and securin. The KEN-box is recognised by APC/C^{Cdh1}, for example in Cdc20. Cdh1 can however also recognise the D-box (Peters, 2006). In vertebrate somatic cells, cyclinA-Cdk2 inhibits APC/C^{Cdh1}. However, cyclin A is also a substrate of APC/C^{Cdc20} and APC/C^{Cdh1} (Peters, 2006). Cyclin A degradation also depends on the levels of the APC-specific ubiquitin-conjugating enzyme (E2) UBCH10, which is itself degraded by APC/C^{Cdh1} during G1 (Rape and Kirschner, 2004). APC/C^{Cdh1} may initiate its own inactivation by ubiquitinating UBCH10, leading to stabilisation of cyclin A, and subsequent inhibition of APC/C^{Cdh1} by cyclin A-Cdk2 (Rape and Kirschner, 2004) (Figure 1.18).

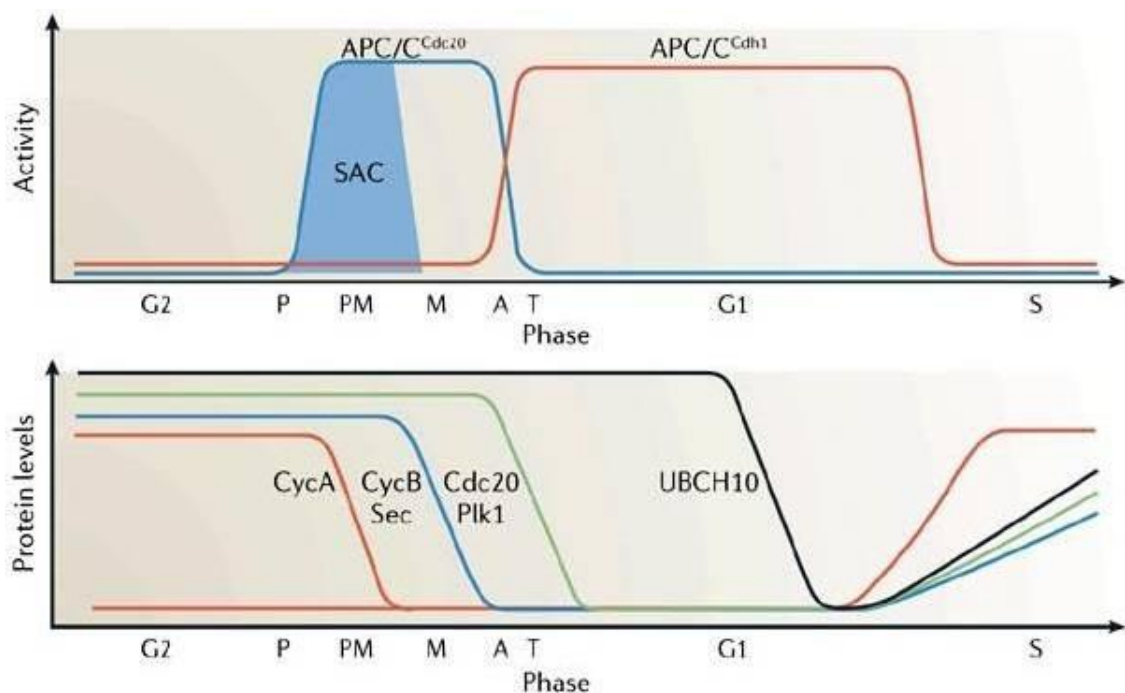


Figure 1.18 - Schematic for securin APC/C activity and associated substrate protein levels in mitosis. APC/C^{Cdc20} is thought to be assembled in prophase (P) and initiates the degradation of cyclin A (CycA) in prometaphase (PM). Proteolysis of cyclin B (CycB) and securin (Sec) also depends on APC/C^{Cdc20} but is delayed until metaphase (M) by the SAC. During anaphase (A) and telophase (T), APC^{Cdh1} is activated, contributes to the degradation of securin and cyclin B, and mediates the destruction of additional substrates such as Plk1 and Cdc20, which leads to the inactivation of APC/C^{Cdc20}. In G1 phase, APC/C^{Cdh1} mediates the destruction of the ubiquitin-conjugating (E2) enzyme UBCH10, and thereby allows for the accumulation of cyclin A, which contributes to the inactivation of APC/C^{Cdh1} at the transition from G1 to S phase (image from (Peters, 2006)).

In mitosis, a period of low Cdk1 activity is required during telophase of G1 in order for pre-replicative complexes to form on origins of replication, followed by an increase in Cdk1 levels for DNA synthesis to occur (Peters, 2006). The high levels of Cdk1 activity inhibit Cdh1 association with the APC/C, so it is Cdc20 instead which is required for APC/C activity at metaphase. APC/C^{Cdc20} is inhibited by the SAC until all chromosomes establish stable bipolar kinetochore-microtubule attachments at metaphase. Cdh1 can only activate the APC/C when APC/C^{Cdc20} has decreased the Cdk1 activity by targeting cyclin B1 for degradation. The drop in Cdk1 activity then promotes the formation of APC/C^{Cdh1} which maintains the cyclin instability and enables pre-replicative complexes to assemble. APC/C dephosphorylation leads to disassembly of APC/C^{Cdc20}, and Cdc20 itself becomes a substrate of APC/C^{Cdh1}. APC/C^{Cdh1} is inactivated later at the G1-S transition for cyclins to reaccumulate and DNA replication to be initiated (Figure 1.18 and Figure 1.19A) (Peters, 2006).

During meiosis, the inactivation of Cdk1 at the MI to MII transition is highly transient. Cyclin B-Cdk1 must be lowered enough for the disassembly of the MI spindle, but kept high enough to repress the initiation of DNA replication between the two meiotic divisions. Separase must also be activated twice, once in MI and again in MII. This requires specialised regulation of the APC/C (Peters, 2006). Cdc20 levels peak in both MI and MII suggesting it is important for both divisions (Salah and Nasmyth, 2000), but the role of Cdh1 is not entirely clear. APC/C^{Cdh1} has a function in maintaining prophase arrest in mouse oocytes (Reis *et al.*, 2006). It has also been proposed that APC/C^{Cdh1} has a role after GVBD in mouse oocytes (Reis *et al.*, 2007). Depletion of Cdh1 in GV oocytes, promotes accelerated progression through MI, resulting in premature anaphase and non-disjunction. Cdc20 is also depleted after GVBD in these oocytes in a Cdh1 dependent manner (Reis *et al.*, 2007). This proposes that APC/C^{Cdh1} is required to prolong prometaphase by the degradation of Cdc20, which then needs to re-accumulate for the proper degradation of cyclin B and securin, allowing time for successful alignment of homologues at the metaphase plate (Figure 1.19B).

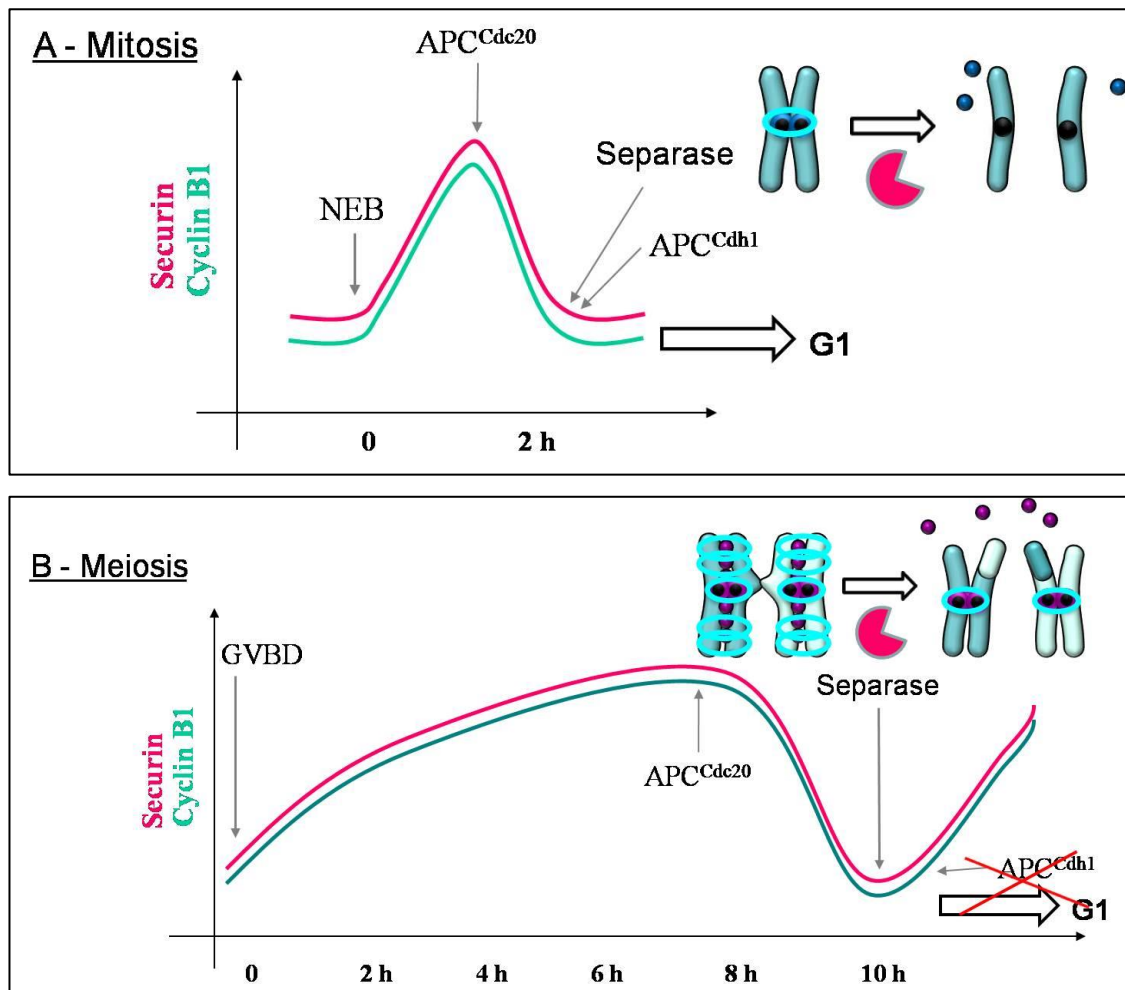


Figure 1.19 - Schematic of securin and cyclin B1 degradation and separase activation in mitosis and meiosis. (A) After nuclear envelope breakdown (NEB) securin and cyclin B1 levels increase. Shortly before anaphase they are targeted for degradation by APC^{Cdc20}. This allows separase to be released to be able to cleave the mitotic cohesin component Scc1 and allow segregation to occur. The APC^{Cdh1} is then activated to degrade Cdc20 and cyclin B, thereby allowing pre replicative complexes to form. APC^{Cdh1} is then later inactivated to allow DNA synthesis to occur.

(B) After GVBD securin and cyclin B1 levels slowly increase. Shortly before anaphase they are targeted for degradation by APC^{Cdc20}. This allows separase to be released to be able to cleave the meiotic cohesin component Rec8 at the chromosome arms, and allow homologue segregation to occur. Cyclin B1 and securin levels quickly increase again, and the APC^{Cdh1} is not activated (in contrast to mitosis). This ensures that separase is inactivated again and that DNA synthesis is repressed during the transition between the two meiotic divisions.

1.8. Regulation of the APC/C by the spindle checkpoint

Tight regulation of APC/C activity by the SAC is essential, as inappropriate activation of the APC/C could cause catastrophic errors in cell cycle progression. The SAC ensures that sister chromatids are evenly divided by inhibiting APC/C-mediated degradation of securin and cyclin B by APC/C^{Cdc20} until each sister kinetochore is correctly attached and under tension at the metaphase plate (Musacchio, 2011; Lara-Gonzalez *et al.*, 2012; Sun and Kim, 2012). The presence of a single unattached kinetochore is sufficient to delay anaphase. Interestingly, although cyclin A is an APC/C substrate, its degradation is SAC independent and starts as soon as the APC/C is activated at NEBD (den Elzen and Pines, 2001; Geley *et al.*, 2001). This indicates the SAC function is directed towards selected substrates only.

The SAC inhibits anaphase in response to improperly attached kinetochores by inactivating Cdc20, thereby preventing degradation of cyclin B1 and securin. The main mediators of this checkpoint are Mad2 and BubR1, which interact directly with APC/C^{Cdc20} to inhibit its ubiquitination activity (Acquaviva and Pines, 2006; Peters, 2006). Mad2 can either bind directly to Cdc20, or to another protein essential for checkpoint function Mad1, which then recruits the Mad2 to unattached kinetochores and can then function as the template for Mad2-Cdc20 interactions (Acquaviva and Pines, 2006; Peters, 2006).

Recent studies indicate that the SAC also functions to ensure timely degradation of securin and cyclin B and proper segregation of homologues during MI. It was found that depletion of Mad2 in oocytes accelerated the onset of anaphase by about 2 hours and resulted in an increased incidence of aneuploidy (Homer *et al.*, 2005). Over expression of Mad2 also inhibits homologue disjunction (Homer *et al.*, 2005). Depletion of Bub1 in oocytes results in a similar defect (McGuinness *et al.*, 2009). These findings indicate that the SAC mediates accurate segregation of homologues by ensuring timely degradation of cyclin B and securin by the APC/C^{Cdc20}. However, it is unclear whether the mechanisms of SAC function are the same as in mitosis. For example, degradation of cyclin B and securin commences 2-3 hr before the onset of anaphase (Herbert *et al.*, 2003; Homer *et al.*, 2005; McGuinness *et al.*,

2009), whereas stable kinetochore-microtubule attachments are not formed until very shortly (14 min) before anaphase (Brunet *et al.*, 1999).

With all these different meiotic events needing to be precisely choreographed by the oocyte, and these are just what have so far been uncovered, it is hardly surprising that when put under the additional strain of time, the process of accurately halving the chromosome number can begin to falter and fall apart.

This work is focussed on investigating and further highlighting the problems of female reproductive ageing. Progress in this field has been hampered by the absence of a convincing animal model. My work is therefore focussed on (i) Comparing the effect of female ageing on fertility and germ cell depletion in humans and mice (ii) Using the mouse model to uncover the cellular and molecular basis for the age-related increase in chromosome segregation errors in oocytes from older females.

Chapter 2. Aims

I. Reproductive ageing and fertility

1. To examine the relationship between oocyte number and oocyte quality using implantation and clinical pregnancy rates, and explore the rate of reduction of each with advancing female age.
2. To study the relationship between oocyte number and fertility in mice of the C57BL/*Icrfa*^f strain, to elucidate whether it is a suitable model for human female ageing.

II. Maternal-age related segregation errors

3. To detect and characterise the incidence of age-related segregation defects by live cell imaging of oocytes from C57BL/*Icrfa*^f females.

III. Mechanisms underlying anaphase defects

4. To determine whether chromosomal cohesin is reduced with female ageing.
5. To investigate the possible methods of cohesin loss, examining the role of the cohesin protector, Shugoshin, in regulating the chromosomal association of cohesin during ageing and progression through MI.

Chapter 3. Methods

3.1. Mouse Strains

Mice were obtained from a long lived colony of the C57BL/1crfa^t strain, housed at the Institute of Ageing and Health, Newcastle University. Female mice were taken between 2 and 14 months of age.

The CD1 mouse colony was housed at the Institute of Genetic Medicine, Newcastle University. Female mice were taken between 2 and 4 months of age.

Generation of the Smc1 β ^{-/-} mice was done in the Jessberger lab, Dresden (Revenkova *et al.*, 2004).

All animal work was carried out under a licence issued by the Home Office and following their regulations.

3.2. Oocyte Harvest

The aged mouse strain, C57BL/1crfa^t, were super-ovulated by injection of 7.5 international units of pregnant mare serum gonadotrophin (PMSG) (Sigma, G4527) 48 hours prior to oocyte retrieval. The CD1 strain mice were not super-ovulated.

Female mice were killed by cervical dislocation before dissection of the ovaries. Ovaries were transported to the lab in pre-warmed M2 media (Sigma, M7167) and dissected in a 60x15mm diameter culture dish (BD Biosciences, 351016) under a microscope in a heated laminar flow hood. Oocytes were released by puncturing the ovarian antral follicles using sterile insulin needles. This was done within M2 media supplemented with 100 μ M isobutylmethylxanthine (IBMX) (Sigma, I7018) to prevent the onset of GVBD prior to experimental treatments. IBMX prevents resumption of meiosis by maintaining elevated

cyclic adenosine monophosphate (cAMP) (Sigma, A6885) concentrations within the oocytes.

GV stage oocytes of sufficient quality were selected for use in experiments. These oocytes were spherical, free of cumulus, and at least 67 μ m diameter with a centrally positioned GV. All oocyte handling was carried out using glass denudation pipettes (BioTipp, 14306). Oocytes were stored in plastic 35x10mm diameter culture dishes (BD Biosciences, 353001) within micro drops of M2+IBMX media, overlaid with filtered mineral oil (Sigma, M8410). These dishes were kept at 37°C until ready for use.

3.3. Oocyte Culture

Plastic 35x10mm diameter culture dishes were set up of 5x 40 μ l drops of G-IVF Plus media (Vitrolife, 10134) overlaid with filtered mineral oil. These dishes were pre-equilibrated in a 5% CO₂ Heraeus incubator at 37°C for at least 4hrs prior to use. Oocytes to be matured were washed thoroughly through 4 micro-drops of G-IVF culture media to remove any IBMX before being left in a fresh drop to mature in the 5% CO₂ 37°C incubator. This allows for synchronous resumption of MI. After 1-2hrs oocytes were scored for GVBD, marked by the absence of the GV. Those oocytes which had undergone GVBD within the first 2hrs of incubation were matured overnight and scored the next morning for PB extrusion.

3.4. Microinjection

Oocytes were injected with message RNA (mRNA) for the expression of fluorophore-tagged proteins.

Glass microinjection pipettes were made from borosilicate glass capillaries (O.D: 1.0mm, I.D: 0.50mm, 10cm length, Harvard Apparatus, GC100T-10), using a P-97 micropipette puller with a 2mm box filament (Sutter Instruments). The settings used were: heat 473; pull 90; velocity 70; time 150 and pressure

200. The end of the pipette was then angled to 30° using an MF-900 Microforge (Research Instruments).

A small section of glass capillary was cut to approximately 2cm using a diamond scribe. This was mounted onto a glass microscope slide with wax and referred to as the loading column. The capillary was loaded with 0.5µl of approximately 2µg/µl mRNA, either mixed with 0.5µl of a second mRNA and 0.2µl of injection buffer, or with 0.7µl of injection buffer (refer to 3.19), to make the concentration of each mRNA approximately 1µg/µl. The column was kept on an ice block until loading to avoid evaporation.

Microinjections were performed on a Nikon TE300 inverted microscope fitted with Narishige MMN-1 micromanipulators and IM300 pressure microinjector. A holding pipette (Hunter Scientific) was attached to an SAS air syringe (Research Instruments) on one side, and an injection pipette on the other.

The injection pipette was attached to the micromanipulators with the balance pressure at zero. The injection column was placed on the microscope stage and the injection pipette tip was gently broken open on the end of the loading column. This was then moved into the mRNA solution. Intake was first observed by capillary action, and then it was filled up to the 30° bend using the standard fill programme. After loading, a small amount of positive pressure was set on the balance in order to prevent oil and media being taken into the pipette from the injection dish. The injection pipette was lowered into an empty drop of the injection dish in order to test the injection size and adjust the balance as necessary. The meniscus of the pipette was continuously monitored and maintained through the injections by adjustments in the balance pressure.

Prophase arrested GV oocytes were transferred to a plastic 50x9mm diameter easy grip petri dish with a tight fitting lid (BD Biosciences, 351006) containing 5µl micro drops of M2+IBMX under filtered mineral oil. Five to ten oocytes were placed into each drop. The oocytes were orientated and held in place using gentle suction through the holding pipette. The injection pipette was introduced opposite the holding pipette, vertically into each oocyte, breaking through the zona pellucid and oolemma and avoiding the GV. Oocytes were injected with approximately 1pg of mRNA solution. This was observed as a cytoplasmic disturbance approximately the same size as the nucleolus. The balance

pressure was equalised before the injection pipette was removed at the exact same angle of entry.

Oocytes were left in the injection dish for at least 1hr to allow recovery before any further manipulation or imaging.

3.5. Fluorescent Construct Cloning

All fluorescent constructs for mRNA synthesis were either cloned by myself or were gifts from collaborators (Table 3.1).

Most constructs made were from a pRN3 plasmid backbone (Figure 3.1). pRN3 contains a T3-RNA polymerase transcription promoter site, a 5' globin untranslated region (UTR) to promote stability of RNA transcripts, a series of restriction sites for common restriction enzymes, a globin 3'-UTR and a poly(A) encoding sequence to enhance translation. The coding sequence for a fluorescent protein was inserted between the cloning site for the gene of interest and the 3'-UTR for most fluorescent constructs used. The gene of interest was either sub-cloned or amplified using a polymerase chain reaction (PCR) from a mouse oocyte cDNA library (constructed using the SMART PCR cDNA Synthesis Kit (Clontech, 634902)), and inserted into the plasmid by restriction digest and ligation. The cloning was confirmed by sequencing (The Sequencing Service, Dundee).

Name	Method	Origin	Fluorescence Tag
pRN3	Empty cloning vector	Mark Levasseur	N/A
pGFP	Empty GFP vector with pRN3 backbone.	Mark Levasseur	Green fluorescent protein (GFP)
pRFP	Empty RFP vector with pRN3 backbone. Primers designed for RFP, 5'EcoRI (incorporated Sall), 3'NotI. Primed from H2-RFP. Cut with EcoRI+NotI. Ligated to similarly cut empty pRN3 vector.	Lisa Lister	Red fluorescent protein (RFP)
pYFP	Empty YFP vector with pRN3 backbone.	Mark Levasseur	Yellow fluorescent protein (YFP)
Histone H2B-RFP	EcoRI+ XbaI cut H2B-RFP into similarly cut pRN3 vector.	Mark Levasseur	RFP
Sgo2 (siRNA resistant)-Venus	pVenus with Sgo2 (resistant to Sgo2 siRNA sequence) insert. pCS2 backbone.	Olaf Stemmann	Venus (brighter version of YFP)
Tubulin-GFP	Primers designed for TUBB 5'EcoRI 3'Sall. Primed from TUBB pCMV-SPORT6. Cut with EcoRI+Sall. Ligated into similarly cut pGFP vector.	Lisa Lister	GFP
Securin-YFP	Primers designed for Securin 5'EcoRI 3'BamHI. Primed from pRN3 Mcy2 Securin vector. Cut with EcoRI+BamHI. Ligated to EcoRI+BglII cut pEYFP-N1 to generate C terminal YFP-tagged Securin. Cut Securin YFP from	Katja Wassmann	GFP

	this with EcoRI+NotI and cloned into similarly cut pRN3.		
Cyclin B-GFP	pGFP with CyclinB insert.	Mark Levasseur	GFP
CyclinB Δ 90	pRN3 with CyclinB Δ 90 insert.	Mark Levasseur	No tag

Table 3.1 - Plasmids designed for mRNA synthesis.

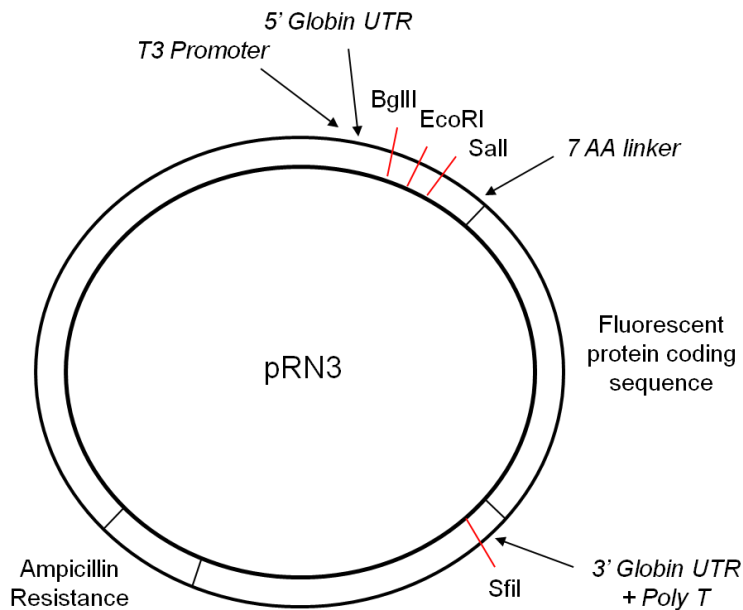


Figure 3.1 - Plasmid map for constructs based on a pRN3 plasmid backbone.

pRN3 contains a T3-RNA polymerase transcription promoter site, a 5' globin untranslated region (UTR), a series of restriction sites for common restriction enzymes, a globin 3'-UTR and a poly(A) encoding sequence. The coding sequence for the gene of interest was inserted between the three restriction sites, minus its STOP codon. The coding sequence for a fluorescent protein was inserted between the cloning site for the gene of interest and the 3'-UTR.

3.6. Message RNA Construction

Plasmid DNA was linearised by enzymatic digest, downstream of the insert to be transcribed. Capped Message RNA (mRNA) was synthesised using the mMessage mMachin (Ambion), either the T3, T7, or SP6 kit, depending on the RNA polymerase promoter site on the plasmid. The resulting mRNA was diluted to approximately 2 μ g/ μ l with sterile nuclease free water.

3.7. Small Interfering RNA

Sgo2-1 siRNA sequence (Invitrogen, sequence design from the Watanabe lab, Japan (Lee *et al.*, 2008)): GGATAAAGACTTCCCAGGAACTTTA

GV stage oocytes were isolated and co-injected (refer to 3.4) with Histone mRNA and a 1uM concentration of Sgo2 siRNA (0.5µl 2µM Sgo2 siRNA + 0.5µl 2µg/µl Histone H2B-RFP). Control oocytes were co-injected with Histone mRNA and a Stealth Negative Control (Invitrogen) of the same concentration. Oocytes were allowed to recover 1hr before being washed thoroughly through 4 micro-drops of G-IVF culture media, supplemented with 50µM IBMX and 50µM cAMP. They were then incubated in a fresh drop for 21hrs in the 5% CO₂ 37°C incubator. Following this incubation, oocytes were washed thoroughly through 4 micro-drops of un-supplemented G-IVF culture media to remove any IBMX and cAMP, before being left in a fresh drop to mature in the 5% CO₂ 37°C incubator. GVBD was monitored and chromosome spreads were performed at the appropriate time points. This protocol gave complete knockdown of Sgo2 when tested at GVBD+3hrs, which persisted until at least GVBD+18-23hrs.

3.8. Chromosome Spreads

The PFA fixation solution was made by dissolving 0.25g of Paraformaldehyde (PFA, Merck, 104005) in 22.5ml of MilliQ (MQ) water in a 50ml falcon tube (Starlab, E1450-0200). In order to dissolve the PFA 4µl of 10M Sodium Hydroxide (VWR, 102524X) was added, and the solution was incubated at 60°C for 20mins, or until dissolved. The solution was then cooled to room temperature before adjusting the pH to 9.2 with 50mM boric acid (Sigma, B6768). This was prepared on the day of chromosome spreads and just before use 175µl of 20% Triton X-100 (Sigma, T8787) and 150µl of 0.5M DTT (Sigma, D9163) were added. The solution was mixed thoroughly and filter sterilised.

Humidified slide chambers were made by taping two glass capillaries (Harvard Apparatus) to the bottom of 100x20mm Petri dishes (SLS, 351005), and placing dampened paper towel to each side. Polysine slides (Fisher Scientific, MNJ-

800-010F) were labelled and a guide line was drawn onto the back of each slide. These were placed into the PFA solution just before use. Oocyte manipulations were carried out using a glass denudation pipette and a bench top microscope. Chromosome spreading is highly temperature dependent so in cooler weather heaters were used to ensure an adequate 'room temperature' was maintained.

Three separate 35x10mm culture dishes were set up, the first containing 2x 40µl drops of acid tyrodes (refer to 3.19), the second containing 4x 40µl drops of warmed M2 media, and the third 2x 40µl drops of 0.5% sodium citrate (VWR, 102425M).

Up to 10 oocytes were transferred at a time from their culture dishes to the first drop of acid tyrodes solution, washed, and moved to the second drop. The oocytes were left for approximately 2mins, or as long as it took for the zona pellucid to no longer be visible. Oocytes were washed thoroughly through the four M2 drops and then washed through the first sodium citrate drop before being left in the second drop for exactly 2min. Just before the end of the 2min incubation the PFA coated slide was taken from the PFA, the excess tapped off onto a paper towel, and placed into a humidified chamber. The oocytes were picked up from the sodium citrate in a minimal volume of media. The humidified chamber containing the slide was moved under the microscope, focused on the guide line, and the oocytes were expelled slowly and in as little media as possible along the line. Swelling and bursting of the oocytes was observed and a rough indication of placement was marked on the slide. The slides were then dried in the closed humidified chamber overnight.

After drying a box was drawn around the spread oocytes using an Immedge Hydrophobic barrier pap pen (Vector Laboratories, H-4000). This was left 30min to dry and then the slides were washed 2x 2min in a coplin jar containing a H₂O+Photoflo (Silverprint, 90662) solution, then 2x 2min in PBS (Melford Laboratories, P3206). The slides were left at 4°C in the final PBS wash until ready to stain. The slides could be left for a few months but the sooner the slides were stained the better the image quality.

3.9. Chromosome Spread Immunofluorescence

A humidified slide staining tray was made by wrapping a large plastic dish in tin foil and sticking down four rows of 1ml serological pipettes with dampened paper towel down each side. Slides were removed from the PBS, the excess tapped off onto a paper towel, and placed in the slide tray.

A blocking solution was pipette into the pap pen box (100-200 μ l depending on the size of the box) and left for 1hr. The blocking solution depended on the antibodies to be used, but was most commonly a 10% donkey or goat (Stratech Scientific Limited, 017-000-121 and 005-000-121 respectively) serum solution in PBS+0.05% Triton and Tween (Sigma, P9416).

After the hour the block solution was carefully pipette off from the corner of the pap box. The primary antibody solution (diluted in blocking buffer) was added in its place. The slides were left overnight in the chamber at 4°C.

The next morning the primary antibody was carefully pipette off (and saved at 4°C for further use), and the slides were put through a series of washes in a plastic screw top coplin jar on a shaking platform. These were 10min in PBS+0.4% Photoflo, 2x 10min PBS+0.01% Triton X-100, 10min in PBS+0.4% Photoflo, then rinsed for 2min in PBS. The excess was tapped off onto a paper towel and the slides were placed back in the humidified slide tray. The secondary antibody, again diluted in blocking solution, was added to the pap box, and left at room temperature for 1hr. It is very important that from this point on any exposure to light is minimised.

After the hour the secondary antibody was removed and discarded. The same series of washes were repeated as for after the primary antibody incubation. Excess PBS was tapped off onto a paper towel and the slides were placed back in the slide tray. A small drop of VectaShield DAPI Mountant Media (Vector Laboratories, H-1200) was placed onto a zero thickness coverslip (SLS) just larger than the size of the pap box. The coverslip was then gently lowered onto the slide to avoid air bubbles becoming trapped. Rubber glue was used to seal around the edges of the coverslip. The slides were kept at 4°C until ready to image. Slides could be left for a few months but the sooner the slides were images the better the image quality.

Chromosomes were found under the 10x magnification, visualised using the DAPI staining. Images were then taken under the 100x magnification.

Antibody dilutions are shown in Table 3.2.

Primary	Source	Dilution	Secondary	Source	Dilution
CREST	Cellon HCT-0100	1:50	Goat α - Human Cy5	Jackson Immuno 109-175- 003	1:400
Rec8	Christer Hôôg	1:100	Donkey α - Guinea Pig TRITC	Jackson Immuno 706-025- 148	1:400
Sgo2	Yoshinori Watanabe	1:50	Donkey α - Rabbit Alexa 488	Invitrogen A21206	1:800
Myc	Millipore 05-724	1:100	Donkey α - Mouse 555	Invitrogen A31570	1:800
Separase	Abcam ab3762	1:100	Donkey α - Rabbit Alexa 488	Invitrogen A21206	1:800

Table 3.2 - Antibody dilutions.

3.10. Whole Oocyte Immunofluorescence

Oocytes were cultured to the required stage of maturation before fixing for 30min at room temperature in 2% PFA + 0.1% Triton, in a 4 well dish. Oocytes could at this stage be stored at 4°C in PBS + 0.1% Poly(vinyl alcohol) (PVA, Sigma, P8136) for staining at a later date. Oocytes were washed on a shaking platform, 3x 5min in Wash Buffer (9ml PBS, 1ml 1% PVA, 25 μ l 20% Tween and 25 μ l 20% Triton) before incubating 1hr in Block (usually 10% serum in Wash Buffer). Oocytes were then incubated overnight at 4°C in a primary antibody

solution diluted with Block. The oocytes were washed 3x 5min in Wash Buffer before incubating 1hr in a secondary antibody solution diluted with Block. Following the final 3x 5min washes the oocytes were incubated in 1:500 Hoechst (Sigma, 861405) in PBS for 2min, before washing through fresh PBS. The oocytes were left in PBS until ready to image.

3.11. Wax Embedding Ovaries

Following dissection, the ovaries were rinsed in PBS, and incubated overnight in 4% PFA at 4°C. The ovaries were then rinsed again in fresh PBS, and put through a series of washes in a 12 well plate (Helena Biosciences, 92012t) on a shaking platform. These were 30min in 50% ethanol, 2x 30min 70% ethanol, and 30min in 95% ethanol. The ovaries were then transferred into a glass bijou (SLS, TUB1236), and washed for 2x 30min in 100% ethanol. They were then washed for 2x 10min in HistoClear (Fisher, HIS-010-010S), 15min in 50/50 HistoClear and Paraffin Wax (VWR, 361336E), then 3x 20min with wax. The wax steps were performed in a hot block to prevent it solidifying. A pasture pipette was used to place each ovary with a pool of wax into separate plastic 7x7x5 dispomoulds (CellPath, GAD-0702-02A). An embedding ring (CellPath, GAB-0102-10A) was placed on top of each mould, and then filled to the top with wax. After 5min they were transferred to 4°C for at least 30min before sectioning.

3.12. Sectioning

The dispomould was removed and the wax block containing the ovary was carefully trimmed using a scalpel, into a topless pyramid shape. This was clamped into the microtome, and 8µm sections cut. The ribbons were collected in the order they were sectioned. Water was placed onto a HistoBond (Griffith & Nielson, GNHISTOTF) glass slide on a 37°C hot plate. The sections were carefully transferred, in order, onto the slide. After 5min the water was gently removed from the slide with a pasture pipette, and any excess was tapped off

on a paper towel. The slides were then placed in a rack, and left at 37°C overnight to allow the sections to properly adhere to the slides. They were kept at room temperature until ready to stain.

3.13. Haematoxylin and Eosin Staining

Using a slide rack and trough, the slides were washed 2x 10min in Histoclear. The slides were then rehydrated by a series of 2min ethanol washes, 2x 100%, 90%, 70%, 50%, then rinsed in dH₂O. Slides were then placed in Haematoxylin (Fisher, SDLAMB/230-D) for 10min. Slides were rinsed in dH₂O (5min or less) until the sections turned blue, before leaving under gently running tap water for an additional 5min. Slides were quickly dipped in a solution of 1% HCl in 70% ethanol, before leaving under running water again, 5min or less, until the sections turned blue. After incubation in 1% Eosin in dH₂O (Fisher, SDLAMB/100-D) for 4min, the slides were placed under running water until clear. The slides were then dehydrated by a series of 1min ethanol washes, 50%, 70%, 90% and 2x 100% (using a clean, dry trough for the final and subsequent washes), followed by 2x 10min in Histoclear before mounting cover slips. Slides were left at least 2hrs before imaging. Nuclei appear blue/black, and the cytoplasm varying shades of pink.

3.14. Microscopy

Timelapse and fixed immunofluorescence imaging was performed using a Nikon TE2000-U inverted microscope. This was fitted with automated excitation and emission filter wheels and shutters; and a Prior Proscan controller for the focus and motorised stage (Prior Scientific). Excitation source was a Xenon Arc Lamp. Also fitted were 10x, 20x, 40x, and 100x Nikon Plan Fluor objectives; a Hamamatsu power supply and a Photmetrix CoolSnap HQ digital camera (Roper Scientific). Filter blocks were used for viewing DAPI (Nikon UV-2A); Rhodamine (Nikon G2-A); GFP (Nikon B-2A); Cy5 (Chroma 41008); GFP/RFP (Chroma 51022); and CFP/YFP/RFP (Chroma Tech Corporation 86006). A heated chamber (Solent) was attached to the microscope frame and custom

made CO₂ chamber (Medical Physics, Newcastle University) was made for timelapse imaging.

Fixed immunofluorescence imaging was also performed on a Zeiss Axio Imager Z1 microscope fitted with a Zeiss ApoTome 2. Images were captured using an EC Plan Apochromat 63x/1.4 Oil DIC objective and a Zeiss AxioCam HRm Rev3 camera, in combination with the Axiovision 4.8 software package. Excitation source was a Mercury short arc HBO® 100 W/2 lamp (Osram, Germany).

3.15. Timelapse Imaging

To image overnight by timelapse microscopy oocytes were placed in a glass bottom dish (Thistle Scientific, IB-81158) containing a central 2µl micro-drop of pre-equilibrated G-IVF under filtered mineral oil maintained at 5% CO₂ and 37°C. Approximately 20 oocytes were imaged at a time, carefully arranged in a 4x5 rectangle.

The dish was secured in a metal holding frame and maintained at 37°C 5% CO₂ through the modified stage incubator thought imaging. Images were collected on a Z-plane of 5 steps of 7.5µM every 20 minutes for bright-field and each fluorophore required using the 20xNikon Fluor oil immersion objective at 1x1 binning and 100-200ms exposure times.

To image fixed oocytes they were placed in glass bottom dish (Intracel, HB-3522St) containing a central 2µl micro-drop of PBS under mineral oil.

3.16. Metamorph analysis of live cell microscopy

A timelapse series for each wavelength was assembled using the multidimensional acquisition tool in Metamorph (Molecular Devices). The best focus for the chromosomes was selected for each oocyte by tracking the histone H2-RFP chromosome movements on the RFP wavelength, and

choosing the plane at each time point where they were best visualised. Any chromosome or spindle associated proteins being imaged at the same time were analysed using the same planes of focus as the chromosomes. Any cytoplasmic proteins were analysed on the central plane of focus of the oocyte. Circular regions were drawn around the oolemma of each oocyte and the fluorescent values for each selected focus plane at each time point were logged into Excel using the 'Graph Intensities' function. Several background regions were also logged to allow background subtraction in Excel. Background subtracted values were plotted for each oocyte and observed chromosome dynamics were correlated to the degradation patterns of the other observed proteins. The stacks were cropped to individual oocytes and any overlays, montages or movies were created using the Metamorph software.

3.17. Metamorph analysis of chromosome spreads

Metamorph imaging software was used to subtract an equal level of background from the images of interest. An Inclusive Threshold was selected for the CREST image, which was adjusted so it was only localised within the CREST signal. The Auto-Trace function was used to define regions around the thresholded centromeres (Figure 3.2), and four background regions elsewhere on the image. Once defined, these regions were transferred to the image for comparison (i.e. Sgo2). The average fluorescence intensities of the regions were measured using the software, logged onto an Excel sheet, and an average of the background regions was subtracted. This data was then used for fluorescence intensity ratios or co-localisation measurements.

Centromere distance measurements were done on background subtracted images, using the callipers tool to measure the distance between the outermost margins of the centromeres (Figure 3.2).

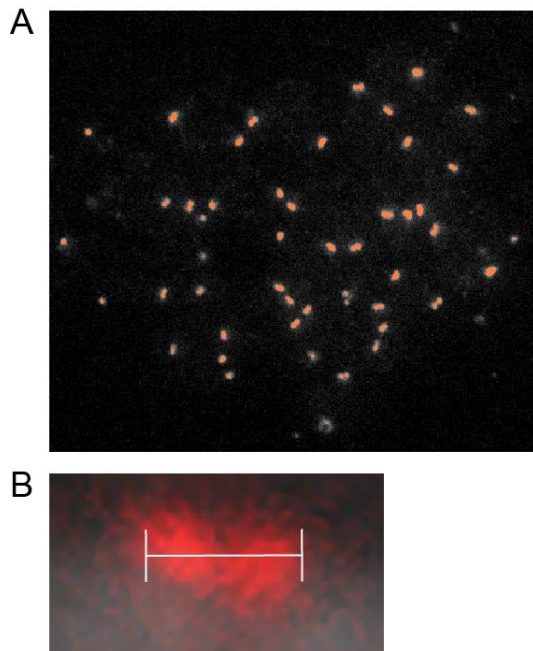


Figure 3.2 - Metamorph analysis functions. (A) Paraformaldehyde chromosome spread prepared at mid prometaphase I (GVBD + 5hrs). Image shows CREST staining (white), thresholded (orange) in order to determine regions for comparative analysis. (B) Image showing the callipers function used to measure the distance between sister centromeres, measuring from the outermost margins of the CREST signals (red).

3.18. Statistical Analysis

Statistical analysis was performed using either Excel or Minitab.

3.19. Stocks and Solutions

20% Triton X-100 - 10ml Triton X-100 to 40ml sterile MilliQ (MQ) dH₂O.

20% Tween 20 - 10ml Tween 20 to 40ml sterile MQ dH₂O.

0.5M DTT - 0.08g/ml sterile MQ dH₂O.

50mM Boric Acid - 0.15g in 50ml sterile MQ dH₂O

0.5% Sodium Citrate - 0.25g NaCl in 50 ml of sterile MQ dH₂O

0.4% Photoflo solution - 4ml of Photoflo in 1L 1xPBS

0.01% Triton solution - 250ul of 20% Triton in 500ml sterile MQ dH₂O.

H₂O + Photoflo solution - 200ul in 400ml of MQ dH₂O.

Acid Tyrodes:

NaCl	0.8g
KCl	0.02g
CaCl ₂ ·2H ₂ O	0.024g
MgCl ₂ ·6H ₂ O	0.01g
Glucose	0.1g
Polyvinylpyrrolidone	0.4g

Made to 90ml with sterile MQ water and dissolved components. Adjusted pH to 2.5 with 5M HCl and made to 100ml with MQ water. Filter sterilised and made aliquots of 1ml. Stored at -20°C.

10M NaOH - 40g in 100ml of MQ dH₂O.

Chromosome Spread Immunofluorescence Wash Solution - 10ml PBS + 25ul 20% Triton + 25ul 20% Tween.

Chromosome Spread Immunofluorescence Block - 100ul serum (goat/donkey) + 900ul Immunofluorescence Wash Solution.

Whole Oocyte Immunofluorescence Wash Solution - 9ml PBS, 1ml 1% PVA, 25µl 20% Tween and 25µl 20% Triton

Whole Oocyte Immunofluorescence Block - 100ul serum (goat/donkey) + 900ul Whole Oocyte Immunofluorescence Wash Solution

Injection Buffer

1M Tris HCL pH 7.5	0.5ml
1M KCL	6ml
In 50ml sterile MQ dH ₂ O	

Chapter 4. Results I – Reproductive Ageing and Fertility

The major determinant of whether a woman will experience difficulty conceiving, either naturally or through the assistance of reproductive technologies, is her age. After pregnancy itself, infertility is the most common reason for a woman between the age of 20 and 45 to seek medical advice. It is defined by the National Institute for Health and Clinical Excellence (NICE) as ‘the failure to conceive after frequent unprotected sexual intercourse for two years’, and it is estimated to affect one in seven couples in the UK (National Health Service (NHS) website - <http://www.hfea.gov.uk/infertility.html>).

Data from the Human Fertilisation and Embryology Authority (HFEA), the UK regulator of fertility clinics and human embryo research, show a decline in female fertility from the age of 30, with a more dramatic decline from around the age of 35. Statistics show that the chance of pregnancy following in vitro fertilization (IVF) treatment declines from 40.2% for women under 35 years of age, to just 20.8% when in their early forties (HFEA Fertility Treatment in 2010, Trends and Figures).

Female reproductive lifespan is curtailed by germ cell depletion which culminates in the menopause at 45-55 years, and by defective segregation of chromosomes during meiosis, resulting in a dramatically increased incidence of infertility, miscarriage and birth defects. The age-related increase in oocyte aneuploidy has a major impact on human reproductive health. Approximately 2–3% of clinically recognised pregnancies among women in their twenties involve trisomic fetuses. However, this dramatically increases to over 35% in women around 40 years of age (Figure 4.1) (Hassold and Hunt, 2001; Hunt and Hassold, 2010).

While it is known that >80% of trisomies involved in birth defects (chromosome 21) and miscarriage (chromosome 16) arise during MI (Hassold and Hunt, 2001), progress in our understanding of the biological basis for the association between female age and MI segregation errors has been remarkably slow.

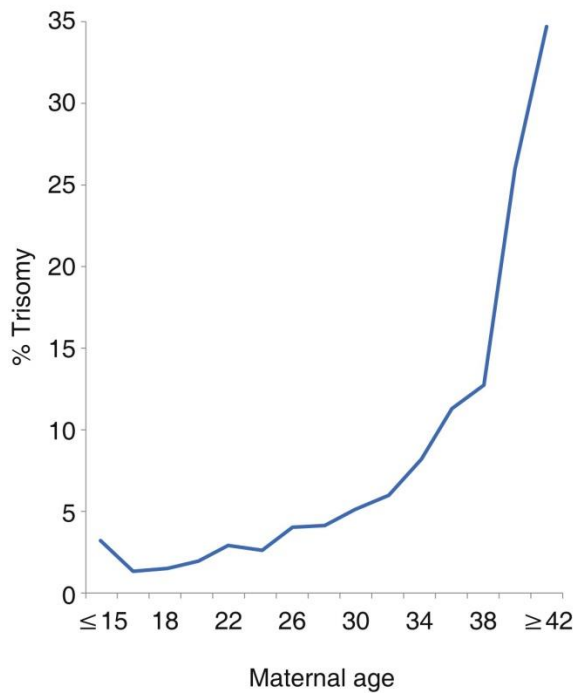


Figure 4.1 - The incidence of trisomy increases with maternal age. Graph showing the correlation between the occurrence of trisomic pregnancies and maternal age. The risk of trisomy rapidly increases after the age of 35 (Hassold and Hunt, 2001; Hunt and Hassold, 2010).

Over the past 20 years the incidence of a Down's syndrome pregnancy has increased by 71% in association with increased maternal age (Morris and Alberman, 2009). However, this is thought to represent just the tip of the iceberg. More complex abnormalities would most likely not be compatible with embryo development to a stage where they would be capable of implanting, resulting in infertility. With the increasing trend for women to delay childbearing (Figure 4.2), elucidating the underlying causes of age-related chromosome segregation errors has become a pressing concern.

A data set was compiled by the HFEA from information relating to 722,067 IVF treatment cycles, in 71 different fertility centres within the UK, between 1991 and 2010. Within this time period, the mean age of women being treated has increased by 1.5 years, from 33.6 to 35.1 years (Figure 4.2A). The data set further revealed a sharp peak in 2010 for women having treatment at 39 years of age (8.3% of the total patient number) (Figure 4.2B). Overall, there has been a 168% increase in the number of women seeking treatment aged 40 and above, and a staggering 400% increase in those over the age of 49.

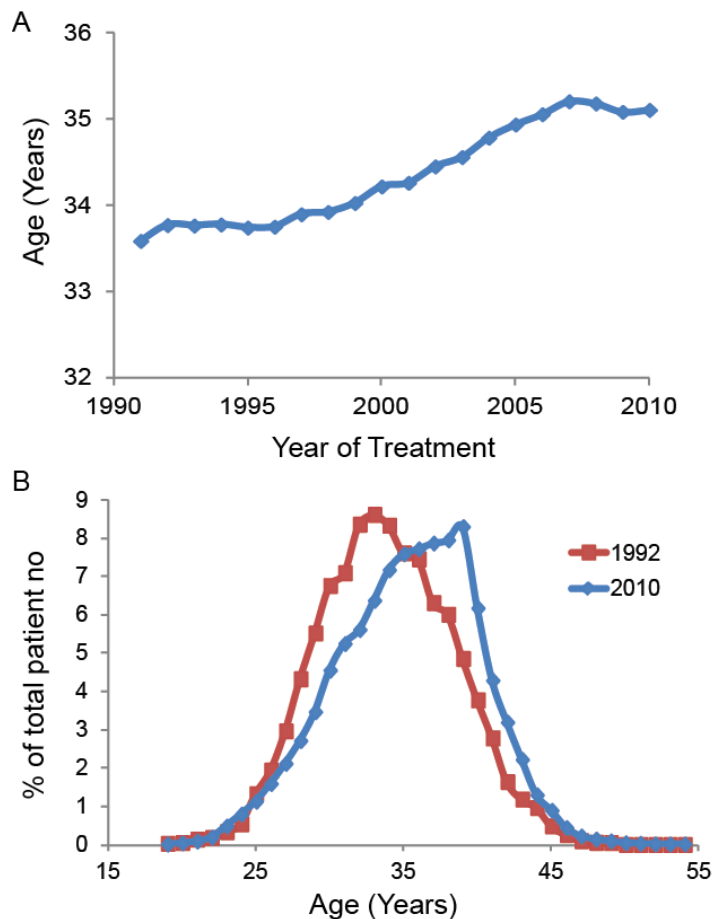


Figure 4.2 - The average age of women undergoing fertility treatment has greatly increased since 1991. (A) Scatter plot representing the mean patient age at egg collection for each year of the HFEA data set (n=722,067 treatment cycles). (B) Plot representing the percentage of the total HFEA recorded treatment cycles represented by each age group in 1992 (n=18,318, red) and 2010 (n=57,643, blue). These graphs are based on data made available on the HFAE website (Data from Fertility Treatment, Trends and Figures).

Human ovaries acquire their lifetime quota of oocytes during foetal life.

However, this pool begins to decline from approximately 7 million human germ cells to only ~2 million remaining at birth. Based on follicle counts of ovarian sections it has been estimated that the pool decreases to only 250,000 by menarcheal age, with just 400 to 500 follicles being ovulated during the reproductive life span (Peters, 1970; Gosden, 1987; Picton, 2001).

This reduction in oocyte number has previously been shown to continue bi-exponentially with age, decreasing more dramatically after 37.5 years (Figure 4.3A) (Faddy *et al.*, 1992). This was a well accepted model as it corresponded to the age related increase in the risk of chromosomal abnormalities and miscarriage (Hassold and Hunt, 2001; Hunt and Hassold, 2010). It further

followed the same pattern as the age related decline in pregnancy rates in women over the age of 35 (Menken *et al.*, 1986). However, realising the biological implausibility of such a sudden acceleration in the rate of decline, re-analysis of the data was more suggestive of a gradual change in rate (Figure 4.3B) (Faddy *et al.*, 1992; Leidy *et al.*, 1998; Faddy, 2000).

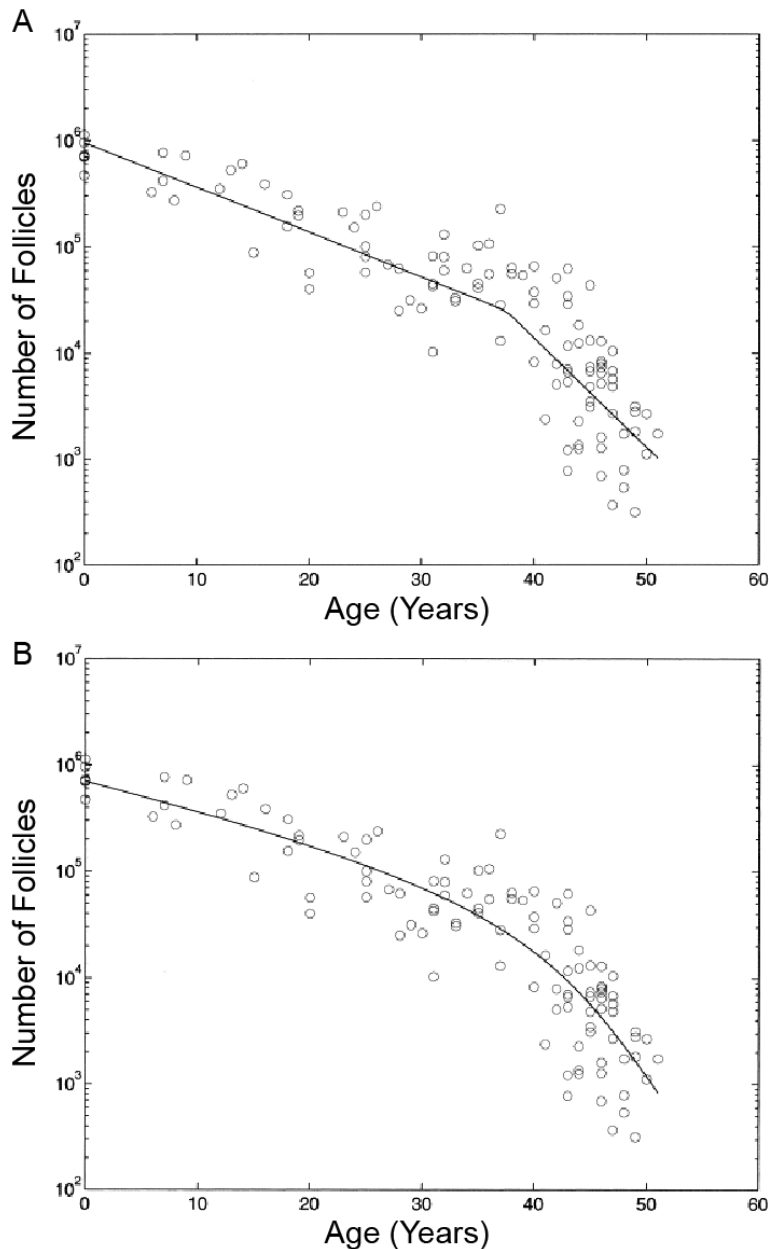


Figure 4.3 - Models of follicular decline in human ovaries. Data from pairs of human ovaries from neonatal age to 51 years of age ($n=110$ from 4 different data sets (Block, 1952; Block, 1953; Richardson *et al.*, 1987; Gougeon *et al.*, 1994) used in (Faddy *et al.*, 1992; Faddy and Gosden, 1996; Faddy, 2000)). (A) Biphasic exponential model of decline showing an increased loss of follicles, and hence oocytes, after 37.5 years of age (Faddy *et al.*, 1992). (B) Revised model, the decay curve a result of performing a differential equation on the data, illustrating a gradual increase in the rate of follicular decline with increasing female age (Faddy, 2000).

The biphasic nature of the previous model was believed to be an artefact produced by the use of a log-linear scale; however, there is a lack of consensus on the best way to model such data (Leidy *et al.*, 1998). There is also the added variability produced by comparing data from multiple studies. Although Faddy observed consistent counts at overlapping ages from each study, incurring errors due to different sampling methods cannot be ruled out.

Studies of non growing (primordial) follicles by ovarian sectioning using modern stereology techniques (Hansen *et al.*, 2008) and antral follicles by ultrasound assessment (Rosen *et al.*, 2010) have also shown that rather than the previously predicted sudden change in the rate of decline, there is instead a gradual acceleration in the rate of follicle loss over time.

Even if the accelerated rate of decline is not occurring at a critical age or follicle number, there is still an undeniable increase in the rate of follicle loss occurring as a woman approaches her late 30's. The coincidence in the timing of the accelerated rate of oocyte depletion and the increased incidence of trisomic pregnancy, raises the possibility that the two are somehow mechanistically linked. Is the cellular ageing of oocytes a chronological phenotype or, have those remaining in the ovary been previously overlooked for ovulation due to a defect, which also predisposition them to aneuploidy? Is there more than one biological clock ticking or is one driving the other?

In this chapter I aim to examine the relationship between oocyte number and oocyte quality using implantation and clinical pregnancy rates, and explore the rate of reduction of each with advancing female age. Analysis is based on data from the HFEA register and from a large series of clinical data collected by the Newcastle Fertility Centre (NFC). As these data are not representative of normal fertility, I also include pregnancy data from a Hutterite population analysed in the same way. Given the scarcity of human oocytes, the mechanistic studies required to uncover the underlying causes of aneuploidy require experiments in an animal model. I study the relationship between oocyte number and fertility in mice of the C57BL/1crfa^t strain, which I used to characterise oocyte chromosome segregation during female ageing in Chapter 5. I also investigate the effect of age on oocyte yield and meiotic competence in the mouse model.

4.1. Depletion of the human female germ cell pool with advancing female age

Based on clinical data from patients of the NFC, I was able to take a closer look at the current trend in the ages of women requiring fertility treatment, and the correlation between oocyte number and female age.

The data set consisted of 4914 treatment cycles from women who underwent fertility treatment between January 2005 and November 2011. Female indicators for treatment included blockage of Fallopian tubes; endometriosis; elevated FSH; ovulatory problems; and polycystic ovary syndrome. Male infertility was due to low sperm count; poor sperm morphology/motility; or azoospermia (no sperm) due to the failed reversal of a vasectomy or other genetic factors. All cycles involved ovarian stimulation using a standard regime of down regulation, using Gonadotropin-releasing hormone (GnRH) analogue, followed by superovulation. This was achieved by injections of Follicle-stimulating hormone (FSH) and Luteinizing hormone (LH) for 10-14 days, followed by injection of human chorionic gonadotropin (hCG) 38 hours before the scheduled time of oocyte harvest by transvaginal ultrasound guided aspiration (Hyslop *et al.*, 2012). Treatments included conventional In vitro fertilisation (IVF), in which the sperm was added to the eggs and allowed to fertilise, and Intracytoplasmic sperm injection (ICSI) treatment, in which the sperm was injected directly into the egg.

The mean female age was 33.47 ± 4.60 years, ranging from 20-44 (Figure 4.4). However, this distribution and range of women attending for treatment is influenced by an upper female age limit of 40 years for NHS-funded treatment, which accounted for 60-80% of all treatments during the 7 year period in which these data were collected. Self-funded patients may be taken on for treatment in their early 40's depending on the outcome of preliminary fertility investigations.

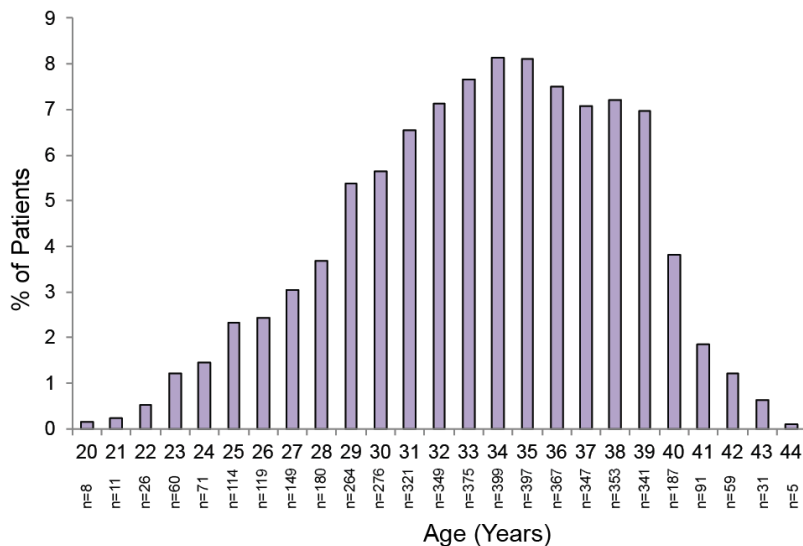


Figure 4.4 - A range of different ages of women attended the Newcastle Fertility Centre for treatment. Bars represent each age group as a percentage of the total number of treatment cycles for women at the NFC between January 2005 and November 2011. Of 4914 treatment cycles, the mean female age was 33.47 ± 4.60 years.

Human ovaries acquire their full quota of oocytes before birth, with numbers in the millions at around five months of gestational age. However, from then on this number declines, leaving only approximately 1000 by 50-51 years of age, around the time of menopause (Richardson *et al.*, 1987; Faddy *et al.*, 1992).

The number of oocytes retrieved at egg collection, after hormonal stimulation for fertility treatment, is determined by the size of the ovarian reserve of oocytes. Consistent with this, I found that the oocyte number declines steadily as a function of age in this patient cohort (Figure 4.5).

As the NFC dataset initially available to me included only patients who had undergone egg collection, it could be possible that excluding any cancelled treatment cycles might mask an accelerated decline in oocyte number at later ages. I repeated the graphs from Figure 4.5, this time including 358 cancelled treatment cycles, where the reason for cancellation was related to the patients poor response to stimulation (Figure 4.6). The graphs were virtually identical to those in Figure 4.5, again showing the oocyte number to decline steadily with female age, with no acceleration in the rate of decline in oocyte number after the mid 30's.

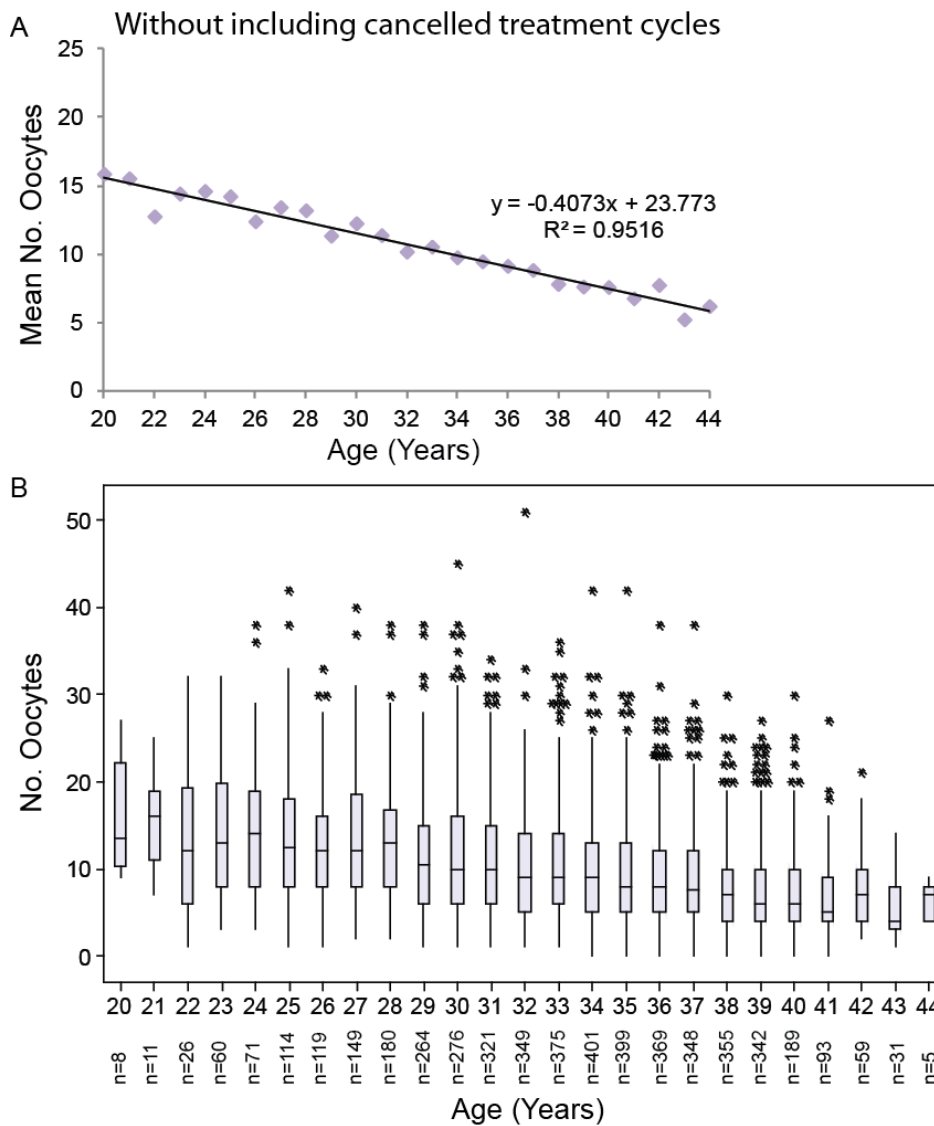


Figure 4.5 - Oocyte numbers decline as a function of female age in humans. The number of oocytes retrieved at egg collection was recorded for NFC patients falling within each age group (n=4914 treatment cycles). (A) The mean oocyte number was calculated for each age and plotted as a scatter plot with a trend line which strongly fits the data. (B) Box plots depicting the range in the data. Both show the steady decline in oocyte number with female age.

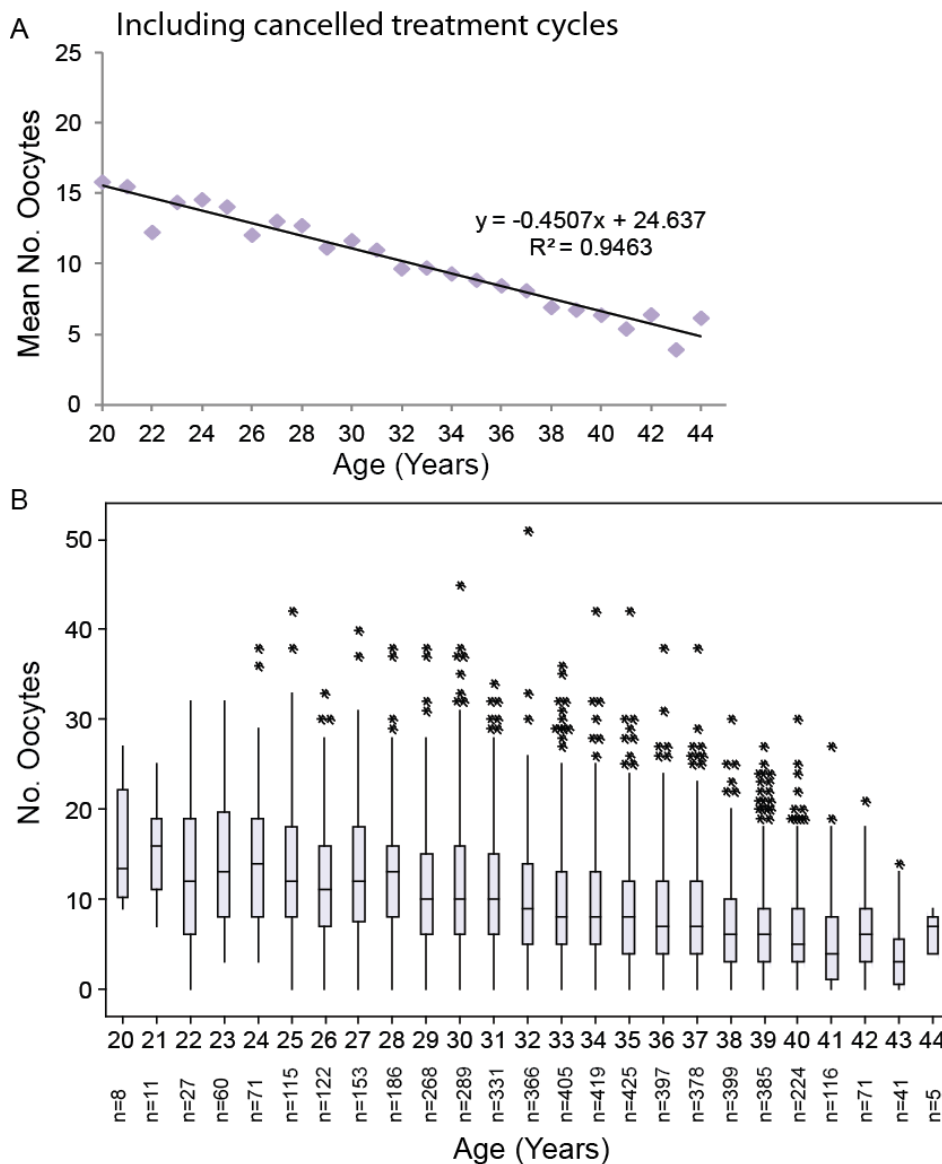


Figure 4.6 - Inclusion of cancelled treatment cycles does not change the pattern of decline in the yield of human oocytes. The number of oocytes retrieved at egg collection (n=4914 treatment cycles), and number of cases where treatment had been cancelled due to a poor response to stimulation (n=358 treatment cycles, represented as 0 oocytes) was recorded for NFC patients falling within each age group. (A) The mean oocyte number was calculated for each age and plotted as a scatter plot with a trend line which strongly fits the data. (B) Box plots depicting the range in the data. Both show the steady decline in oocyte number with female age.

This discrepancy could be due to differences between the different data sets. The NFC data were obtained from the number of oocytes collected after hCG injection and egg collection, whereas the Faddy *et al.* data were taken from the total follicle number observed in ovarian sections of multiple autopsy studies (ranging from neonatal to adults up to 44 years of age) and post surgery of premenopausal women (19-50 years of age) (Block, 1952; Block, 1953;

Richardson *et al.*, 1987; Faddy *et al.*, 1992). It could also be that as our data only include women between 20 and 44 years of age, that we are missing some of the initial gradual decline and some of the more dramatic decline at the later ages. It could be that this pattern is only observed in a 'healthy' population, not experiencing fertility problems.

Menopause is triggered by the number of ovarian follicles, and hence oocytes, falling below a threshold number (Richardson *et al.*, 1987). Being able to accurately predict the number of "fertile years" remaining would be advantageous to many women. This is particularly so in the current climate with the ever growing trend for women in developed economies to postpone parenthood. This tendency has been found to be due to many factors, including the rise in effective contraception, making family planning easier; increases in women's education and career opportunities; gender equality; partnership changes; and economic uncertainty (Mills *et al.*, 2011). However, this postponement, if left too long, can lead to infertility and involuntary childlessness. Therefore, a predictor of female fecundity (the monthly chance of a clinical pregnancy) would be valuable in informing the reproductive choices of women in developed economies

4.2. Is the competence to complete MI affected by advancing female age?

To determine whether the timing of meiotic progression is affected by advancing female age I analysed the maturation of oocytes collected for ICSI treatment (Figure 4.7). These oocytes are stripped of their cumulus cells straight after egg collection to facilitate injection of sperm into the oocyte during the ICSI procedure. The percentage of oocytes that developed to MII did not appear to be reduced with female ageing (Figure 4.7). If anything, there was a trend towards increased PB formation in older women (>41 years). This indicates that although older women have fewer oocytes, the competency to complete MI is not hindered by age.

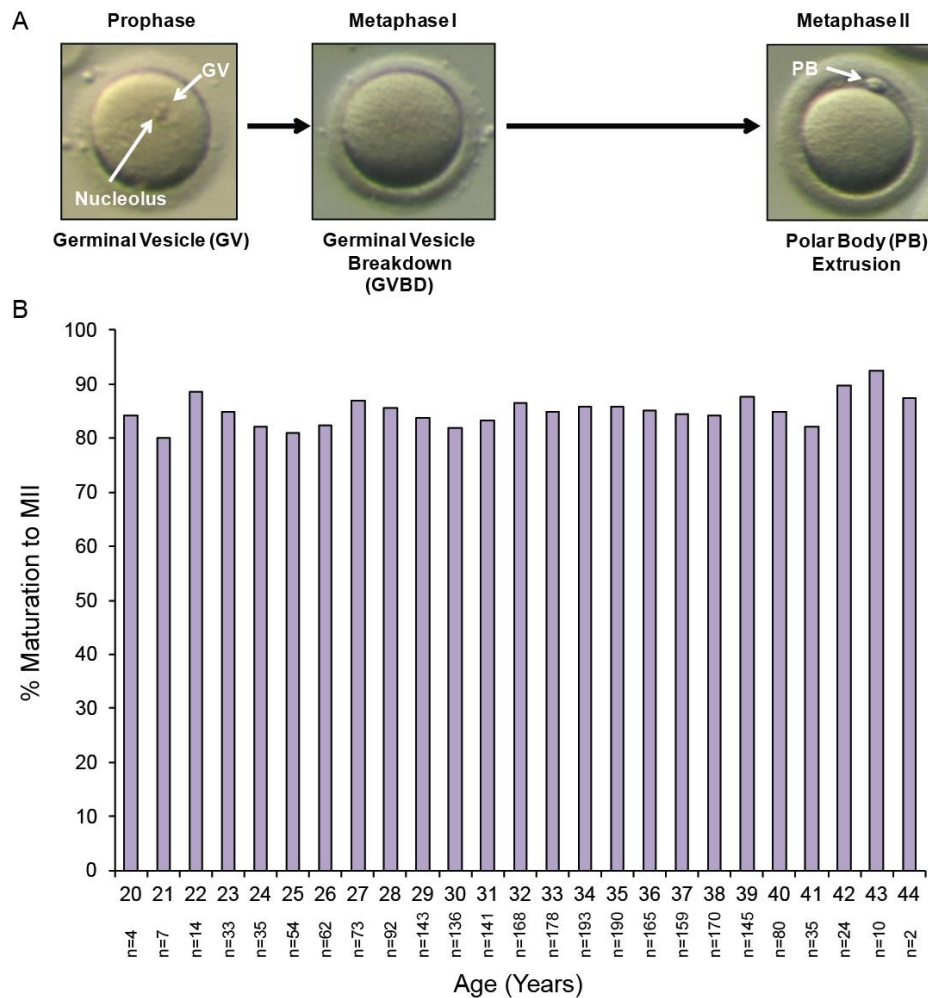


Figure 4.7 - Maturation to MII was not inhibited by female age in humans.

Oocytes were collected for ICSI treatment and stripped of their cumulus cells. They were then scored for their stage of maturation (A) by looking for the presence of a polar body, indicating maturation to MII. (B) The percentage of oocytes maturing to MII does not fall below 80% for any age group.

It could be that the checkpoint is somehow compromised in these oocytes. Alternatively, as meiotic competence is acquired gradually through oocyte growth (Wickramasinghe *et al.*, 1991) some of the oocytes from the younger age groups may not yet be fully grown.

4.3. Decline in clinical pregnancy rates with advancing female age

Of 4900 treatment cycles which resulted in oocyte collection, 93% had successful fertilisation and embryo development to a stage at which they were considered suitable for transfer to the uterine cavity. For this patient cohort I

analysed the correlation between clinical pregnancy rates and female age (Figure 4.8). A clinical pregnancy is defined as an ultrasound-detectable fetal heartbeat six weeks after IVF treatment. As expected, the data show a decline in the percentage of clinically recognised pregnancies as female age increases. They decreased from 40% at 21 years of age to only 10.34% at 43 years, with no pregnancies recorded after this age. There was an accelerated rate of decline from around the age of 36 onwards (Figure 4.8B). This is consistent with other studies illustrating that female fertility declines more rapidly from the mid 30's (Menken *et al.*, 1986; van Balen *et al.*, 1997; Larsen and Yan, 2000).

It should be noted that our NFC data set was from a group of women already experiencing problems conceiving naturally. Although this may not always be due to a female factor, we do need to take into account that some of these patients may show lower pregnancy rates because of ongoing fertility problems. This was more likely to be observed in the younger age groups where women were referred for treatment because of early known conditions such as polycystic ovaries or tubal complications and pelvic inflammatory disease. This may explain the fluctuations observed in the pregnancy rates before the age of 30.

Ideally we would want to compare these pregnancy rates to those of a healthy population with no known fertility complications. However, such a baseline is difficult to achieve as unlike most mammals, which copulate only during the estrous phase of their estrous cycle, human reproduction is influenced by many social and economic factors. A study which comes the closest to the possible biological maximum is that of a Hutterite population, who for religious reasons are opposed to any form of birth control, and are encouraged to have as many children as possible after marriage at a median age of 22 (Eaton and Mayer, 1953). On average each Hutterite woman gives birth to 12-14 children (Eaton and Mayer, 1953). As expected, the fluctuations observed in young women undergoing fertility treatment were not observed in Hutterite women. By contrast, the peak fertility was observed at 20 years of age (Figure 4.9). Fertility declines gradually until the age of 35, after which the rate of decline is accelerated (Eaton and Mayer, 1953).

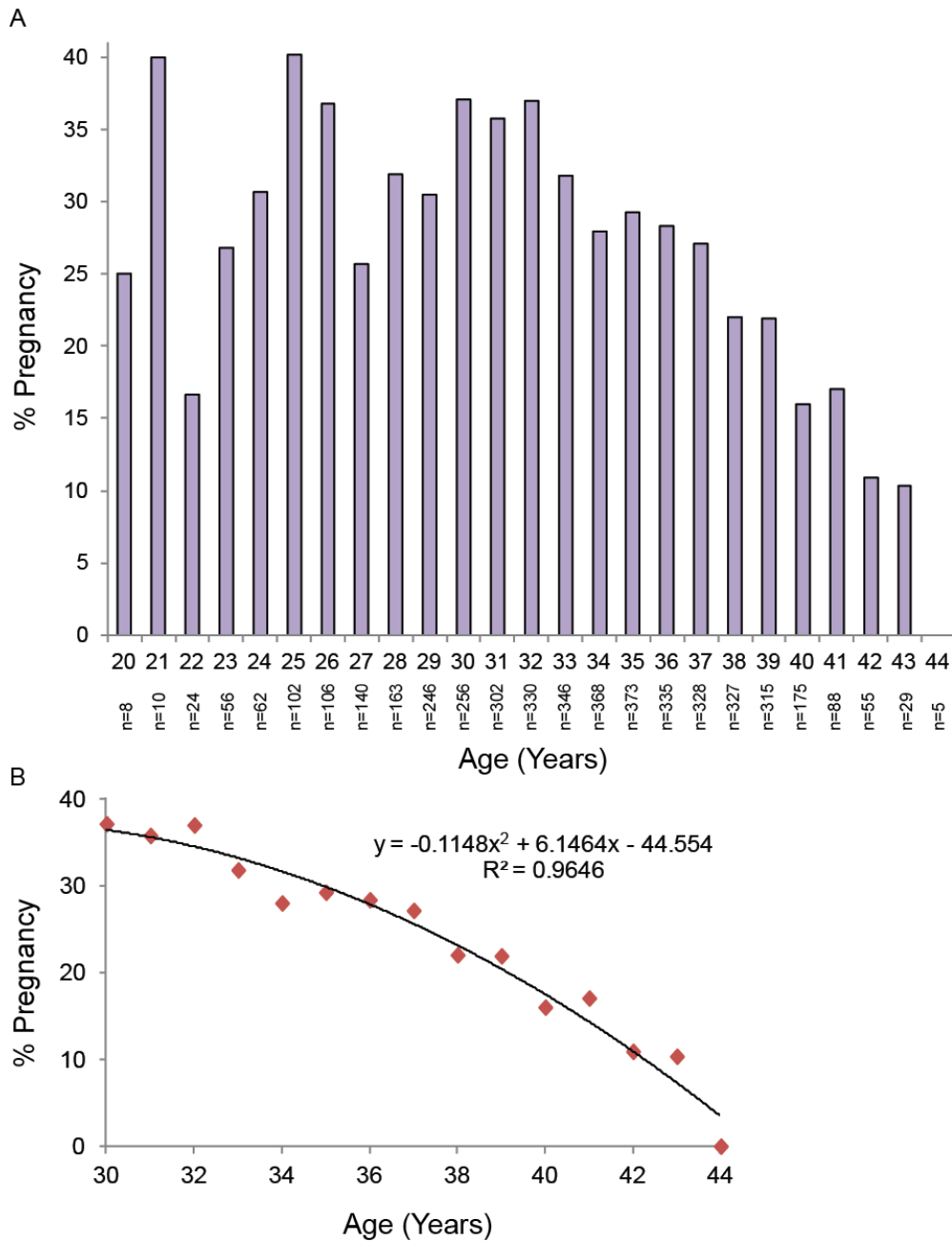


Figure 4.8 - Pregnancy rates decline as a function of female age. The percentage of pregnancies was recorded for each age group and plotted as (A) a bar chart (n=4549 treatment cycles) and (B) a scatter plot from the age of 30 with a trend line fitted (n=3632 treatment cycles). Pregnancy rates decline with female age, with an acceleration in the rate of decline around the mid 30's.

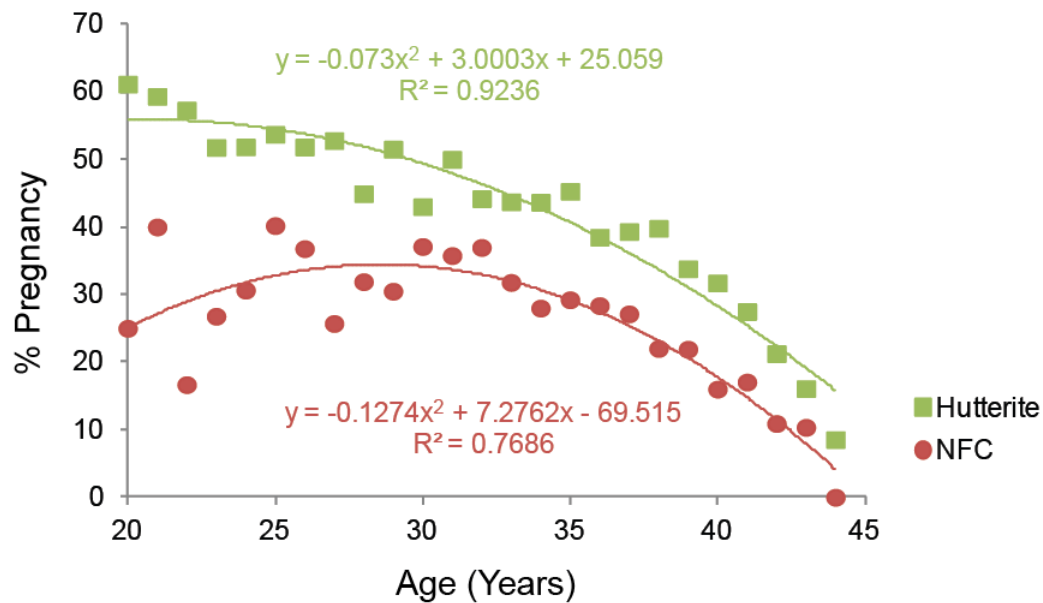


Figure 4.9 - Fertility rates decline as a function of female age during natural and assisted conception. The percentage probability of a live birth at each age was recorded from a Hutterite population (green; n=12,638 women, graph produced using original data (Eaton and Mayer, 1953)). This was plotted against the percentage pregnancy rates for the NFC data set (red; n=4549 treatment cycles). A decline in pregnancy was observed with advancing female age, with the rate of decline accelerating after ~35 years of age.

This is similar to the initially described biphasic decline in oocyte number with female age observed by Faddy *et al.* (Faddy *et al.*, 1992), and certainly to the revised theory of a gradual acceleration in follicular decline (Faddy, 2000) (Figure 4.3).

I compared this data set to the pregnancy rates recorded by the NFC. Although the pregnancy rates are lower for the NFC, reflecting the fertility problems and perhaps suboptimal procedures during IVF treatment, both show a similar rate of decline in pregnancy from around 34 years of age, and an increased rate of decline after the mid 30's (Figure 4.9).

However, a more recent study of Hutterites using a convolution model of fecundability shows the decline to be almost linear from the age of 20 to 45 (Larsen and Yan, 2000). Although this model takes into account additional factors such as postpartum amenorrhea, the study by Eaton and Mayer (Eaton and Mayer, 1953) includes a larger number of women. In addition the raw data from the Eaton and Mayer study was available and I was therefore able to analyse it for myself, in the same manner as for our own data (Figure 4.9).

4.4. Decline in implantation rates with advancing female age

The implantation rate reflects the proportion of embryos giving rise to a viable foetus, with a heartbeat detectable by ultrasound at ~6 weeks. Implantation is affected by both endometrial receptivity and oocyte quality, with embryos of low quality being less likely to implant after replacement.

More than 80% of trisomies associated with birth defects and miscarriage are due to errors arising during MI (Hassold and Hunt, 2001). There is over a 30% increase in clinically recognised pregnancies involving trisomic foetuses in women ~40 years of age, compared to women in their 20's (Hassold and Hunt, 2001; Hunt and Hassold, 2010). However, trisomy likely only represents the tip of the iceberg. More severe and complex oocyte abnormalities would not be compatible with embryo development to a stage where they would be capable of implantation.

The decline in the birth rates with age can be rescued by using oocytes from younger donors (35 years of age or younger) (Figure 4.10). Analysing the IVF data available from the HFEA for 2009 indicated that women aged 40-42 are 2.6 times more likely to have a live birth using donor oocytes, rather than their own. Even more strikingly women aged 43-44 years are 6.8 times more likely, and those over 45 years of age are 25.4 times more likely to give birth following treatment using donor oocytes.

As the age related decline in birth rates was completely rescued by using donor oocytes from younger women, it can be concluded that the quality of the oocytes, rather than other factors such as endometrial receptivity, is the overriding factor affecting the decline in pregnancy rates with advancing female age.

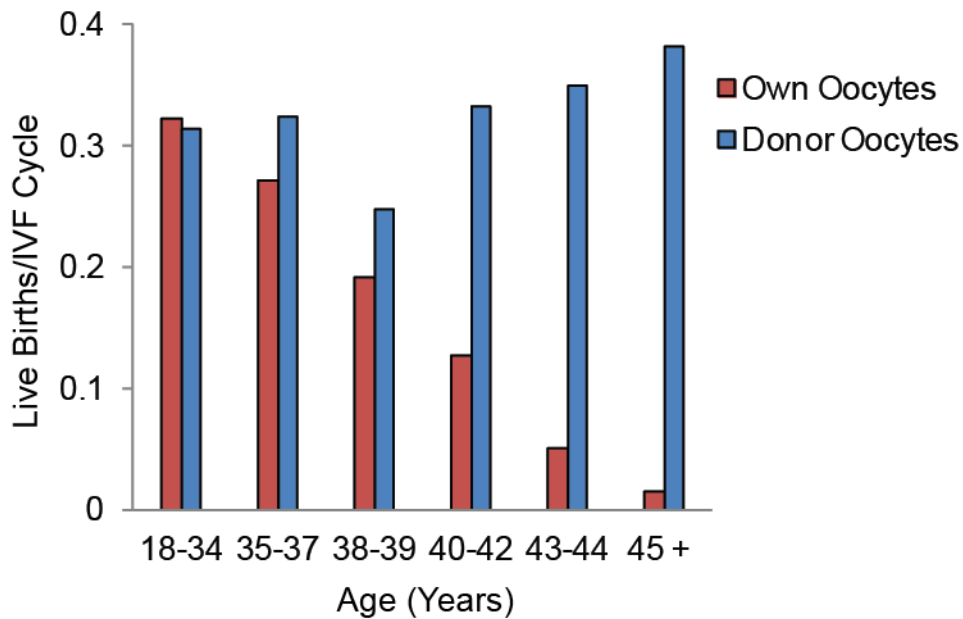


Figure 4.10 - Birth rates are rescued when using donor oocytes. Bar chart showing the number of birth events per IVF cycle for women undergoing treatment in 2009 using their own oocytes (43166 treatment cycles, 10869 births; red), or those donated from younger women (1254 treatment cycles, 417 births; blue). This graph is based on data made available on the HFEA website (Data from Fertility Treatment, Trends and Figures).

For the NFC patient cohort I analysed the correlation between implantation rates and female age (Figure 4.11). As expected, consistent with the decline in oocyte numbers and pregnancy rates, the data show a decline in the percentage implantation as female age increases. Implantation decreased from 27.3% at 25 years of age to only 4.84% at 43 years. After showing fluctuation in the 20's, again likely due to the more severe nature of fertility problems represented at these earlier ages, the implantation rates declined dramatically from the age of 30 onwards (Figure 4.11B).

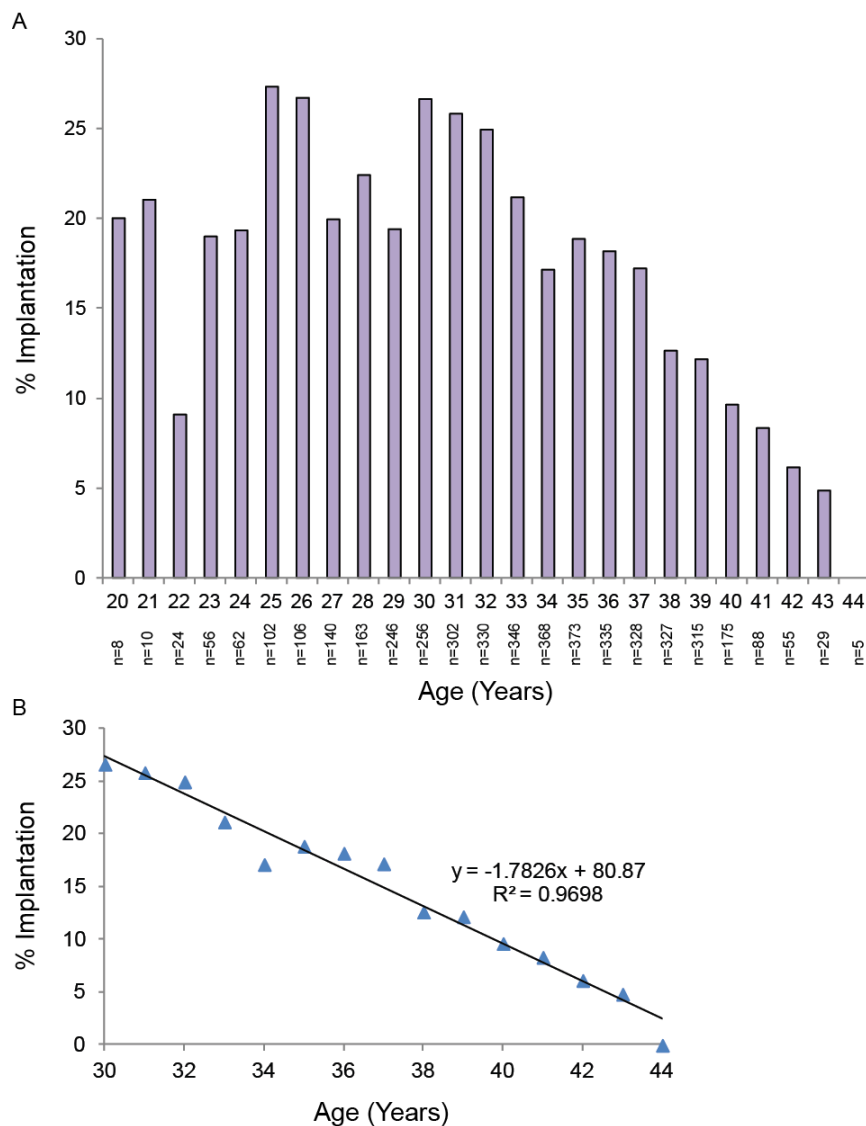


Figure 4.11 - Implantation rates decline as a function of female age. The percentage of implantation was recorded for each age group and plotted as (A) a bar chart (n=4549 treatment cycles) and (B) a scatter plot from the age of 30 with a trend line fitted (n=3632 treatment cycles). An almost linear decline in implantation rates were observed with advancing female age.

Both oocyte quantity (mean oocyte numbers) and oocyte quality (implantation rates) decline as a function of female age. The key question is, are the two linked? To answer this I directly compared mean oocyte numbers and implantation rates from the age of 30 onwards. The implantation rate declines twice as fast as the rate of decline in the mean oocyte number (Figure 4.12). This reflects a decline in oocyte quality faster than the decline in oocyte yield. This suggests that the reduction in oocyte number is not the only factor affecting pregnancy rates, and there are instead two independent factors contributing to this decline.

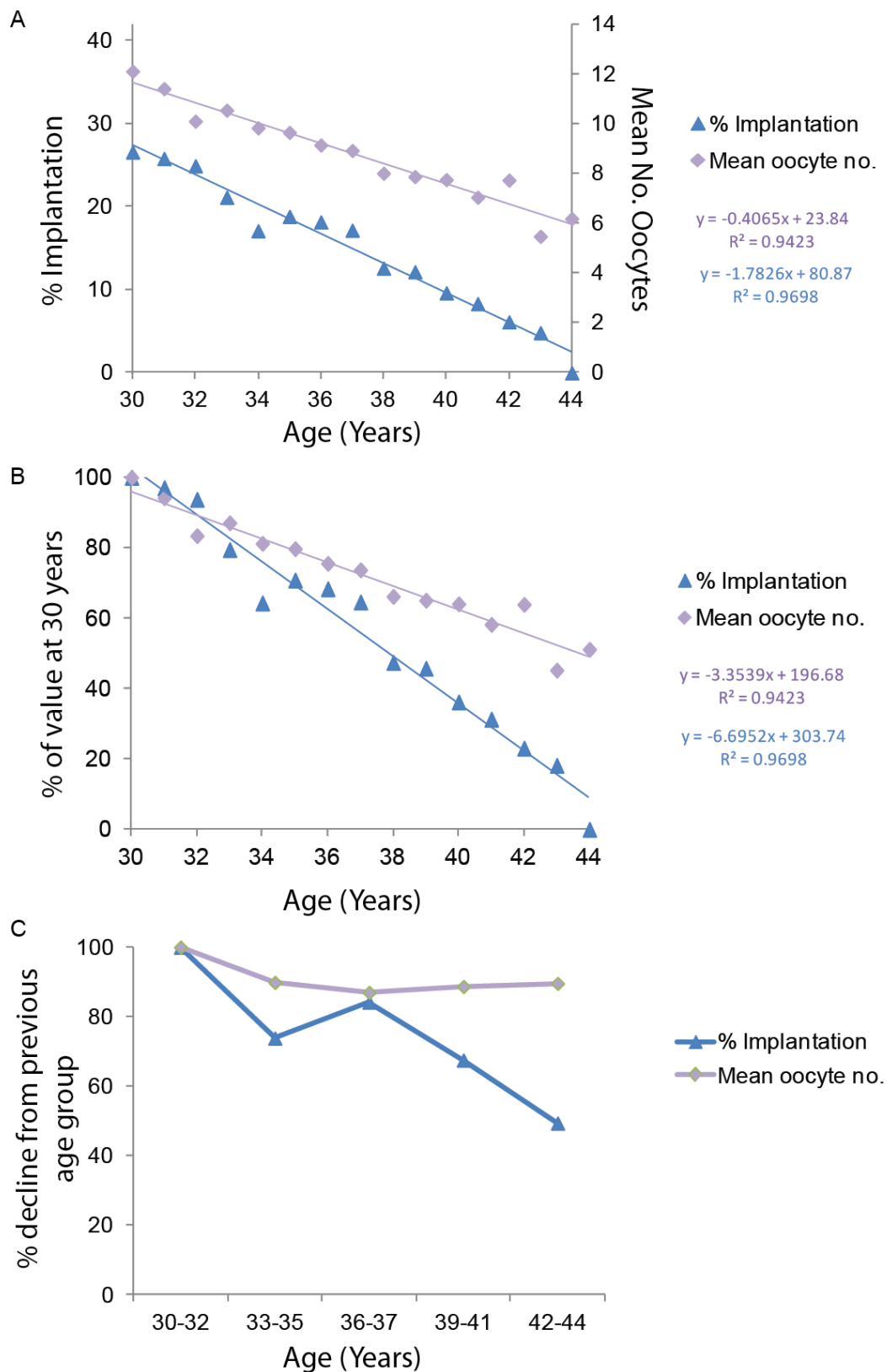


Figure 4.12 - Implantation rates decline at a faster rate than the decline in the mean oocyte number as a function of female age. (A) Scatter plots showing the percentage implantation (blue) and the mean oocyte number (purple) recorded for each age group from 30 onwards (n=3632 treatment cycles). (B) Scatter plot showing the data in (A) as a percentage of the value at 30 years of age. (C) Line graph showing the changes in the rate of decline in implantation and mean oocyte number as a function of female age.

This conclusion could be strengthened by comparing implantation rates in young and older women who produced equivalent numbers of oocytes.

While the decline in quantity can be explained by the depletion of the endowment of oocytes present at birth, the decline in oocyte quality is less straightforward. The question of why oocyte quality declines as we get to the end of the pool has remained unanswered. As reproductive biology is so difficult to study in humans, mainly due to the limited number of oocytes available for research, finding a convincing animal model was extremely important.

4.5. Use of a mouse model for female reproductive ageing

Although multiple mouse strains have been used, much of the earlier research on female reproductive ageing was performed using mice of a CBA strain (Martin *et al.*, 1976; Speed, 1977; Eichenlaub-Ritter *et al.*, 1988; Eichenlaub-Ritter, 1998). Although exhibiting a reduction in follicle number and a modest increase in aneuploidy toward the end of their reproductive lifespan, they had a relatively short general lifespan linked to a high incidence of lung tumours (Strong, 1936). Thus, it is not clear whether the reproductive defects were linked to the underlying pathology.

In order to better investigate the maternal age effect in a wild type mouse strain, we used oocytes from the aged mouse colony of a C57BL/*Icrfa*^t strain. This colony has been housed at Newcastle University's Institute for Ageing and Health since 2000. It is a non-mutant strain free of specific familial pathologies and is long lived (the mean female age at death is 25.1 ± 0.35 (s.e.) months), making it a good model for studies related to ageing as observed in humans (Rowlatt *et al.*, 1976).

By contrast, the C57BL/*Icrfa*^t strain females do not exhibit lung tumours, and are not observed to form lymphomas until after approximately 27 months of age, and hepatic tumours after 29 months. In addition, heart failure has never been observed in females under the age of 35 months. This gives us confidence that

any defects we saw can be attributed to age rather than to any underlying pathology.

These mice have been allowed to age as naturally as possible with minimal intervention from technicians or research staff. They are housed conventionally but in larger, non standard cages with higher lids so they have more space to move and climb. A forage mix is provided in their bedding of sunflower seeds and flaked maize to encourage natural activity. They are also provided with an enriched environment by means of a cardboard box, which they can use their own cognitive ability to adapt as they wish (Figure 4.13). Finally, the females are only ever mated with one male, and the breeding pairs/trios are kept together for life.



Figure 4.13 - C57BL/1crfa^f strain female in its enriched environment. Image taken from a poster entitled 'A retrospective review of the causes of death in an aged mouse colony' by Adele Kitching.

Survival data from the Institute of Ageing and Health (courtesy of Adele Kitching, Senior Animal Technologist) reveal that there is very little difference in mortality rates between males and females up until approximately 20 months of age, after which the mortality of females exceeds that of males. Interestingly, breeding females have a shorter lifespan than the non-breeding females.

Based on a linear extrapolation estimate using the average life expectancy of our female mice as 25.1 months (Adele Kitching and Rowlatt *et al.* (Rowlatt *et al.*, 1976)), and human females as 82.1 years (National Statistics Office 2010), I deduced that each month of female mouse life was equal to 3.27 years of human female life (Figure 4.14).

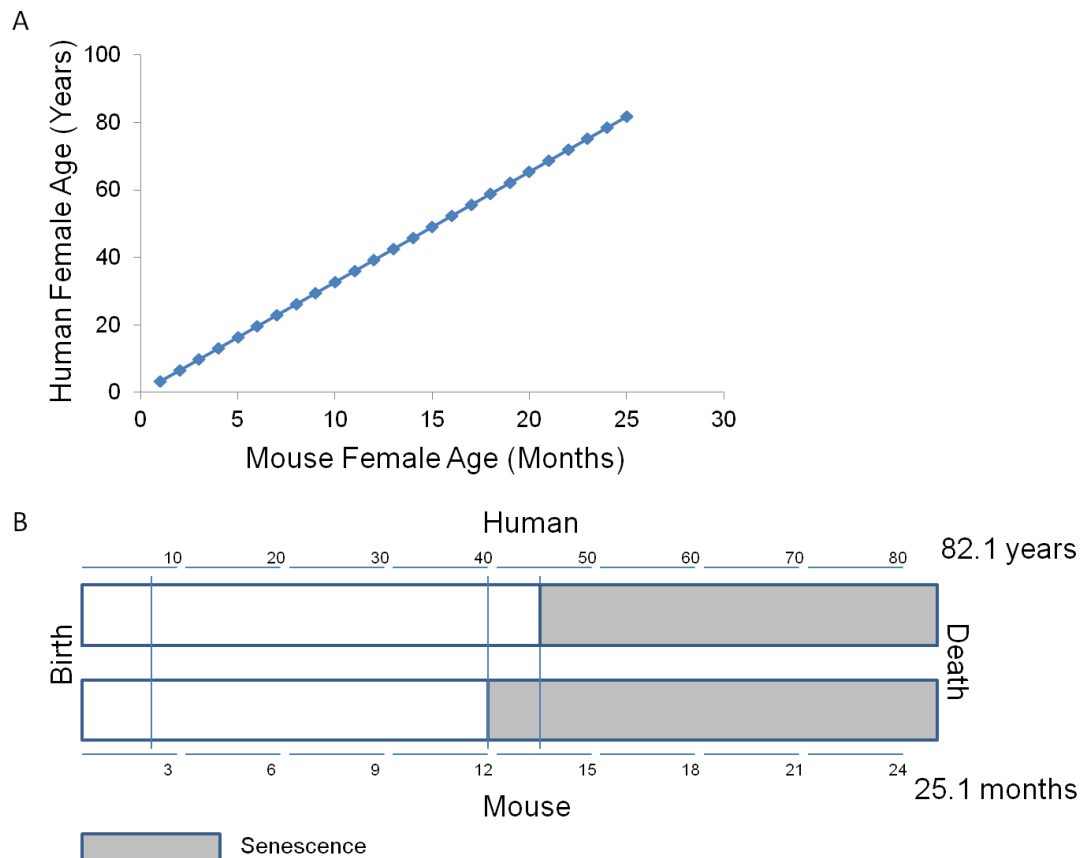


Figure 4.14 - Linear extrapolation model to determine the corresponding ages of mouse and human females. (A) Using the average life expectancy of our female mice as 25.1 months, and human females as 82.1 years, we assumed a linear relationship to produce a linear extrapolation model for calculating the corresponding human female ages of our mice. (B) Timeline of the linear extrapolation model. Blue lines indicate the corresponding human ages of mice aged 2, 12 and 14 months.

Litter size declines after 8 months of age, and by 12 months (~40 human years), which is half their lifespan, most females are sterile. However, litters have been recorded up to 16 months of age (Franks and Payne, 1970; Rowlatt *et al.*, 1976).

This decline in reproductive capacity with female ageing is comparable to that observed in humans. In principle, this is a very useful animal model.

We used this mouse strain in Chapter 5, for the investigation of female age-related chromosome segregation defects in oocytes. In this Chapter, I compare the age related decline in oocyte numbers and fecundity with that observed in our NFC data set.

4.6. Dimensions of the C57BL/1crfa^t mouse breeding data

As the previous study of fertility of the C57BL/1crfa^t strain was performed more than 30 years ago (Rowlatt *et al.*, 1976), I was keen to revisit this to obtain a contemporary profile of fertility under the husbandry conditions applied in our aged mouse colony. To achieve this I analysed the breeding information from the past 6 years (mid 2004 till mid 2010), which included records of the number and size of litters produced, in relation to maternal age.

The data were provided, courtesy of Adele Kitching, in the form of breeding cage cards. Males were paired with either one or two females, which were housed together for life from ~10 months of age. Recorded on each card was the date of birth of the breeding pair/trio; the date of first mating; the date of litter birth and number in each litter; and the date of weaning and number which survived till weaning. Also noted was the date of death of the breeders, if it occurred whilst they were still being kept for breeding purposes.

A caveat of these experiments is that we cannot rule out reduced frequency of coitus or male factors as being the cause of a decline in fertility. However, it is likely that if the male were infertile it would have been discovered and retired early on in the breeding regime. As male mice are not subject to many factors associated with a deterioration in sperm quality, as has been observed in humans (such as obstructive problems due to the failed reversal of a vasectomy, trauma or infection; or external factors such as drug use, smoking or excessive alcohol intake), we can be fairly confident that any decline in fertility will be a result of female ageing. However, we also cannot rule out that any observed decline in fertility could be due to endometrial factors. Unlike human studies showing that there is no decline in endometrial receptivity with advancing female age (Figure 4.10), there are as yet no donor oocytes studies showing this to be the case in mice.

There were some cases where the birth of a litter was recorded, but some pups, or the complete litter, did not survive until weaning (where the pups are separated from the mother, 3 weeks after birth). Where possible, the litter size has been recorded at both birth, and the time of weaning. However, in some

cases the litter died before the number born could be recorded. In these cases the number born is recorded as zero.

4.7. Fertility of the C57BL/*Icrfa*^t mouse

A total of 431 litters were recorded from 111 females. Litters were produced between 2 and 15 months of age, with just under a third of all the litters recorded being from females aged 5-6 months (Figure 4.15A). The number of litters produced initially increased with maternal age, peaking at 16% of the total being born to females around 6 months of age. Just under 12% of the total were born to females aged 8 months, and from here the number of litters steadily declined, with less than 1% of the total being born to females aged 13 months and older (Figure 4.15A).

Another factor which should be taken into account when measuring fertility in mice is the number of pups produced in each litter. As well as litter frequency, the size of the litter was also found to decrease with maternal age (Figure 4.15B and C). This may be due to fewer oocytes being ovulated, or fewer embryos successfully implanting. The mean litter size fluctuates at around 5 pups per litter until ~7 months of age, after which it then begins to rapidly decline. A mean of 4 pups are produced between 7 and 10 months of age, and females older than 10 months only produced a mean of 2 pups per litter.

However, as mentioned previously, not all litters survive till weaning. Almost 20% of the total number of litter births recorded no longer had any pups by the time of weaning (n=85 litters) (Figure 4.16). In these cases the pups were either still born; the mothers were unable to produce enough milk; or in some cases, infanticide (the termination of a neonate after it has been born) may occur (Hrdy, 1979). This was highly evident in the older age groups as 50% of the litters born to females over 10 months did not survive till weaning (n=19 litters), compared with 17% in females 10 months and younger (n=66 litters) (Figure 4.16).

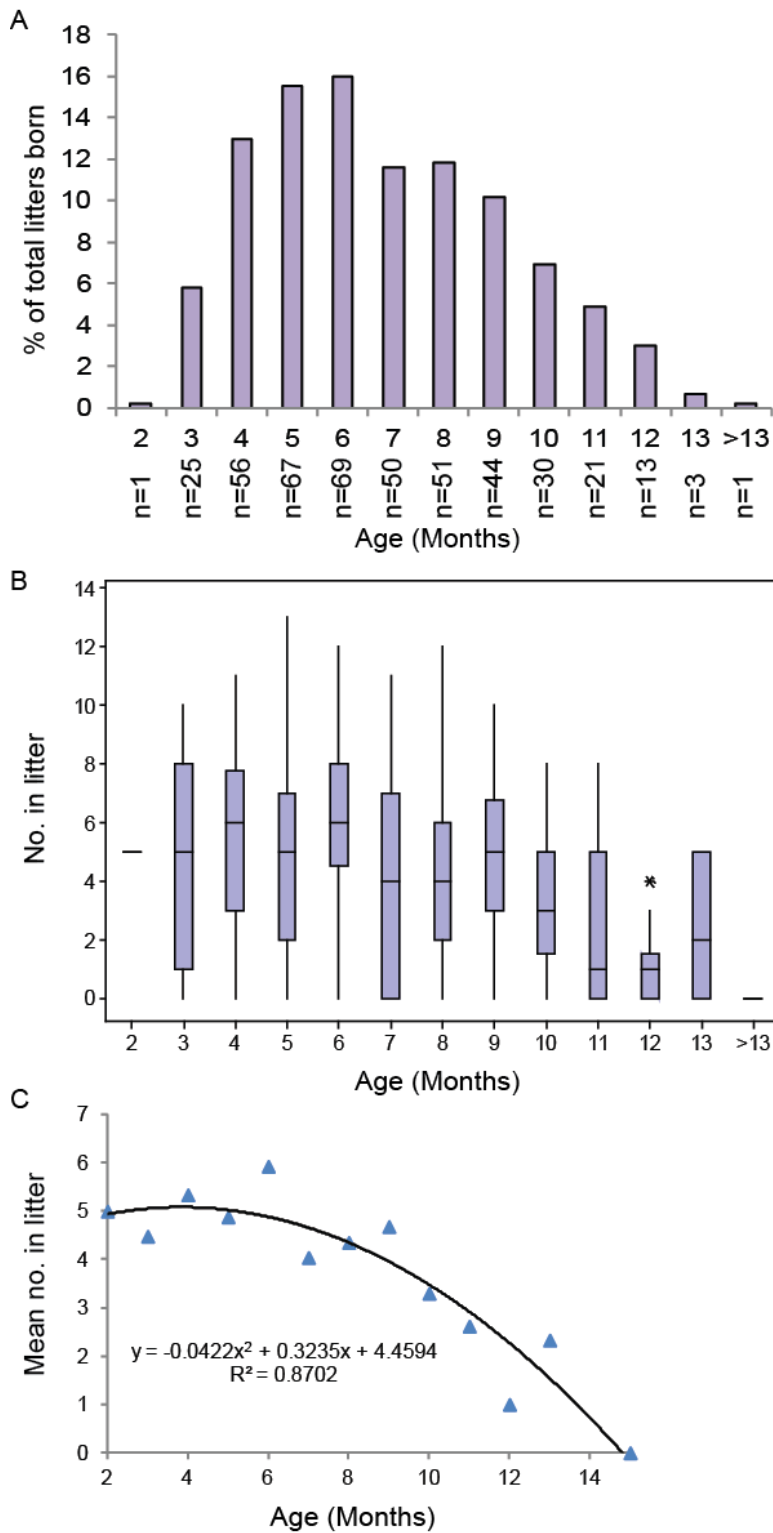


Figure 4.15 - Litter frequency and size decrease gradually with advancing maternal age. (A) Bar chart depicting the maternal age at litter birth as a percentage of the total number of litters recorded (n=431 litters from 111 females). (B) Box plot illustrating the range in litter size per age group, and (C) a scatter plot showing the mean number born per litter for each age group. Litter size and fertility decrease with advancing maternal age.

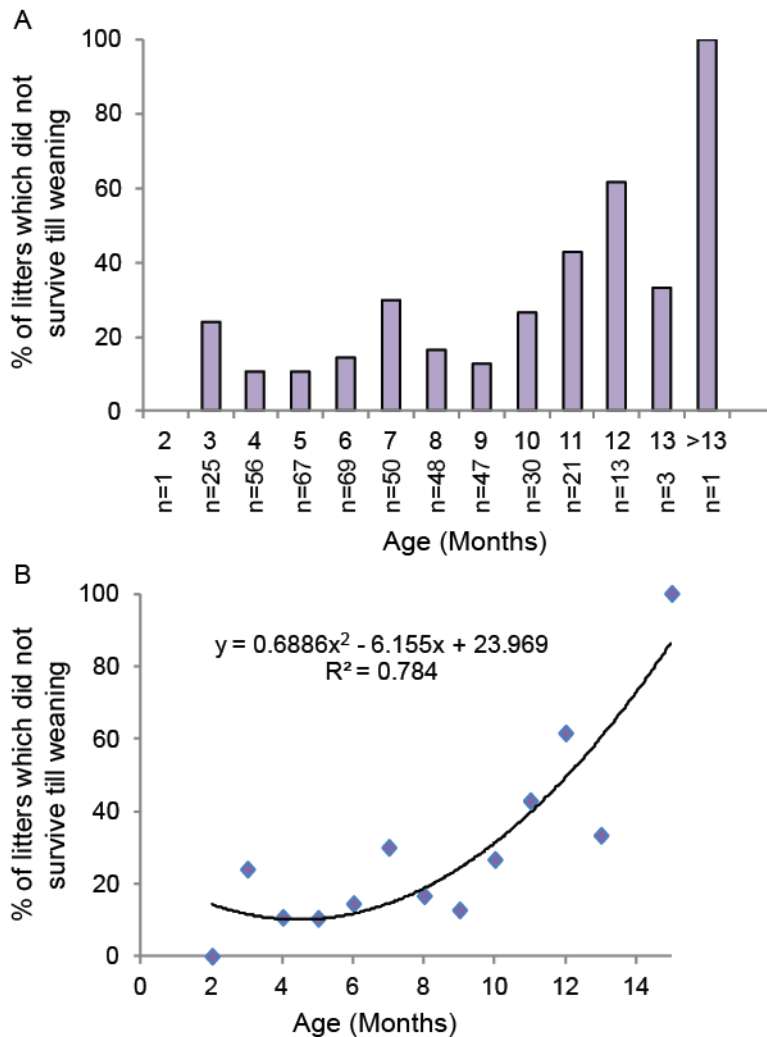


Figure 4.16 - There is an increased incidence of neonatal death with advancing maternal age. (A) Bar chart and (B) scatter plot depicting number of litters which were either still born, or died before weaning, as a percentage of the total number of litters produced by the age group (n=431 litters from 111 females, 85 litters did not survive).

One of the most common reasons for infanticide is when a pup is deformed or wounded. If it is unlikely to survive, continuing to feed it would take away sustenance from the mother and the rest of the litter (Hrdy, 1979). The increased frequency of litter death, either before birth or by infanticide, may reflect an increased incidence of aneuploidy in the oocytes of the aged females giving rise to genetically unfit offspring. Supporting this is the striking resemblance of Figure 4.16B to Figure 4.1 showing the increased rate of trisomy with increased female age in humans.

However, in contrast to humans, where three autosomal trisomies routinely survive beyond birth (trisomy 13, 18 and 21), trisomies are rarely observed in

mice. Where their frequency has been artificially increased through breeding schemes, aneuploid embryos rarely survive to mid-gestation (Lightfoot *et al.*, 2006). This is consistent with the reduced litter size relative to oocyte number observed in my study. However, the few aneuploidies that survive to birth have fairly distinct phenotypes, with all mouse autosomal trisomies being retarded in growth and development (Hernandez and Fisher, 1999).

Although the results drawn from our older mothers are strikingly similar to the results previously shown for the increased rate of aneuploidy in human females, the low incidence of trisomic embryos surviving to birth indicated the possibility of other reasons for the increased frequency of neonatal death in offspring of older females.

In addition to litter size, the frequency of litters was reduced, with longer intervals occurring between litters with advancing maternal age (Figure 4.17), and increasing more dramatically after 9 months of age. There was however no strong correlation observed between the litter size and the interval between litters.

These data show that fertility in this strain begins to decrease gradually after 6 months, with a dramatic reduction in fertility after 9 months of age. After this point there is an accelerated rate of decline in litter size (Figure 4.15); an increased incidence of neonatal death (Figure 4.16); and a dramatic increase in the length of time between litters (Figure 4.17).

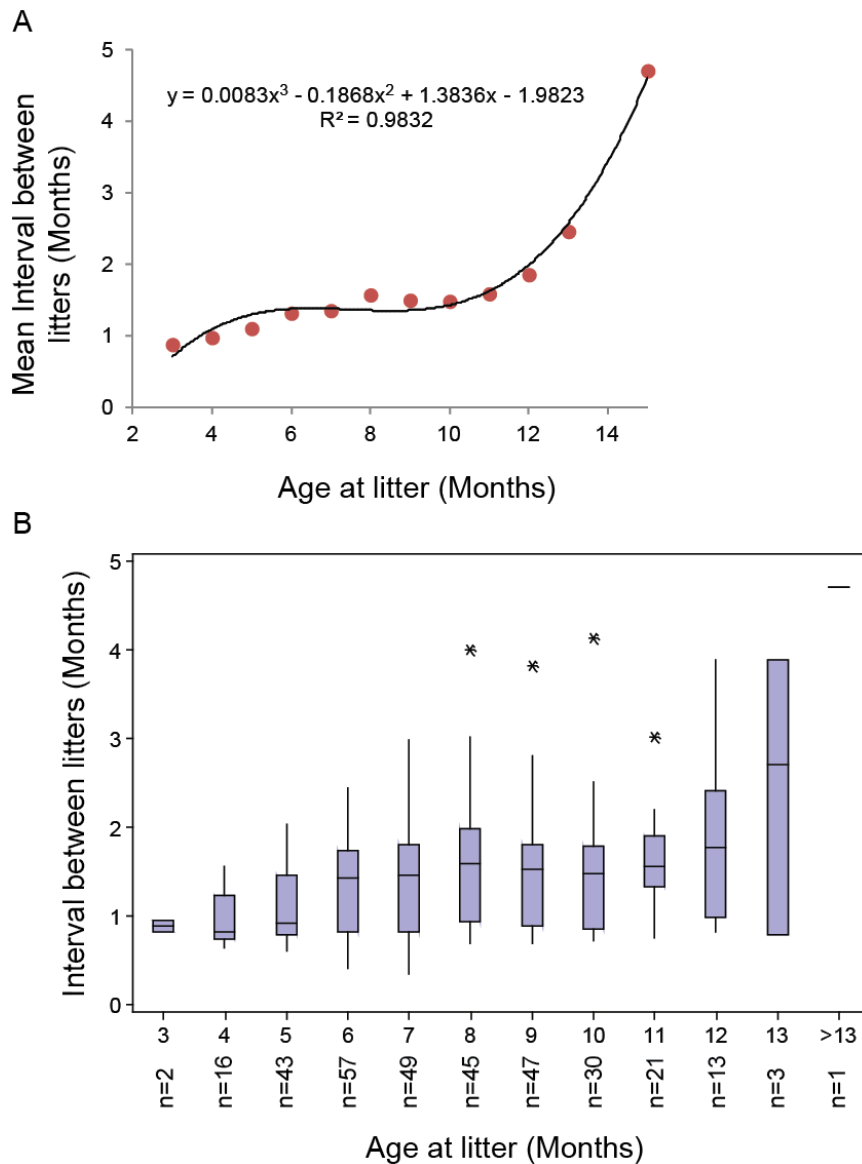


Figure 4.17 - The interval between litters increases with advancing maternal age. (A) The mean interval between litters was calculated (n=431 litters in total; 104 first litters and 327 subsequent litters) and plotted against the age of the female when the litter was produced. (B) Box plot illustrating the range in the interval length for each age group.

According to the linear extrapolation of age presented above (Figure 4.14), a 6 month aged mouse is the equivalent of a 20 year old human female. This decline in fertility after 6 months of age is consistent with that observed in the Hutterite population (Figure 4.9). As discussed earlier, the peak fertility among the NFC infertility patients is not equivalent to a normal fertile population, likely because of aetiological factors in the younger women, so is more difficult to compare to the mouse data.

Although there was an observed decline in litter size with maternal ageing, fertility did not decline to the same extent in all individuals, with some females still being capable of giving birth to large litters. These females were perhaps better equipped than the others to continue breeding, maybe with a larger pool of oocytes remaining within the ovaries.

4.8. Depletion of the germ cell pool with advancing female age in the C57BL/1crfa^t mouse

To elucidate whether the decline in fertility correlated with a decline in the ovarian reserve of oocytes, as has been observed during human female ageing (Faddy *et al.*, 1992; Faddy and Gosden, 1996; Faddy, 2000; Hansen *et al.*, 2008; Rosen *et al.*, 2010), we harvested mature GV stage oocytes from a range of ages of superovulated C57BL/1crfa^t mice (Figure 4.18). The number of oocytes harvested after ovarian stimulation reflects the number of follicles which have been recruited for growth from the primordial pool. This hormone dependent growth phase lasts ≥ 14 days in mice (and 85 days in humans).

The number of oocytes collected from the 2, 6 and 8 month aged mice did not greatly differ. However, when the mice were aged 10 months and over, an increased rate of decline in oocyte numbers was strikingly clear (Figure 4.18). The number of oocytes obtained from the 2, 6 and 8 month old mice, was significantly greater than from the 12 or 14 month old mice ($p < 0.001$).

It was further observed that the number of oocytes from the 12 month aged mice was greater than that of the 14 month age group ($p < 0.05$; Figure 4.18). These data indicate that, consistent with litter size data, there is depletion in the germ cell pool with increasing female age for the C57BL/1crfa^t mice.

To determine whether the competence to complete MI was affected by female age, I analysed the maturation of mature GV stage oocytes from 2 month and 14 month aged C57BL/1crfa^t mice, harvested and matured overnight using timelapse microscopy (Figure 4.19).

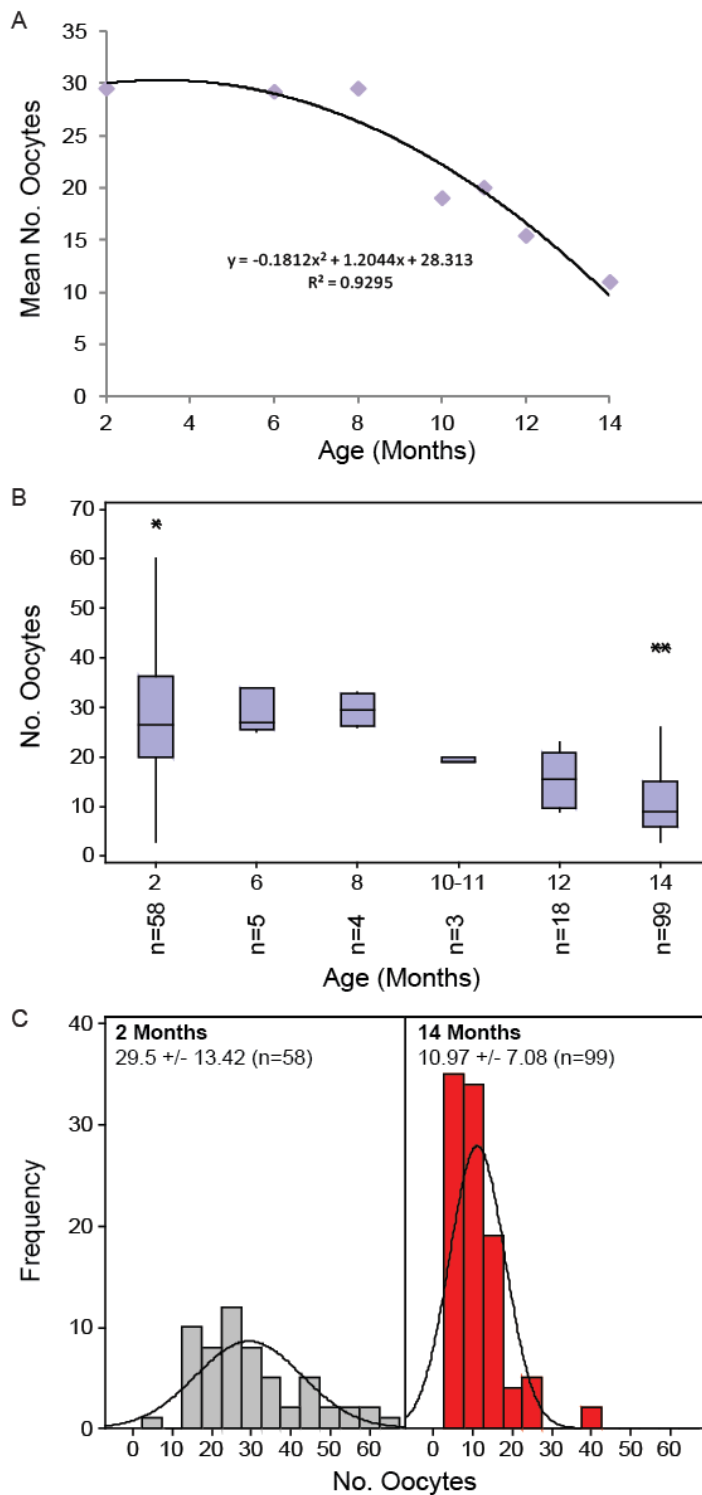


Figure 4.18 - Oocyte numbers decline as a function of female age. Fully grown GV stage oocytes were harvested from the ovaries of super-ovulated 2; 6; 8; 10; 11; 12 and 14 month old C57BL/1crfa^f mice (n=187 mice). (A) Scatter plot with a trend line showing the decrease in the mean oocyte number with advancing female age. (B) Box plots representing the range in the number of oocytes obtained from each age group. The number of oocytes obtained per 2 month (29.50 ± 13.42); 6 month (29.20 ± 4.44); and 8 month (29.50 ± 3.51) old mouse, were significantly greater than per 12 month (15.39 ± 5.50) or 14 month old mouse (10.97 ± 7.08) ($p < 0.001$). The number of oocytes per 12 month old mouse was also significantly greater than that per 14 month old mouse ($p < 0.05$). (C) Histograms representing the range in the number of oocytes obtained from 2 month and 14 month old mice.

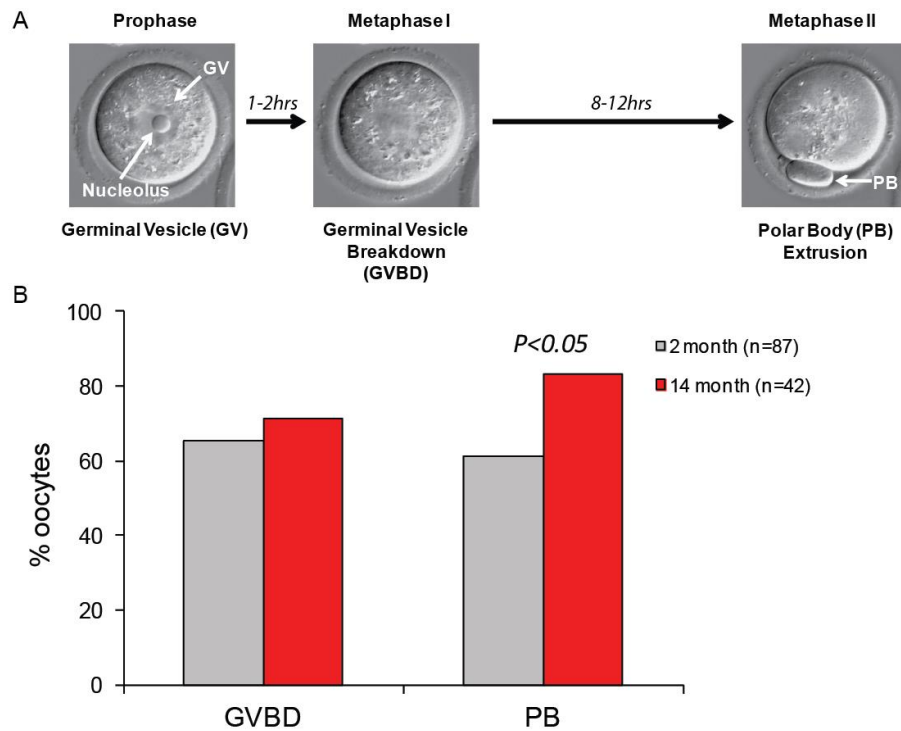


Figure 4.19 - GVBD was not influenced by increased female age, but PB formation was increased in oocytes from older mice. Oocytes were matured overnight whilst being imaged using timelapse microscopy. (A) Images depicting mouse oocyte maturation from GV to PB extrusion. (B) The proportion of oocytes maturing to MI was not significantly different between the oocytes of 2 month (n=87) and 14 month (n=42) mice (65.5% and 71.4% respectively). However, of these oocytes, a significantly higher proportion from 14 month old mice matured to PB extrusion (83.3%) compared to the 2 month old mice (61.4%; $p < 0.05$). *Experiment performed in collaboration with Louise Hyslop and Sarah Pace (Lister et al., 2010).*

The number of oocytes progressing from the GV stage to MI arrest was higher in oocytes from 14 month old mice (71.4%) than 2 month old mice (65.5%). Of the oocytes imaged which underwent GVBD, PB extrusion was monitored. As observed in the human data, the proportion of oocytes producing a PB was not reduced in older females, in fact in mice the proportion of oocytes that produced a PB was significantly higher for 14 month old mice compared with 2 month old ($p < 0.05$). Thus, despite the decline in oocyte number observed as a function of increasing female age, competency to develop to MII was not hindered in mice or humans. While it is tempting to speculate to impairment of the SAC, two independent studies have reported that canonical measures of spindle checkpoint function show no deterioration during female ageing (Duncan *et al.*, 2009; Lister *et al.*, 2010).

There was however some discrepancy between the number of oocytes collected within each age group and the number of litters produced. Where there was the greatest number of oocytes recorded for the 2 month age group, there was just 1 litter produced at this age (0.23% of the total number of litters; Figure 4.15A and Figure 4.20A). This may be because the females are not yet sexually mature. Furthermore, whilst I observed that the mice still had oocytes at 14 months of age, there was again just 1 litter born to this group (Figure 4.15A and Figure 4.20A). This indicates that these older oocytes may not be capable of producing a viable pregnancy.

The number of oocytes collected is probably more translatable to litter size, however, there is again some discrepancy between the two (Figure 4.20A). In addition, the rate of decline in litter size is 1.2 times faster than the rate of decline in oocyte number (Figure 4.20B-D).

This difference suggests that, similar to my observation in humans (Figure 4.12), the decline in oocyte number is not the only factor affecting fertility rates. While the litter size may be our best measure of implantation and oocyte quality for the mouse model, it is not as straight forward an extrapolation as with humans. Implantation rates from the NFC data set are based on the percentage implantation of oocytes which had undergone successful fertilisation and embryo development to a stage where they were considered suitable for transfer to the uterine cavity. The reduced litter sizes recorded from older C57BL/*Icrfa*^t strain females could reflect either reduced oocyte number or oocyte quality. However, as the oocyte number exceeded the litter size, it can be concluded that number of oocytes is not the limiting factor. I therefore propose that it is oocyte quality rather than quantity which is resulting in the reduced litter size (implantation) with advancing female age in C57BL/*Icrfa*^t mice.

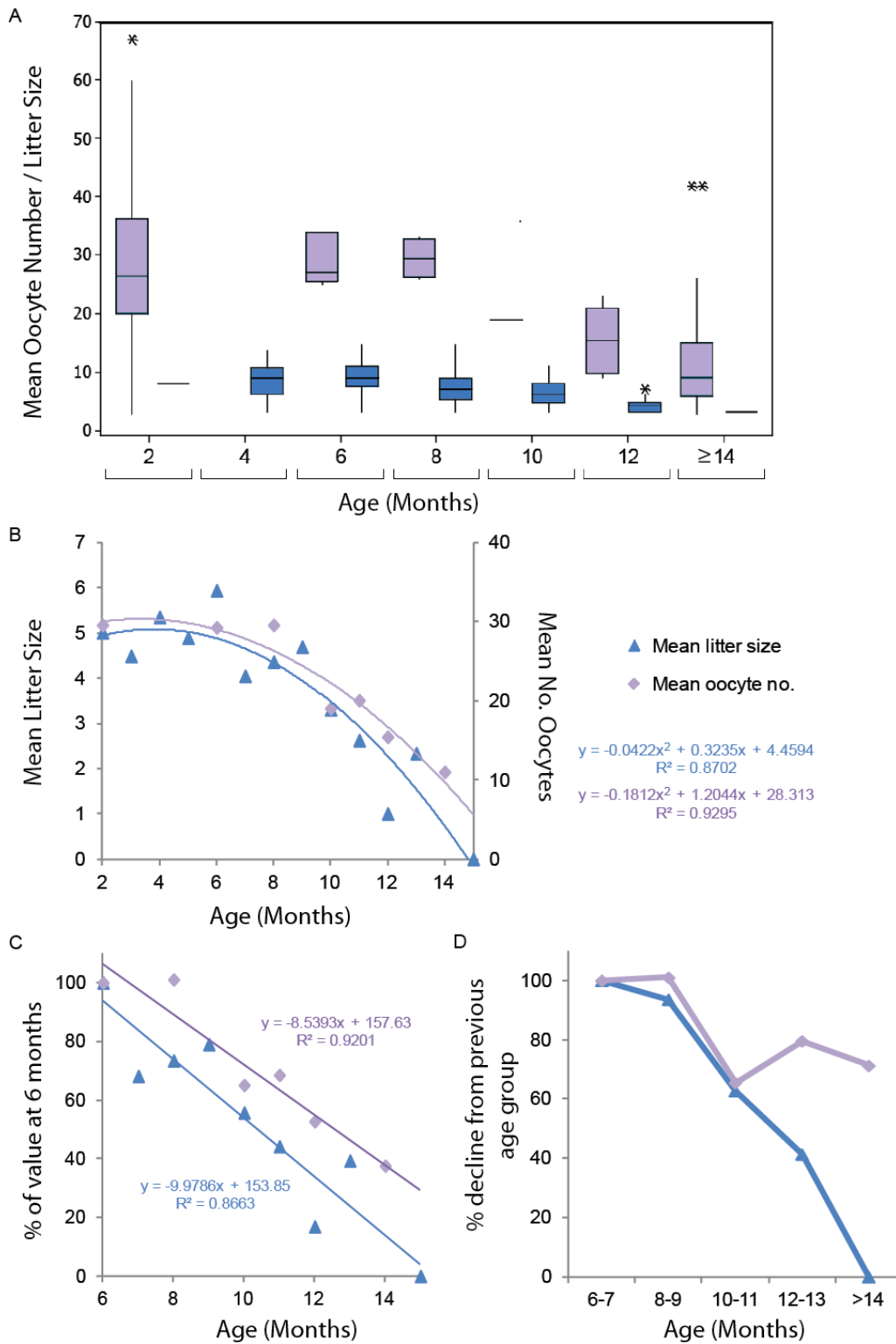


Figure 4.20 - Oocyte numbers and litter size decline at different rates as a function of female age. (A) Box plots representing the range in the number of oocytes collected (left, purple, n=187 mice), and the litter size (right, blue, n=431 litters) for each age group. It should be noted that no 4 month old mice were taken for oocyte collection. (B) Scatter plot showing the mean oocyte number (purple), and mean litter size (blue) recorded for each age group. (C) Scatter plot showing the data in (B) as a percentage of the value at 6 months of age (the age of peak fertility). (D) Line graph showing the changes in the rate of decline in mean oocyte number and litter size, by showing each age group as a percentage of what it was in the age group which precedes it.

4.9. What is the equivalence between human and mouse female ageing?

Based on information from the UK National Statistics Office for 2010, the female life expectancy is 82.1 years of age. By comparing this to the observed life expectancy of our C57BL/1crfa^f mice (Adele Kitching and Rowlatt *et al.* (Rowlatt *et al.*, 1976)) of 25.1 months, I designed a linear extrapolation model (Figure 4.14). Using the fertility data obtained from each species, I annotated the model, highlighting trends observed in each species (Figure 4.21). I used the model to determine the corresponding human ages of the mice, and directly compared the mean oocyte numbers and pregnancy rates observed in human females after the age of 30 (Figure 4.22).

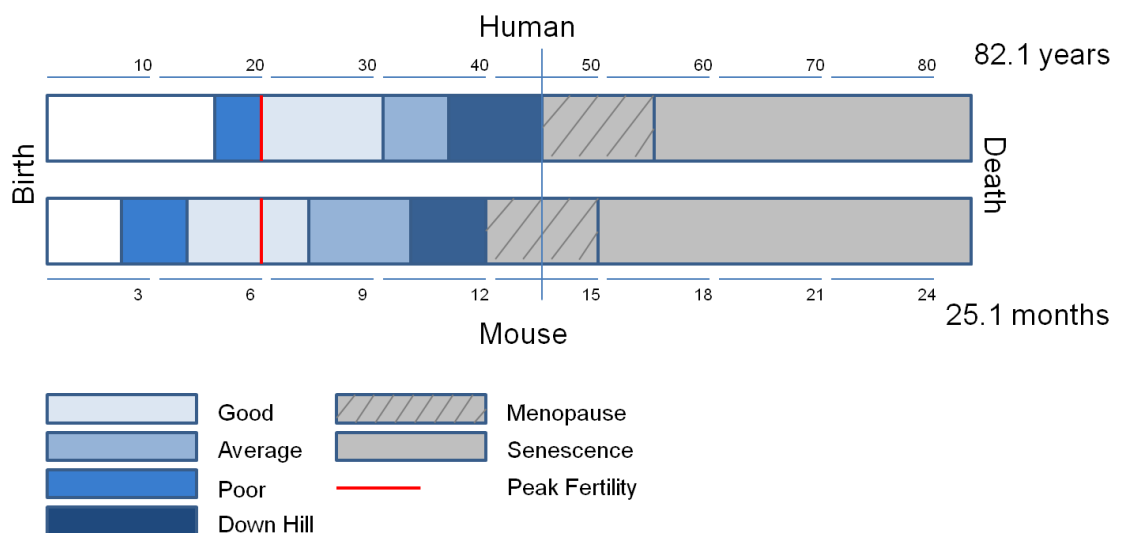


Figure 4.21 - Linear extrapolation model of reproductive trends in humans and mice. Human data taken from a normal fertile population (Eaton and Mayer, 1953), and mouse data a combination of our findings and those from Rowlatt *et al.* (Rowlatt *et al.*, 1976)). Using the average life expectancy of our female mice as 25.1 months, and human females as 82.1 years, we assumed a linear relationship to produce a linear extrapolation model for calculating the corresponding human female ages of our mice. Graphical representation of the model (Figure 4.14A) highlighting fertility trends for each species. Based on the model, a 45 year old woman is roughly equivalent to a 14 month aged C57BL/1crfa^f mouse.

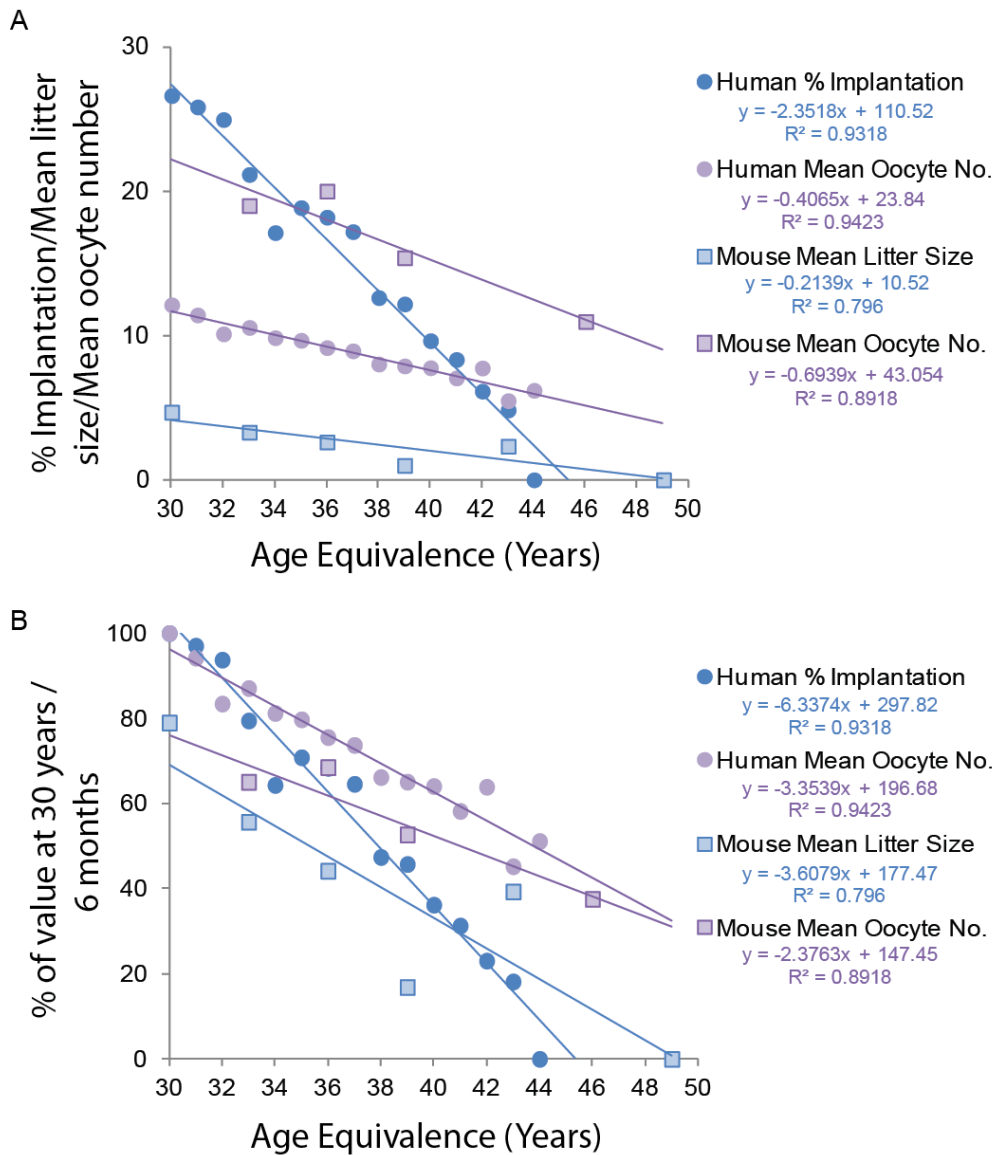


Figure 4.22 - Oocyte numbers and fertility decline at different rates in mice and humans as a function of female age. (A) Scatter plot showing the mean oocyte number (purple) and implantation rate (percentage implantation or mean litter size, blue) recorded for each age group. The mouse ages are converted to their human equivalence using my linear extrapolation model (Figure 4.14). Human data are represented by circles, the mouse human age equivalence by squares. (B) Scatter plot showing the data in (A) as a percentage of the value at 30 years of age for human data; and 6 months of age for mouse data.

Although the patterns are similar, implantation rates and oocyte numbers decline faster in the human data set compared with the mouse (1.76 and 1.41 times faster respectively).

When implementing the model and comparing the fertility trends of each species, it became evident that a linear model was not the best comparison (Figure 4.21). Although the relationship was fairly linear after 6 months of age

in mice (20 years in humans), the earlier sexual maturity in this species cannot be equally matched to the human population. The C57BL/1crfa^t mice reproduce earlier; however, less than a third of the way through their lifespan, fertility begins to decline. This is earlier than that observed in humans. An altered model can be used for better comparing the two species (Figure 4.23).

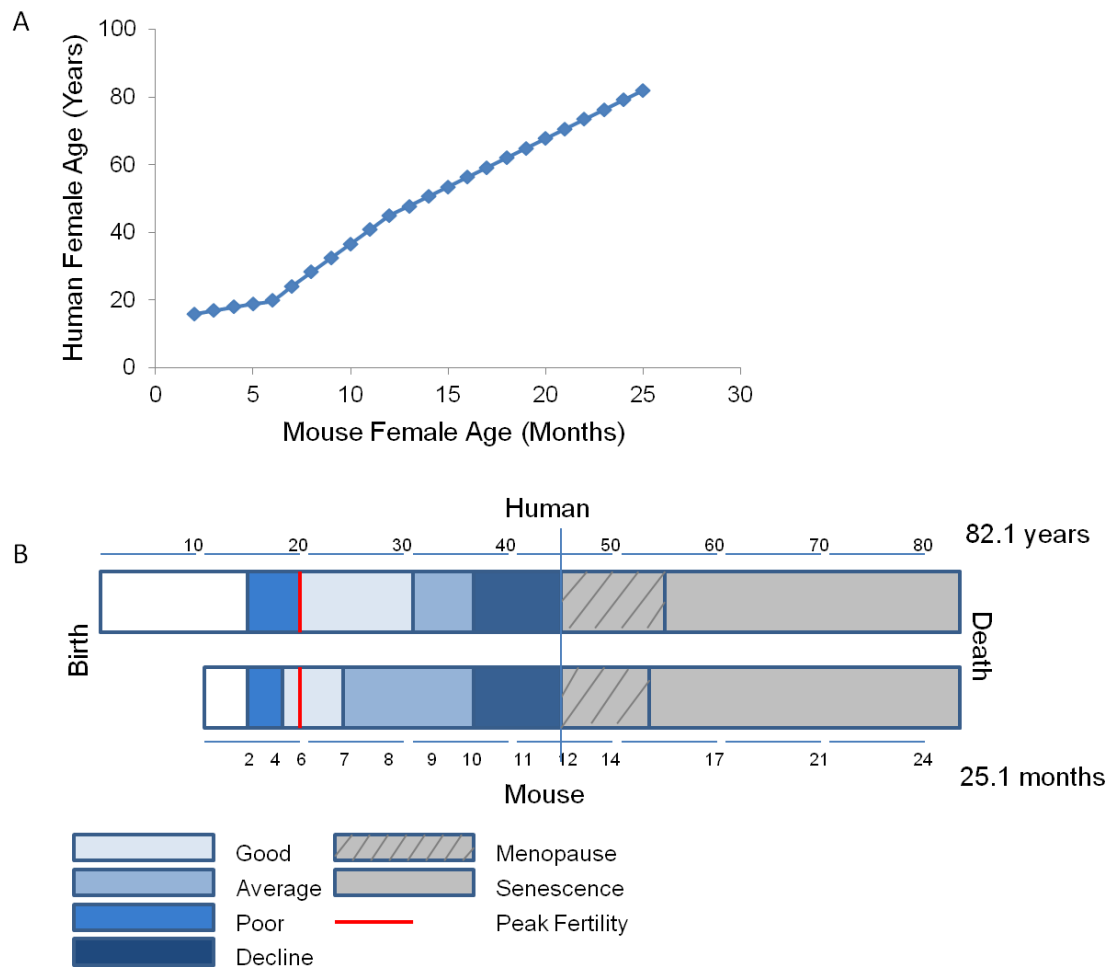


Figure 4.23 - Non-linear extrapolation model of the reproductive lifespan in humans and mice. Human data taken from a normal fertile population (Eaton and Mayer, 1953), and mouse data a combination of our findings and those from Rowlett *et al.* (Rowlett *et al.*, 1976)). (A) By comparing the mouse peak fertility and senescence data to that found of humans, a model was created to calculate the corresponding human female ages of our mice. (B) Graphical representation of the model. Based on fertility data a 45 year old woman is roughly equivalent to a 12 month aged C57BL/1crfa^t mouse.

In both humans and mice, oocyte quantity (mean oocyte numbers) and oocyte quality (implantation rates, represented by litter size in the mouse model) decline as a function of female age. These seem to be independent factors contributing to the overall decline in fertility, with oocyte quality declining faster than the oocyte yield. The fact that this occurs in both species strengthens our use of this strain as an animal model for female ageing.

Chapter 5. Results II - Maternal-age related segregation errors

The data presented in Chapter 4 indicate that female reproductive ageing is accompanied by a decline in the number of oocytes, which despite high rates of meiotic maturation, apparently have a poor capacity to develop into viable embryos when a woman is in her late 30's. This is consistent with the dramatic increase in the incidence of infertility, miscarriage and birth defects observed ~10 years before the menopause. While it has long been known that the majority of chromosomal abnormalities leading to miscarriage and birth defects are the result of segregation errors during the oocyte meiotic divisions (Hassold and Chiu, 1985), remarkably little is known about the biological basis for the association between female age and chromosome missegregation.

The different types of segregation errors are numerous. During MI segregation errors may arise due to a failure to resolve chiasmata between homologous chromosomes at anaphase I, or aberrant segregation of univalents may occur due to absence of chiasmata. Alternatively, segregation errors may arise due to premature loss of cohesion between centromeres, leading to segregation of sisters rather than homologous chromosomes. Most errors of MII are thought to result from a failure of the sisters to separate correctly, or random segregation of sisters due to their premature separation (Hassold and Hunt, 2001). Much of our current knowledge on the causes of meiotic chromosome segregation errors is based on inference from genetic mapping studies in cases of trisomy (Chakravarti *et al.*, 1989; Hassold *et al.*, 1995; Lamb *et al.*, 1997), and on cytogenetic analysis of oocytes that fail to undergo fertilisation during IVF treatment (Pacchierotti *et al.*, 2007). However, insights into the pathways and mechanisms leading to meiotic errors and how these are affected by female ageing have remained elusive. Progress in this field has been impeded by scarcity of human oocytes, the intractability of MI, and absence of a convincing animal model.

Early studies in mice indicated that incidence of chromosome segregation errors increases only modestly during female ageing (Brook *et al.*, 1984;

Eichenlaub-Ritter *et al.*, 1988). However, these data were based largely on analysis of fertilised and ovulated MII oocytes. Furthermore, much of the earlier work was performed on oocytes from the CBA strain (Martin *et al.*, 1976; Speed, 1977; Brook *et al.*, 1984; Eichenlaub-Ritter *et al.*, 1988; Eichenlaub-Ritter, 1998), which although similar to humans in exhibiting a depletion in the pool of follicles towards the end of its reproductive lifespan, the age-related increase in the incidence of aneuploidy is only modest (Eichenlaub-Ritter, 1998). Additionally, the CBA mouse has a relatively short general lifespan linked to a high incidence of lung tumours (Strong, 1936). It is therefore not clear whether the defects reported are linked to the tumourogenic phenotype.

It could further be argued that the short reproductive lifespan of the CBA strain reflects an underlying problem in ovarian function. A similar argument would apply to the Senescence Accelerated Mouse (SAM) which has been another strain utilised in the studies of reproductive ageing (Liu and Keefe, 2002; Liu and Keefe, 2004). These mice exhibit age-related meiotic defects, specifically chromosome misalignments, resembling those found in human female aging. However, there is questionable value of these mice in characterising maternal age-related meiotic defects as nuclear transfer experiments where defects could be rescued by young wild type cytoplasm but not young SAM cytoplasm, suggest an inherent problem in the regulation of SAM oocytes (Liu and Keefe, 2004).

We therefore believed that it was worth revisiting this question using oocytes from the C57BL/*Icrfa*^f mouse strain, which has no underlying pathologies (Rowlatt *et al.*, 1976). Furthermore, advancement in live cell imaging of oocytes raised the possibility of overcoming the intractability of MI by monitoring chromosomes during progression through MI in real time. This chapter describes the detection and incidence of age-related segregation defects by live cell imaging of oocytes from C57BL/*Icrfa*^f females.

5.1. Imaging of oocyte chromosome dynamics by timelapse fluorescence imaging

To determine whether female ageing is associated with aberrant chromosome dynamics, we used epi-fluorescence live cell imaging to monitor chromosomes, in oocytes expressing a red fluorescent protein (RFP)-tagged variant of the nucleosomal protein Histone H2B. Chromosomes were imaged for a period of 16-18 hours to track them during progression from prophase arrest (GV stage) to metaphase II arrest.

To prevent oocytes from undergoing GVBD (exit from prophase) before being placed on the time-lapse microscope, oocytes from C57BL/1crfa^f mice were harvested from excised ovaries in M2 medium supplemented with IBMX. IBMX is a phosphodiesterase inhibitor, which inhibits the transition from prophase to M phase of meiosis I by preventing the breakdown of cAMP. Elevated cAMP prevents activation of the M phase kinase Cdk1 by activating protein kinase A (PKA), which in turn inhibits the Cdk1 activating phosphatase Cdc25B (Mitra and Schultz, 1996; Lincoln *et al.*, 2002; Oh *et al.*, 2010).

Following harvest, oocytes were transferred to fresh droplets of M2-IBMX medium for micro-injection with mRNA encoding histone H2B-RFP. This was made from a plasmid constructed by cloning mouse histone H2B into a pRN3 backbone plasmid, upstream of a red fluorescent protein tag (Figure 5.1). The H2B was inserted minus its STOP codon so that the RFP would be directly transcribed with the histone. The mRNA was transcribed using the Ambion T3 mMessage mMachine, which incorporates cap analog to maximise the yield of RNA and the proportion of capped transcripts. Capping of RNA promotes the correct initiation of protein synthesis as well as the stability and processing of mRNA (Gallie, 1991; Preiss and Hentze, 1998; Kapp and Lorsch, 2004). Most eukaryotic mRNA's found in vivo are capped. The plasmid design also allows incorporation of a Poly(A) tail to the transcript. Polyadenylation plays an important role in the stabilization of RNA and enhances efficient initiation of translation (Gallie, 1991; Preiss and Hentze, 1998; Kapp and Lorsch, 2004).

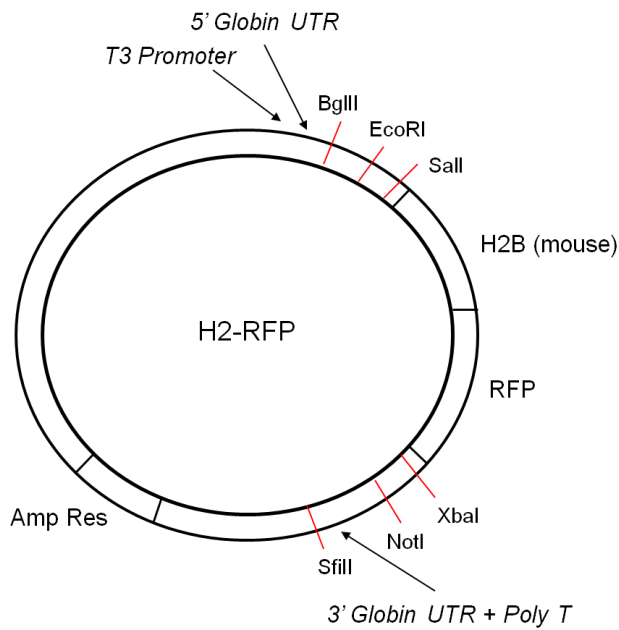


Figure 5.1 - H2B-RFP Plasmid Map. Map showing the components of the H2B-RFP plasmid. The mouse H2B sequence is directly followed by the sequence encoding RFP. Red lines represent restriction enzyme sites.

The mRNA was diluted with injection buffer to give a concentration of approximately 1µg/µl. Oocytes were injected with a single bolus, approximately the same size as the nucleolus (10µm diameter) equalling approximately 12.5-13.5pl. Injected oocytes were left 2-4 hours to recover in M2-IBMX medium. During this time the oocytes translated the injected mRNA and incorporated the Histone H2B-RFP protein into the oocyte chromatin (Figure 5.2).

At this concentration of mRNA and injection volume, the levels of H2B-RFP translated within the oocyte are fairly constant, and mostly remain constant through oocyte maturation, with a modest increase around the time of anaphase (Figure 5.2B-F). Occasionally the volume injected is larger due to either a blockage in the pipette, or an oocyte being mistakenly injected twice, which sometimes occurred if the first injection attempt was not clearly observed as being successful. This generally results in higher levels of protein expression and hence higher levels of fluorescence (Figure 5.2F, oocyte represented by upper green line). However, these oocytes were easily identified and omitted from further analysis. This was also the case with any falsely injected oocytes, or those of insufficient size to be competent of maturation (less than 67µm diameter).

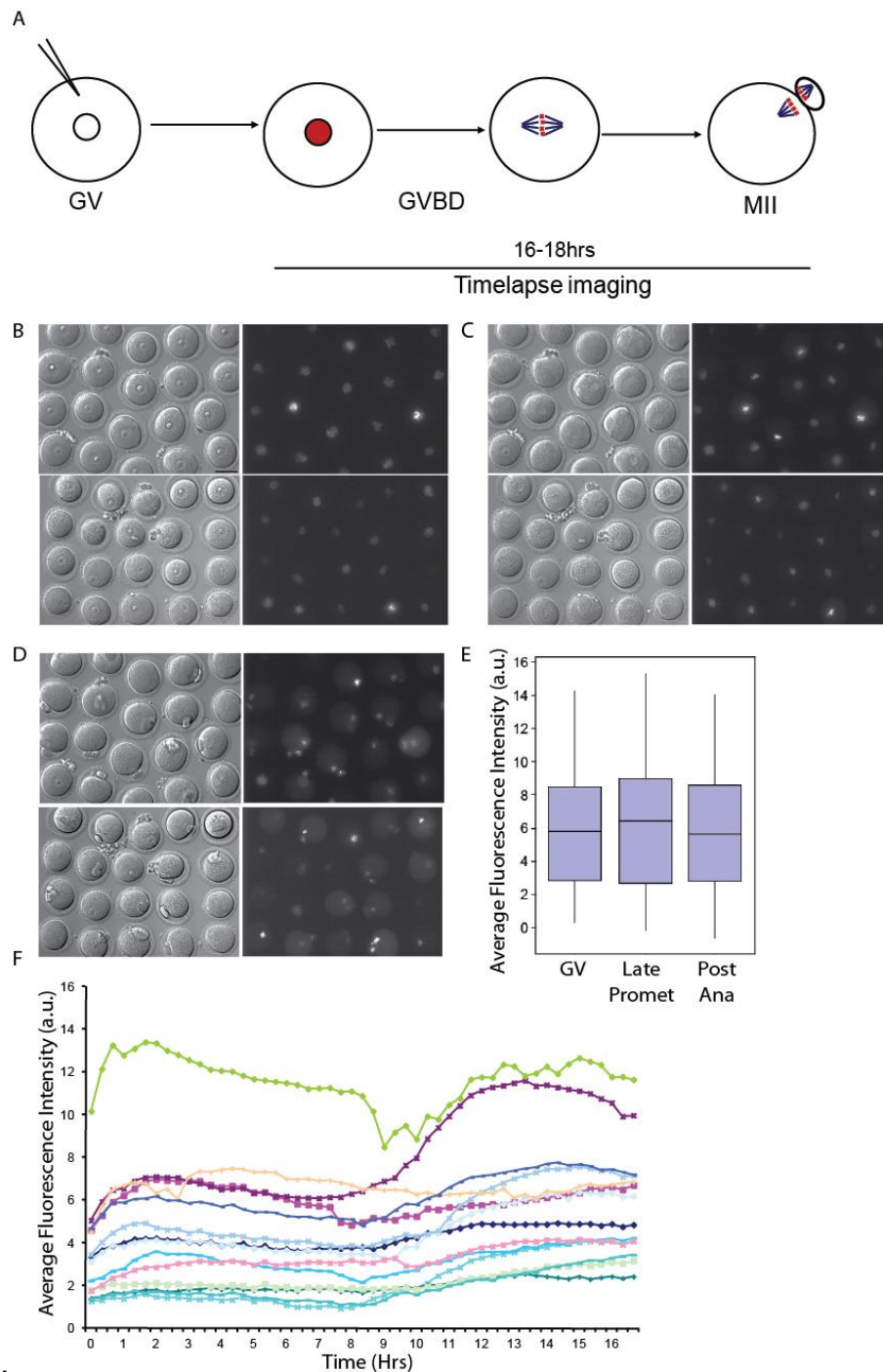


Figure 5.2 - Oocyte micro-injection and translation of histone H2B-RFP. (A) GV stage oocytes were injected with H2B-RFP mRNA. Oocytes were left 2-4hrs to allow mRNA translation and the incorporation of the H2B-RFP protein into the oocyte chromatin. The chromosomes were then visible by immunofluorescence. (B-D) Using the 20x objective 20 oocytes can be imaged at any one time. DIC (left) and H2B-RFP (right) images are shown for 2 different experiments where the majority of the oocytes were at (B) the GV stage; (C) late prometaphase; and (D) post anaphase. Scale bar represents 50 μ m. (E) Box plots showing the mean average fluorescent intensities of H2B-RFP in PB producing oocytes over 3 experiments (n=34) at the GV stage, late prometaphase and post anaphase. Non-fluorescent oocytes and oocytes of high fluorescence intensity were left out of this analysis. (F) Graph showing the average fluorescent intensities over time for the PB producing oocytes in one experiment. These results show that histone injections are fairly constant in size and in the subsequent amount of mRNA being translated.

After recovery, oocytes were washed from the M2-IBMX media into droplets of G-IVF maturation media in a glass-bottomed dish with an oil overlay. This was placed in a chamber mounted on a microscope stage, maintained at 37°C in a gas phase of 5% CO₂ in air.

Because the M phase of MI lasts for 6-12 hours in mouse oocytes (Polanski, 1986; Polanski, 1997), it was necessary to optimise imaging parameters to enable us to track chromosomes from GVBD until PB extrusion while minimizing phototoxic effects. This was done as part of an undergraduate project by Vasileios Floros who found that 100ms acquisitions taken at 5x 7.5µm z-steps at 20 minute intervals was optimal for the 20x 0.75 n.a. oil immersion objective. Importantly he found that oocyte survival and maturation was greatly enhanced by replacing the commonly used M16 culture medium with the more complex G-IVF medium, a “new generation” medium for human IVF which is bicarbonate buffered and contains amino acids, human serum albumin, and gentamicin as an antibacterial agent. Using these conditions, we were able to image up to 20 oocytes simultaneously (Figure 5.2B-D). For visualising chromosomes, the best focus images were selected from the Z stack of each acquisition and analysed using Metamorph imaging software.

Pilot experiments indicated that the above imaging conditions were compatible with maturation of oocytes from 2 month old C57BL/1crfa^f mice, and enabled us to visualise chromosomes from prophase arrest until metaphase II arrest in the majority of oocytes (Figure 5.3 and Figure 5.4).

We found that fully grown (> 67µm diameter) oocytes underwent GVBD, which marks entry into M phase of MI, within 1-2hrs of removal from IBMX or cAMP-containing medium. Oocytes unable to mature within this timeframe were not included in subsequent analyses. Chromosomes from 2 month old mice typically became visible as individual entities 0.67-2hrs after GVBD and congressed on the spindle equator (Figure 5.4F), before becoming tightly aligned prior to anaphase onset (Figure 5.4D). During this time they migrated to the oocyte cortex where they underwent anaphase and PB formation (Figure 5.4G). This was followed by realignment of the MII chromosomes (Figure 5.4E).

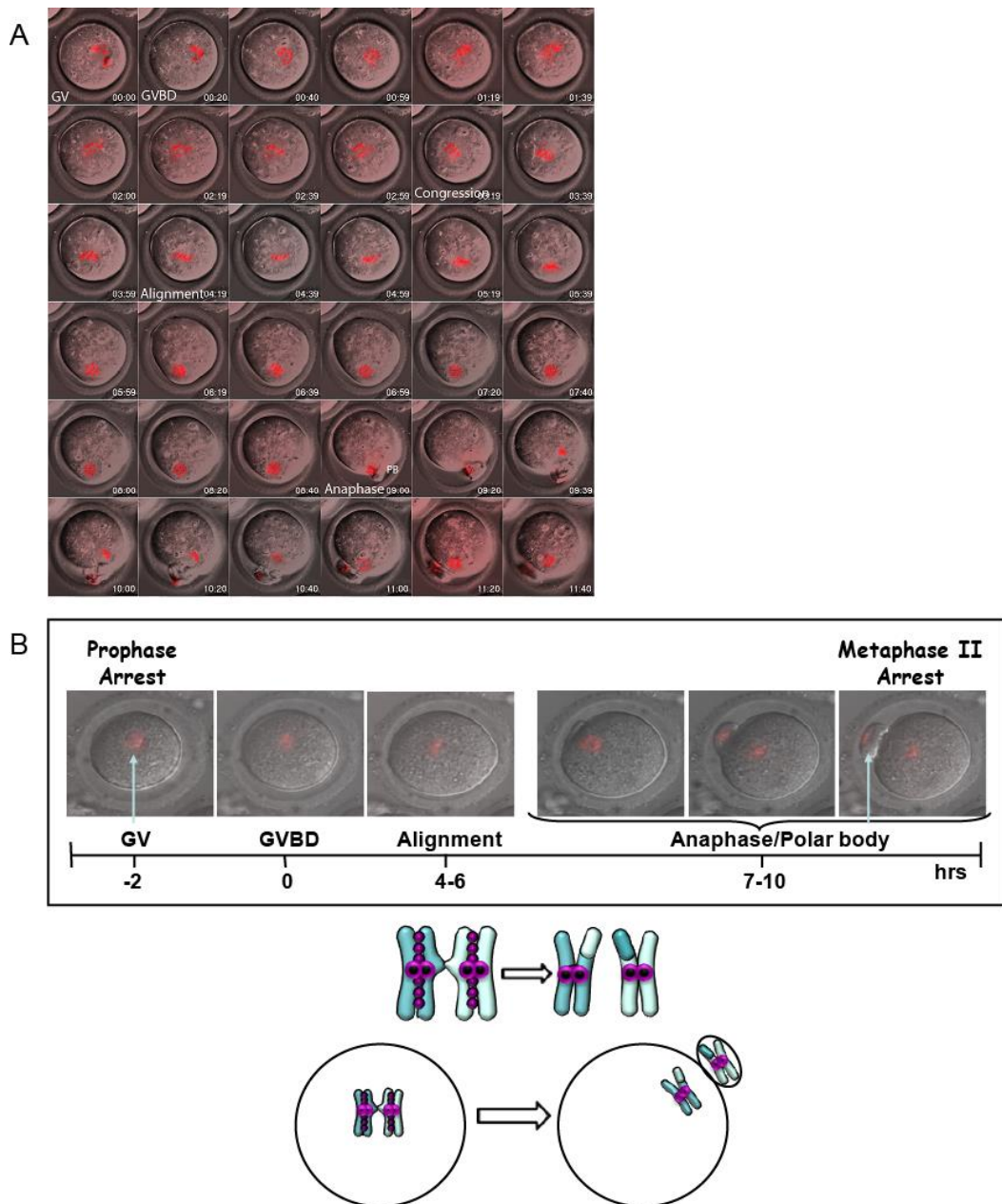


Figure 5.3 - A representative example of chromosome behaviour in an oocyte from a 2 month old mouse. The chromosome dynamics of 2 month old mouse oocytes ($n=16$) injected with mRNA encoding H2B-RFP were visualised by live cell imaging. Images were acquired on $5 \times 7.5\mu\text{m}$ z-planes every 20 minutes for 16-18hrs. (A) Montage of a representative 2 month old mouse oocyte, matured after microinjection with H2B-RFP. The DIC (grey) and histone fluorescence (red) images were overlaid to enable the chromosomes to be visualised in the context of oocyte maturation, from GVBD through to PB extrusion. The montage shows the GV oocyte undergoing GVBD, followed by chromosome congression, alignment and segregation during anaphase of MI. This is then followed by realignment at MII (refer to Figure 5.4A for a montage of the magnified chromosomes). (B) Images summarising the timing of key chromosome events. Arrows show the GV and the PB. The illustration beneath depicts the metaphase to anaphase transition, shown in relation to PB formation.

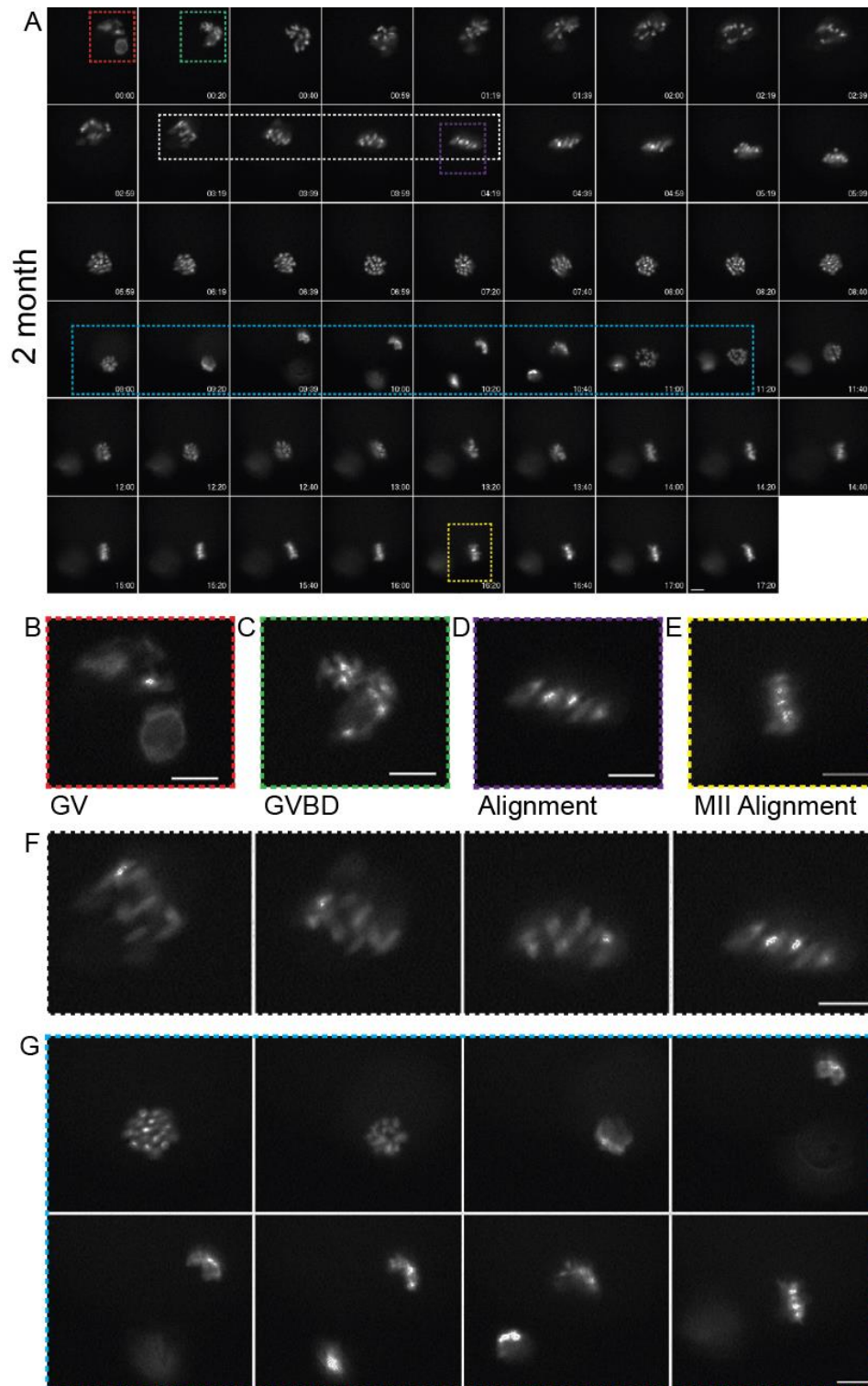


Figure 5.4 - Meiotic progression of an oocyte from a 2 month old mouse. The chromosomal dynamics of 2 month old mouse oocytes ($n=16$) injected with mRNA encoding H2B-RFP were visualised by live cell imaging. Images were acquired on $5 \times 7.5\mu\text{m}$ z-planes every 20 minutes for 16-18hrs. (A) A representative montage showing typical chromosomal behaviour. Individual frames are highlighted and enlarged showing (B) the GV (red box); (C) GVBD (green box); (D) MI alignment (purple box); and (E) MII alignment (yellow box). (F) Frames showing normal congression (white box, left to right). (G) Frames showing anaphase (blue box) starting at the time point before anaphase (top left), early anaphase (top 3 images right) to late anaphase (bottom images). Scale bars represent $10\mu\text{m}$. *Experiment performed in collaboration with Louise Hyslop and Sarah Pace (Lister et al., 2010).*

5.2. Age-dependence of defective chromosome dynamics during progression through MI

Initial experiments using oocytes from 12 month old mice revealed no obvious defects in chromosome behaviour (Sarah Pace, PhD. thesis). We therefore performed live cell imaging on oocytes from 14 month old mice, which in preliminary experiments, have revealed a number of striking defects (Figure 5.5).

As the chromosomes can move in and out of focus during the period of timelapse imaging, not all chromosome events could be monitored in every imaged oocyte. Therefore, we analysed the following events only where they could be clearly visualised from the H2-RFP images: (i) timing and extent of congression; (ii) MI alignment; (iii) anaphase; and (iv) MII alignment. As our interest lay in determining the precise nature of segregation defects, oocytes that failed to mature to MII were excluded from the analysis. Data were obtained from 14 separate experiments in which oocytes (n=87) from 2 month old females (n=9), and oocytes (n=42) from 14 month old females (n=7) were imaged. Under the imaging conditions described above, PB formation was observed in 61.4% and 83.3% of oocytes from 2 and 14 month old mice respectively ($p < 0.05$) (Figure 4.19). Thus, using these criteria, we were able to analyse chromosome dynamics in a total of 16 oocytes from 2 month and 21 oocytes from 14 month old females.

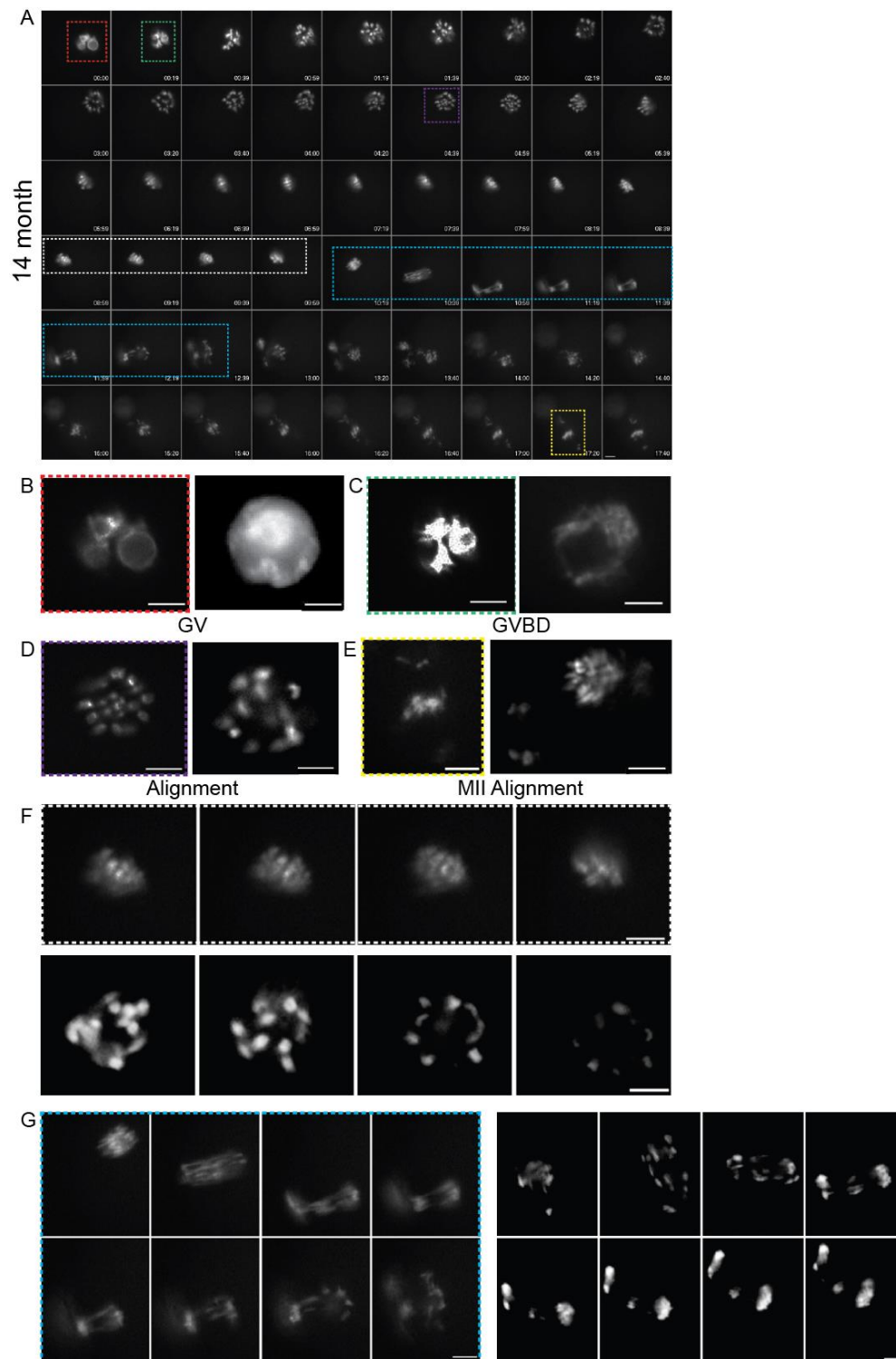


Figure 5.5 - Meiotic progression of oocytes from a 14 month old mouse.

Chromosome dynamics were visualised in 14 month aged mouse oocytes ($n=21$) as in Figure 5.4. (A) A representative montage showing abnormal chromosomal behaviour. Individual frames are highlighted and enlarged showing (B) the GV (red box); (C) GVBD (green box); (D) MI alignment (purple box); and (E) MII misalignment (yellow box). (F) Frames showing abnormal congression (white box, left to right). (G) Frames showing anaphase with severe chromosome bridges (blue box) starting at the time point before anaphase (top left), early anaphase (top 3 images right) to late anaphase (bottom images). Images are also displayed from a second oocyte for each chromosome event. Scale bars represent 10 μ m. *Experiment performed in collaboration with Louise Hyslop and Sarah Pace (Lister et al., 2010).*

5.3. Classification and incidence of age-related chromosome defects

Timelapse images of oocytes from 2 and 14 month old mice which produced a PB were analysed for defects in alignment at MI, segregation defects during anaphase of MI, and realignment during MII. Defects were scored according to their severity (Figure 5.6).

The proportion of oocytes showing a normal MI alignment in the image preceding anaphase was greater in oocytes from 2 month old mice compared with those from 14 month old mice ($p < 0.05$).

The incidence of anaphase defects was also markedly increased in oocytes from 14 month old mice compared with those from 2 month old mice ($p < 0.01$). These ranged in severity from a single lagging chromosome to severe chromosome bridging and trapping of clumps of chromatin at the spindle midzone (Figure 5.6).

In contrast to oocytes from 2 month old mice, we observed misalignment of MII chromosomes in oocytes from aged mice (Figure 5.6). Interestingly the degree of misalignment at MII in aged oocytes often increased progressively following anaphase I (Figure 5.7). Consistent with this the MII spindle was also observed to become progressively more disorganised (S. Pace PhD thesis); (Lister *et al.*, 2010). Higher magnification z-stack images taken at the end of the timelapse experiment (GVBD + 17-20hrs) indicated that misaligned chromosomes consisted of single sisters as well as intact pairs (Figure 5.8A). The presence of single sisters during MII was confirmed by performing chromosome spreads on MII oocytes from 2 month and 14 month aged mice (Figure 5.8B). Precociously separated sister chromatids were observed in 13/14 oocytes from 14 month mice, compared with none observed in oocytes from 2 month old mice ($n=8$).

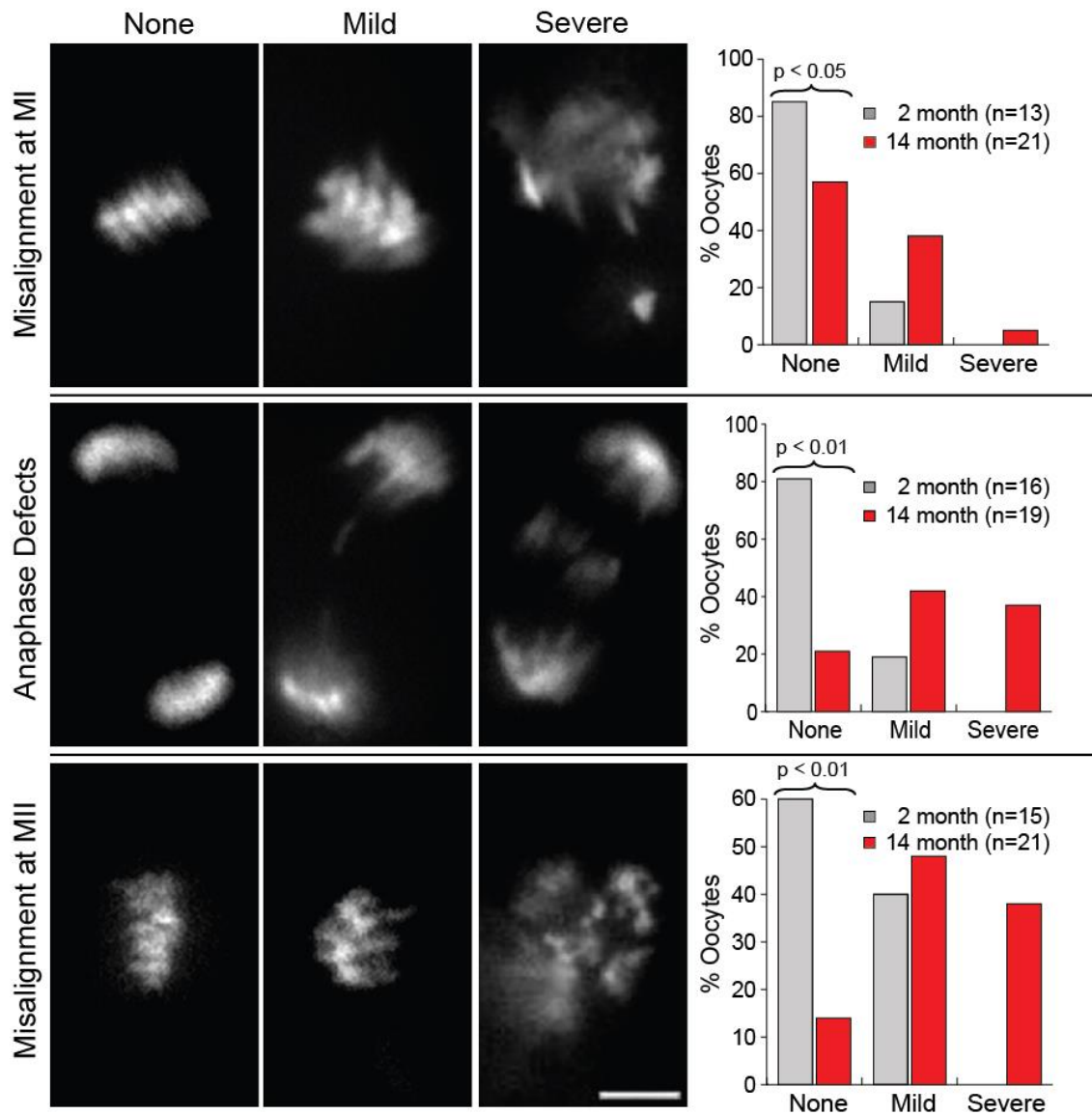


Figure 5.6 – Aberrant chromosome dynamics are more prevalent in oocytes from 14 month old mice. Images from the timelapse microscopy of oocytes from 2 month (n=16) and 14 month (n=21) old mice, show the range of chromosomal defects observed ranging from none, to severe. The top panels show misalignment at MI (in the image preceding anaphase), middle panels show anaphase defects, and the bottom panels show misalignment at MII. Scale bar represents 10 μ m. To the right of each panel are the frequencies of chromosomal defects in oocytes from each age group, scored for misalignment at MI, anaphase I and MII. Only data from oocytes in which each event could be clearly visualized were included in these data sets. The proportion of oocytes showing normal alignment at MI ($p < 0.05$) and MII ($p < 0.01$) was significantly higher in the oocytes from 2 month aged mice. The incidence of anaphase defects was significantly higher ($p < 0.01$) in oocytes from 14 month old mice. *Experiment performed in collaboration with Louise Hyslop and Sarah Pace (Lister et al., 2010).*

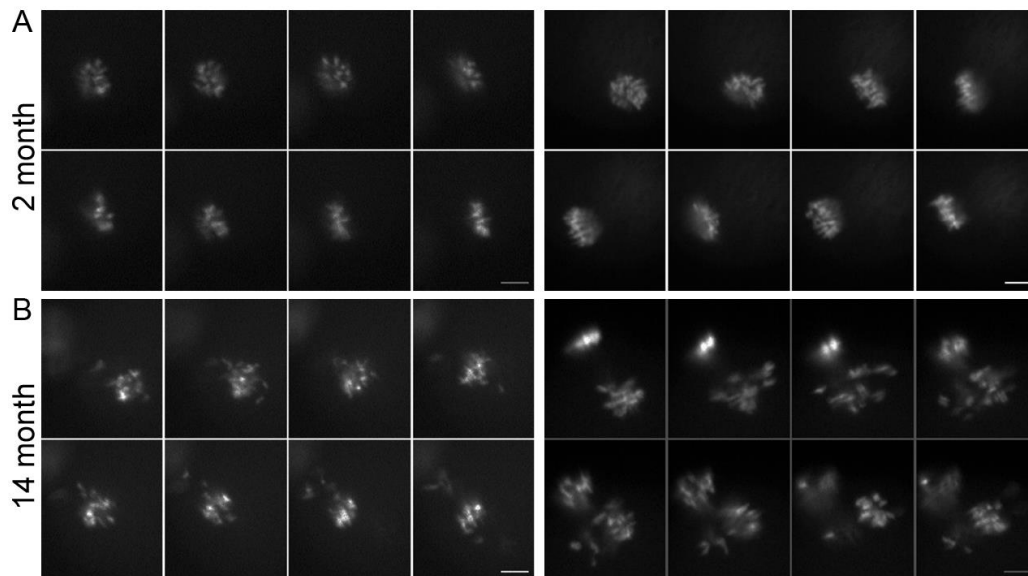


Figure 5.7 - MII misalignment increases progressively after anaphase I in oocytes from 14 month old mice. Chromosome dynamics were visualised in 2 month (n=16) and 14 month aged mouse oocytes (n=21) as in Figure 5.4. (A) Representative montages showing normal MII alignment in 2 oocytes from 2 month old mice. (B) Representative montages showing worsening MII misalignment in 2 oocytes from 14 month old mice. Scale bars represent 10 μ m. *Experiment performed in collaboration with Louise Hyslop.*

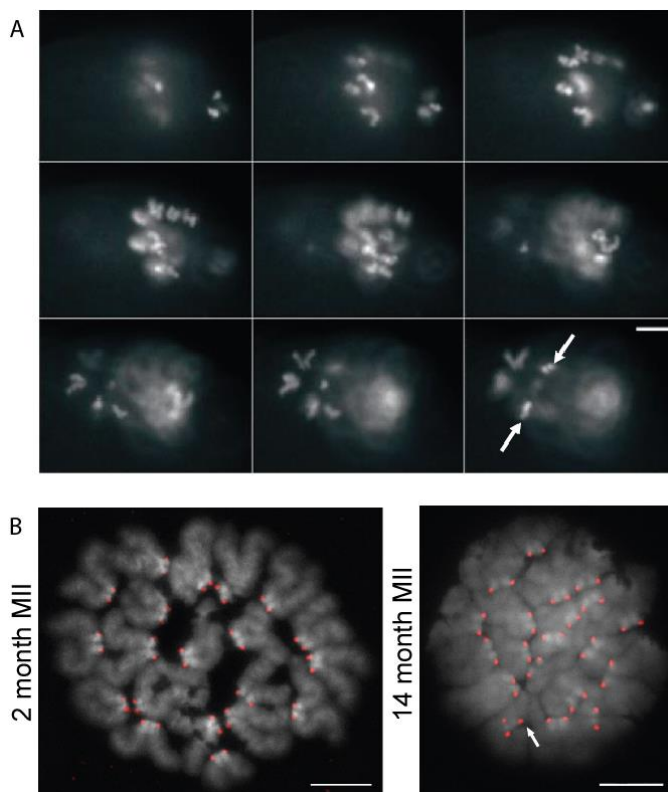


Figure 5.8 - Single sisters are observed in MII oocytes from 14 month old mice. (A) Z-stack images of MII chromosomes taken at the end of a timelapse experiment (GVBD + 17-20hr) in a representative oocyte from a 14 month old mouse expressing

histone-RFP. Images acquired at 1.5 μ m z-steps from the top to the bottom of the spindle. Single sister chromatids were observed, indicated by the white arrows. Scale bar represents 6 μ m. (B) Paraformaldehyde chromosome spreads of a representative MII oocyte from a 2 month old mouse showing a normal MII configuration of 20 dyads, and a 14 month old mouse showing an extra single chromatid, indicated by the white arrow. Spreads are labelled with CREST (red) and DAPI (grey). Single sisters were present in 13/14 MII spreads analysed from 14 month oocytes compared with 0/8 for 2 month oocytes. Scale bar represents 10 μ m. *Experiment performed in collaboration with Louise Hyslop (Lister et al., 2010).*

These data indicate that failure to undergo synchronous segregation of chromosomes during anaphase of MI, followed by misalignment and premature separation of sisters, are the major age-related defects in mouse oocytes. While it is not known whether lagging and trapped chromosomes are a feature of reproductive ageing in human oocytes, it has been reported that misalignment at MII is prevalent in oocytes from older women (Battaglia *et al.*, 1996). Moreover, a large scale analysis of the types of aneuploidy in human MII oocytes indicated that the presence of single sisters showed the strongest correlation with female age (Pellestor *et al.*, 2003). Thus, our findings indicate that the mouse provides a promising model for elucidating the mechanistic basis of maternal age related oocyte chromosome segregation defects. The difference between our findings and previous reports (Brook *et al.*, 1984; Eichenlaub-Ritter *et al.*, 1988) may be attributable to the higher resolution analysis provided by live cell imaging and the advanced age of the females we studied.

5.4. Timing of key events during progression through meiotic M phases

To better understand the pathways leading to defective segregation during MI in oocytes of aged mice, I analysed the timing of key chromosomal events from the time of GVBD. Alignment of bivalents during metaphase I is preceded by a period of pronounced chromosome movements in which bivalents congress on the spindle equator and undergo repeated rounds of kinetochore-microtubule interactions before becoming stably aligned on the metaphase plate (Figure 5.4F, white box). This is termed congression. The majority of oocytes from 2 month (75%, n=12) and 14 month old mice (89%, n=19) underwent congression between 2 and 6 hours after GVBD. While there was no difference in the mean time of congression between the two age groups, 37% of oocytes from the aged females had already congressed by 2.33 hours of GVBD compared with 8% for the young mice (Figure 5.9). It has recently been discovered that mammalian oocyte chromosome congression forms an intermediate configuration, now known as the prometaphase belt (Kitajima *et al.*, 2011). The chromosomes then invade the spindle to form the metaphase plate, which precedes chromosome biorientation. It was observed that 86% of all chromosomes undergo at least one round of error correction of their kinetochore-microtubule attachments, before achieving accurate biorientation (Kitajima *et al.*, 2011). This trend towards early congression may reflect reduced error-correction in oocytes from older females. Failure to correct aberrant kinetochore-microtubule attachments would explain the alignment and segregation defects we observed in oocytes from aged mice. In support of this, lagging chromosomes are the hallmarks of aberrant attachment in mitosis (Cimini *et al.*, 2001; Cimini *et al.*, 2002) and in yeast meiosis (Pidoux *et al.*, 2000).

Congression is followed by alignment of bi-oriented bivalents on the metaphase plate (Schuh and Ellenberg, 2007; Kitajima *et al.*, 2011). In those oocytes in which alignment was captured by live cell imaging, we found that there was no difference in the mean time of alignment between young (n= 11) and aged oocytes (n=13; Figure 5.10). However, the distribution was greater in aged oocytes, with a trend towards delayed alignment. For example, 72% of oocytes from 2 month old mice showed alignment by 6.33 hours of GVBD compared

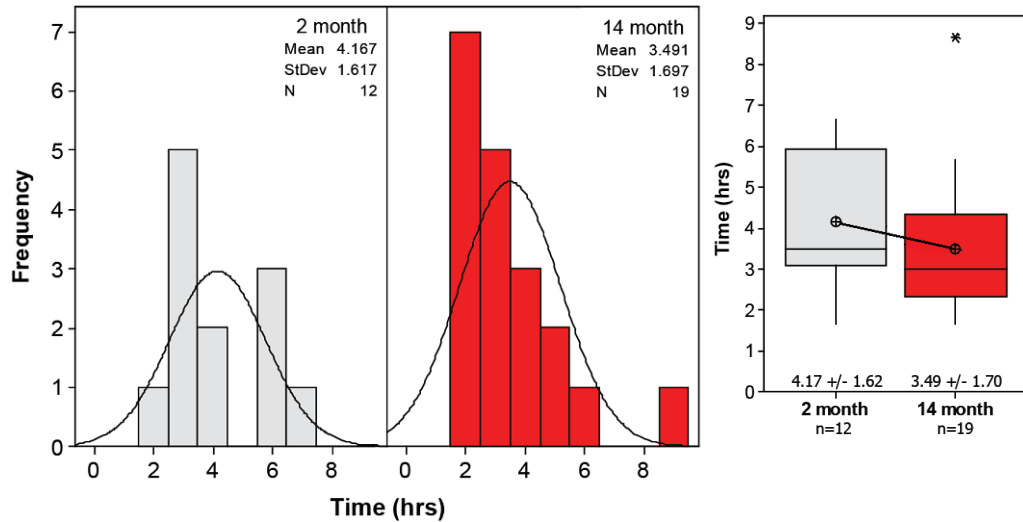


Figure 5.9 - The interval from GVBD to chromosome congression. Graphs showing the range of intervals and the difference in the mean intervals between GVBD and congression in oocytes from 2 month (4.17 ± 1.62 ; $n=12$) and 14 month (3.49 ± 1.70 ; $n=19$) old mice \pm s.d. Although there is a trend towards a shorter mean interval in 14 month aged oocytes, there was no significant difference observed ($p = 0.278$).

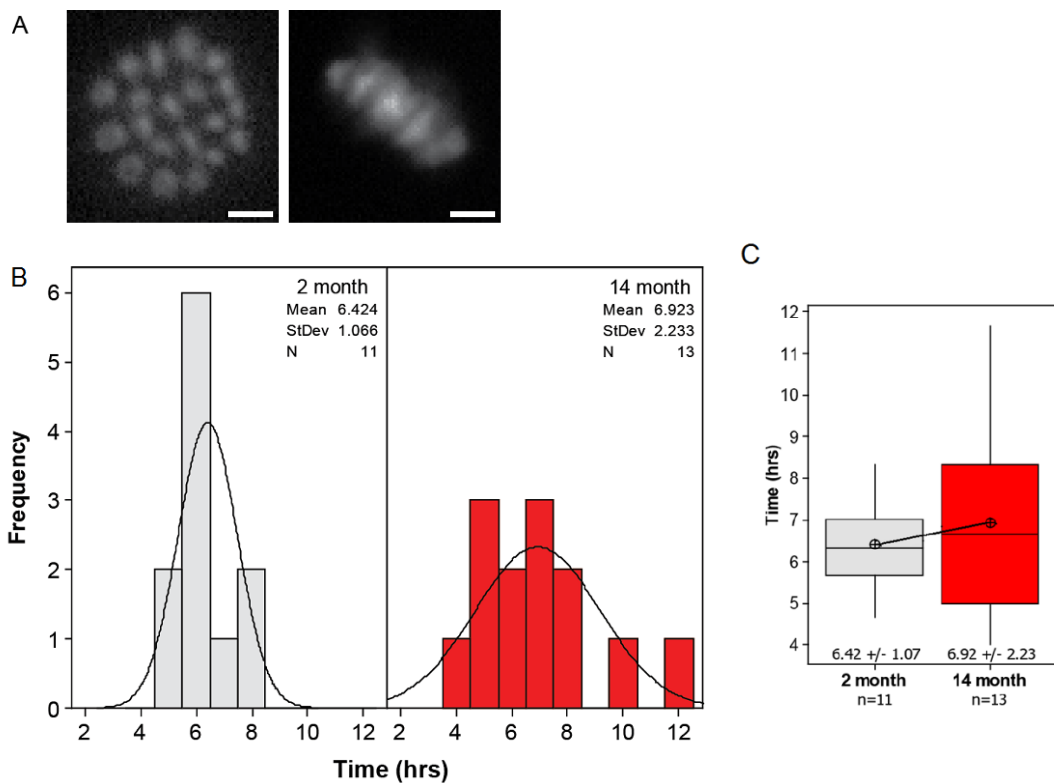


Figure 5.10 - The interval from GVBD to chromosome alignment. (A) Images showing alignment as viewed by looking down the spindle (left image) or across it, perpendicular to the plane of focus (right image). Scale bars represent $5\mu\text{m}$. (B-C) Graphs showing the range of intervals and the difference in the mean intervals between GVBD and alignment in oocytes from 2 month (6.42 ± 1.07 ; $n=11$) and 14 month (6.92 ± 2.23 ; $n=13$) old mice \pm s.d. There was no significant difference observed ($p = 0.484$).

with only 46% in the older age group. Oocytes from the aged mice also showed a trend towards delayed anaphase. Notably, the distribution was tighter in oocytes from the younger mice; 75% had undergone anaphase between 8-10 hours after GVBD, compared with only 60% in the oocytes from the older females (Figure 5.11).

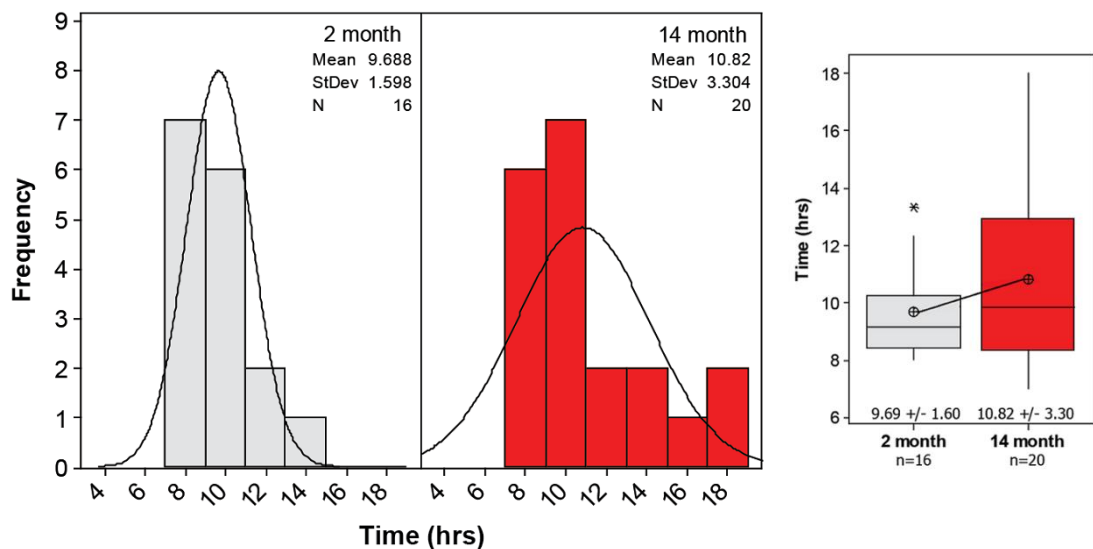


Figure 5.11 - The interval from GVBD to anaphase. Graph showing the range of intervals and the difference in the mean intervals between GVBD and anaphase in oocytes from 2 month (9.69 ± 1.60 ; $n=16$) and 14 month (10.82 ± 3.30 ; $n=20$) old mice \pm s.d. There was no significant difference observed ($p = 0.190$).

Following anaphase the chromosomes emerge from a telophase-like state to realign on the metaphase II plate. Comparison of the interval between the anaphase of MI to MII alignment revealed that MII alignment occurred later in oocytes from 14 month old mice compared to 2 month old mice (Figure 5.12).

However, it should be noted that MII alignment was often not observed in the 14 month oocytes. In 11 of the aged mouse oocytes ($n=17$), compared with just 3 of the 2 month old mouse oocytes ($n=12$), the chromosomes were still in focus and analysable post anaphase, but MII alignment was never observed.

Consequently these could not be included in the analysis of the timing of MII alignment.

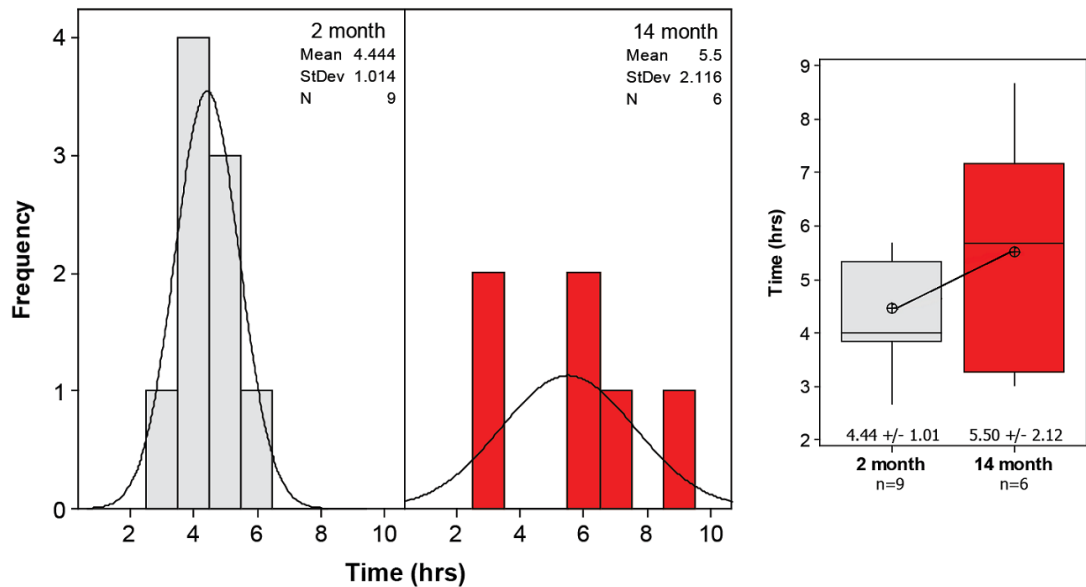


Figure 5.12 - The interval from anaphase of MI to MII alignment. Graph showing the range of intervals and the difference in the mean intervals between anaphase and MII alignment in oocytes from 2 month (4.44 ± 1.01 ; $n=9$) and 14 month (5.50 ± 2.12 ; $n=6$) old mice \pm s.d. There was no significant difference observed ($p = 0.214$).

The data presented above, which is based on oocytes in which the individual events were observed, indicate a trend towards accelerated chromosome congression and delayed anaphase in oocytes from aged females. Consistent with this, analysis of the timing of congression and anaphase in a subset of 2 month ($n=12$) and 14 month ($n=19$) oocytes in which all chromosomal events were observed (Figure 5.13), revealed that the interval between GVBD and anaphase was significantly longer in the oocytes from 14 month old mice compared with 2 month old mice ($p < 0.05$). We found that this was due to a prolonged interval between congression and anaphase ($p < 0.01$) rather than a delay in congression itself.

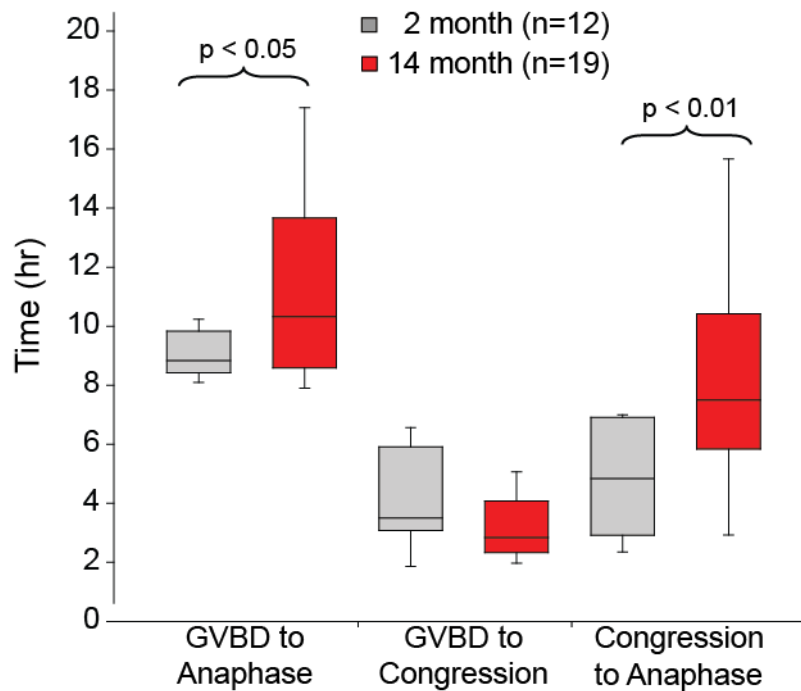


Figure 5.13 - Meiotic progression was delayed in oocytes from 14 month old mice. Graph showing the difference in the intervals between chromosome events in oocytes from 2 month (n=12) and 14 month (n=19) old mice, in which each event could be clearly visualised. The interval from GVBD to anaphase was significantly longer in oocytes from 14 month (10.91 ± 3.37) compared to 2 month old mice (9.22 ± 1.24 ; $p < 0.05$). The interval from GVBD to congression was not significantly different between oocytes from 2 month (4.17 ± 1.62) and 14 month (3.49 ± 1.70) old mice, but the interval from congression to anaphase was significantly longer in oocytes from 14 month aged mice (7.54 ± 4.12) compared those from the younger mice (5.06 ± 2.33 ; $p < 0.01$). Error bars represent s.d. (Lister *et al.*, 2010).

5.5 Is the interval from GVBD to anaphase linked to segregation defects, and how does this fit with spindle checkpoint function?

To determine whether the interval from GVBD to anaphase is linked to the observed segregation defects, we mapped the timeline for each oocyte in which the relevant events could be visualised and scored (Figure 5.14A). This revealed that the majority of oocytes with severe segregation defects showed delayed anaphase (Figure 5.14B).

A plausible explanation for delayed anaphase is that the spindle checkpoint, which is functional in mammalian oocytes (Brunet *et al.*, 2003; Wassmann *et al.*, 2003; Homer *et al.*, 2005; McGuinness *et al.*, 2009) enforces a “wait anaphase” signal until such time as its requirement for kinetochore-microtubule attachment

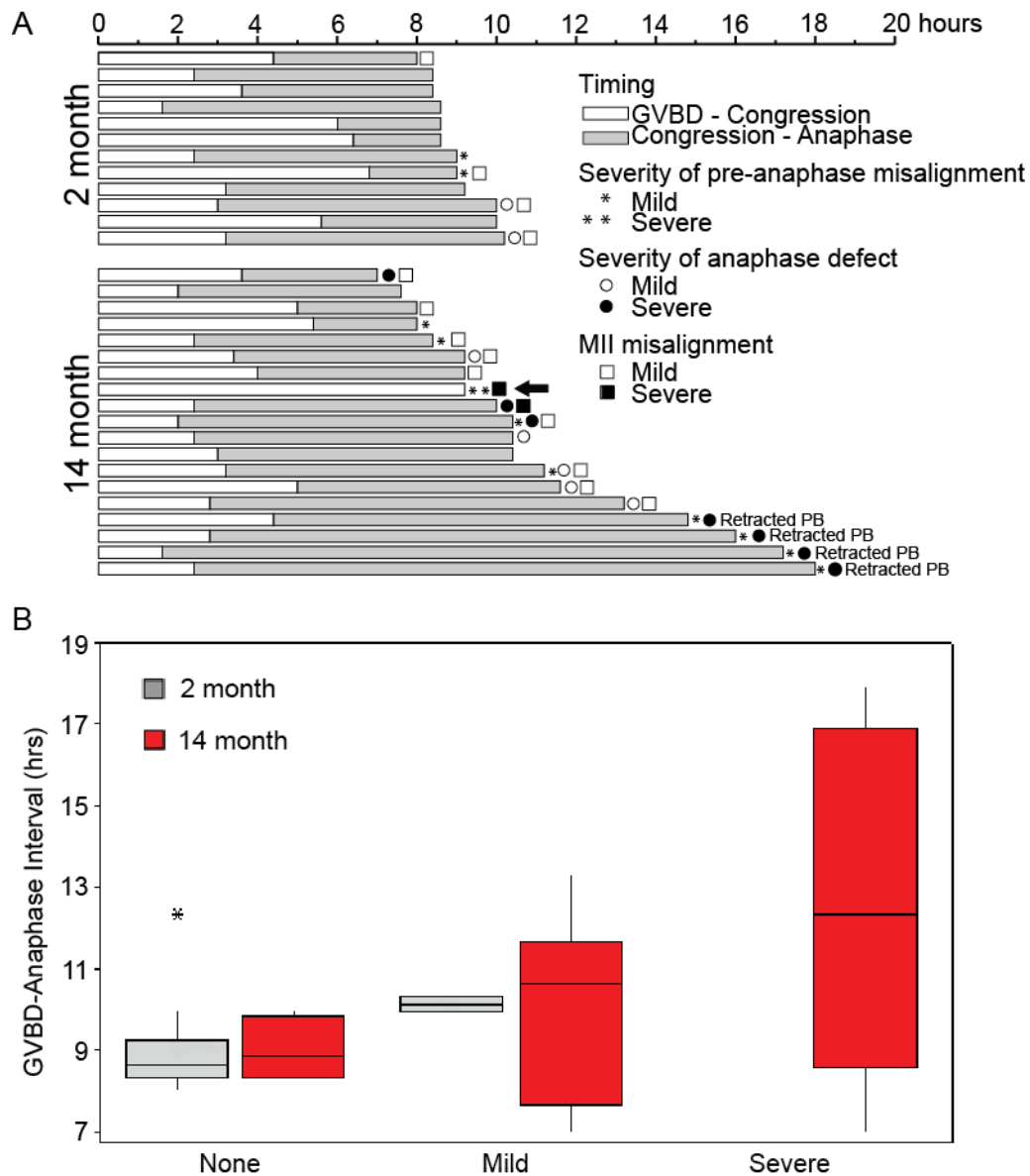


Figure 5.14 - Timeline depicting the incidence of defects. (A) A timeline was drawn for each oocyte from Figure 5.13, a sub-set of oocytes from 2 month (n=12) and 14 month (n=19) old mice in which the chromosomes could be tracked through each event and scored for the severity of any defects. Defects are shown in relation to the interval from GVBD to congression (white bar) and congression to anaphase (shaded bar). The black arrow indicates the failed congression observed in 1/19 oocytes from 14 month old mice. Polar body retraction was observed in association with delayed anaphase and severe segregation defects in 4/19 oocytes from 14 month old mice (Lister *et al.*, 2010). (B) Box plots representing the mean interval between GVBD and anaphase, grouped in relation to the class of severity of the anaphase defect observed (grey=2 month old, red=14 month old). There was no significant difference in the mean interval between oocytes of 2 month and 14 month old mice, where no anaphase defects could be observed (9.03 ± 1.28 and 9.00 ± 0.82 respectively), or where only mild defects were observed (10.17 ± 0.24 and 10.10 ± 2.24 respectively). However, there was a strong trend towards delayed anaphase in oocytes from 14 month old mice with severe defects (12.58 ± 4.31) compared with those which showed no defects ($p=0.057$).

and tension is satisfied. In support of this our lab (S. Pace PhD thesis); (Lister *et al.*, 2010), and others (Duncan *et al.*, 2009) have reported that canonical measures of spindle checkpoint function show no deterioration during female ageing. So, if the checkpoint is functional, why does it not prevent a defective anaphase?

5.6. The spindle checkpoint can be satisfied in the absence of correct monopolar attachments in meiosis I.

Assuming that anaphase occurred upon compliance with the checkpoint's requirement for correct kinetochore-microtubule attachments and tension (Pinsky and Biggins, 2005), the prevalence of lagging chromosomes, which are indicative of aberrant kinetochore-microtubule attachments (Pidoux *et al.*, 2000; Cimini *et al.*, 2001; Cimini *et al.*, 2002) indicate that the spindle checkpoint can be satisfied in the absence of correct monopolar attachment of sister kinetochores in mammalian oocytes. In accordance with this, my previous collaborative work with the Höög lab indicates that univalent chromosomes can evade the spindle checkpoint through the establishment of bipolar rather than monopolar attachment of sister kinetochores (Kouznetsova *et al.*, 2007) (Figure 5.15).

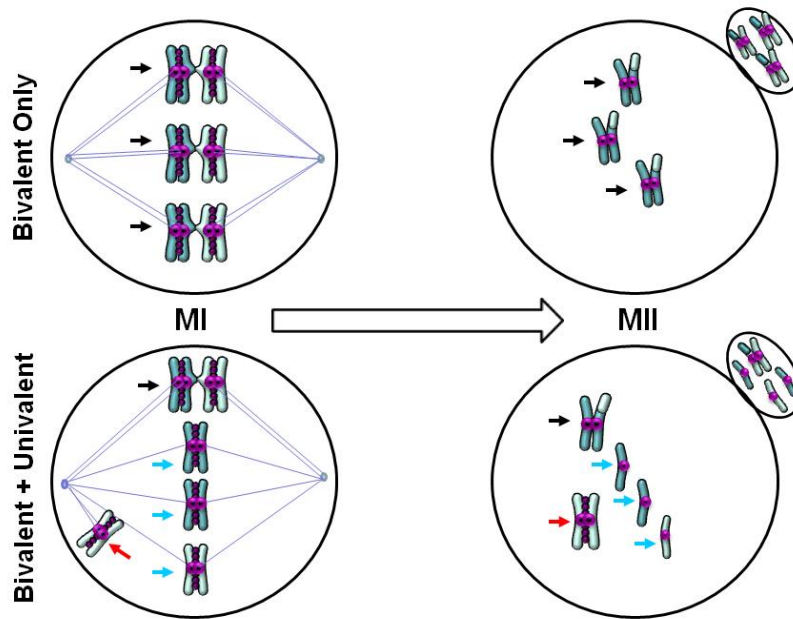


Figure 5.15 - Schematic illustrating segregation patterns for univalent chromosomes. Homologous chromosomes with chiasmata (MI, black arrows) should attach to opposite spindle poles and segregate reductionally, giving rise to dyads (MII, black arrows). A univalent can form a monopolar attachment (MI, red arrow) and segregate intact (MII, red arrow). Alternatively, univalents could form bipolar attachments and segregate equationally (MI, blue arrows) resulting in single sister chromatids (MII, blue arrows).

In a study aimed at tracking the behaviour of univalent chromosomes, we used oocytes from the *Sycp3*^{-/-} mouse strain, which contain 1-4 univalents due to defective synaptonemal complex and crossover formation during meiotic prophase (Yuan *et al.*, 2002; Kouznetsova *et al.*, 2007). Evaluation of the MII karyotype following timelapse imaging, revealed that 93% of *Sycp3*^{-/-} oocytes yield at least one single sister chromatid at MII. Lagging chromosomes at anaphase were found to be a feature in 77% of *Sycp3*^{-/-} mouse oocytes imaged by timelapse microscopy (n=13, Figure 5.16). No such defects were observed in the wild type oocytes (n=5). *Sycp3*^{-/-} oocytes were also prone to chromosome scattering during early prometaphase (69%) followed by marked stray chromosomes (31%). Despite this they were able to achieve tight alignment (75%) before the onset of anaphase.

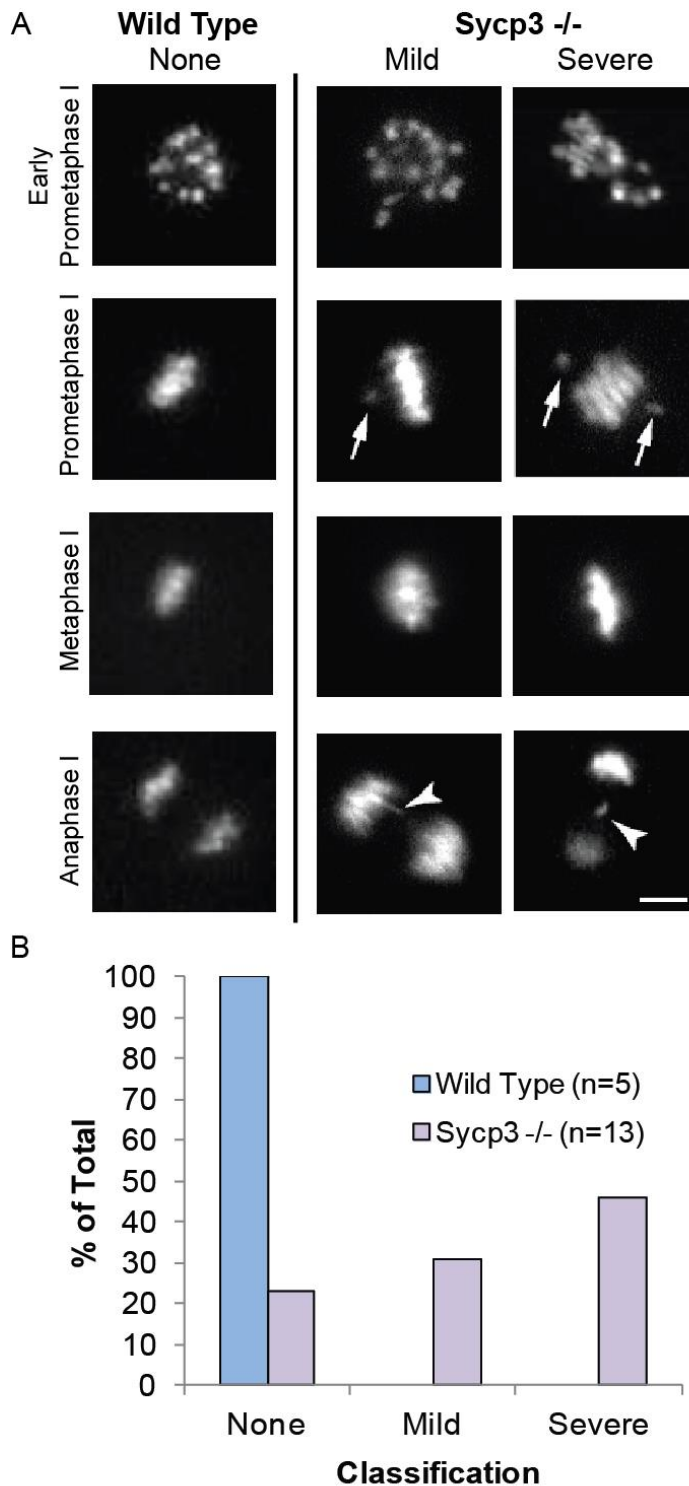


Figure 5.16 - Chromosomes in *Sycp3*^{-/-} mice achieve alignment before undergoing an error prone anaphase. The chromosome dynamics of wild type (n=8) and *Sycp3*^{-/-} (n=13) mouse oocytes, injected with mRNA encoding H2B-RFP were visualised by live cell imaging. Images were acquired on 5 x 7.5 μ m z-planes every 20 minutes for 16-18hrs. (A) Representative timelapse images are shown illustrating wild type and *Sycp3*^{-/-} oocyte maturation. Scale bar represents 10 μ m. The wild type oocytes displayed good congression and maintained a tight alignment until anaphase, where no defects were observed (5/5). The chromosomes of the *Sycp3*^{-/-} oocytes were scattered during early prometaphase (9/13) which was followed by the presence of misaligned stray chromosomes (4/13, white arrows). Most oocytes achieved a tight

alignment (9/12) before anaphase onset where lagging and stray chromosomes were observed (10/13, white arrow heads). *Experiment performed in collaboration with Anna Kouznetsova (Kouznetsova et al., 2007).* (B) Graph depicting the different classes of anaphase defect observed in wild type (n=5) and *Sycp3*^{-/-} mouse oocytes (n=13) where anaphase could be clearly visualised.

Univalent chromosomes are associated with a high incidence of lagging and trapped chromosomes during anaphase of MI. High resolution analysis of the kinetochore-microtubule attachments indicated that bipolar attachment was prevalent in univalent chromosomes of *Sycp3*^{-/-} mouse oocytes (Kouznetsova *et al.*, 2007). These data support the hypothesis that aberrant kinetochore-microtubule attachment may contribute to the lagging/trapped chromosomes observed in oocytes from aged mice, and such attachments can evade the spindle checkpoint.

The delayed onset of anaphase in oocytes with lagging and trapped chromosomes (Figure 5.11) is also consistent with the presence of univalent chromosomes. Recent findings in fission yeast indicate that anaphase onset is delayed in the presence of univalent chromosomes, and that this delay is correlated with the number of univalents detected (Sakuno *et al.*, 2011). In light of these findings, I re-analysed the *Sycp3*^{-/-} timelapse images to determine whether there was a correlation between the presence of univalent chromosomes, and the timing of anaphase in *Sycp3*^{-/-} mouse oocytes (Figure 5.17).

There was a tendency for the interval from GVBD to anaphase to be longer in *Sycp3*^{-/-} oocytes (9.18 ± 2.37 , n=15) compared with wild type controls (8.53 ± 1.43 , n=5, p=0.575). In addition, *Sycp3*^{-/-} oocytes in which lagging chromosomes were observed (n=6) showed a trend towards a longer interval from GVBD to anaphase (9.71 ± 2.60) compared with those in which no anaphase defects were observed (8.23 ± 0.87 , n=4, p=0.312). Thus, the association between anaphase defects and the delayed onset of anaphase observed above in the aged oocytes (Figure 5.17) may be a general feature of MI in mammalian oocytes.

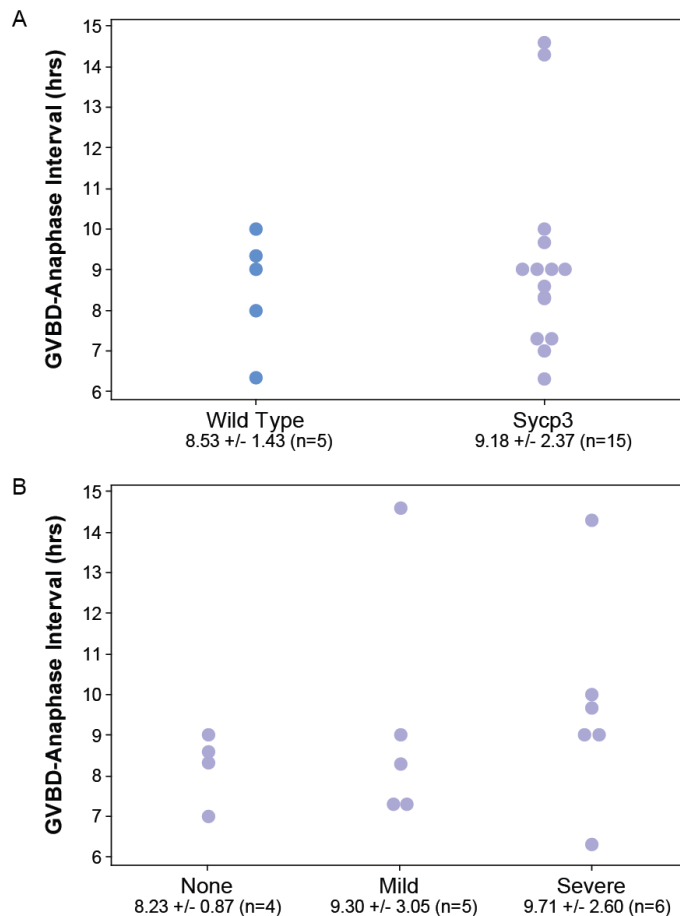


Figure 5.17 - Anaphase is delayed in *Sycp3*^{-/-} oocytes which display lagging chromosomes at anaphase. Dot plots depicting the range observed in the interval from GVBD and anaphase in (A) Wild type (n=5) and *Sycp3*^{-/-} oocytes (n=15), and (B) for the different classifications of anaphase defects in *Sycp3*^{-/-} oocytes. Anaphase was delayed where lagging chromosomes were observed.

Given the similarities between the timing and type of anaphase defects observed in aged oocytes with those of *Sycp3*^{-/-} mice, my next step was to investigate whether univalent chromosomes were present in oocytes from aged females.

5.7. Are lagging chromosomes and a delayed anaphase due to the presence of univalent chromosomes in oocytes from aged mice?

In order to investigate whether univalent chromosomes are present in MI oocytes from aged mice, surface spread chromosomes were prepared during mid prometaphase I (GVBD + 5hrs) in oocytes from 2 month and 14 month old mice.

Surprisingly, we observed no univalent chromosomes in oocytes from aged mice. However, there was a prevalence of homologous pairs which appeared to be associated at telomeres, but without visible chiasmata (Figure 5.18).

Such distally associated homologous chromosomes were observed in 63% of 14 month old oocytes (n=37) compared with just 14% of 2 month old oocytes (n=19). The mean number of distally associated homologues per oocyte was 0.19 ± 0.52 and 5.21 ± 6.86 for 2 and 14 month old mice respectively (Figure 5.18B and C). Analysis of all the homologous chromosomes imaged revealed that 33.9% of the homologs in 14 month aged mouse oocytes had distally associated chromosomes (n=292 pairs) compared with only 1% of 2 month oocytes (n=693 pairs) (Figure 5.18D).

Classification of homologues according to the number of visible chiasmata revealed that female ageing was associated with a significant increase ($p < 0.001$) in the proportion of homologues with distal associations in oocytes from aged females (Figure 5.18). There was also a significant decline in the proportion of aged oocyte bivalents showing just single chiasmata ($p < 0.001$). There was no difference in the proportion of oocytes showing multiple chiasmata between the two age groups. Thus, these data indicate that single chiasmate bivalents are prone to destabilisation during female ageing. Chiasmata destabilisation may affect the ability of the chromosomes to establish correct monopolar attachments (Sakuno *et al.*, 2011), which could contribute to the anaphase defects observed in oocytes from aged females.

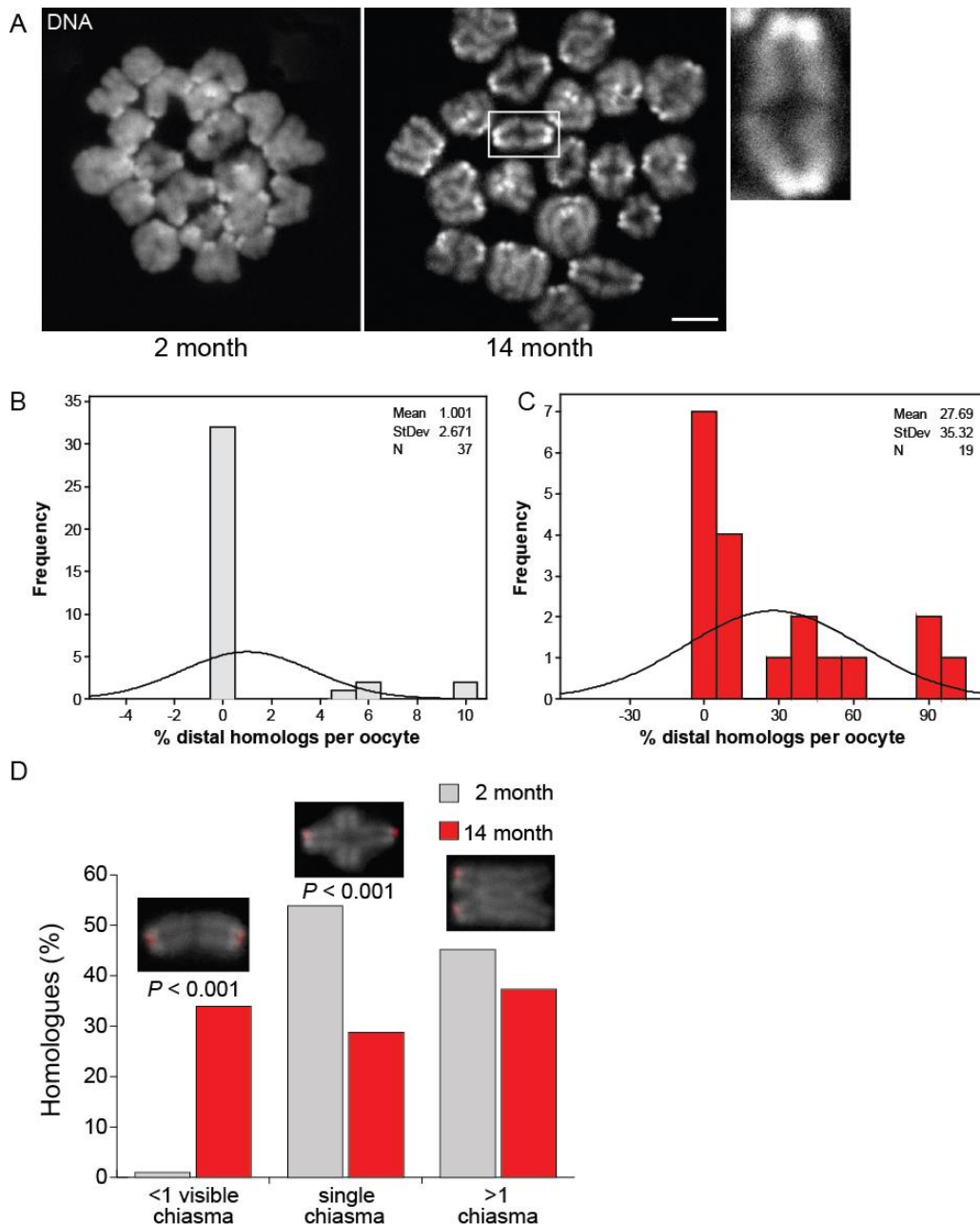


Figure 5.18 - Distally associated chiasmata are prevalent in oocytes from 14 month old mice. Paraformaldehyde chromosome spreads were prepared at prometaphase I (GVBD + 5hrs) in 2 month (n=37 oocytes from 5 mice) and 14 month old (n=19 oocytes from 7 mice) mouse oocytes. These were stained for DAPI (grey) with or without CREST (red). (A) Representative image from a 2 month oocyte showing normal bivalent configurations with one or more chiasmata, and a 14 month oocyte showing an increased proportion of distally associated chiasmata. The inset in the 14 month image shows an example of a distally associated homolog with no visible chiasmata. Scale bar represents 10 μ m. (B) Histograms depicting the percentage of distally associated chromosomes observed per oocyte in 2 month and (C) 14 month old mice. (D) Analysis of the proportions of homologs classified as having either no visible chiasmata, one chiasmata, or more than one chiasmata in 2 month and 14 month oocytes, with representative images of each classification. The analysis was based on pairs of homologs where the chiasmata classification could be clearly determined (n= 693 pairs from 2 month and n= 292 pairs from 14 month aged mouse oocytes). *Experiment performed in collaboration with Dimitrios Kalleas (Lister et al., 2010).*

To summarise, the data presented in this chapter indicate that C57BL/1crfa^t mice exhibit a maternal age effect. With advanced maternal age aberrant chromosome dynamics become more prevalent, observed as an increased incidence of anaphase defects followed by misalignment and single sister chromatids observed at MII. Meiotic progression is delayed in these aged oocytes, with an increased interval between GVBD and anaphase due to a prolonged interval between congression and anaphase. This delay may be due to the chromosomes trying to achieve correct alignment, by undergoing multiple rounds of biorientation. Although a delay in anaphase has also been attributed to the presence of univalent chromosomes, none were observed in oocytes from aged mice. There was however a prevalence of distally associated homologous chromosomes with no visible chiasmata due to destabilisation of single chiasmate bivalents. If the integrity of the bivalent is being compromised by the destabilisation of chiasmata, it may be unable to establish the tension required for the stable biorientation of homologous chromosomes.

Chapter 6. Results III – Mechanisms underlying anaphase defects

Despite the 14 month aged mouse oocytes showing largely normal congression, spindle formation and alignment preceding anaphase I, a large proportion of these oocytes failed to segregate their chromosomes faithfully. This was observed by lagging chromosomes and anaphase bridges, followed by spindle destabilisation and misalignment at MII. The compromised bivalent structure and presence of prematurely separated sister chromatids, suggests that this is due to errors in the biorientation and accurate segregation of homologous chromosomes.

As the previous data have now very clearly established that there is a maternal age effect in the C57BL/1crfa^f mouse strain, the next step was to explore the mechanisms underlying the observed anaphase defects.

The distally associated homologues observed in oocytes from aged mice were reminiscent of an earlier report from a study on oocytes lacking the meiosis-specific cohesin sub-unit SMC1 β (Hodges *et al.*, 2005). It was found that while SMC1 β deficient oocytes have reduced crossover formation, the position of Mlh1 foci, which mark the sites of crossover formation during early prophase (Svetlanov and Cohen, 2004), were similar to wild type control oocytes (Hodges *et al.*, 2005). By contrast, chromosome spreads prepared during prometaphase revealed a prevalence of distally associated homologues in which the chiasmata were said to have “terminalized” (Hodges *et al.*, 2005) (Figure 6.1). Crucially, this defect was amplified during female ageing (Hodges *et al.*, 2005). We therefore asked whether the chromosomal configuration observed in our aged oocytes (Figure 5.18), might also be explained by the depletion of cohesin.

As well as SMC1 β , another well researched meiotic cohesin component is the alpha-kleisin subunit Rec8. Rec8 containing cohesin is essential for cohesion during MI, and for recombination (Klein *et al.*, 1999; Watanabe and Nurse, 1999) (Figure 6.2). It has been shown that Rec8 cleavage is essential for homologue disjunction in mouse oocytes (Kudo *et al.*, 2006).

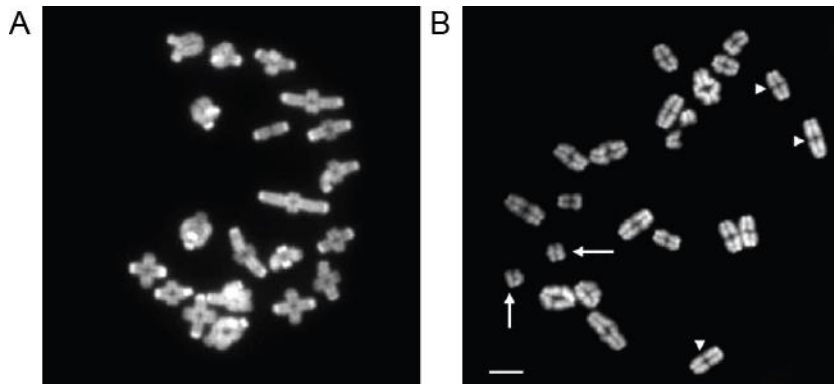


Figure 6.1 - Distally associated chiasmata are prevalent in oocytes from SMC1 β knockout mice. Air dried preparations of diakinesis–metaphase I chromosomes from (A) wild-type and (B) SMC1 β -deficient mouse oocytes, stained with DAPI. SMC1 β deficient oocytes show an increased incidence in distal chiasmata (arrowheads) and the presence of unpaired univalent chromosomes (arrows). Scale bar represents 5 μ m. (Hodges *et al.*, 2005).

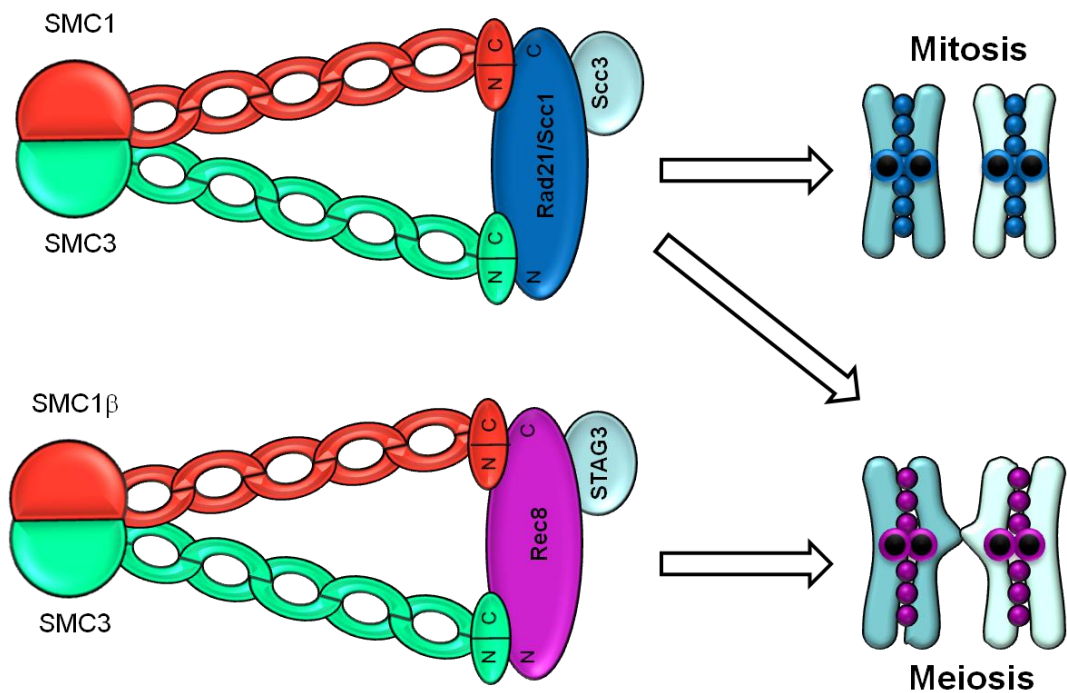


Figure 6.2 - The cohesin complex. A diagrammatic representation of the architecture of the cohesin complex. Scc1 (also known as Rad21, or the meiotic variant Rec8) connects the nuclear binding domains of the Smc1 and Smc3 heterodimer forming a ring like structure. Scc1 then recruits Scc3. Meiotic cohesin complexes can contain either Rec8 or Scc1, but it is only the Rec8 containing cohesin that is necessary for cohesion during MI. Mammalian meiotic cohesin complexes also consist of SMC1 β , and STAG3.

Remarkably, more recent findings indicate that Rec8 containing complexes loaded during the pre-meiotic S phase are sufficient to maintain cohesion in mouse oocytes until sexually maturity and beyond (Tachibana-Konwalski *et al.*, 2010). Similar findings were reported for SMC1 β (Revenkova *et al.*, 2010). These data together with the SMC1 β null oocyte phenotype (Hodges *et al.*, 2005) make cohesin depletion a strong candidate mechanism for the age-related loss of bivalent structure reported in the previous chapter.

In this chapter I use oocytes from the C57BL/1crfa^f females to determine whether chromosomal cohesin is reduced with female ageing. I also investigated the mechanisms by which cohesin might be depleted, and examine the role of the cohesin protector Sgo in regulating chromosomal-association of cohesin during ageing and during progression through MI.

6.1. Is cohesin depleted during maternal ageing?

We addressed this question by immunofluorescence staining for Rec8 during mid-late M phase of MI (GVBD + 5hrs). Staining of surface spread chromosomes revealed reduced levels of Rec8 in the oocytes from 14 month old mice (n=9) compared with those from 2 month old mice (n=14) (Figure 6.3).

Rec8 staining was markedly reduced on the chromosome arms of the oocytes of 14 month old mice. Notably, the intense pericentromeric Rec8 staining which was very clearly visible in the 2 month oocytes was largely absent from the aged oocytes.

The CREST antibody recognises the centromeric proteins CENP-A, CENP-B and CENP-C (Earnshaw and Cooke, 1989), which are positioned on the inner kinetochore (Hemmerich *et al.*, 2008; Santaguida and Musacchio, 2009). To determine whether Rec8 was specifically reduced at the centromeres, we measured the fluorescence intensity of Rec8 at CREST foci and calculated the ratio of Rec8 to CREST fluorescence intensities. Comparison of the Rec8:CREST fluorescence intensity between oocytes from 2 month and 14 month mice revealed that the ratio was significantly reduced in 14 month oocytes compared with those from 2 month old mice ($p < 0.001$) (Figure 6.4).

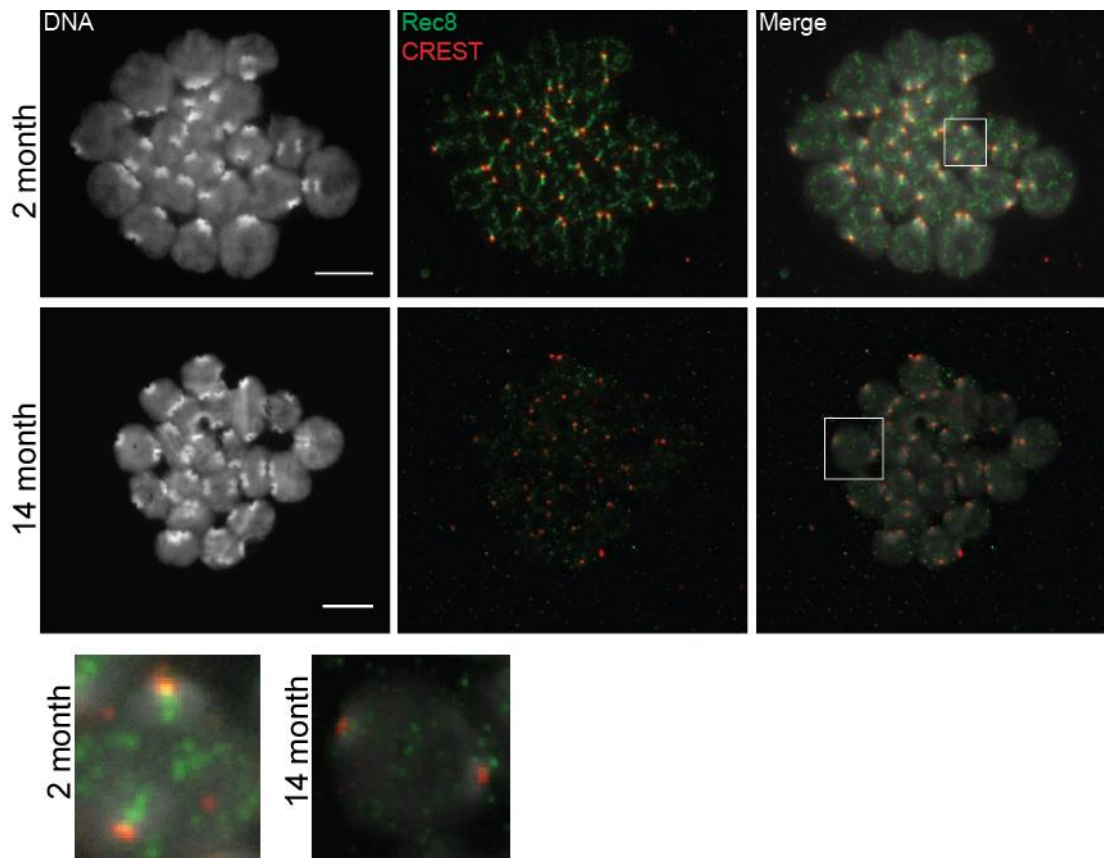


Figure 6.3 - Chromosome associated cohesin is reduced in the oocytes of aged mice. Paraformaldehyde chromosome spreads were prepared at mid prometaphase I (GVBD + 5-6hrs) in oocytes from 2 month (n=14 oocytes from 4 mice) and 14 month (n=9 oocytes from 6 mice) old mice. Representative images show DAPI DNA (grey), Rec8 (green) and CREST (red) staining. Insets show enlarged images of chromosomes at 2 months (left) and 14 months (right). Scale bar represents 10 μ m. Rec8 staining was reduced in the 14 month oocytes, which is particularly noticeable by the absence of the intense Rec8 staining under the centromere, which was evident in the oocytes from 2 month aged mice. *Experiment performed in collaboration with Dimitrios Kalleas and Anna Kouznetsova (Lister et al., 2010).*

This indicates that the centromeric cohesin is vulnerable to depletion during female ageing.

It was not possible to perform ratiometric analysis of cohesin loss on chromosome arms due to the absence of an appropriate marker for normalising arm cohesin. However, reduced arm cohesin, particularly in the peri-centromeric region, is obvious from the immunolabelled chromosome spreads. I therefore conclude that cohesin is lost from chromosome arms as well as centromeres during female ageing.

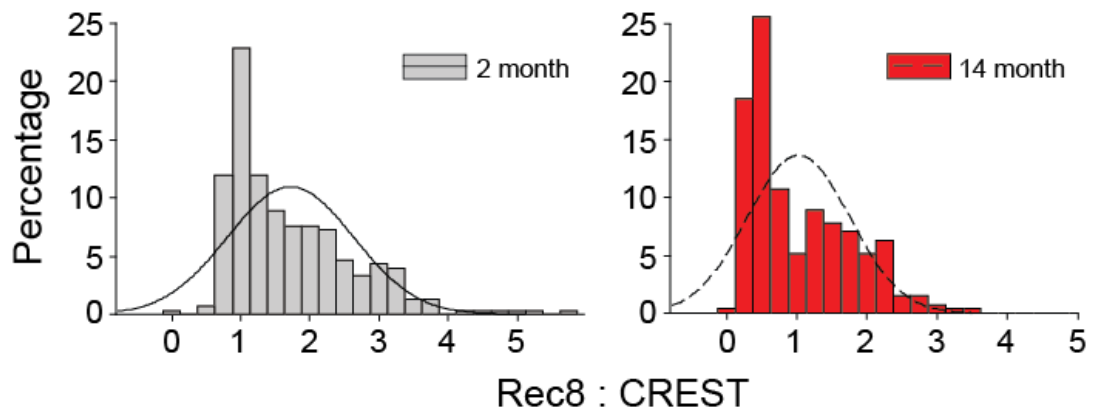


Figure 6.4 - Centromeric cohesin is reduced in the oocytes of aged mice.

Frequency distributions of the Rec8:CREST fluorescence intensity ratios, measured at the centromeres of 2 month (n=302 centromeres; 8 oocytes from 4 mice) and 14 month (n= 270 centromeres; 7 oocytes from 6 mice) oocyte chromosome spreads, from Figure 6.3. There was significantly reduced colocalisation of Rec8 with the CREST foci observed in oocytes of 14 month old mice (1.02 ± 0.73) compared with 2 month old mice (1.71 ± 0.91) ($p < 0.001$) (refer to methods 3.17). *Experiment performed in collaboration with Dimitrios Kalleas and Anna Kouznetsova (Lister et al., 2010).*

6.2. Is depletion of cohesin during maternal ageing associated with individualisation of sister centromeres?

The closely apposed structure of sister centromeres is essential for mono-orientation of sister chromatids, and accurate segregation of homologues during MI (Petronczki *et al.*, 2003; Hauf and Watanabe, 2004; Marston and Amon, 2004; Brar and Amon, 2008). Work in fission yeast indicates that cohesin at the core centromere is essential for maintaining the unified structure of sister centromeres (Sakuno *et al.*, 2009). During analysis of the prometaphase I chromosome spreads, it became evident that the distance between sister centromeres was increased in oocytes from aged mice. In oocytes from young mice, the CREST signal at sister centromeres predominantly appeared as a single focus. By contrast, aged oocytes showed a prevalence of two foci, separated to varying degrees. Quantification of the different types of signals revealed that CREST appeared as single foci in 90% of centromeres from 2 month old mouse oocytes compared with only 32% of centromeres in 14 month oocytes ($p < 0.001$). The majority of centromeres from the older females were observed as either two separate but adjacent foci, or two well separated foci (Figure 6.5).

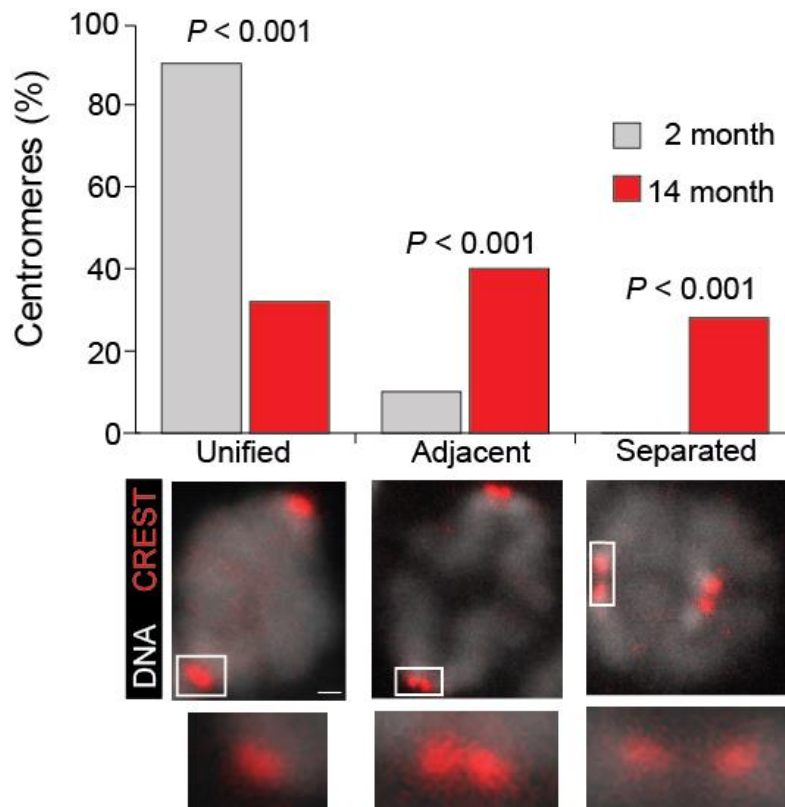


Figure 6.5 - Splitting of sister centromeres occurs in oocytes of aged mice. The chromosome spreads from Figure 6.3 were further analysed and classed depending on the configuration of the sister centromeres. These were either “unified”, where the CREST staining was observed as a single focus, “adjacent”, where the CREST signal appeared as two separate but adjacent foci, or “separated”, where the CREST foci were well separated but the sister chromatids had not segregated. Insets show magnified images of the centromeres. Scale bar represents 1 μ m. The graph shows the percentage of centromeres in 2 month (n=360 centromeres; 8 oocytes from 4 mice) and 14 month (n=293 centromeres; 7 oocytes from 6 mice) old mouse oocytes which were organised into each classification. The proportion of centromeres showing a unified structure was significantly reduced in the oocytes from 14 month old mice ($p < 0.001$), whereas the prevalence of adjacent and separated centromeres was significantly greater ($p < 0.001$). *Experiment performed in collaboration with Dimitrios Kalleas (Lister et al., 2010).*

The incidence of adjacent or separated centromeres was significantly increased in the oocytes from 14 month old mice compared with those from 2 month old mice ($p < 0.001$). In accordance with these data, measurement of the distance between the extremities of the CREST signals revealed a significantly increased distance in oocytes from aged mice ($p < 0.001$) (Figure 6.6A). We also found that the Rec8: CREST fluorescence intensity ratio, was negatively correlated with the distance between the sister centromeres in oocytes from 14 month old mice (Figure 6.6B). This indicates that increased distance may be caused by cohesin loss.

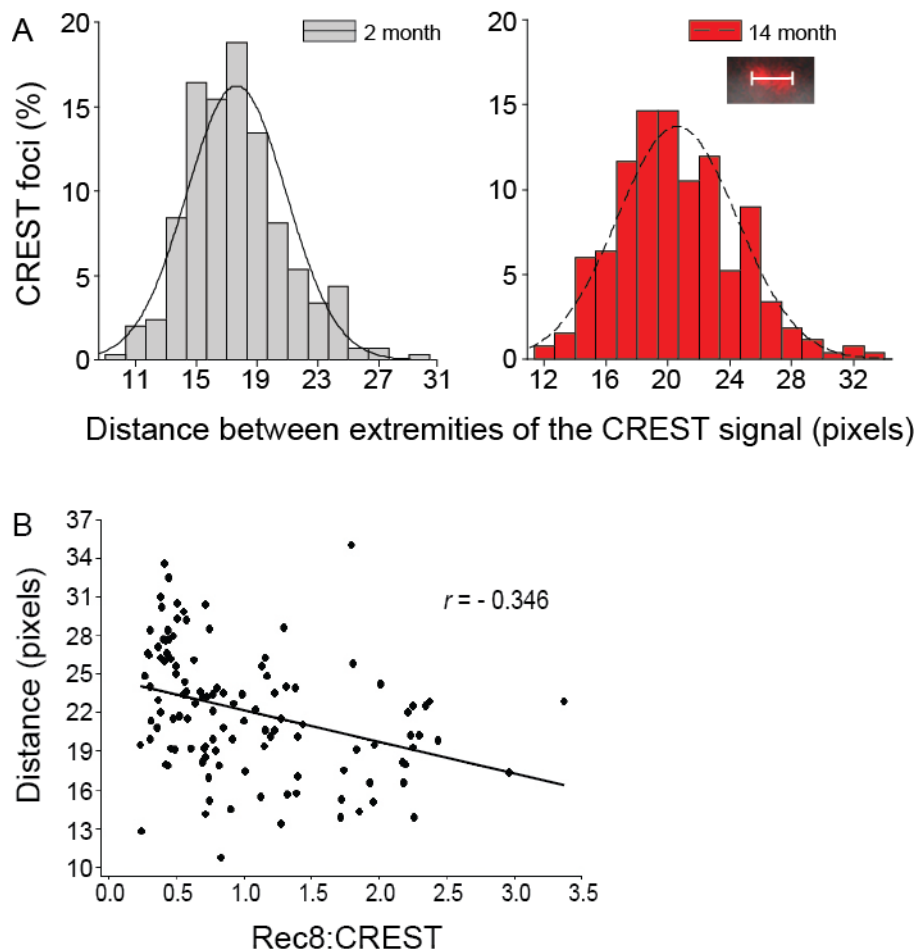


Figure 6.6 - Reduced cohesin is associated with centromere splitting in aged mice. (A) Frequency distribution of the range in the distance measured between sister centromeres in chromosome spreads from Figure 6.3. The distance was measured as shown inset, measuring from the outermost margins of the CREST signals. The mean distance was significantly greater between the sister centromeres in oocytes from 14 month old mice (771.77 ± 145.32 ; $n=267$ centromeres; 7 oocytes from 6 mice) compared with 2 month old mice (698.75 ± 123.04 ; $n=298$ centromeres; 8 oocytes from 4 mice) ($p < 0.001$). (B) Scatter plot showing the negative correlation between the sister centromere distance and the Rec8:CREST fluorescence intensity ratio, in 14 month old mouse oocytes. The calibrated pixel size for the microscope objective is 66.89nm. *Experiment performed in collaboration with Dimitrios Kalleas and Anna Kouznetsova (Lister et al., 2010).*

These findings gave foundation to the hypothesis that depletion of centromeric cohesin disrupts the unified structure of sister centromeres, thereby compromising their ability to establish and maintain monopolar sister kinetochore-microtubule attachments. This hypothesis provides a plausible explanation for the observed splitting of sister chromatid centromeres and anaphase defects observed in oocytes from aged mice. In support of this hypothesis we have previously identified splitting of sister centromeres in

association with bipolar attachments and lagging chromosomes in *Sycp3*^{-/-} mouse oocytes (Kouznetsova *et al.*, 2007). The intercentromere distance between sister chromatids was found to be substantially higher in the aligned univalents compared with aligned bivalents.

As I have previously described, for accurate homologous chromosome segregation to faithfully occur, there are three main rules which must be followed: I) Chiasmata must be maintained until the onset of anaphase I. (II) Sister kinetochores must establish monopolar attachments. (III) Cohesin must be lost from the arms of sister chromatids, but not from the centromeres before anaphase I (Figure 6.7).

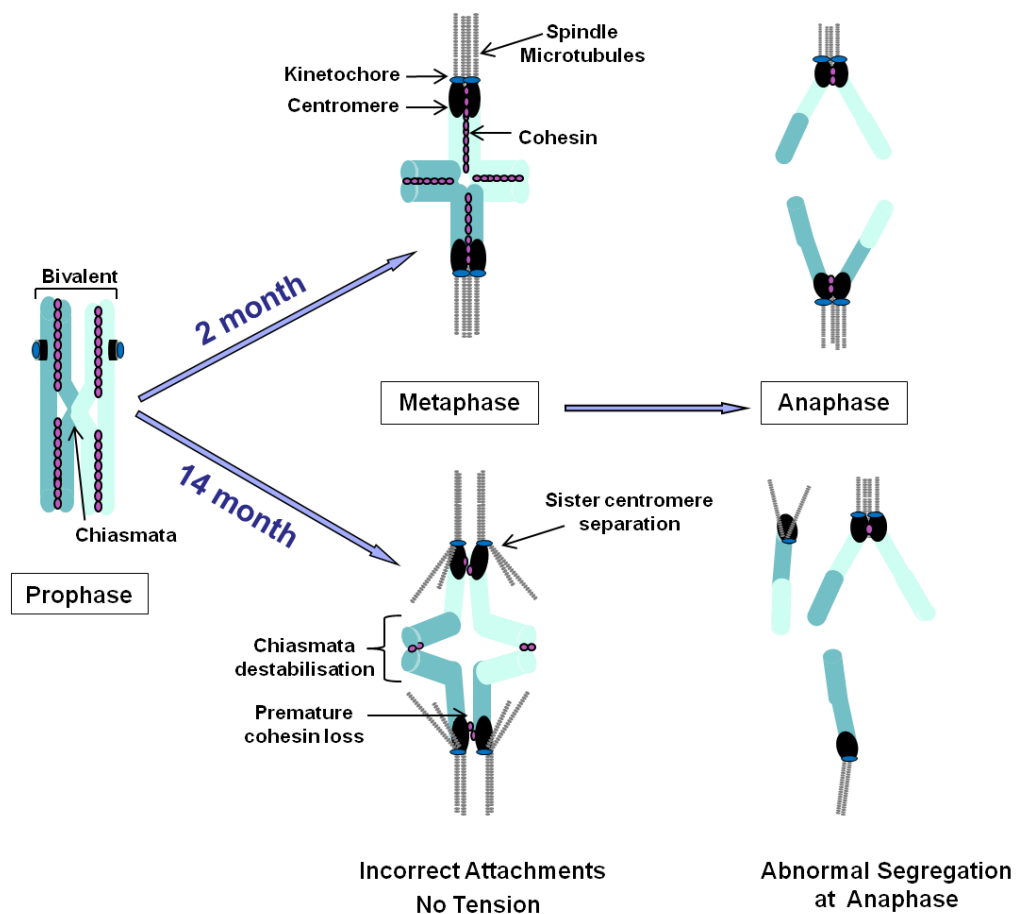


Figure 6.7 - Errors leading to abnormal chromosome segregation at anaphase I. Diagrammatic representation of chromosomes from a 2 month and 14 month aged mouse. The 14 month schematic shows the errors I have elucidated so far as occurring with advancing maternal age, contributing to abnormal chromosome segregation. I) Chiasmata are not maintained. II) Sister centromeres are splitting which may render kinetochores unable to establish monopolar attachments. III) Cohesin is prematurely lost from the centromeres, before anaphase I. These three events may be creating a bias against monopolar attachments and thereby faithful chromosome segregation.

My results so far have demonstrated the breaking of these essential rules in the oocytes of aged females, creating a bias against monopolar attachments, thereby rendering the oocyte unable to undergo a successful meiotic division (Figure 6.7).

Our next questions are whether cohesin loss occurs gradually; whether loss occurs during the prolonged prophase arrest; and what might the mechanisms be behind this loss?

6.3. Sister centromere splitting occurs gradually during female ageing.

Due to repeated problems with the transport of the Rec8 antibody we were unable to get it to work reproducibly in our hands. Even when it was considered to be working many chromosome spread images had to be excluded from our analysis because of high levels of background fluorescence. This made testing cohesin loss using fluorescence intensity measurements difficult, so instead we used the distance between sister centromeres as an indicator of cohesin loss.

In order to determine whether the increasing intercentromere distance occurred progressively during female ageing, we measured the distance between sister centromeres in oocytes from the intermediate age groups of 8 and 11 months. Oocytes from 2, 8, 11 and 14 month old mice were spread during mid prometaphase I (GVBD + 5hrs) using paraformaldehyde fixation. The distance between sister centromeres was measured as in Figure 6.6, and analysed using Minitab (Figure 6.8). The data revealed that the intercentromere distance does increase progressively with advancing female age. However, there is no further increase after 11 months. This is surprising, given that we did not observe any striking defects in preliminary experiments conducted with oocytes from 12 month old females. However, the increased intercentromere distance observed from 8 months of age is consistent with the observation that C57BL/1crfa^t mice show a decline in fertility after ~9 months (Figure 4.15), and are found to be mainly sterile after ~12 months of age (Rowlatt *et al.*, 1976).

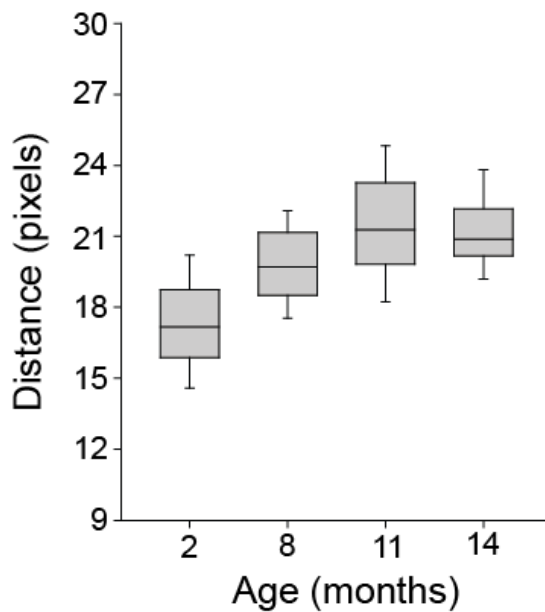


Figure 6.8 - The distance between sister centromeres increases with advancing maternal age. Box plots showing the distance between the sister chromatid CREST signals measured as in Figure 6.6, in oocytes from 2 month (n=218 centromeres; 10 oocytes from 1 mouse), 8 month (n=127 centromeres; 6 oocytes from 2 mice), 11 month (121 centromeres; 4 oocytes from 1 mouse), and 14 month (n=199 centromeres; 9 oocytes from 4 mice) old mice. The distance was significantly increased in the 11 and 14 month oocytes, compared with the 2 and 8 month oocytes ($p < 0.001$). The calibrated pixel size for the microscope objective is 66.89nm. *Experiment performed in collaboration with Dimitrios Kalleas and Abinaya Nathan (Lister et al., 2010).*

It is conceivable that the problem of splitting centromeres is compounded by an accumulation of distally associated homologues in oocytes from 14 month old mice.

However, all of the analysis I have done so far has been during the progression through M phase. What about prophase? Given the prolonged prophase arrest of oocytes, especially in humans, cohesin depletion during prophase could provide an explanation as to the increased incidence of aneuploidy and infertility with advancing female age.

6.4. Is cohesin lost during prophase arrest in oocytes?

When oocytes are in prophase arrest they are predominantly at the primordial stage. Primordial oocytes are continuously recruited for growth through life, but do not mature (enter into M phase of MI) until after puberty (Figure 6.9). The fully grown oocytes enter the M phase of MI (prometaphase) in response to cyclic hormonal triggers (Gougeon, 1996; Mehlmann, 2005).

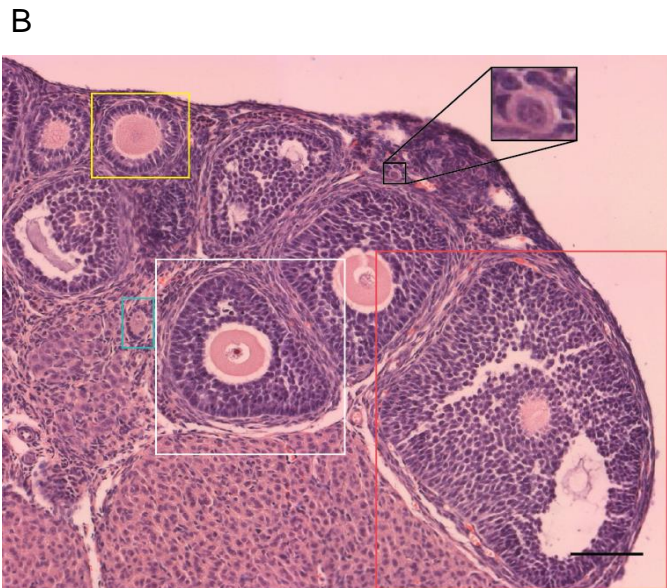
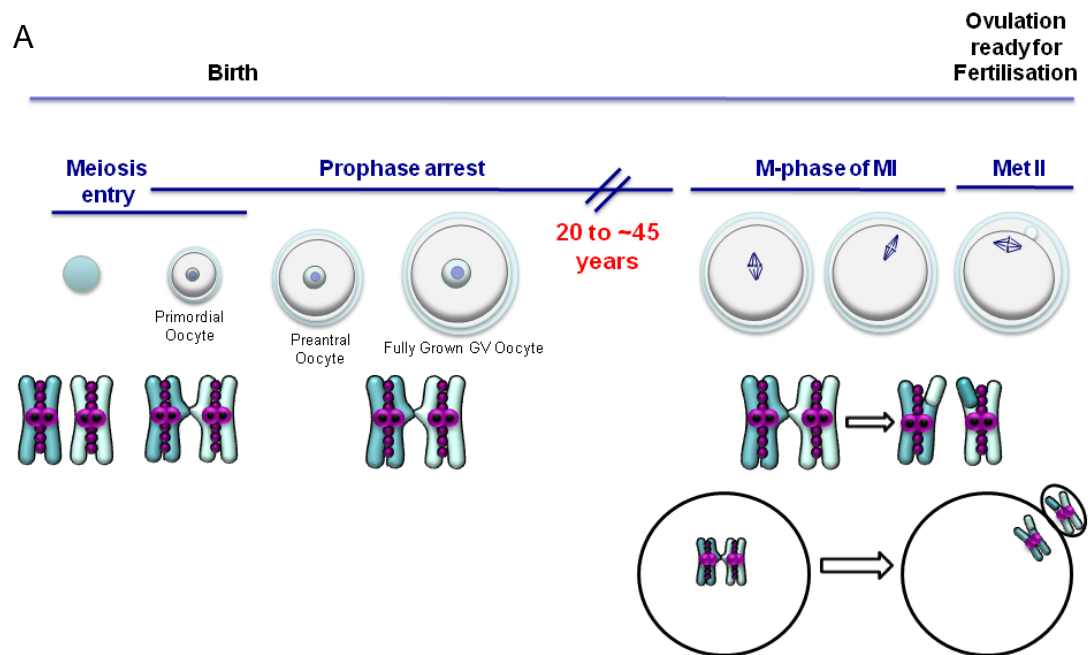


Figure 6.9 - Stages of oocyte growth. (A) Diagrammatic representation of the stages of oocyte growth. (B) Section from a wax embedded ovary stained with Hematoxylin-Eosine. Image shows the ovarian cortex highlighting the first stages of follicular growth: a primordial follicle (black box); a primary follicle (blue box); a transitional follicle (yellow box); a secondary follicle (white box) and an antral follicle (red box). Scale bar represents 50 μ m.

To test the theory that cohesin is lost during the long prophase arrest in aged oocytes, Dimitrios Kalleas, a PhD student in our lab, measured cohesin levels in fully grown GV, and preantral stage oocytes of 2 month and 14 month aged females. His results showed that cohesin loss occurs gradually during maternal ageing, and as well as being depleted in the prometaphase of MI, is also depleted during prophase, even in the later growth stages of oocytes (Lister *et al.*, 2010).

Our findings, together with those of others (Chiang *et al.*, 2010), support the hypothesis that cohesin is lost gradually during prophase arrest. As cohesin loss occurs at all stages of oocyte growth, its gradual depletion during the prolonged prophase arrest of aged oocytes may be responsible for the observed age related chromosome segregation defects observed in Chapter 5, and the observed increase in intercentromere distance with female ageing (Figure 6.8).

6.5. Cohesin loss from oocyte chromosomes during female ageing.

At the anaphase of mitosis, centromeric cohesin is cleaved at the Scc1 subunit by the protease separase (Uhlmann *et al.*, 1999; Hauf *et al.*, 2001). Separase is kept inactive through a majority of the cell cycle by an inhibitory binding partner known as securin, and by the inhibitory phosphorylation of Cyclin B-Cdk1 (Shirayama *et al.*, 1999; Stemmann *et al.*, 2001).

Meiotic cohesin is removed from the chromosome arms for anaphase I, and the centromeres for anaphase II. Homologous chromosome disjunction in MI of mammalian oocytes requires degradation of cyclin B and securin (Herbert *et al.*, 2003), the timing of which is regulated by the spindle checkpoint to ensure that anaphase does not occur until all the chromosomes are properly aligned (Herbert *et al.*, 2003; Homer *et al.*, 2005; McGuinness *et al.*, 2009).

An age related deterioration of the spindle checkpoint itself could lead to premature activation of separase accounting for the observed reduction in the level of chromosome associated cohesin. In mouse oocytes, functional disruption of the spindle checkpoint results in accelerated PB formation

(Tsurumi *et al.*, 2004; Homer *et al.*, 2005; Niauxt *et al.*, 2007; McGuinness *et al.*, 2009), premature degradation of securin and cyclin B (Homer *et al.*, 2005; McGuinness *et al.*, 2009), and failure to inhibit their degradation in the presence of nocodazole, a microtubule depolymerising drug which would normally activate the checkpoint due to spindle damage (Wassmann *et al.*, 2003; Homer *et al.*, 2005; Niauxt *et al.*, 2007; McGuinness *et al.*, 2009).

I have already shown that anaphase and PB formation did not occur earlier in the oocytes from 14 month old mice compared with those from the 2 month old mice (Figure 5.11). Consistent with these findings, live cell imaging of oocytes injected with securin-YFP mRNA reveal that there was no difference in the timing of securin degradation between the oocytes of 14 month and 2 month old mice (Lister *et al.*, 2010; Sarah Pace PhD thesis). Furthermore, aged oocytes injected with cyclin B-GFP were not shown to degrade cyclin B in the presence of nocodazole (Lister *et al.*, 2010; Sarah Pace PhD thesis). This supports the hypothesis that the spindle checkpoint is still functional in aged oocytes, and is therefore not compromised by maternal ageing. This is consistent with the findings of another group (Duncan *et al.*, 2009).

The spindle assembly checkpoint however, does not exist in prophase. Cyclin B-Cdk1 is suppressed in prophase-arrested oocytes (Reis *et al.*, 2006), which implies that if separase is expressed in prophase, its inhibition is entirely reliant on securin binding. The simplest explanation for the removal of cohesin during female ageing would be the premature activation of separase. In support of this idea separase is present in prophase of yeast meiosis I (Katis *et al.*, 2010). I therefore asked whether separase is expressed in prophase-arrested oocytes.

My preliminary experiments have shown that separase is expressed during the different stages of growth in prophase arrested oocytes (Figure 6.10). This is consistent with findings in budding yeast (Katis *et al.*, 2010). While the securin/separase complex is thought to be stable (Ciosk *et al.*, 1998), it is possible that a small fraction of separase might become active due to securin dissociation or degradation (Marangos and Carroll, 2008). Even if this occurs infrequently over a prolonged period of time, such as the decades it can take to complete prophase, it could still have significant consequences.

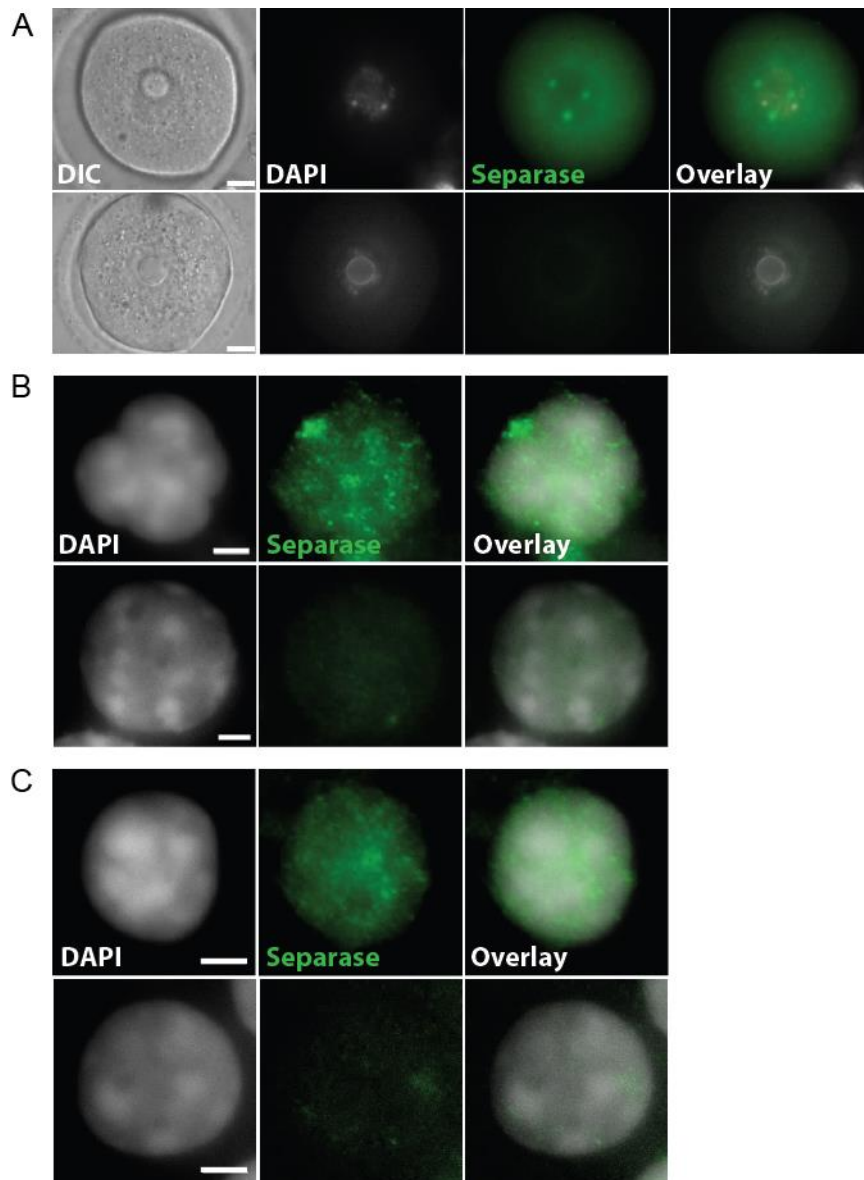


Figure 6.10 - Separase is expressed in fully grown GV, preantral, and primordial stage oocytes. Paraformaldehyde chromosome spreads were prepared from (A) fully grown GV oocytes; (B) preantral oocytes; and (C) primordial oocytes. Representative images show the nuclei of each oocyte stained for the DNA (grey) and separase (green). Scale bar represents 5 μ m in (A) and 3 μ m in (B) and (C).

Separase is an obvious candidate for investigation, and needs to be either ruled in or out of the ageing equation. It is also highly testable with a separase knockout mouse. My experimental strategy would be to age these mice and use the methods previously described to measure cohesin levels at the centromeres. Rescue experiments would also be conducted by microinjecting separase mRNA. If separase was the culprit in prophase cohesin depletion, then upon its rescue we would not observe any anaphase defects.

However, as it would take some time to age the mice to continue these experiments, in the meantime I investigated whether cohesin might be lost due to a separase-independent mechanism, such as one analogous to the prophase pathway of mitosis.

6.6. Is there a separase-independent mechanism of cohesin removal in meiosis?

In vertebrate cells, the bulk of arm cohesin is removed by a mechanism known as the prophase pathway (Losada *et al.*, 1998; Darwiche *et al.*, 1999; Sumara *et al.*, 2000). The classic X shape of chromosomes in metaphase arrested cells is thought to be attributable to the removal of arm cohesin by this pathway, with the centromeres still remaining connected (Waizenegger *et al.*, 2000).

Removal of cohesin by the prophase pathway is separase-independent but requires phosphorylation of the cohesin subunit SA2 by Plk1 (Hauf *et al.*, 2005) in association with Aurora B (Losada *et al.*, 2002; Gimenez-Abian *et al.*, 2004) and Wapl (Gandhi *et al.*, 2006; Kueng *et al.*, 2006; Shintomi and Hirano, 2009). Studies in human cells have revealed that Wapl physically interacts with cohesin to help promote its resolution via the prophase pathway (Gandhi *et al.*, 2006; Kueng *et al.*, 2006; Shintomi and Hirano, 2009).

It is not yet known whether a mechanism analogous to the prophase pathway is active during meiosis. If so, it would need to be very tightly regulated to protect against premature resolution of chiasmata until the onset of anaphase.

Preliminary experiments indicate that Plk1 is not localised to the nucleus during prophase arrest (work by Randy Ballesteros Mejia, a PhD student in our group). However, it is active in prometaphase (D. Kalleas PhD thesis, (Pahlavan *et al.*, 2000)) raising the possibility that cohesin might be removed by a separase-independent mechanism during progression through M phase. As this can last ~20 hours in human oocytes, it could significantly exacerbate the effects of cohesin depletion during prophase.

Sgo was first discovered to have a conserved role in protecting centromeric cohesin from separase-mediated cleavage during anaphase of MI (Kitajima *et*

et al., 2004). Shugoshin has two splice variants in mammalian meiosis, Sgo1 and Sgo2. Both are expressed in proliferating cells, with Sgo2 being notably stronger in germ cells (Lee *et al.*, 2008). Sgo1 and Sgo2 are both localised to the inner kinetochore region in MI and MII.

In mammalian oocytes, Sgo2 has been found to protect centromeric cohesin at anaphase I (Lee *et al.*, 2008). Deletion of Sgo2 in mammalian oocytes results in a loss of centromeric cohesion and premature sister chromatid separation (Lee *et al.*, 2008). This leads to single sister chromatids being observed at MII (with no observed defect at MI). By contrast depletion of Sgo1 results in failure of ~10% of homologous pairs to disjoin (Lee *et al.*, 2008). Therefore, in mouse oocytes, Sgo2 appears to act alone in protecting centromeric cohesion, while the precise role and mechanism of action of Sgo1 remains unclear.

Sgo was also found to protect centromeric cohesin from removal by the prophase pathway in vertebrate somatic cells (Kitajima *et al.*, 2005; McGuinness *et al.*, 2005). Sgo recruits PP2A to counteract phosphorylation of SA2 by Plk1 until the onset of anaphase (Kitajima *et al.*, 2006; Riedel *et al.*, 2006). We therefore asked whether Sgo2 might serve to protect cohesin from removal by a mechanism analogous to the prophase pathway during progression through MI. This idea is supported by the observed decline in cohesin levels at the centromeres of aged mice (Figure 6.3 and Figure 6.4) and by the incidence of single sisters at MII (Figure 5.8). To test this possibility, we asked whether (I) Sgo2 recruitment to chromosomes is reduced in oocytes from aged mice (II) Depletion of Sgo2 in oocytes of young mice results in reduced chromosomal cohesin.

6.7. Is recruitment of the cohesin protector Sgo2 compromised during female ageing?

In order to determine whether there was a reduction in recruitment of Sgo2 to chromosomes in oocytes of aged mice, I prepared chromosome spreads of young and aged oocytes during prometaphase I (GVBD + 5hrs) and used immunolabelling to analyse the localisation and levels of Sgo2 on the chromosomes (Figure 6.11A). Sgo2 was detected along the chromosome arms, as well as at the centromeres, however the level of Sgo2 detected was greatly reduced in the oocytes of 14 month old mice compared to those of 2 month old mice (Figure 6.11B).

High resolution images indicate that splitting of sister centromeres, which was prevalent in oocytes from aged mice, was associated with mislocalisation of Sgo2 (Figure 6.12). Instead of being positioned between the centromeres, which is presumably required to protect centromeric cohesin during anaphase of MI, Sgo2 was frequently off-centre, being predominantly localised under one or other of the CREST signals (Figure 6.12). Thus, Sgo2 mislocalisation together with reduced levels is likely to compromise protection of centromeric cohesin from separase-mediated cleavage during anaphase I. This provides a ready explanation for the prevalence of prematurely separated single sister chromatids observed in the MII oocytes of 14 month old mice (Figure 5.8). However, it remains to be established whether reduced recruitment of Sgo2 might also contribute to the lower levels of centromeric cohesion observed during prometaphase I in oocytes from aged mice (Figure 6.3).

Surprisingly, we detected intense Sgo2 staining on chromosome arms. This was not consistent with a previous report in which Sgo2 was confined to centromeres (Gomez *et al.*, 2007). However this was based on findings in mouse spermatocytes, rather than oocytes (Gomez *et al.*, 2007). While Lee *et al.* used the same antibody as we used, they did not report arm-associated Sgo2. However, arm-staining was obvious in some of their images (Lee *et al.*, 2008, Figure S2). Lee *et al.* also used whole oocyte immunofluorescence rather than chromosome spreads. It is a possibility that the arm staining may be an artefact of soluble cohesin within the oocyte becoming associated with the chromosomes during our spreading procedure.

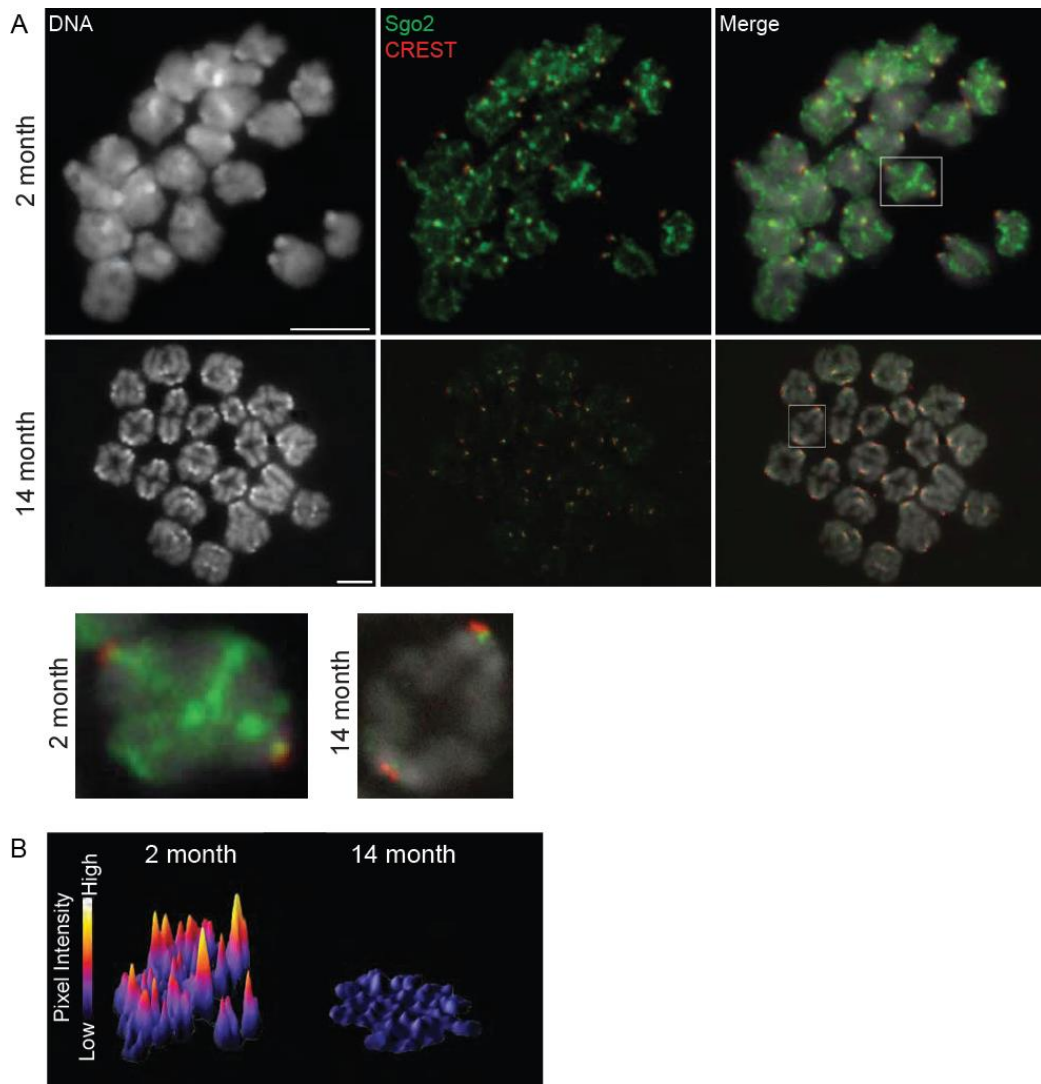


Figure 6.11 - Sgo2 levels are reduced in oocytes of aged mice. (A)

Paraformaldehyde chromosome spreads were prepared during mid prometaphase I (GVBD + 5hrs) in oocytes from 2 month (n = 20 from 3 mice) and 14 month (n = 10 from 4 mice) old mice. Representative images show DAPI (grey), Sgo2 (green) and CREST (red) immunolabelling. Insets show enlarged images of chromosomes at 2 months (left) and 14 months (right). Scale bar represents 10 μ m. Reduced levels of Sgo2 are observed on the chromosomes of oocytes from 14 month old mice compared with 2 month oocytes. (B) Representative 3D surface plots of chromosome spreads from (A) illustrate higher Sgo2 fluorescence intensity on the chromosomes of 2 month old compared with 14 month old oocytes. *Experiment performed in collaboration with Dimitrios Kalleas (Lister et al., 2010).*

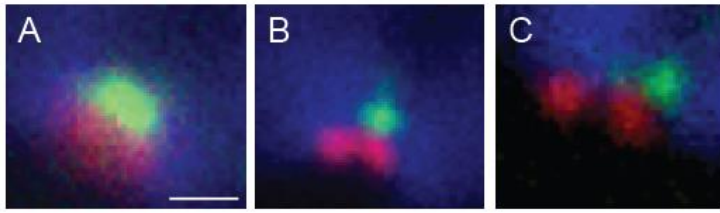


Figure 6.12 - Sister centromere splitting with advanced female age is associated with Sgo2 mislocalisation. Enlarged images of representative centromeres from (A) 2 month and (B-C) 14 month aged mouse oocytes from Figure 6.11. Scale bar represents 1 μ m. The usual pericentromeric localisation of Sgo2 was observed to be increasingly off-centre in association with increased sister centromere separation.

Further studies are required to test the reproducibility of arm staining under different fixation and staining conditions. However, in support of our findings, communications with another research group using a different Sgo2 antibody concur with our observations (Ahmed Rattani, personal communications).

To test the specificity of the antibody, I stained chromosome spreads from oocytes injected with Sgo2 siRNA. No Sgo2 was detected on the arms or centromeres following siRNA-mediated knock down of Sgo2 (Figure 6.16). To gain insight into the function of Sgo2 on the arms, I also stained for PP2A, which protects cohesin from the prophase pathway, by counteracting its phosphorylation by Plk1 (Kitajima *et al.*, 2006; Riedel *et al.*, 2006; Tang *et al.*, 2006). I found that PP2A co-localised with Sgo2 (Figure 6.13), localising greatest during late prometaphase (GVBD + 6-7 hours), indicating a role in protecting arm cohesin during M phase.

In addition to cohesin being reduced at the centromeres of aged oocytes, it was found to be reduced along the chromosome arms during female ageing. Thus, if Sgo2 has a role in protecting arm cohesin during progression through M phase, its loss is likely to contribute to the destabilisation of chiasmata in oocytes from aged mice. Sgo2 may protect the chromosome arm cohesin against any premature activation of separase during the 2-3 hour degradation period of securin and Cyclin B-Cdk1 (Herbert *et al.*, 2003), coordinating cohesin loss with entry to anaphase. Sgo2 could also be protecting the arm cohesin against a meiotic equivalent of the prophase pathway.

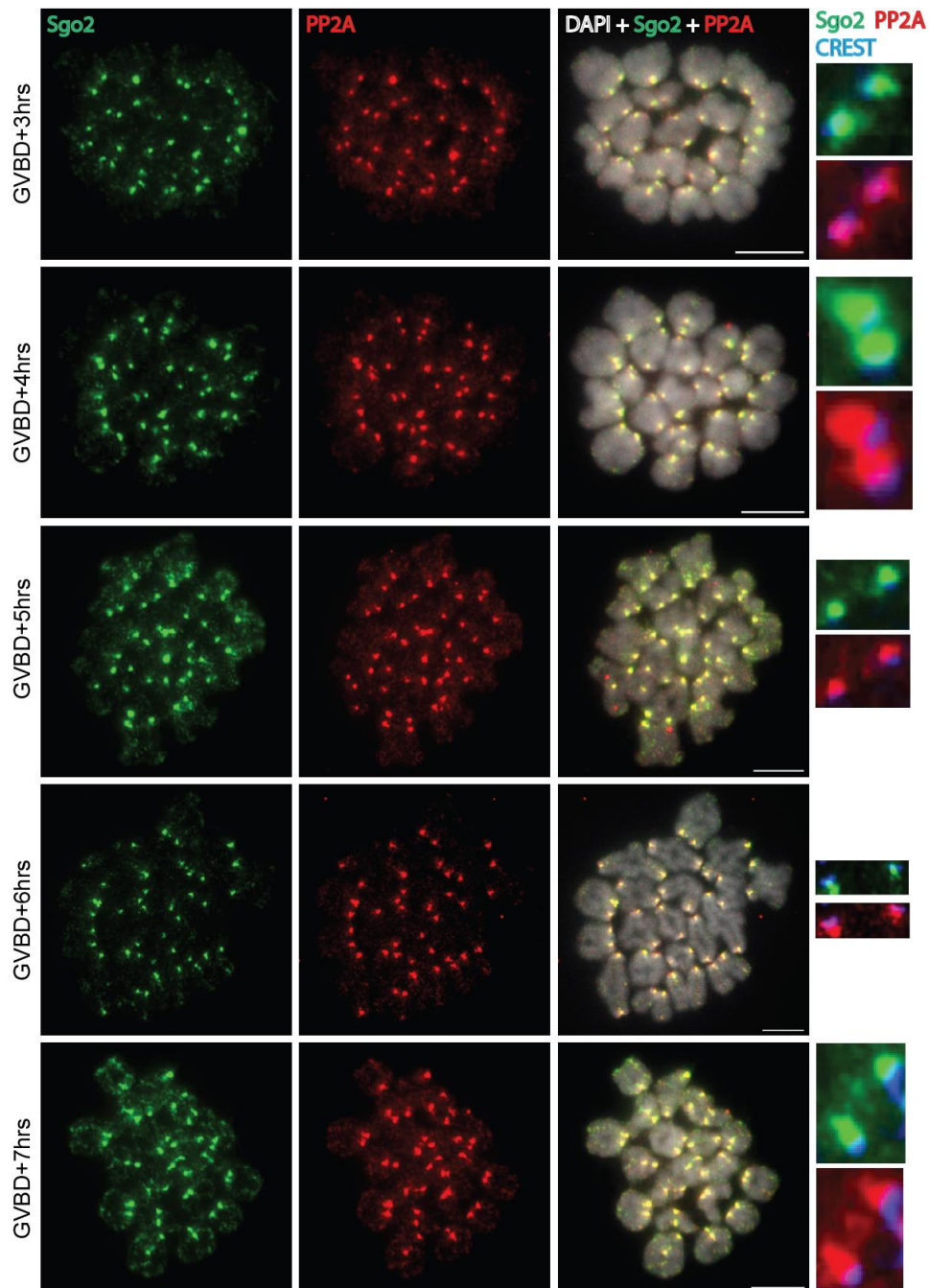


Figure 6.13 - Time course staining of Sgo2 and PP2A in prometaphase oocytes. Paraformaldehyde chromosome spreads were prepared at different time points through prometaphase I (GVBD + 3-7hrs) in oocytes from CD1 mice. Representative images show DAPI DNA (white), Sgo2 (green) and PP2A (red) staining. Insets show enlarged images of selected centromeres. Scale bar represents 10 μ m. Sgo2 and PP2A co-localise, showing greatest association with the chromosomes at 6 and 7 hrs post GVBD.

Immunolabelling of fully grown GV oocytes revealed that Sgo2 is predominantly localised to the nucleolus at prophase, and is not enriched on DNA or at CREST foci, as is the case at prometaphase (Figure 6.14).

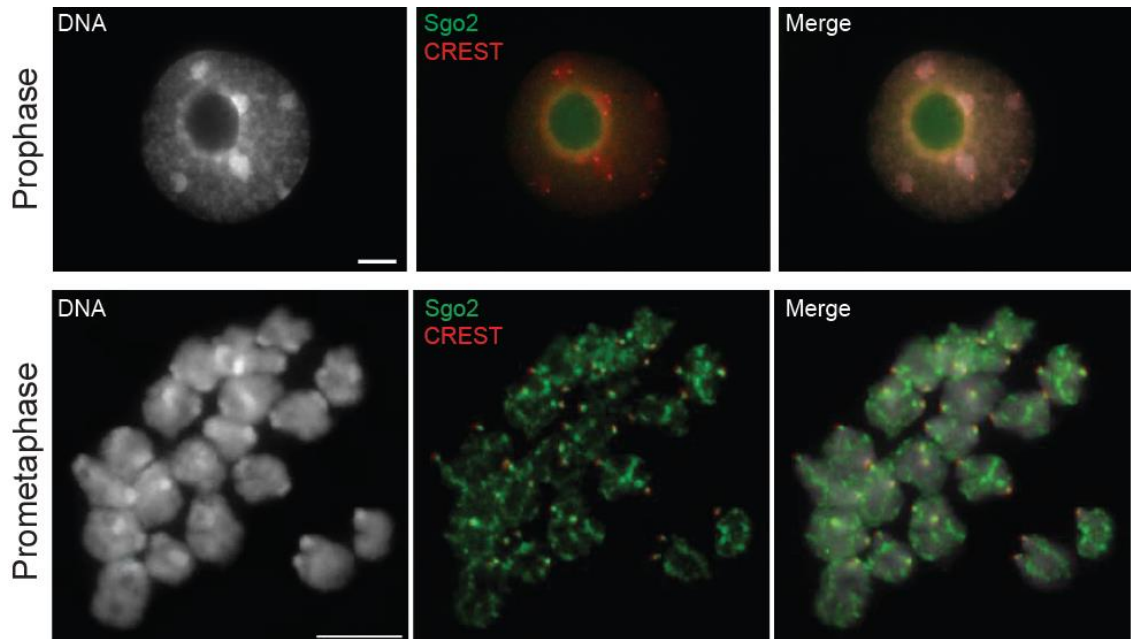


Figure 6.14 - Sgo2 is recruited to chromosomes at the prophase to metaphase transition in oocytes. Paraformaldehyde chromosome spreads were prepared of fully grown prophase arrested oocytes, and during mid prometaphase I (GVBD + 5hrs) in oocytes from 2 month (n = 20 from 3 mice) old mice. Representative images show DAPI (grey), Sgo2 (green) and CREST (red) immunolabelling. Scale bar represents 10 μ m. Note – the prometaphase image is repeated from figure 6.11A. Sgo2 is localised to the nucleolus during prophase, and does not appear to localise to the chromosomes as observed during prometaphase. *Experiment performed in collaboration with Dimitrios Kalleas (Lister et al., 2010).*

Thus, recruitment of Sgo2 appears to occur at the prophase to metaphase transition in oocytes. This suggests that Sgo2 might not be involved in the protection of cohesin during the prolonged prophase arrest of oocytes. However, we cannot rule out the possibility that Sgo2 moves on and off chromosomes during prophase arrest.

In conclusion, Sgo2 is reduced at both the centromeres and chromosome arms during ageing in female meiosis. This provides an explanation for the separation of sister chromatids and destabilisation of chiasmata (Figure 5.18), and hints at a new function for Sgo2 in protecting arm cohesin before anaphase I. If this hypothesis is correct, and the protective function of Sgo2 is only relevant during the M phase of MI, knockdown of Sgo2 at this stage should cause a reduction in the level of chromosome associated cohesin.

6.8. Does depletion of Sgo2 result in loss of chromosomal cohesin during progression through M phase of meiosis I?

6.8.1 Optimisation of siRNA techniques.

Based on the successful use of Sgo2 siRNA in mouse oocytes by Yoshinori Watanabe's research group (Lee *et al.*, 2008), I used the same Sgo2 siRNA sequence and used their protocol as a starting point for my own experiments.

The antisense strand of the siRNA duplex becomes part of a complex which identifies the corresponding cellular mRNA and cleaves it at a specific site. The cleaved message is then targeted for degradation, which consequently results in the loss of protein expression (Hammond *et al.*, 2000; Zamore *et al.*, 2000; Paddison *et al.*, 2002).

Getting the correct level of expression of the Sgo2 siRNA was challenging, and took a great deal of optimisation. Lee *et al.* used a transfection method for the uptake of the Sgo2 siRNA, which first required the removal of the zona pellucida. This makes the oocytes subsequently very difficult to handle or further manipulate. As I was intending to perform timelapse imaging of these treated oocytes, I used a microinjection technique, co-injecting with histone H2B-RFP to enable visualisation of the chromosomes. The co-injection was also a valuable tool in isolating oocytes of consistent injection sizes for analysis. Stealth negative siRNA (Invitrogen) was used as a control for each condition tested.

Although the siRNA prevents further translation of Sgo2, as it is already expressed in prophase I had to allow time for protein turnover to occur in order to achieve a complete knockdown. This was done by maintaining GV arrest for a significant period of time after siRNA microinjection, before incubating the oocytes in G-IVF media for maturation.

I initially injected a 5 μ M concentration of Sgo2 siRNA, and allowed 45hrs incubation in IBMX and cAMP-containing medium for knockdown, mimicking the 6hr transfection period and 39hr incubation in IBMX and cAMP done by Lee *et al.* (Lee *et al.*, 2008). However, this resulted in the majority of oocytes remaining in prophase arrest (Sgo2 siRNA 34.15% GVBD; (n=41); Stealth

negative siRNA 7.14% GVBD (n=14)) (Figure 6.15A). In those oocytes that did enter M phase, chromosome spreads and immunolabelling at early prometaphase showed no detectable Sgo2 signal, indicating that a successful knockdown was achieved.

In order to improve maturation of siRNA-injected oocytes I systematically decreased the period of incubation in IBMX and cAMP-containing medium. I found that a large proportion of oocytes maintained in prophase-arrest for 16hrs or more did not resume meiosis following removal from IBMX and cAMP-containing medium (Figure 6.15A). However incubations of 16hrs or less resulted in only a partial knockdown. I therefore asked whether the problem of poor maturation (entry into M phase) could be overcome by reducing the concentration of siRNA. I kept the incubation time at 20-22hrs, and reduced the concentration of the injected siRNA. This improved the proportion of oocytes which were able to exit prophase. However, concentrations below 1 μ M were insufficient to achieve a successful knockdown of Sgo2 (Figure 6.15B). Further attempts to reduce the incubation period in IBMX and cAMP-containing medium compromised the efficiency of the knockdown.

This dose dependency of Sgo2 siRNA lead me to fix my protocol at an injection concentration of 1 μ M siRNA followed by a 20-22hr incubation in G-IVF containing IBMX and cAMP (Figure 6.16).

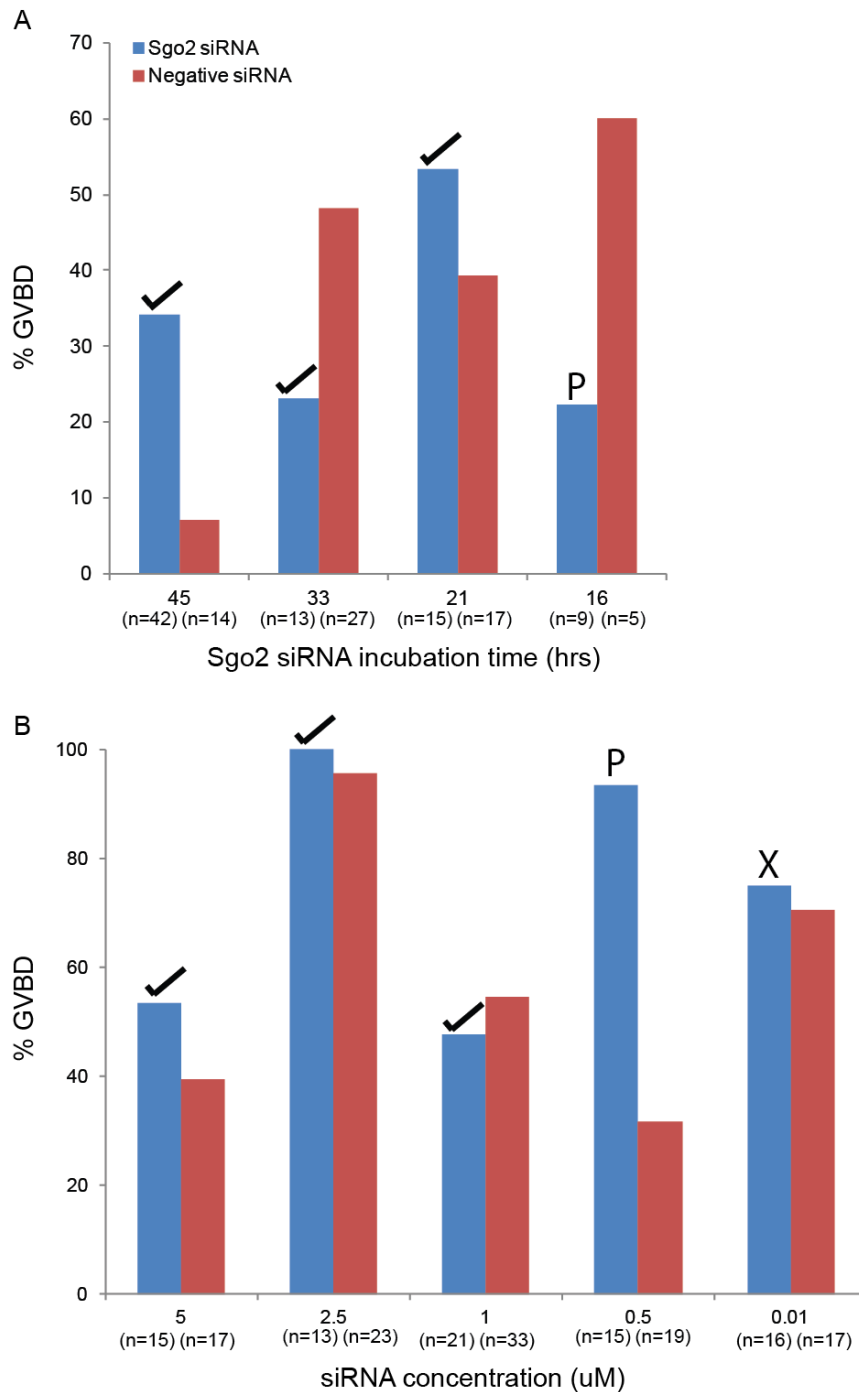


Figure 6.15 - Maturation after siRNA injection. Oocytes were co-injected with mRNA encoding histone-RFP and either Sgo2 siRNA (blue) or Stealth negative siRNA (red). Oocytes expressing equivalent levels of histone-RFP were incubated in media supplemented with IBMX and cAMP to allow knockdown before incubating in un-supplemented G-IVF media for maturation, and scored for GVBD after 2hrs. Chromosome spreads were prepared on paraformaldehyde-coated slides during prometaphase (GVBD + 3hrs) and immunofluorescence labelling of Sgo2 and CREST was performed to assess knockdown (tick = complete knockdown; P = partial knockdown; x = no knockdown). (A) Oocytes injected with 5 μ M siRNA and incubated 45hrs; 33hrs; 21hrs or 16hrs in media supplemented with IBMX and cAMP. (B) Oocytes injected with either 5; 2.5; 1; 0.5; or 0.01 μ M siRNA, and incubated 20-22hrs in media supplemented with IBMX and cAMP.

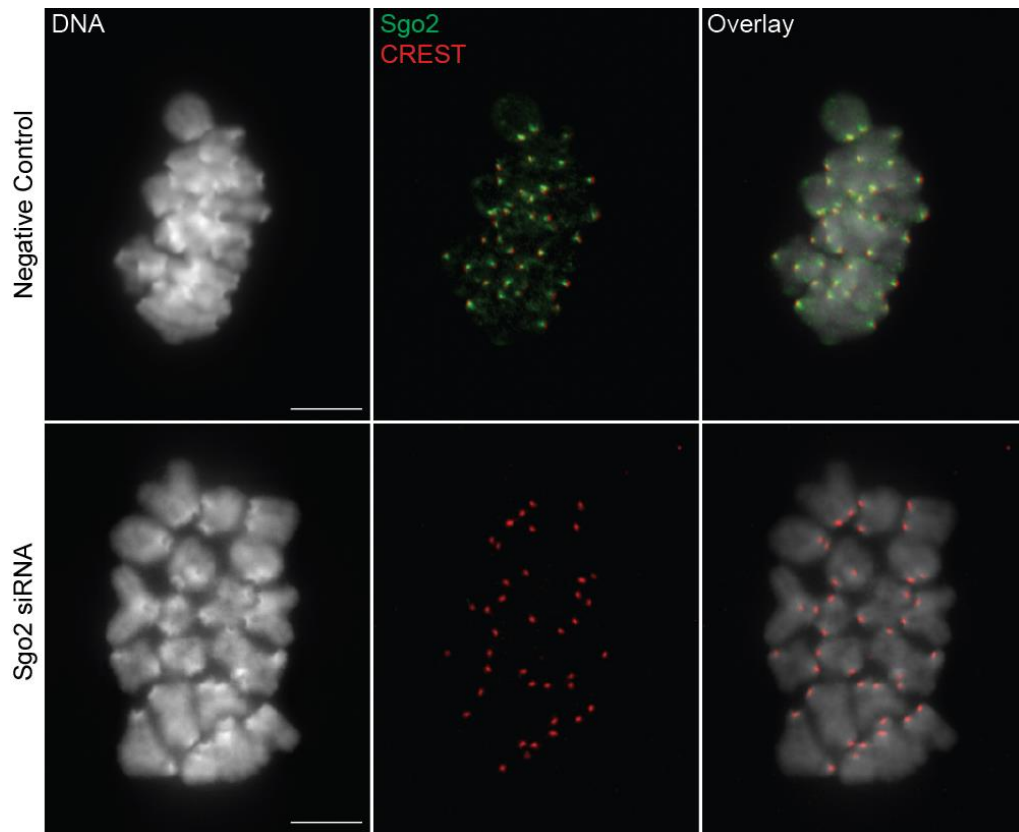


Figure 6.16 - Sgo2 siRNA knockdown. Oocytes were co-injected with mRNA encoding histone-RFP and either Stealth negative siRNA (top panel; n=4) or Sgo2 siRNA (bottom panel; n=5). Oocytes expressing equal levels of histone were incubated in G-IVF medium supplemented with IBMX and cAMP for 20-22hrs to allow knockdown, before incubating in un-supplemented G-IVF media for maturation. Chromosome spreads were prepared on paraformaldehyde-coated slides during prometaphase (GVBD + 3hrs) and immunofluorescence labelling of Sgo2 and CREST was performed. Scale bar represents 10µm. Immunofluorescence labelling shows Sgo2 is localized to the centromeres and chromosome arms in control oocytes but is not detected in oocytes injected with Sgo2 siRNA.

As an additional control I stained Sgo2 knockdown oocytes for PP2A, which I have previously shown to co-localise with Sgo2 (Figure 6.13). Both PP2A and Sgo2 were completely absent from the centromeres (Figure 6.17A). However, I cannot draw any conclusions as to whether the PP2A arm staining was also lost, due to the fact that the illumination required for my secondary fluorophore also excited the tag of the histone-RFP, of which mRNA had been co-injected with the Sgo2 siRNA.

I also injected Sgo2 knockdown oocytes with mRNA encoding Sgo2-Venus. The localisation of the exogenous Sgo2-Venus to both the centromeres and chromosome arms further validated the specificity of the Sgo2 antibody (Figure 6.17D).

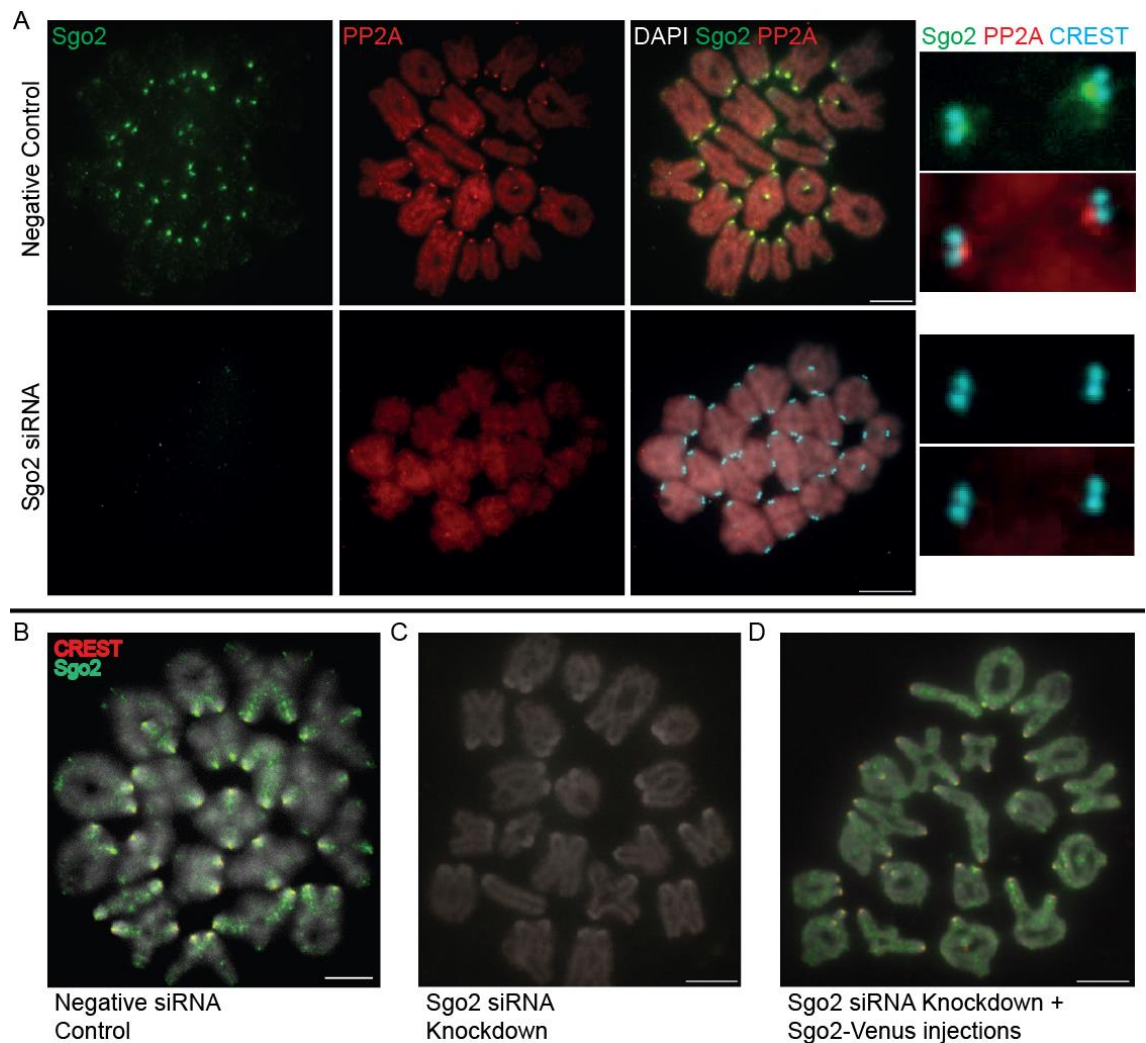


Figure 6.17 - PP2A localisation is disrupted in Sgo2 knockdown oocytes.

Oocytes were co-injected with mRNA encoding histone-RFP and 1 μ M of either Stealth negative siRNA or Sgo2 siRNA. Oocytes expressing equal levels of histone were incubated in G-IVF medium supplemented with IBMX and cAMP for 20-22hrs to allow knockdown, before incubating in un-supplemented G-IVF media for maturation. Chromosome spreads were prepared on paraformaldehyde-coated slides during prometaphase and immunofluorescence labelling was performed. Scale bars represent 10 μ m.

(A) Immunofluorescence labelling of Sgo2 (green), PP2A (red) and CREST (blue) at GVBD + 6hrs show that PP2A is lost from the centromeres in oocytes injected with Sgo2 siRNA (bottom panel; n=5), compared with the Stealth negative control (top panel; n=5).

(B-D) Immunofluorescence labelling of Sgo2 (green) and CREST (red) at GVBD + 3hr. (B) Stealth negative oocytes (n=5 from 3 mice) show Sgo2 localisation to both the centromeres and chromosome arms. (C) Sgo2 knockdown oocytes (n=7 from 3 mice) show complete absence of Sgo2 staining, indicating a complete knockdown was achieved. (D) After the 20-22hr incubation period to allow knockdown, a subset of oocytes (n=3 from 1 mouse) were injected with mRNA encoding Sgo2-Venus. These oocytes were left to recover 1hr after microinjection, before incubating in un-supplemented G-IVF media for maturation before performing chromosome spreads. Sgo2-Venus staining is clearly observed at both the centromeres and chromosome arms.

Oocytes co-injected with siRNA and mRNA encoding histone-RFP, followed by incubation in IBMX and cAMP for 20-22hrs, showed a prevalence of symmetric cell divisions rather than the usual highly asymmetric PB formation, during MI (Figure 6.18A and B). This was evident in both Sgo2 siRNA and Stealth negative siRNA injected oocytes (10.4% and 58.8% respectively), and was rescued by reducing the duration of incubation in IBMX and cAMP-containing medium (Figure 6.18C). However, these symmetric divisions were not solely a consequence of the duration of arrest. PB formation of un-injected oocytes incubated in IBMX and cAMP for 20-22hrs was not significantly different from control oocytes (70.5% normal and 9.8% symmetric) (Figure 6.18D).

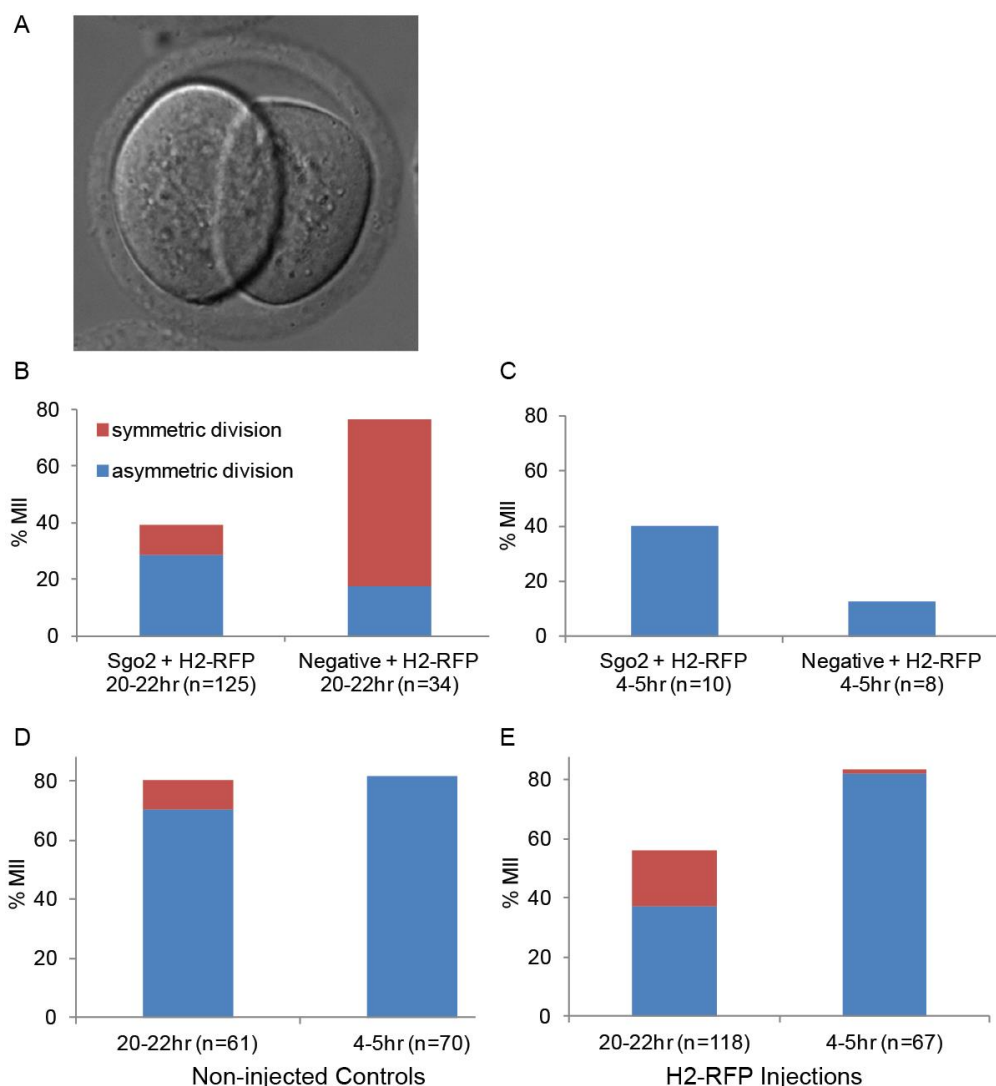


Figure 6.18 - Prolonged incubation in media supplemented with IBMX+cAMP and translation of Histone H2B compromises asymmetric division during MI. (A) Representative image of an abnormal symmetric cell division. Oocytes were co-injected with mRNA encoding histone-RFP and either 1 μ M Sgo2 siRNA or Stealth negative siRNA. Oocytes expressing histone were incubated in G-IVF medium

supplemented with IBMX and cAMP for (A) 20-22hrs or (B) 4-5hrs to allow knockdown, before incubating in un-supplemented G-IVF media for maturation. (C) Non-injected control groups, incubated in G-IVF medium supplemented with IBMX and cAMP for either 20-22hrs or 4-5hrs, before incubating in un-supplemented G-IVF media for maturation. (D) Control groups injected with only mRNA encoding histone-RFP, incubated in G-IVF medium supplemented with IBMX and cAMP for either 20-22hrs or 4-5hrs, before incubating in un-supplemented G-IVF media for maturation. The percentage maturation to MII was scored for each group the next morning. Each bar is broken into the percentage of normal asymmetric cell divisions (blue) and the abnormal symmetric cell divisions (red) which occurred.

This indicates that the combination of injection and prolonged incubation results in loss of asymmetry during MI.

To determine whether this was a peculiarity of siRNA injection, I performed a series of experiments in which I injected only mRNA encoding histone-RFP, followed by incubation in G-IVF media containing IBMX and cAMP for either 20-22hrs or for 4-5hrs (Figure 6.18E). I found that 18.6% of oocytes showed symmetric PB formation when incubated for 20-22hrs compared with 1.5% when incubated for 4-5hrs. These data indicate that, as well as a prolonged incubation in media containing IBMX and cAMP, the increased time allowed for translation of histone H2B compromises the ability of oocytes to undergo the asymmetric division required to minimise loss of cytoplasm during MI (Figure 6.18A).

The abnormal near symmetrical division at exit from MI was a concern of the siRNA experiments. The cleavage furrow is usually restricted to a domain near the cortex, which is enriched in actin microfilaments and devoid of microvilli (Longo and Chen, 1985). The spindle migrates from the centre of the oocyte, to the closest part of the oocyte cortex before PB extrusion. Chromosome segregation in vertebrate oocytes is preceded by spindle elongation, followed by a shortening of kinetochore-microtubules (FitzHarris, 2012). This early spindle elongation stage determines the extent of chromosome segregation and the size of the resulting polar body (FitzHarris, 2012).

In mouse oocytes the migration of the spindle involves an interaction between the chromosomes and actin microfilaments, not microtubules (Longo and Chen, 1985; Maro *et al.*, 1986; Maro and Verlhac, 2002; Schuh and Ellenberg, 2008). Spindle migration requires a continuously reorganising cytoplasmic actin

network, organised by the actin-filament nucleators Formin-2 (Azoury *et al.*, 2008; Schuh and Ellenberg, 2008) and Spire1/2 (Pfender *et al.*, 2011) which pull and/or push on the microtubule spindle. The spindle and actin network both migrate to the closest part of the oocyte cortex (Verlhac *et al.*, 2000; Schuh and Ellenberg, 2008). Spindle migration promotes cortical differentiation, resulting in the area absent of microvilli and rich in actin (Longo and Chen, 1985). This is the first sign of oocyte polarisation and defines the site of PB formation.

Precedent for abnormal positioning of the cleavage furrow comes from a number of studies. Mice lacking Mos, an upstream activator of mitogen-activated protein kinase (MAPK), have also been found to form larger PBs at anaphase (Verlhac *et al.*, 2000). This was due to the spindle not migrating to the oocyte cortex before anaphase. Instead, the spindle elongated, with the pole closest to the cortex moving towards it, while the innermost pole remained tethered to the central region resulting in the cleavage plane forming deeper into the oocyte (Verlhac *et al.*, 2000). Spindle migration has also been inhibited in the presence of brefeldin A (BFA), a fungal toxin which inhibits Golgi-based membrane vesicle fusion, resulting in the formation of large PBs (Wang *et al.*, 2008). Previous work in our lab indicates that depletion of the spindle checkpoint protein Mad2 also results in a prevalence of large PBs (Homer *et al.*, 2005). This is most likely linked to accelerated onset of anaphase, which occurs in Mad2-depleted oocytes (Homer *et al.*, 2005).

My findings indicate that large PBs in oocytes maintained in IBMX for 20-22hrs are linked to over-expression of Histone H2 rather than exposure to IBMX alone. It is not clear from my studies whether anaphase is accelerated, like the Mad2 phenotype, or whether histone expression is interfering with the mechanisms of spindle migration in another way. It would however be interesting to investigate.

6.8.2 Injection of Sgo2 siRNA induces premature separation of sister centromeres.

To determine whether depletion of Sgo2 resulted in separation of sisters I fixed oocytes after maturation to MII. Single sisters were observed (Figure 6.19), consistent with the observations of Lee *et al.* (Lee *et al.*, 2008).

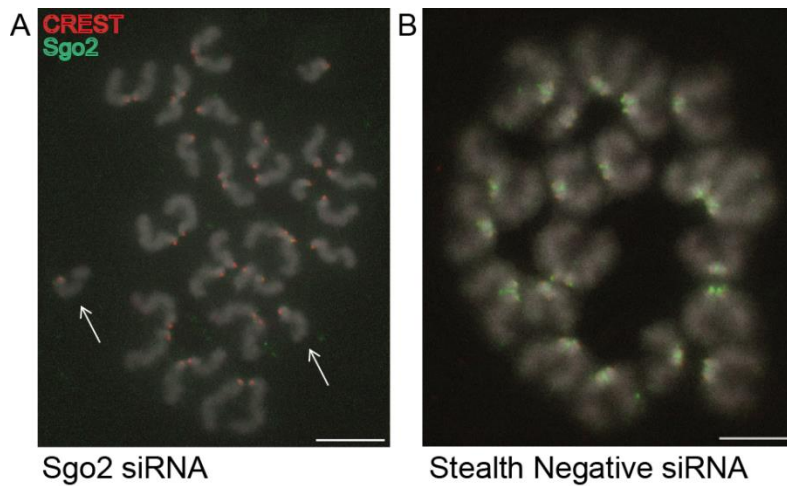


Figure 6.19 - Single sister chromatids are observed at MII in Sgo2 knockdown chromosome spreads. (A) Oocytes were co-injected with mRNA encoding histone-RFP and (A) 1 μ M Sgo2 siRNA, or (B) 1 μ M Stealth negative siRNA. Oocytes expressing histone were incubated 5-6hrs to allow knockdown in G-IVF supplemented with IBMX and cAMP, before incubating in un-supplemented G-IVF media to allow overnight maturation using timelapse microscopy. MII chromosome spreads were prepared the next day on paraformaldehyde-coated slides and immunofluorescence labelling of Sgo2 and CREST was performed. Scale bar represents 10 μ m. (A) 2/9 oocytes (from 2 mice) produced a PB with both showing single sister chromatids (white arrows). (B) 3/9 oocytes (from 2 mice) produced a PB, none of the 3 showed single sister chromatids.

Of the oocytes which produced a PB after injection with 1 μ M Sgo2 siRNA followed by 22hr incubation, 100% (2/2) showed single sisters (0/3 for Stealth negative control). 8/14 PB oocytes showed single sister chromatids across all the experiments done over the range of Sgo2 siRNA concentrations and incubation times.

6.9. What is the effect of Sgo knock down on chromosomal cohesin?

Having optimised the protocol for the efficient knockdown of Sgo2, the next step was to determine whether silencing of Sgo2 affected cohesin's association with chromosomes during progression through M phase of MI (Figure 6.20). Given the difficulty associated with the Rec8 antibody, I measured cohesin levels by chromosome immunofluorescence using oocytes from a Rec8-myc transgenic mouse strain, in which the endogenous cohesin subunit Rec8 is entirely

replaced by a Myc (GEQKLISEEDLN) tagged Rec8 (Kudo *et al.*, 2006; Kudo *et al.*, 2009). These mice express Rec8 from a bacterial artificial chromosome (BAC), with nine tandem copies of the human c-myc epitope at its C terminus (Kudo *et al.*, 2006; Kudo *et al.*, 2009).

These experiments reveal that cohesin remains on the arms despite the absence of Sgo2. However, its levels do appear to be reduced, indicating that Sgo2 may be required for retention of a subset of cohesin complexes during MI.

The more striking finding of these experiments is that the CREST signal was markedly reduced in the absence of Sgo2, indicating that Sgo2 is directly or indirectly required for recruitment or retention of the centromeric proteins CENP-A, CENP-B and CENP-C. The reduced CREST signal made it impossible to perform a ratiometric measurement of Rec8-myc at the centromeres. However, measurement of the distance between extremities of the CREST foci at sister centromeres indicates that the Sgo2 knockdown promotes splitting of sister centromeres ($p=0.000$) (Figure 6.21). While this is similar to the effect of cohesin depletion, I cannot rule out the possibility that the distance is increased due to mislocalisation of the centromeric proteins targeted by CREST.

From these experiments we can only conclude that Sgo2 is clearly required to protect centromeric cohesin from separase-mediated cleavage during anaphase of MI, consistent with the observations of Lee *et al.* (Lee *et al.*, 2008). I need to develop a more robust method to determine whether I am truly observing a reduction in cohesin upon knocking down Sgo2. A protein that localises to the chromosome axes and whose levels remain constant would be very useful for normalising cohesin. We are currently investigating the potential of Topo 2 for this purpose.

These data so far indicate that Sgo2 may have a role in protecting cohesin during progression through M phase of MI. This role could be important in humans, which have a prolonged M phase.

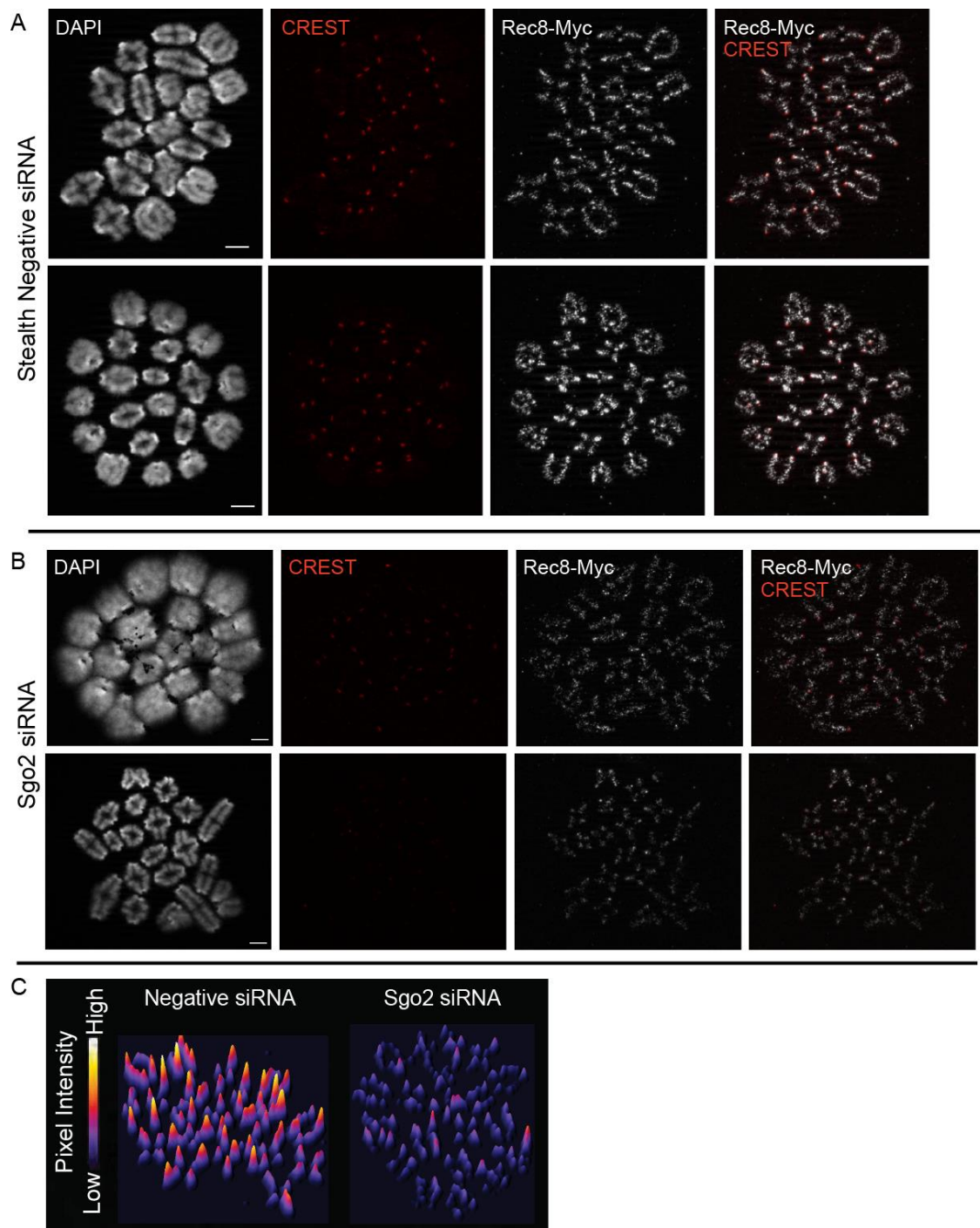


Figure 6.20 - Rec8 and CREST are reduced in Sgo2 knockdown oocytes.

Paraformaldehyde chromosome spreads were prepared during mid prometaphase I (GVBD + 5hrs) in oocytes from 2 month old Rec8-Myc mice, which had been microinjected with either (A) Stealth Negative siRNA (n = 38 from 9 mice), or (B) Sgo2 siRNA (n = 15 from 9 mice). Oocytes were incubated 21hrs to achieve knockdown before being matured to prometaphase. Representative images show DAPI (grey); CREST (red) and Rec8-Myc (grey) immunolabelling. The CREST and Rec8-Myc images are overlaid in the right hand panel. The chromosomes were further stained for Sgo2 to verify complete knockdown (image not shown). Scale bar represents 10 μ m. Reduced levels of Rec8-Myc and CREST are observed on the chromosomes of Sgo2 knockdown oocytes. (C) Representative 3D surface plots of chromosome spreads from (A) and (B) illustrate reduced Rec8-myc fluorescence intensity on the chromosomes of Sgo2 siRNA injected oocytes compared with Stealth negative siRNA injected.

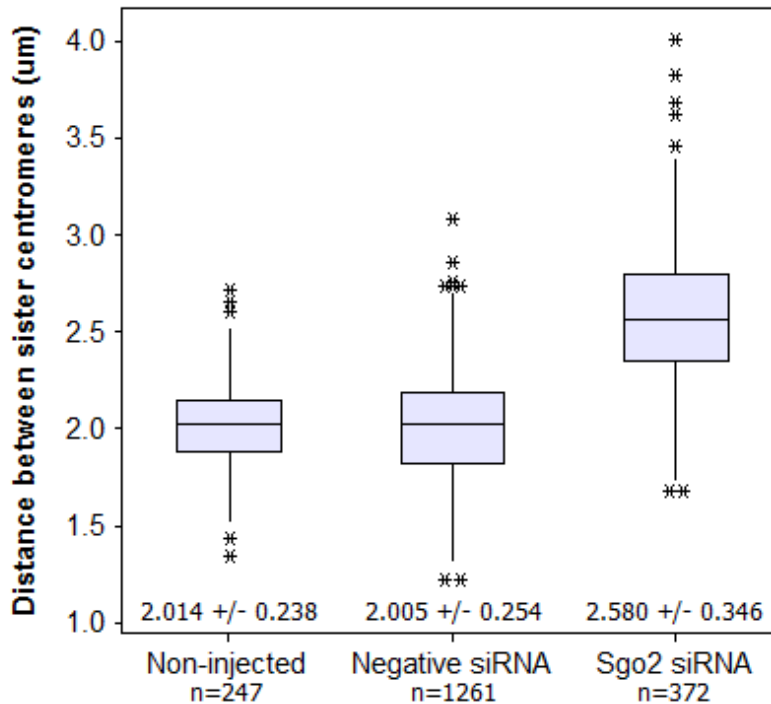


Figure 6.21 - Sgo2 knockdown is associated with increased sister centromere splitting. The distance was measured from the outermost margins of the CREST signals in chromosome spreads from Figure 6.20 (as performed previously in Figure 6.6). The mean distance was significantly greater between the sister centromeres in oocytes which had been injected with Sgo2 siRNA (2.580 ± 0.346 ; $n=372$ centromeres; 13 oocytes from 6 mice) compared with those injected with Negative siRNA (2.005 ± 0.254 ; $n=1261$ centromeres; 35 oocytes from 9 mice) ($p < 0.000$). There was no significant difference between the centromere distances of oocytes injected with Negative siRNA, compared with non-injected controls (2.014 ± 0.238 , $n=247$ centromeres; 7 oocytes from 3 mice) ($p=0.595$).

6.10. Do reduced levels of cohesin influence the recruitment of Shugoshin?

To determine whether the reduced levels of Sgo were a cause or a consequence of reduced levels of cohesin, I prepared chromosome spreads of oocytes from mice deficient for the meiotic cohesin subunit Smc1 β (*Smc1 β ^{-/-}*). Prometaphase I chromosome spreads revealed reduced levels of chromosome associated Sgo2 compared to those from the wild type (wt) strain (Figure 6.22). This raised the possibility that the recruitment or retention of Sgo2 is either directly or indirectly influenced by the level of cohesin.

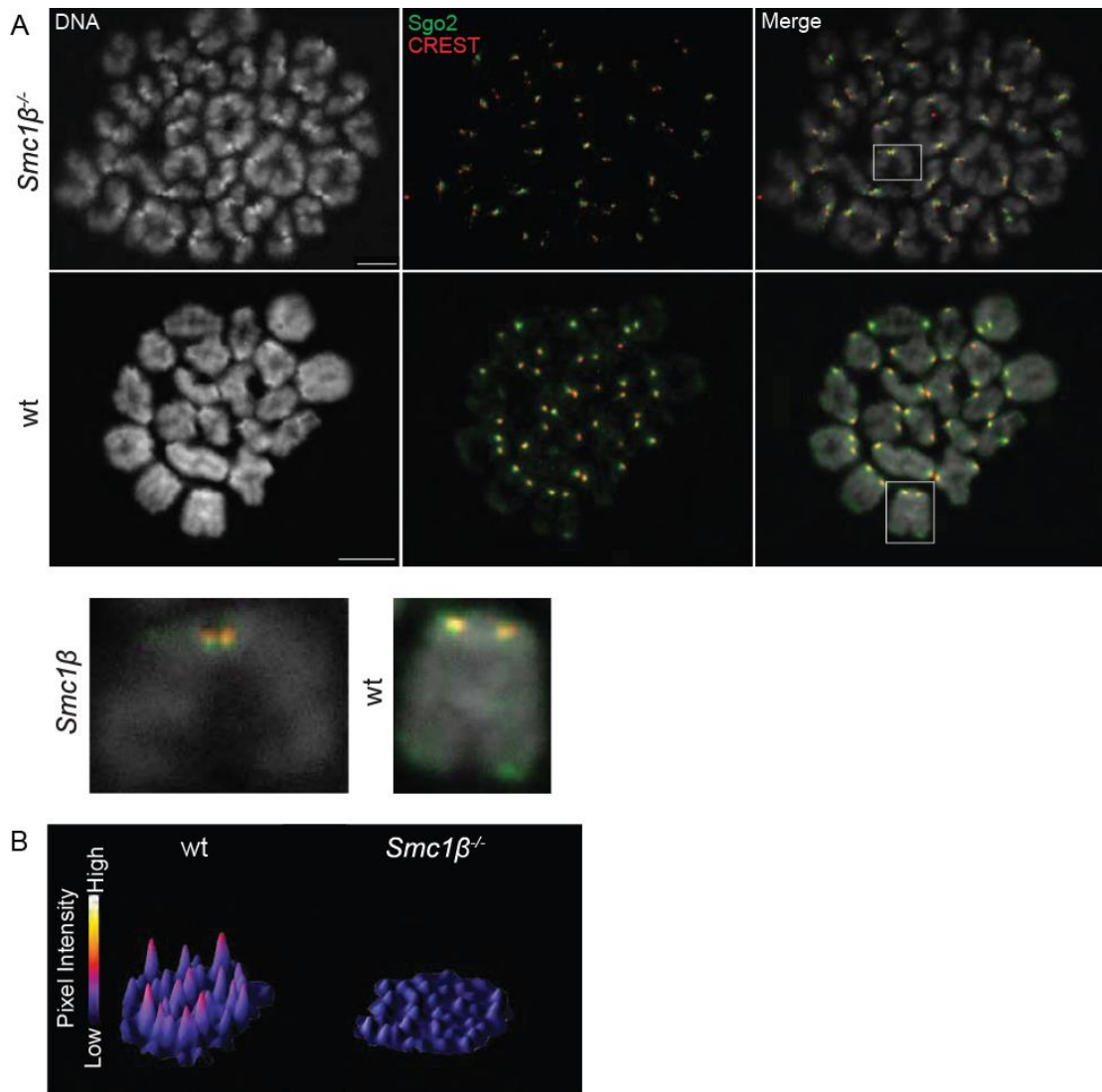


Figure 6.22 - Sgo2 levels are reduced in oocytes of *Smc1β* deficient mice. (A) Paraformaldehyde chromosome spreads were prepared during mid prometaphase I (GVBD + 5hrs) in oocytes from *Smc1β*^{-/-} mice (n = 20 from 3 mice) and *Smc1β* heterozygous and wild type mice (wt, n = 32 from 3 mice). Representative images show DAPI (grey), Sgo2 (green) and CREST (red) immunolabelling. Inset shows enlarged images of chromosomes from *Smc1β*^{-/-} (left) and wild type (right) mice. Scale bar represents 10μm. Reduced levels of Sgo2 are observed on the chromosomes of oocytes from *Smc1β*^{-/-} mice compared with wild type oocytes. (B) Representative 3D surface plots of chromosome spreads from (A) illustrate reduced Sgo2 fluorescence intensity on the chromosomes of *Smc1β*^{-/-} mice compared with wild type. *Experiment performed in collaboration with Dimitrios Kalleas (Lister et al., 2010).*

These results give ground to the hypothesis that depletion of cohesin during the prolonged prophase arrest experienced by aged oocytes, results in reduced recruitment or retention of Sgo2, which consequently further contributes to a greater loss of cohesin during prometaphase.

To summarise, the data presented in this chapter show that chromosomal cohesin is depleted with female ageing in C57BL/1crfa^t mice. This disrupts the unified structure of sister centromeres, thereby compromising their ability to establish and maintain monopolar sister kinetochore-microtubule attachments. This provides an adequate explanation for the observed splitting of sister chromatid centromeres, and the increased incidence of segregation errors with female ageing described in Chapter 5. Cohesin is lost gradually through female ageing, depleted in the later growth stages, prophase, and prometaphase of mouse oocytes. The underlying mechanisms for this are still under investigation, but it could be through either a separase dependent, or independent pathway. The centromeric protector Sgo2 was also found to be reduced with advanced female age, at both the centromeres and on the chromosome arms. Furthermore, Sgo2 seemed to mislocalise more frequently in these aged females, which likely compromises its protection of centromeric cohesin from separase at anaphase I. The reduction of Sgo2 on the chromosome arms could contribute to the destabilisation of chiasmata described in Chapter 5. This suggests a previously unidentified role for Sgo2 in mammalian meiosis. As cohesin appears to be reduced in Sgo2 knockdown oocytes, Sgo2 may be required for protecting a subset of cohesin complexes during MI. Finally, as Sgo2 was also depleted in oocytes from mice deficient for the meiotic cohesin subunit Smc1 β , this suggests that a reduction in cohesin during the prolonged prophase arrest of aged oocytes, may result in the reduced recruitment or retention of Sgo2 to the chromosomes, thereby contributing to a greater loss of cohesin through M phase.

Chapter 7. Discussion

The major determinant of female fecundity is age. As women become older there is a decline in their reserve of oocytes culminating in the menopause. However, reproductive fitness begins to decline ~12 years in advance of menopause. This is characterised by a decline in fertility and an increase in the incidence of miscarriage, predominantly caused by trisomy of chromosome 16. Female ageing is also marked by a dramatic increase in trisomy 21, which causes Down's syndrome. The relationship between age and meiotic chromosome segregation errors is also evident from analysis of oocytes produced during IVF treatment. The question of why segregation errors become prevalent as the oocyte pool declines has remained elusive. This is largely due to the lack of a convincing animal model and the intractability of anaphase of MI, which have combined to delay progress towards identifying the underlying molecular mechanisms. The work presented in my thesis addresses these problems by (i) providing evidence that mice exhibit a strong maternal age effect; (ii) using live cell imaging to identify precisely where the fault-lines lie in relation to missegregation of chromosomes during MI; and (iii) by identifying cohesin as a molecular link between chromosome missegregation and female age.

7.1. The mouse provides a promising model for female reproductive ageing

Previous studies in mice indicated that females showed only a slight age-related increase in oocyte aneuploidy (Brook *et al.*, 1984; Eichenlaub-Ritter *et al.*, 1988). Indeed our early experiments with oocytes from the age mice colony might have led us to the same conclusion. Live cell imaging of oocytes from 12 month old females revealed no striking defects in chromosome segregation errors. However, by allowing the females to age a further two months, we found that 80% of oocytes showed anaphase defects ranging in severity from single lagging chromosomes to clumps of chromatin trapped at the spindle midzone.

Thus, by allowing the females to reach a sufficiently advanced age and by performing the analysis at sufficiently high resolution, we were able to uncover a marked age-related increase in MI chromosome segregation errors.

Because males and females from the breeding colony are caged together until they die of natural causes, we were able to investigate the relationship between female age, oocyte yield, and fertility. By analysing the birth statistics over a 6 year period, I found that peak fertility, as determined by the proportion of litters born to each female age group, is attained at around the age of 6 months, and declines from ~9 months. Consistent with this, the relationship between female age and the interval between litters increases with age. This is consistent with the age-related decline in pregnancy and implantation rates observed from the human data.

Oocyte number also declines in mice, although, in contrast to humans, an accelerated rate of decline was evident from ~10 months of age. This is consistent with findings from oocyte counts obtained from human ovarian tissue (Faddy *et al.*, 1992; Faddy, 2000; Hansen *et al.*, 2008), but was not evident from my analysis of the large IVF data set generated from treatments conducted here at the Newcastle Fertility Centre. It is not clear whether this might be related to the fact that our human oocyte data are obtained from patients with underlying fertility problems.

For the purposes of investigating the relationship between the two known drivers of female reproductive ageing, I compared the rate of decline in oocyte number and oocyte quality. To do this I used our data on the number of oocytes retrieved at egg collection after hormonal stimulation for fertility treatment, and the implantation rate following embryo transfer after IVF. Given that age-related infertility is completely rescued by using donor eggs from younger women (Figure 4.10), I have used implantation rate as an indicator of oocyte quality (Figure 4.11). I repeated the comparison in the mouse model, using litter size as an indicator of implantation rates and oocyte quality. I believe this to be valid as the oocyte number retrieved after superovulation exceeded the number of pups born. Based on these assumptions, the data indicate that oocyte number declines at a slower rate than oocyte quality, and

that this is true for mice and humans. I therefore propose that oocyte quality is the greater determinant of female reproductive lifespan.

I also found that the incidence of neonatal death in mice increased with female age. Around 50% of the total number of litters born to females older than 10 months did not survive till weaning. This may reflect an increased incidence of aneuploidy in females of advanced age, highlighting a further possible parallel in the reproductive ageing process in mouse and human females. However, as aneuploid embryos rarely survive to mid-gestation (Lightfoot *et al.*, 2006) other factors must account for this increased frequency.

Surprisingly, I found that despite the lower yield, a higher proportion of oocytes from older females developed to metaphase II. This was true for both mouse and human oocytes and indicates that meiotic competence, in the sense of being able to complete MI, is not compromised by ageing. However, the ability to accurately segregate chromosomes is clearly compromised.

7.2. The effect of female age on chromosome dynamics

Live cell imaging revealed a dramatically increased incidence of aberrant chromosome dynamics during MI in oocytes from aged mice. These included mild misalignment at MI but the most striking of all were anaphase defects. Lagging chromosomes and chromatin bridges were persistent, followed by misalignment at MII. This did not appear to be due to a failure in spindle formation as oocytes from aged females assembled an apparently normal bipolar spindle.

In meiosis, homologous chromosomes must be bi-oriented on the spindle. This requires that sister kinetochores form attachments with spindle microtubules emanating from the same pole. The anaphase defects we observed were indicative of erroneous attachments (Pidoux *et al.*, 2000; Cimini *et al.*, 2001; Cimini *et al.*, 2002). This indicates that the spindle checkpoint, which is functional in oocytes of aged mice (Duncan *et al.*, 2009; Lister *et al.*, 2010), may be satisfied in the absence of correct monopolar attachment of sister kinetochores to spindle microtubules. Previous collaborative work has indicated

that univalent chromosomes can evade the spindle checkpoint by forming bipolar attachments (Kouznetsova *et al.*, 2007). Further studies will be required to determine whether sisters establish bipolar attachments in oocytes from aged mice.

7.3. The structural integrity of the bivalent, and cohesin depletion during female ageing

Genetic mapping studies in cases of Down's syndrome, indicate that the risk of trisomy 21 is correlated with the number and chromosomal position of crossovers (Lamb *et al.*, 1997). It was found that the highest risk is absence of a crossover giving rise to univalent segregation (Lamb *et al.*, 1997). This was followed by the presence of a single sub-telomeric or peri-centromeric crossover (Lamb *et al.*, 1997). However, more recently it was reported that the association between the risk of trisomy 21 and absence of any crossover, or a single sub-telomeric crossover, is lost with maternal ageing (Lamb *et al.*, 2005; Oliver *et al.*, 2008). Thus, the increased incidence of trisomy in older women appears to be due to events occurring subsequent to crossover formation.

Analysis of surface spread chromosomes revealed that oocytes from our aged females showed a prevalence of distally associated chiasmata. This was accompanied by a decline in the proportion of bivalents with a single chiasma, indicating that single chiasmate bivalents are susceptible to destabilisation during female ageing (Chapter 5). The prevalence of distally associated homologues was reminiscent of the SMC1 β knockout mouse phenotype (Hodges *et al.*, 2005). Thus, cohesin seemed an obvious candidate for investigation. Chromosomal cohesin, required to mediate cohesion between sister centromeres and stabilise chiasmata between bivalent chromosomes during meiosis I, was found to be markedly reduced in oocytes from aged mice. The reduced cohesin levels were obvious on arms and at centromeres, particularly in the pericentromeric region, where cohesin was highly enriched in oocytes from younger mice.

Our results indicate that depletion of oocyte chromosomal cohesin during female ageing gives rise to a prevalence of bivalents with no discernible chiasmata. The barriers to accurate segregation of these distally associated homologues are presumably similar to those of achiasmate or single sub-telomeric configurations. In this sense, it could be argued that depletion of cohesin leads to the acquisition of susceptible chiasmate configurations that do not necessarily reflect the position at which crossovers were formed.

Sub-telomeric recombination events are susceptible as they only need to lose the very little cohesin distal to the exchange. If the cohesin at the centromere is already weakened, then this could be all it takes for the sisters to prematurely separate. There was a notable absence of univalent chromosomes (completely separated homologues) in our results. Instead homologous pairs remained associated at telomeres. The sustained association of telomeres raises the possibility that the telomere region is endowed with a property that enables them to withstand cohesin depletion during ageing. It remains to be determined whether this is due to enrichment of cohesin at telomeres or whether other factors are contributing.

Centromeric cohesin is important for maintaining the closely apposed structure of sister centromeres (Watanabe *et al.*, 2001; Sakuno *et al.*, 2009). This joins the sister kinetochores, enabling monopolar orientation and correct spindle attachment. Consistent with this, we found that the distance between sister centromeres was increased in oocytes of aged mice.

We are not the only lab to have shown a connection between defective cohesin and the increased incidence of MI segregation errors with advancing maternal age. Our findings have been corroborated by two other studies.

Liu and Keefe (2008) reported reduced levels of Rec8 and SMC1 β in oocytes from aged mice, in association with an increased frequency of chromosome misalignment and precocious separation of sister chromatids (Liu and Keefe, 2008). These experiments were performed on both young and aged hybrid F1 and SAM mice, with much greater reductions observed in the SAM oocytes. This was found with two different Rec8 antibodies, one being our own (Kouznetsova *et al.*, 2005), and using a similar chromosome spread protocol (Hodges and Hunt, 2002). However, the value of these mice is questionable for

characterising maternal age-related meiotic defects, as nuclear transfer experiments where defects could be rescued by young wild type cytoplasm but not young SAM cytoplasm, suggest an inherent problem in the regulation of SAM oocytes (Liu and Keefe, 2004). Another limitation of these experiments was that misalignment was only looked at in fixed whole oocyte samples. Although the MI misalignment defects observed concur with our observations by live cell imaging (Lister *et al.*, 2010), the natural variation between oocytes in the timing of alignment needs to be taken into account. Although they did not comment on it in their publication, it is obvious from the images that they also observed an increased distance between sister centromeres at MI (Liu and Keefe, 2008, Figure 3B). In contrast, their evidence of MII misalignment does also not look to be to the same extent as we have observed (Lister *et al.*, 2010).

Published alongside our paper in Current Biology (Lister *et al.*, 2010) was the work of another group reporting very similar results to our own (Chiang *et al.*, 2010). They used B6D2F1/J and CB6F1/J mice, but in contrast to our model, their aged mice were much older than our own (16-19 months). However, their aged females were obtained from a separate facility, so it could be argued that the differences between young and aged oocytes could have been explained by environmental factors. In this sense, I believe that our findings strengthened the data presented by Chiang *et al.* (2010).

In contrast to our cohesin measurements, which were done on chromosome spreads, Chiang *et al.*, (2010) performed cohesin staining on intact fixed oocytes. Nonetheless, their findings confirmed that cohesin is markedly reduced in aged oocytes. Moreover, they extended our understanding by performing western blots to determine whether the reduction in Rec8 was due to a global decline. They found no noticeable difference between the total cohesin in oocytes of young and aged mice (Chiang *et al.*, 2010). Thus, the problem appears to lie with maintaining cohesin on the chromosomes. Consistent with our data, Chiang *et al.* also reported an increased incidence of distal chiasmata at MI, and increased distances between sister kinetochores at MI, and MII (Chiang *et al.*, 2010). The intercentromere distances were measured in oocytes fixed after treatment with monastrol to generate monopolar spindles, thereby allowing distance measurements with no tension across the sister kinetochore pairs. This has also been reported for MII oocytes

of CD1 mice fixed by a similar method (Merriman *et al.*, 2012). Interkinetochore distances not only increased with age, but were also found to be greater in aneuploid oocytes when compared with euploid oocytes (Merriman *et al.*, 2012). Furthermore, this increased distance has recently been observed in oocytes of young mice which have a predisposition to become aneuploid (Merriman *et al.*, 2013). This further strengthens the link between the loss of chromosomal cohesion and segregation errors.

Chiang *et al.* were able to link the reduction in cohesin to chromosome segregation errors by live cell imaging of oocytes, followed by chromosome spreads of each imaged MII oocyte, to then compare the chromosome count to any defects observed at anaphase. This enabled them to elucidate what errors may have occurred at MI (Figure 7.1) (Chiang *et al.*, 2010). This is a very precise technique and one I have since tried to incorporate with my own timelapse experiments. If centromeric cohesion was compromised, but remained functional, and the sister kinetochores biorient at MI, the chromosome pair would be pulled in opposite directions by spindle microtubules, leading to a lagging chromosome pair at anaphase. This would then be pulled to the wrong pole, resulting in its gain or loss to the oocyte (Figure 7.1B). However, the most common abnormalities found in MII oocytes by both ourselves and Chaing *et al.* were separated sister chromatids and the loss or gain of single chromatids, which can be explained by the premature loss of centromeric cohesin (Figure 7.1C and D). The increased distance between sister centromeres could be resulting in biorientation, rather than the mono-orientation of sister kinetochores. Either the bioriented sisters could separate early, whereby no chromosomes would lag at anaphase (Figure 7.1C), or a single kinetochore could biorient and lag at anaphase (Figure 7.1D). Both would result in the gain or loss of a single chromatid. Another possibility would be for the sister kinetochores to mono-orient, but if cohesin was weakened the pair could separate prematurely, resulting in an apparently normal segregation at anaphase, but the MII oocyte would be euploid with a pair of separated chromatids (Figure 7.1E).

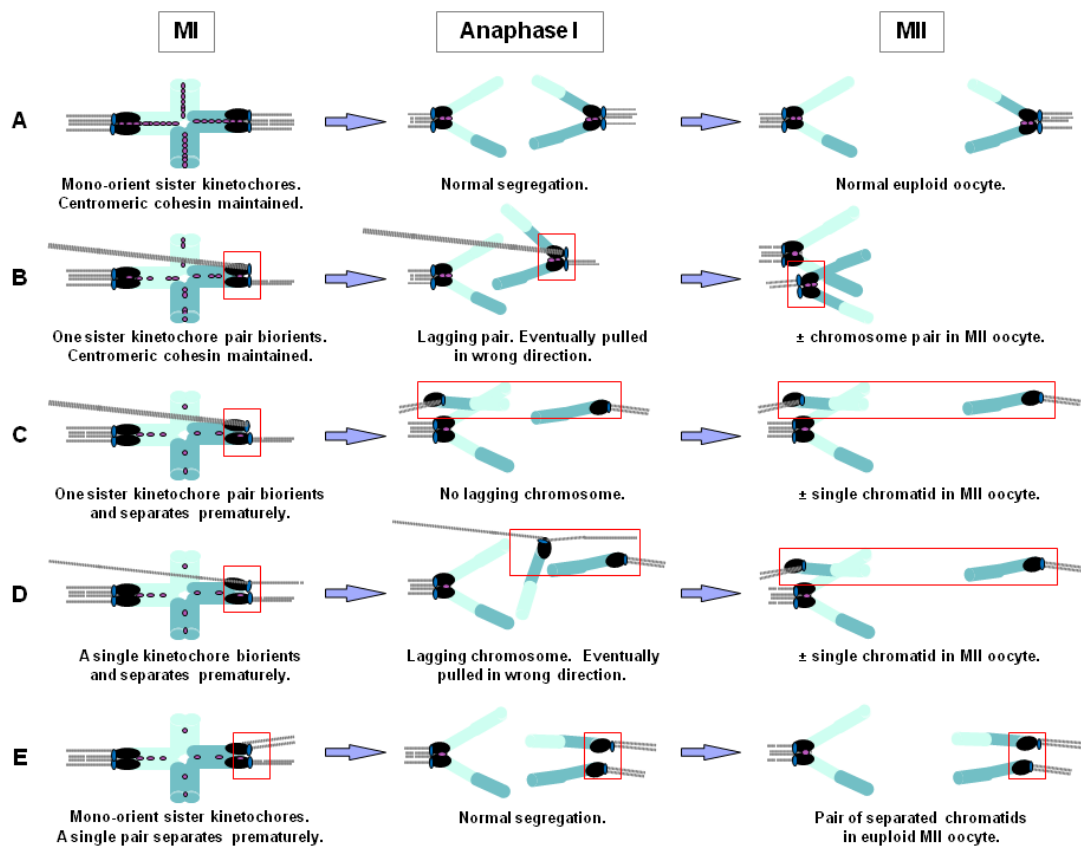


Figure 7.1 - Errors associated with cohesin loss at MI. Schematic illustrating the possible outcomes of normal (A) or compromised (B–E) centromere cohesion in MI. (A) Normal chromosome segregation resulting in a euploid oocyte. (B) If centromeric cohesion is compromised but still functional and sister kinetochores biorient at MI, the chromosome would be pulled in opposite directions by spindle microtubules, leading to a lagging chromosome pair at anaphase. The chromosome pair would be pulled toward the wrong pole, resulting in its gain or loss in the MII oocyte. (C) If the bioriented sisters separate prematurely, then no chromosomes lag at anaphase, and the oocyte would gain or lose a single chromatid. (D) If a single kinetochore biorients and separates prematurely, the single bioriented chromatid would lag at anaphase, resulting in the gain or loss of a single chromatid in the MII oocyte. (E) If sister kinetochores mono-orient, but a single pair separates prematurely, then segregation would be normal at anaphase, and the MII oocyte would be euploid with a pair of separated chromatids. Red boxes follow the progression of a single sister kinetochore pair. Adapted from (Chiang *et al.*, 2010).

One of the limitations of our data was that our live cell images were only taken every 20 minutes, with 5 images planes 7.5 μ m apart. Although these were the optimised parameters compatible with maturation to MII on our microscope, it is likely that we underestimated our incidence of anaphase defects, as they may have been just missed, or, not as clearly viewed in our selected planes of focus. In contrast, Chiang *et al.* used a confocal microscope for their live cell

experiments, and were able to acquire images at 13 intervals of 1 μm , every 1-2 minutes (Chiang *et al.*, 2010). Our group is optimising a protocol for timelapse imaging on the confocal microscope, with increased acquisitions around the time of anaphase.

In summary, these findings indicate that cohesin depletion, observed in different aged mouse strains using a range of cohesin antibodies (Liu and Keefe, 2008; Chiang *et al.*, 2010; Lister *et al.*, 2010) results in increased intercentromere distances between sister centromeres. Along with the destabilisation of chiasmata, this contravenes the structural requirements for the bivalents to establish monopolar attachments and accurately biorient in order for normal segregation to occur (Petronczki *et al.*, 2003), thereby explaining the anaphase defects we observed in mouse oocytes.

Our findings in mice also provide plausible explanations for clinical observations on the risk of trisomy in relation to age and bivalent configuration, in particular, the increased prevalence of peri-centromeric crossovers in trisomy 21 offspring of older mothers (Oliver *et al.*, 2008). Given that homologue disjunction requires cleavage of arm cohesin distal to chiasmata (Petronczki *et al.*, 2003), it follows that resolution of peri-centromeric chiasmata requires that separase-mediated cohesin cleavage occurs in close proximity to the centromeres. In such a situation, an age-related reduction of Sgo2, such as we found in mouse oocytes, would render centromeric cohesin particularly vulnerable to cleavage by separase during anaphase of MI. The resultant single sisters would be at high risk of missegregation leading to trisomy during MII. This problem would be greatly compounded by an increased distance between sister centromeres, which was prevalent in mouse oocytes (Chiang *et al.*, 2010; Lister *et al.*, 2010). In the case of peri-centromeric crossovers the two sets of sister kinetochores would be in relatively close proximity when the bivalent is establishing bipolar attachment. Under these conditions, the loss of tight associations between sister centromeres may render mono-orientation of sisters particularly challenging.

7.4. Chromosomal association of Sgo2 is impaired in cohesin deficient mice

We found that the mammalian centromeric protector Sgo2, which appears to be recruited during the prophase to M phase transition (experiments performed in collaboration with D. Kalleas), was also reduced in oocytes from aged mice. To determine whether this was related to cohesin depletion, we asked whether Sgo2 was also reduced in oocytes lacking the cohesin subunit SMC1 β . We found that Sgo2 staining was reduced on the chromosomes of SMC1 β ^{-/-} oocytes compared with wild type oocytes. These data suggest that cohesin is either directly or indirectly required for efficient recruitment or retention of Sgo2. This is consistent with findings in maize (Hamant *et al.*, 2005).

Given that Sgo2 is known to protect cohesin from separase during anaphase of MI, reduced Sgo2 at centromeres provides a likely explanation for the presence of single sisters in MII oocytes from aged mice. However, Sgo2 also localised strongly to chromosome arms during M phase of MI. This did not appear to be due to non-specific binding as the arm staining was lost in oocytes injected with Sgo2 siRNA. In support of the idea that arm-associated Sgo2 is protecting cohesin on the arms during M phase, I found that it recruits its binding partner PP2A, and that arm cohesin appeared to be reduced following knock down of Sgo2 by siRNA. These data suggest that, in addition to its canonical function in protecting cohesin at centromeres during anaphase of MI, Sgo2 may also protect cohesin on the arms during progression through M phase. It would presumably be necessary to move Sgo2 off the arms to enable separase to cleave cohesin at the onset of anaphase. However, in preliminary experiments (Figure 6.13), I found that Sgo2 and PP2A persist late into M phase. It is conceivable that this acts a mechanism to tightly co-ordinate anaphase with exit from M phase. This may be particularly important in oocytes, which, according to our current understanding, begin to degrade securin and cyclin B approximately 2 hours before the onset of anaphase (Herbert *et al.*, 2003).

7.5. Proposed model for cohesin depletion and chromosome segregation errors during female ageing

Together these data give foundation to the hypothesis that depletion of cohesin during the prolonged prophase arrest of aged oocytes, leads to the reduced recruitment or retention of Sgo2 (Figure 7.2). This in turn may further contribute to increased loss of cohesin during progression through M phase.

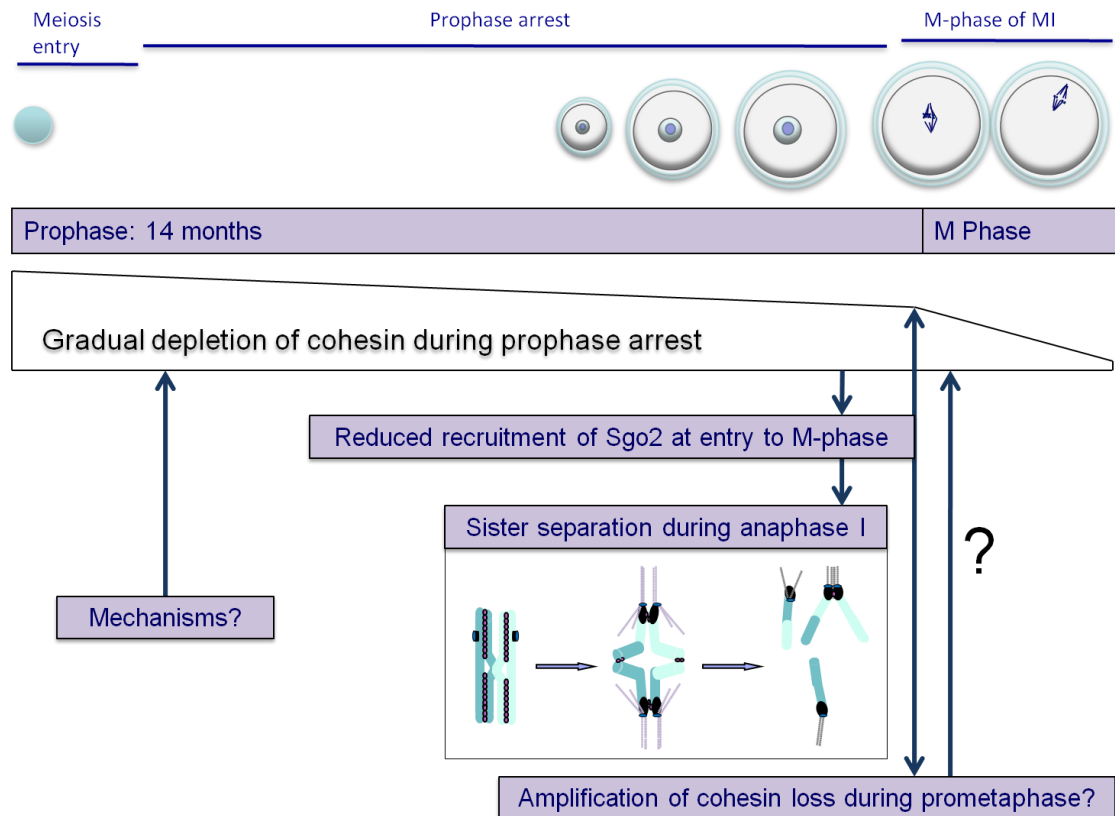


Figure 7.2 - Schematic representing the hypothesised processes contributing to MI segregation errors. Cohesin is gradually lost throughout prometaphase, which leads to reduced recruitment or retention of Sgo2. This then further contributes to amplifying cohesin loss during prometaphase to below the level required to maintain the bivalent integrity required for correct segregation at anaphase I.

We believe that could have a significant impact, especially in the case of human oocytes, which remain in M phase for at least 20 hours. Such an amplification step could lead to depletion below a threshold level needed to maintain the structural requirements for a normal reductional division during MI. Specifically, destabilisation of chiasmata, and loss of the closely apposed structure of sister centromeres, would make it difficult to establish the required tension and

monopolar kinetochore-microtubule attachments required for normal segregation during anaphase of MI. On the basis of the data showing the greater prevalence of sister centromere separation presented in Chapter 6, I propose that this defect is the major contributor to aberrant segregation during anaphase. In support of this, lagging and trapped chromosomes are a hallmark of aberrant kinetochore-microtubule attachments both in mitosis (Cimini *et al.*, 2001; Cimini *et al.*, 2002) and meiosis (Watanabe and Nurse, 1999).

7.6. What might be the mechanisms of cohesin depletion?

During mitosis, cohesin loss occurs by two pathways. First there is Plk1-mediated removal of the bulk of arm cohesin before the onset of anaphase (Darwiche *et al.*, 1999; Losada *et al.*, 2002; Sumara *et al.*, 2002). Secondly, centromeric cohesin is cleaved by the protease separase (Uhlmann *et al.*, 1999; Hauf *et al.*, 2001). While removal of cohesin from arms and centromeres during anaphase at MI and MII requires cleavage by separase, it is not known whether a meiotic equivalent of the prophase pathway is functional in meiosis.

The protein Sgo was first discovered in fission yeast to have a conserved role in protecting centromeric cohesin from separase-mediated removal during anaphase of MI (Kitajima *et al.*, 2004). Deletion of Sgo2 in mammalian oocytes gives rise to a reduction in centromeric cohesin, resulting in premature sister chromatid separation (Lee *et al.*, 2008). Furthermore, in vertebrate somatic cells, Sgo was found to protect centromeric cohesin from removal by the prophase pathway.

While reduced Sgo2 may contribute to cohesin loss during progression through M phase, and likely explains the presence of prematurely separated sisters in MI oocytes, our observations suggest that it is not a major player in protecting cohesin from removal during prophase arrest. However, my findings indicate that Sgo2 may have a role in protecting arm cohesin during progression through M phase. While this may act as a mechanism to prevent premature cleavage by separase, it may also prevent removal of cohesin by a meiotic equivalent of the prophase pathway. However, the work of my colleague Dimitrios Kalleas

indicates that cohesin is only very slightly enriched in the presence of a small molecular inhibitor of Plk1. This implies that the Plk1-mediated removal of cohesin, which is a defining feature of the prophase pathway, is not a major contributor to cohesin loss during progression through prophase of MI. Moreover, the work of another colleague, Randy Ballesteros Mejia, indicates that while Plk1 is present in the cytoplasm from the primordial stage onwards, it is not detectable in the nucleus, indicating that Plk1-mediated removal does not contribute to cohesin loss during prophase arrest. Thus, it is unlikely that a meiotic equivalent of the prophase pathway contributes significantly to the depletion of cohesin from oocyte chromosomes during female ageing.

The simplest explanation for the removal of cohesin during female ageing would be the premature activation of separase. Separase has been shown to be present during prophase of yeast meiosis I (Katis *et al.*, 2010); and my results have shown it to be expressed during the different stages of growth in prophase arrested oocytes (Figure 6.10). At this point, separase activity would be exclusively under the control of securin, as Cyclin B-Cdk1 is suppressed in prophase (Reis *et al.*, 2006). Even a small fraction of separase activity, either due to securin dissociation or degradation (Marangos and Carroll, 2008), would have extremely detrimental effects over a prolonged period of time, such as the human prophase arrest.

My ongoing work is aimed at testing this hypothesis using a separase knockout mouse. Separase deletion causes embryonic lethality in mice (Kumada *et al.*, 2006; Wirth *et al.*, 2006). Previous investigations into separase function, specifically during oocyte maturation, have utilised a mouse strain which expresses Cre recombinase during the growth stage of oocytes from the *Zona pellucid 3* promoter (*Zp3-cre*), to delete a floxed version of the separase gene (Kudo *et al.*, 2006). Separase^{flox/flox} *Zp3-cre* females were found to be sterile, however their ovaries held normal numbers of GV oocytes, indicating that an active form of separase is not required for oocyte growth. It is however required for the removal of Rec8 from the chromosome arms and the resolution of chiasmata (Kudo *et al.*, 2006). As *Zp3* is not expressed until oocytes are recruited for growth, a more useful strain would be one in which separase is deleted at the primordial stage, which is where the oocyte spends the vast majority of its life in prophase arrest. To determine whether separase is indeed

responsible for removal of cohesin at the primordial stage, we are currently breeding a Separase^{flox/flox} GDF9-cre mouse strain. In this strain Cre recombinase is driven from the growth differentiation factor-9 promoter (*GDF9-cre*). As GDF9 is expressed in primordial oocytes, floxed separase will be deleted in primordial as well as growing oocytes (Rajkovic *et al.*, 2004; Wu *et al.*, 2004).

My experimental strategy is to age these mice and use the methods previously described to measure cohesin levels at the centromeres. Rescue experiments would also be conducted by microinjecting separase mRNA. If separase is the culprit in prophase cohesin depletion, then upon its rescue we would not observe any anaphase defects. We already have these mice in our animal unit, and are in the process of breeding and ageing females.

7.7. Is it possible that cohesin depletion reflects a problem with its replenishment during ageing?

According to our current understanding in yeast, cohesion between sisters during MI depends on the cohesin complexes loaded during DNA replication (Uhlmann and Nasmyth, 1998; Haering *et al.*, 2004). In view of the extended period of prophase arrest in oocytes, it was considered unlikely that the maintenance of cohesin between sisters, required to stabilise bivalent chromosomes, would depend on cohesin loaded in pre-meiotic S phase during fetal life. If so, then the depletion of oocyte cohesin could reflect an age-related deficiency in the replenishment of cohesin complexes. Remarkably, this appears not to be the case.

Genetic studies in mice indicate that cohesin loaded in pre-meiotic S phase in mouse oocytes, has to hold the chromosomes together until the end of meiosis I (Revenkova *et al.*, 2010; Tachibana-Konwalski *et al.*, 2010).

Revenkova *et al.* first showed evidence of an age-related decline in cohesin with a transgenic mouse deficient in the meiotic cohesin subunit SMC1 β (Revenkova *et al.*, 2004). They later developed a new mouse model carrying a floxed SMC1 β gene and Cre recombinase under the control of Gdf9. As Gdf9 is

expressed shortly after birth, it is from this point that no more SMC1 β protein can be produced. Any SMC1 β found on the chromosomes would have had to be synthesised and loaded during the meiotic prophase before birth. In contrast to the original knockout mouse, these new mice were fertile and showed no cohesin loss. This indicates that the reloading of cohesin was not required.

These findings were supported by Tachibana-Konwalski *et al.* using mice in which Rec8 was made cleavable by TEV protease (Tachibana-Konwalski *et al.*, 2010). If non-TEV-cleavable Rec8 mRNA was expressed after the initial establishment of cohesin during fetal prophase, and cohesin turnover and reloading does exist, then it should rescue the oocyte from TEV cleavage. As the bivalent chromosomes were converted to chromatids upon injection of TEV mRNA, this indicated that the injected Rec8 mRNA did not form functional TEV resistant cohesin complexes on the chromosomes.

These data provide strong evidence as to the lack of further cohesion establishment by cohesin reloading after the primordial stage. If cohesin in human oocytes also depends on cohesin complexes loaded in S Phase, this raises the amazing spectre of cohesin complexes remaining stable for decades.

7.8. How do the meiotic defects of mouse oocytes fit with what we know about reproductive ageing in humans?

The dynamics of the cohesin proteins Rec8; SMC1 β ; SMC3 and STAG3, were analysed by immunofluorescence at different stages of meiosis in human oocytes (Garcia-Cruz *et al.*, 2010). As expected, they were found to be present in meiosis I along the chromosome arms, and persisted at the centromeres until MII. Thus, bivalent integrity in human oocytes is likely to be mediated by cohesin.

Consistent with our mouse data, and the work observed by others (Chiang *et al.*, 2010; Revenkova *et al.*, 2010), it was recently reported that the inter-kinetochore distance between sister chromatids was increased in oocytes from older women. Furthermore, oocytes from older women showed an increased incidence of unpaired sister chromatids (Duncan *et al.*, 2009; Duncan *et al.*,

2012). These findings, which are consistent with a large scale study of human oocytes from IVF treatment (Pellestor *et al.*, 2003), support the idea that cohesin depletion contributes to the age-related increase in meiotic segregation errors in human oocytes.

7.9. What can we conclude?

The work presented in my thesis provides evidence that mice exhibit a strong maternal age effect. Using live cell imaging we identify precisely where the fault-lines lie in relation to missegregation of chromosomes during MI, and identify cohesin as a molecular link between chromosome missegregation and female age.

These data indicate that oocyte number declines at a slower rate than oocyte quality and that this is true for both mice and humans. I therefore propose that oocyte quality is the greater determinant of female reproductive lifespan. We found that female ageing was associated with loss in the integrity of bivalent chromosome structure. This was accompanied by a decline in the proportion of bivalents with a single chiasma, indicating that single chiasmata bivalents are susceptible to destabilisation during female ageing. We also found that cohesin depletion results in increased intercentromere distance. Along with the destabilisation of chiasmata, this contravenes the structural requirements for the bivalents to establish monopolar attachments and accurately bi-orient in order for normal segregation to occur, thereby providing a plausible explanation for the observed anaphase defects. We further found that cohesin is either directly or indirectly required for efficient recruitment or retention of Sgo2. In somatic cells and yeast, Shugoshin localisation has been found to require Bub1 (Kitajima *et al.*, 2004), in association with histone H2A (Kawashima *et al.*, 2010). However, we believe that our observed reduction of Sgo2 is unlikely to be due to a reduction or mislocalisation of Bub1 as previous experiments have shown it not to be impaired in aged oocytes (Sarah Pace, PhD thesis). Moreover, oocytes depleted of Bub1 did not show widespread loss of centromeric cohesin (McGuinness *et al.*, 2009).

In addition to its canonical function in protecting cohesin at centromeres during anaphase of MI, Sgo2 may also protect cohesin on the arms during progression through M phase. Together these data gave foundation to the hypothesis that depletion of cohesin during the prolonged prophase arrest of aged oocytes, leads to the reduced recruitment or retention of Sgo2 (Figure 7.2). This in turn could further contribute to increased loss of cohesin during progression through M phase.

However, while my Sgo2 siRNA experiments confirm the role of Sgo2 in protecting centromeric cohesin during anaphase of MI, there was no striking reduction in levels of arm cohesin present during late M phase. This argues against Sgo2 having a major role in protecting arm cohesin before the onset of anaphase.

7.10. What are the next steps for this research?

The key questions are how and when is cohesin lost? What is causing cohesin loss during the prolonged prophase arrest associated with oocytes, in particular those of women of advanced maternal age? Furthermore, is cohesin depleted as early as in the primordial oocyte stages? If this were the case it is no wonder the oocytes from aged females become so vulnerable, given that the oocyte will spend most of its life arrested at the primordial stage. This is an even greater concern in human females of advanced age. We are beginning further studies into the depletion of cohesin across the different types of oocytes populations (Randy Ballesteros Mejia). Doing this across a range of ages of C57BL/1crfa^t females should take us closer to answering the question of when cohesin is first depleted. If cohesin is not lost at the primordial stage then there may be scope for developing intervention strategies, to reduce the genetic risk to children of older women.

Determining whether cohesin loss and age-related meiotic errors are mechanistically linked to germ cell depletion is vital to our understanding of the biology of female reproductive ageing. The recent creation of mouse models of premature ovarian depletion, provide a means of uncoupling germ cell depletion

from chronological age. Mice carrying an oocyte-specific deletion of Pten, a phosphatase which restrains the recruitment of primordial oocytes into the growing pool (Reddy *et al.*, 2008) undergo premature exhaustion of the germ cell pool by 14-16 weeks, though reproductive function is otherwise normal. If cohesin loss and germ cell depletion occur by independent pathways, cohesin levels should be equivalent in oocytes with and without the oocyte specific deletion.

The relationship between germ cell depletion and cohesin depletion is very important in relation to predicting a woman's useful reproductive lifespan. Biochemical assays of ovarian reserve are now increasingly used to assess a woman's future chance of conception. One such biochemical marker is Anti-Müllerian hormone (AMH), which is expressed by the granulosa cells of growing follicles (Vigier *et al.*, 1984), and had been shown to decline with age (Rosen *et al.*, 2012). AMH inhibits the recruitment of primordial follicles to the pool of growing follicles (Durlinger *et al.*, 1999; Durlinger *et al.*, 2002). Knockout mice deficient in AMH have been found to undergo premature depletion of their ovarian reserve of primordial follicles (Durlinger *et al.*, 1999). This mouse strain could also be used in our future experiments to uncouple germ cell depletion from chronological age.

Obviously, this is a valuable tool for women; however, it could lead to a false sense of complacency if cohesin loss occurs in a time dependent fashion (i.e. if there are two independent clocks ticking). If this were the case then even a large pool of oocytes will be subject to cohesin depletion and may not be useful in terms of predicting fertility.

It would be extremely interesting to expand our current data set to include patient AMH levels, and analyse how these correlate with oocyte numbers and age, compared with that previously observed in literature. Being uniquely positioned as a research lab within a fertility centre, there is the possibility for testing chromosomal cohesin levels in oocytes which have been consented for research, and correlating this with the patients AMH level. This would be highly informative in terms of determining whether AMH is truly a useful tool in the measurement of ovarian reserve.

Appendix I - Abbreviations

APC/C	Anaphase promoting complex/cyclosome
ATP	Adenosine triphosphate
Bub1	Budding uninhibited by benzimidazoles 1
CAK	Cdk activating kinase
cAMP	Cyclic adenosine monophosphate
Cdc5	Cell-division control protein 5
Cdc20	Cell-division cycle protein 20
Cdk	Cyclin dependent kinase
cDNA	Complementary DNA
CENP	Centromere Protein
CFP	Cerulean fluorescent protein
CO ₂	Carbon dioxide
C-terminus	Carboxyl terminus
DAPI	4',6-diamidino-2-phenylindole
D-box	Destruction box
DIC	Differential interference contrast
DNA	Deoxyribonucleic acid
DSBs	Double strand breaks
DTT	Dithiothreitol
Eco1	Establishment of cohesin protein
F actin	Filamentous actin
FSH	Follicle stimulating hormone
GFP	Green fluorescent protein
GV	Germinal vesicle
GVBD	Germinal vesicle breakdown
Homologs	Homologous Chromosomes
I.D.	Inside diameter
IBMX	Isobutylmethylxanthine
ICSI	Intracytoplasmic sperm injection
IVF	In vitro fertilisation
KEN-box	Additional degradation signal
L	Litre
LH	Luteinising hormone
M	Molar
Mad2	Mitotic arrest deficient 2
MCAK	Mitotic-centromere-associated kinesin
mg	Milli gram
ml	Milli litre
mM	Mili molar
Moa1	Monopolar attachment protein 1
MQ	MilliQ
mRNA	Message RNA

MTOCs	Microtubule organising centre
MI	The first meiotic division/Metaphase I
MII	The second meiotic division/Metaphase II
n.a.	Numerical aperture
NaOH	Sodium Hydroxide
NBD	Nuclear binding domain
NEB	Nuclear envelope breakdown
nl	Nano litre
nM	Nano molar
N-terminus	Amino terminus
O.D.	Outside diameter
OSC	Oogonial stem cells
PB	Polar body
PBS	Phosphate buffered saline
pc	Post-coitum
PCR	Polymerase chain reaction
Pds5	Precocious dissociation of sisters protein 5
PFA	Paraformaldehyde
PGCs	Primordial germ cells
PKA	Protein kinase A
Plk1	Polo-like kinase 1
PMSG	Pregnant mare's serum gonadotropin
PP2A	Protein phosphatase 2A
PVA	Poly(vinyl alcohol)
RFP	Red fluorescent protein
RNA	Ribonucleic acid
s.d.	Standard deviation
s.e.	Standard error
SA	Stromal antigen
SAC	Spindle assembly checkpoint
SC	Synaptonemal complex
Scc	Sister chromatic cohesion protein
Sgo	Shugoshin
Sycp3	Synaptonemal complex protein 3
siRNA	Small interfering RNA
SMC	Structural maintenance of chromosomes protein
Spo13	Sporulation-specific protein 13
STAG	Stromal antigen
UTR	Untranslated region
UV	Ultra violet
Venus	Bright yellow fluorescent protein
YFP	Yellow fluorescent protein
µg	Micro gram
µl	Micro litre
µM	Micro molar

Appendix II - Definitions

Acetylation	A reaction that introduces an acetyl group into a compound.
Achiasmatic	No chiasma.
Amino terminus	The start of an amino acid chain terminated by a free amine group (-NH ₂).
Amphitelic	Where sister kinetochores on each chromosome are positioned so that they can form stable attachments with microtubules from opposing spindle poles.
Anaphase I	First anaphase event of meiosis. Stage at which the kinetochore microtubules shorten, severing the recombination nodules and pulling homologous chromosomes apart.
Aneuploidy	An abnormal number of chromosomes.
Atresia	The degeneration and subsequent reabsorption of one or more immature ovarian follicles.
Bi-orientation	Where microtubules emanating from different microtubule organizing centres attach to kinetochores of sister chromatids, with each homologue attached to a different pole.
Bivalent	A pair of homologous chromosomes linked by at least one chiasma.
Cantination	Extensive intertwining of DNA when two adjacent replication forks collide.
Carboxyl terminus	The end of an amino acid chain terminated by a free carboxyl group (-COOH).
Cell Cycle	The series of events that lead to the reproduction of a cell.
Centromere	The part of a chromosome that links sister chromatids.
Centrosome	An organelle that serves as the main microtubule organising centre in mammalian cells.
Chiasmata	Physical linkages between homologs marking cross over sites.
Cohesin	A protein complex which holds sister chromatids together and regulates their segregation.
Dictyate	Prolonged prophase arrest in oogenesis. It starts late in foetal life and is terminated shortly before ovulation by the LH surge.
Diplotene	Final stage of prophase I where the chromosomes decondense, the synaptonemal complex gradually disassembles and the homologous chromosomes remained linked at chiasmata. The chromosomes continue to be held together as they condense and enter prophase arrest of MI.
Eukaryote	An organism whose cells contain complex structures enclosed within membranes (i.e. the nucleus).

G0 phase	A period in the cell cycle in which cells exist in a quiescent state.
G1 phase	A period in the cell cycle during interphase, before the S phase. Normally a major period of cell growth.
G2 phase	The final subphase of interphase in the cell cycle, directly preceding mitosis. G2 phase ends with the onset of prophase.
Germ Cell	A cell that gives rise to the gametes of an organism.
Germinal Vesicle	The nucleus of the oocyte.
Granulosa cell	Somatic cell closely associated with the developing oocyte.
Homologous Chromosomes	Chromosomes which share the same genes, but not necessarily the same alleles. One homologous chromosome is inherited from the mother; the other from the father.
Homologous Recombination	A type of genetic recombination by which nucleotide sequences are exchanged between two sister chromatids.
Kinetochores	Multiple conserved protein complexes which assemble on the centromeres of chromosomes, linking centromeric DNA to spindle microtubules
Leptotene	The first stage of prophase I where chromosomes are visible under the microscope as long thin strands. Homologous chromosomes begin to pair.
M phase	The period in which cell division takes place.
Meiosis	Specialised form of cell division in which diploid progenitors form haploid gametes by undergoing two rounds of chromosome segregation without an intervening round of DNA synthesis.
Merotelic	Where one chromatid is anchored simultaneously to microtubules emanating from both poles.
Metaphase I	Stage at which homologous chromosomes move together along the metaphase plate.
Metaphase plate	An imaginary line equidistant from the two centrosome poles where the centromeres of chromosomes align.
MI	The first meiotic division - a reductional division whereby the number of chromosomes is halved following segregation of recombinant maternal and paternal homologous chromosomes.
Microtubule	Rope-like polymers of tubulin important for forming the spindle.
MII	The second meiotic division - an equational division in which sister chromatids segregate.
Mitosis	Process of eukaryotic cell division.
Mono-orientation	Where microtubules emanating from one microtubule organizing centre attaches to the kinetochores of sister

	chromatids, with both of the sister chromatids within each homologous pair being attached to the same pole.
Monopolin	A protein complex required for the segregation of homologous chromosomes.
Monotelic	Where only one of the chromatids is anchored to microtubules, and the second kinetochore is not anchored.
Non-disjunction	The failure of chromosome pairs to separate properly during meiosis.
Oogenesis	The formation of fully grown oocytes from primordial germ cells.
Pachytene	Prophase I stage where synaptonemal complex assembly is completed and recombination occurs.
Pericentromeric	The region near to, or either side of the centromere.
Phosphorylation	The addition of a phosphate group to a protein.
Polar Body	The by-product of a meiotic division containing segregated chromosomes and very little cytoplasm.
Prophase I	Stage at which homologous recombination occurs. Is a protracted process in female meiosis. Can be split into leptotene, zygotene, pachytene and diplotene.
Proteosome	A large protein complex, the main function of which is to degrade unneeded or damaged proteins by proteolysis.
Proteolysis	A chemical reaction that breaks peptide bonds.
Securin	A protein which binds to separase, making it non-functional.
Shugoshin	A protein responsible for protecting cohesin.
Separase	A protease responsible for triggering anaphase by cleaving a cohesin subunit.
Sister Chromatids	Two copies of a chromatid.
Spermatogenesis	The process where male primary germ cells undergo division, and produce many cells termed spermatogonia, from which the primary spermatocytes (sperm) are derived.
S phase	The synthesis phase, the part of the cell cycle in which DNA is replicated, occurring between G1 and G2.
Spindle Checkpoint	Mechanisms which prevent anaphase in the presence of unattached or incorrectly attached kinetochores.
Spindle	A structure for organizing and separating the chromosomes during division.
Synaptonemal Complex	A protein structure that forms between homologous chromosomes that is thought to mediate chromosome pairing and synapsis.
Syntelic	Where both the sister chromatids within each homologous pair are attached to microtubules from same spindle pole.
Telomere	A region of repetitive DNA sequences at the end of a chromosome.

Trisomy	The presence of three copies of a chromosome instead of the usual two.
Ubiquitination	An enzymatic post-translational modification process.
Univalent	Single chromosome, unpaired with its homologous chromosome.
Zygotene	Prophase I stage where the chromosomes line up in homologous pairs. Synapsis takes place with the help of the synaptonemal complex.

References

- Acquaviva, C. and Pines, J. (2006) 'The anaphase-promoting complex/cyclosome: APC/C', *J Cell Sci*, 119(Pt 12), pp. 2401-4.
- Adhikari, D. and Liu, K. (2009) 'Molecular mechanisms underlying the activation of mammalian primordial follicles', *Endocr Rev*, 30(5), pp. 438-64.
- Andrews, P.D., Ovechkina, Y., Morrice, N., Wagenbach, M., Duncan, K., Wordeman, L. and Swedlow, J.R. (2004) 'Aurora B regulates MCAK at the mitotic centromere', *Dev Cell*, 6(2), pp. 253-68.
- Azoury, J., Lee, K.W., Georget, V., Rassinier, P., Leader, B. and Verlhac, M.H. (2008) 'Spindle positioning in mouse oocytes relies on a dynamic meshwork of actin filaments', *Curr Biol*, 18(19), pp. 1514-9.
- Battaglia, D.E., Goodwin, P., Klein, N.A. and Soules, M.R. (1996) 'Influence of maternal age on meiotic spindle assembly in oocytes from naturally cycling women', *Hum Reprod*, 11(10), pp. 2217-22.
- Baxter, J., Sen, N., Martinez, V.L., De Carandini, M.E., Schwartzman, J.B., Diffley, J.F. and Aragon, L. (2011) 'Positive supercoiling of mitotic DNA drives decatenation by topoisomerase II in eukaryotes', *Science*, 331(6022), pp. 1328-32.
- Beroukhim, R., Mermel, C.H., Porter, D., Wei, G., Raychaudhuri, S., Donovan, J., Barretina, J., Boehm, J.S., Dobson, J., Urashima, M., Mc Henry, K.T., Pinchback, R.M., Ligon, A.H., Cho, Y.J., Haery, L., Greulich, H., Reich, M., Winckler, W., Lawrence, M.S., Weir, B.A., Tanaka, K.E., Chiang, D.Y., Bass, A.J., Loo, A., Hoffman, C., Prensner, J., Liefeld, T., Gao, Q., Yecies, D., Signoretti, S., Maher, E., Kaye, F.J., Sasaki, H., Tepper, J.E., Fletcher, J.A., Taberner, J., Baselga, J., Tsao, M.S., Demichelis, F., Rubin, M.A., Janne, P.A., Daly, M.J., Nucera, C., Levine, R.L., Ebert, B.L., Gabriel, S., Rustgi, A.K., Antonescu, C.R., Ladanyi, M., Letai, A., Garraway, L.A., Loda, M., Beer, D.G., True, L.D., Okamoto, A., Pomeroy, S.L., Singer, S., Golub, T.R., Lander, E.S., Getz, G., Sellers, W.R. and Meyerson, M. (2010) 'The landscape of somatic copy-number alteration across human cancers', *Nature*, 463(7283), pp. 899-905.
- Block, E. (1952) 'Quantitative morphological investigations of the follicular system in women; variations at different ages', *Acta Anat (Basel)*, 14(1-2), pp. 108-23.
- Block, E. (1953) 'A quantitative morphological investigation of the follicular system in newborn female infants', *Acta Anat (Basel)*, 17(3), pp. 201-6.
- Brar, G.A. and Amon, A. (2008) 'Emerging roles for centromeres in meiosis I chromosome segregation', *Nat Rev Genet*, 9(12), pp. 899-910.
- Brook, J.D., Gosden, R.G. and Chandley, A.C. (1984) 'Maternal ageing and aneuploid embryos--evidence from the mouse that biological and not chronological age is the important influence', *Hum Genet*, 66(1), pp. 41-5.
- Brunet, S., Maria, A.S., Guillaud, P., Dujardin, D., Kubiak, J.Z. and Maro, B. (1999) 'Kinetochore fibers are not involved in the formation of the first meiotic spindle in mouse oocytes, but control the exit from the first meiotic M phase', *J Cell Biol*, 146(1), pp. 1-12.
- Brunet, S., Pahlavan, G., Taylor, S. and Maro, B. (2003) 'Functionality of the spindle checkpoint during the first meiotic division of mammalian oocytes', *Reproduction*, 126(4), pp. 443-50.
- Buonomo, S.B., Clyne, R.K., Fuchs, J., Loidl, J., Uhlmann, F. and Nasmyth, K. (2000) 'Disjunction of homologous chromosomes in meiosis I depends on proteolytic cleavage of the meiotic cohesin Rec8 by separin', *Cell*, 103(3), pp. 387-98.
- Chakravarti, A., Majumder, P.P., Slauchaupt, S.A., Deka, R., Warren, A.C., Surti, U., Ferrell, R.E. and Antonarakis, S.E. (1989) 'Gene-centromere mapping and the

- study of non-disjunction in autosomal trisomies and ovarian teratomas', *Prog Clin Biol Res*, 311, pp. 45-79.
- Chiang, T., Duncan, F.E., Schindler, K., Schultz, R.M. and Lampson, M.A. (2010) 'Evidence that weakened centromere cohesion is a leading cause of age-related aneuploidy in oocytes', *Curr Biol*, 20(17), pp. 1522-8.
- Cimini, D., Fioravanti, D., Salmon, E.D. and Degrossi, F. (2002) 'Merotelic kinetochore orientation versus chromosome mono-orientation in the origin of lagging chromosomes in human primary cells', *J Cell Sci*, 115(Pt 3), pp. 507-15.
- Cimini, D., Howell, B., Maddox, P., Khodjakov, A., Degrossi, F. and Salmon, E.D. (2001) 'Merotelic kinetochore orientation is a major mechanism of aneuploidy in mitotic mammalian tissue cells', *J Cell Biol*, 153(3), pp. 517-27.
- Cimini, D., Moree, B., Canman, J.C. and Salmon, E.D. (2003) 'Merotelic kinetochore orientation occurs frequently during early mitosis in mammalian tissue cells and error correction is achieved by two different mechanisms', *J Cell Sci*, 116(Pt 20), pp. 4213-25.
- Ciosk, R., Shirayama, M., Shevchenko, A., Tanaka, T., Toth, A. and Nasmyth, K. (2000) 'Cohesin's binding to chromosomes depends on a separate complex consisting of Scc2 and Scc4 proteins', *Mol Cell*, 5(2), pp. 243-54.
- Ciosk, R., Zachariae, W., Michaelis, C., Shevchenko, A., Mann, M. and Nasmyth, K. (1998) 'An ESP1/PDS1 complex regulates loss of sister chromatid cohesion at the metaphase to anaphase transition in yeast', *Cell*, 93(6), pp. 1067-76.
- Cohen-Fix, O., Peters, J.M., Kirschner, M.W. and Koshland, D. (1996) 'Anaphase initiation in *Saccharomyces cerevisiae* is controlled by the APC-dependent degradation of the anaphase inhibitor Pds1p', *Genes Dev*, 10(24), pp. 3081-93.
- Conn, P.M., McArdle, C.A., Andrews, W.V. and Huckle, W.R. (1987) 'The molecular basis of gonadotropin-releasing hormone (GnRH) action in the pituitary gonadotrope', *Biol Reprod*, 36(1), pp. 17-35.
- Darwiche, N., Freeman, L.A. and Strunnikov, A. (1999) 'Characterization of the components of the putative mammalian sister chromatid cohesion complex', *Gene*, 233(1-2), pp. 39-47.
- den Elzen, N. and Pines, J. (2001) 'Cyclin A is destroyed in prometaphase and can delay chromosome alignment and anaphase', *J Cell Biol*, 153(1), pp. 121-36.
- DiNardo, S., Voelkel, K. and Sternglanz, R. (1984) 'DNA topoisomerase II mutant of *Saccharomyces cerevisiae*: topoisomerase II is required for segregation of daughter molecules at the termination of DNA replication', *Proc Natl Acad Sci U S A*, 81(9), pp. 2616-20.
- Dorsett, D., Eissenberg, J.C., Misulovin, Z., Martens, A., Redding, B. and McKim, K. (2005) 'Effects of sister chromatid cohesion proteins on cut gene expression during wing development in *Drosophila*', *Development*, 132(21), pp. 4743-53.
- Duncan, F.E., Chiang, T., Schultz, R.M. and Lampson, M.A. (2009) 'Evidence that a defective spindle assembly checkpoint is not the primary cause of maternal age-associated aneuploidy in mouse eggs', *Biol Reprod*, 81(4), pp. 768-76.
- Duncan, F.E., Hornick, J.E., Lampson, M.A., Schultz, R.M., Shea, L.D. and Woodruff, T.K. (2012) 'Chromosome cohesion decreases in human eggs with advanced maternal age', *Aging Cell*, 11(6), pp. 1121-4.
- Durlinger, A.L., Gruijters, M.J., Kramer, P., Karels, B., Ingraham, H.A., Nachtigal, M.W., Uilenbroek, J.T., Grootegoed, J.A. and Themmen, A.P. (2002) 'Anti-Mullerian hormone inhibits initiation of primordial follicle growth in the mouse ovary', *Endocrinology*, 143(3), pp. 1076-84.
- Durlinger, A.L., Kramer, P., Karels, B., de Jong, F.H., Uilenbroek, J.T., Grootegoed, J.A. and Themmen, A.P. (1999) 'Control of primordial follicle recruitment by anti-Mullerian hormone in the mouse ovary', *Endocrinology*, 140(12), pp. 5789-96.

- Earnshaw, W.C. and Cooke, C.A. (1989) 'Proteins of the inner and outer centromere of mitotic chromosomes', *Genome*, 31(2), pp. 541-52.
- Eaton, J.W. and Mayer, A.J. (1953) 'The social biology of very high fertility among the Hutterites; the demography of a unique population', *Hum Biol*, 25(3), pp. 206-64.
- Eichenlaub-Ritter, U. (1998) 'Genetics of oocyte ageing', *Maturitas*, 30(2), pp. 143-69.
- Eichenlaub-Ritter, U., Chandley, A.C. and Gosden, R.G. (1988) 'The CBA mouse as a model for age-related aneuploidy in man: studies of oocyte maturation, spindle formation and chromosome alignment during meiosis', *Chromosoma*, 96(3), pp. 220-6.
- Faddy, M.J. (2000) 'Follicle dynamics during ovarian ageing', *Mol Cell Endocrinol*, 163(1-2), pp. 43-8.
- Faddy, M.J. and Gosden, R.G. (1996) 'A model conforming the decline in follicle numbers to the age of menopause in women', *Hum Reprod*, 11(7), pp. 1484-6.
- Faddy, M.J., Gosden, R.G., Gougeon, A., Richardson, S.J. and Nelson, J.F. (1992) 'Accelerated disappearance of ovarian follicles in mid-life: implications for forecasting menopause', *Hum Reprod*, 7(10), pp. 1342-6.
- FitzHarris, G. (2012) 'Anaphase B precedes anaphase A in the mouse egg', *Curr Biol*, 22(5), pp. 437-44.
- Foley, E.A. and Kapoor, T.M. (2013) 'Microtubule attachment and spindle assembly checkpoint signalling at the kinetochore', *Nat Rev Mol Cell Biol*, 14(1), pp. 25-37.
- Franks, L.M. and Payne, J. (1970) 'The influence of age on reproductive capacity in C57BL mice', *J Reprod Fertil*, 21(3), pp. 563-5.
- Funabiki, H., Yamano, H., Kumada, K., Nagao, K., Hunt, T. and Yanagida, M. (1996) 'Cut2 proteolysis required for sister-chromatid separation in fission yeast', *Nature*, 381(6581), pp. 438-41.
- Gallie, D.R. (1991) 'The cap and poly(A) tail function synergistically to regulate mRNA translational efficiency', *Genes Dev*, 5(11), pp. 2108-16.
- Gandhi, R., Gillespie, P.J. and Hirano, T. (2006) 'Human Wapl is a cohesin-binding protein that promotes sister-chromatid resolution in mitotic prophase', *Curr Biol*, 16(24), pp. 2406-17.
- Ganem, N.J., Godinho, S.A. and Pellman, D. (2009) 'A mechanism linking extra centrosomes to chromosomal instability', *Nature*, 460(7252), pp. 278-82.
- Garcia-Cruz, R., Brieno, M.A., Roig, I., Grossmann, M., Velilla, E., Pujol, A., Cabero, L., Pessarrodona, A., Barbero, J.L. and Garcia Caldes, M. (2010) 'Dynamics of cohesin proteins REC8, STAG3, SMC1 beta and SMC3 are consistent with a role in sister chromatid cohesion during meiosis in human oocytes', *Hum Reprod*, 25(9), pp. 2316-27.
- Geley, S., Kramer, E., Gieffers, C., Gannon, J., Peters, J.M. and Hunt, T. (2001) 'Anaphase-promoting complex/cyclosome-dependent proteolysis of human cyclin A starts at the beginning of mitosis and is not subject to the spindle assembly checkpoint', *J Cell Biol*, 153(1), pp. 137-48.
- Gimenez-Abian, J.F., Sumara, I., Hirota, T., Hauf, S., Gerlich, D., de la Torre, C., Ellenberg, J. and Peters, J.M. (2004) 'Regulation of sister chromatid cohesion between chromosome arms', *Curr Biol*, 14(13), pp. 1187-93.
- Gomez, R., Valdeolmillos, A., Parra, M.T., Viera, A., Carreiro, C., Roncal, F., Rufas, J.S., Barbero, J.L. and Suja, J.A. (2007) 'Mammalian SGO2 appears at the inner centromere domain and redistributes depending on tension across centromeres during meiosis II and mitosis', *EMBO Rep*, 8(2), pp. 173-80.
- Gomperts, M., Garcia-Castro, M., Wylie, C. and Heasman, J. (1994) 'Interactions between primordial germ cells play a role in their migration in mouse embryos', *Development*, 120(1), pp. 135-41.
- Gordon, D.J., Resio, B. and Pellman, D. (2012) 'Causes and consequences of aneuploidy in cancer', *Nat Rev Genet*, 13(3), pp. 189-203.

- Gosden, R.G. (1987) 'Follicular status at the menopause', *Hum Reprod*, 2(7), pp. 617-21.
- Gougeon, A. (1996) 'Regulation of ovarian follicular development in primates: facts and hypotheses', *Endocr Rev*, 17(2), pp. 121-55.
- Gougeon, A., Ecochard, R. and Thalabard, J.C. (1994) 'Age-related changes of the population of human ovarian follicles: increase in the disappearance rate of non-growing and early-growing follicles in aging women', *Biol Reprod*, 50(3), pp. 653-63.
- Gregan, J., Polakova, S., Zhang, L., Tolic-Norrelykke, I.M. and Cimini, D. (2011) 'Merotelic kinetochore attachment: causes and effects', *Trends Cell Biol*, 21(6), pp. 374-81.
- Gruber, S., Haering, C.H. and Nasmyth, K. (2003) 'Chromosomal cohesin forms a ring', *Cell*, 112(6), pp. 765-77.
- Guacci, V., Koshland, D. and Strunnikov, A. (1997) 'A direct link between sister chromatid cohesion and chromosome condensation revealed through the analysis of MCD1 in *S. cerevisiae*', *Cell*, 91(1), pp. 47-57.
- Gui, L. and Homer, H. (2012) 'Spindle assembly checkpoint signalling is uncoupled from chromosomal position in mouse oocytes', *Development*, 139(11), pp. 1941-6.
- Haering, C.H., Schoffnegger, D., Nishino, T., Helmhart, W., Nasmyth, K. and Lowe, J. (2004) 'Structure and stability of cohesin's Smc1-kleisin interaction', *Mol Cell*, 15(6), pp. 951-64.
- Hamant, O., Golubovskaya, I., Meeley, R., Fiume, E., Timofejeva, L., Schleiffer, A., Nasmyth, K. and Cande, W.Z. (2005) 'A REC8-dependent plant Shugoshin is required for maintenance of centromeric cohesion during meiosis and has no mitotic functions', *Curr Biol*, 15(10), pp. 948-54.
- Hammond, S.M., Bernstein, E., Beach, D. and Hannon, G.J. (2000) 'An RNA-directed nuclease mediates post-transcriptional gene silencing in *Drosophila* cells', *Nature*, 404(6775), pp. 293-6.
- Hansen, K.R., Knowlton, N.S., Thyer, A.C., Charleston, J.S., Soules, M.R. and Klein, N.A. (2008) 'A new model of reproductive aging: the decline in ovarian non-growing follicle number from birth to menopause', *Hum Reprod*, 23(3), pp. 699-708.
- Hartman, T., Stead, K., Koshland, D. and Guacci, V. (2000) 'Pds5p is an essential chromosomal protein required for both sister chromatid cohesion and condensation in *Saccharomyces cerevisiae*', *J Cell Biol*, 151(3), pp. 613-26.
- Hassold, T. and Chiu, D. (1985) 'Maternal age-specific rates of numerical chromosome abnormalities with special reference to trisomy', *Hum Genet*, 70(1), pp. 11-7.
- Hassold, T. and Hunt, P. (2001) 'To err (meiotically) is human: the genesis of human aneuploidy', *Nat Rev Genet*, 2(4), pp. 280-91.
- Hassold, T. and Hunt, P. (2007) 'Rescuing distal crossovers', *Nat Genet*, 39(10), pp. 1187-8.
- Hassold, T., Merrill, M., Adkins, K., Freeman, S. and Sherman, S. (1995) 'Recombination and maternal age-dependent nondisjunction: molecular studies of trisomy 16', *Am J Hum Genet*, 57(4), pp. 867-74.
- Hauf, S., Roitinger, E., Koch, B., Dittrich, C.M., Mechtler, K. and Peters, J.M. (2005) 'Dissociation of cohesin from chromosome arms and loss of arm cohesion during early mitosis depends on phosphorylation of SA2', *PLoS Biol*, 3(3), p. e69.
- Hauf, S., Waizenegger, I.C. and Peters, J.M. (2001) 'Cohesin cleavage by separase required for anaphase and cytokinesis in human cells', *Science*, 293(5533), pp. 1320-3.
- Hauf, S. and Watanabe, Y. (2004) 'Kinetochore orientation in mitosis and meiosis', *Cell*, 119(3), pp. 317-27.
- Hemmerich, P., Weidtkamp-Peters, S., Hoischen, C., Schmiedeberg, L., Erliandri, I. and Diekmann, S. (2008) 'Dynamics of inner kinetochore assembly and maintenance in living cells', *J Cell Biol*, 180(6), pp. 1101-14.
- Henderson, S.A. and Edwards, R.G. (1968) 'Chiasma frequency and maternal age in mammals', *Nature*, 218(5136), pp. 22-8.

- Herbert, M., Levasseur, M., Homer, H., Yallop, K., Murdoch, A. and McDougall, A. (2003) 'Homologue disjunction in mouse oocytes requires proteolysis of securin and cyclin B1', *Nat Cell Biol*, 5(11), pp. 1023-5.
- Hernandez, D. and Fisher, E.M. (1999) 'Mouse autosomal trisomy: two's company, three's a crowd', *Trends Genet*, 15(6), pp. 241-7.
- Hodges, C.A. and Hunt, P.A. (2002) 'Simultaneous analysis of chromosomes and chromosome-associated proteins in mammalian oocytes and embryos', *Chromosoma*, 111(3), pp. 165-9.
- Hodges, C.A., Revenkova, E., Jessberger, R., Hassold, T.J. and Hunt, P.A. (2005) 'SMC1beta-deficient female mice provide evidence that cohesins are a missing link in age-related nondisjunction', *Nat Genet*, 37(12), pp. 1351-5.
- Homer, H.A., McDougall, A., Levasseur, M., Yallop, K., Murdoch, A.P. and Herbert, M. (2005) 'Mad2 prevents aneuploidy and premature proteolysis of cyclin B and securin during meiosis I in mouse oocytes', *Genes Dev*, 19(2), pp. 202-7.
- Howe, J.A., Howell, M., Hunt, T. and Newport, J.W. (1995) 'Identification of a developmental timer regulating the stability of embryonic cyclin A and a new somatic A-type cyclin at gastrulation', *Genes Dev*, 9(10), pp. 1164-76.
- Hrdy, S.B. (1979) 'Infanticide among animals', *Ethology and Sociobiology*, pp. 13-40.
- Hunt, P. and Hassold, T. (2010) 'Female meiosis: coming unglued with age', *Curr Biol*, 20(17), pp. R699-702.
- Hurst, P.R., Mora, J.M. and Fenwick, M.A. (2006) 'Caspase-3, TUNEL and ultrastructural studies of small follicles in adult human ovarian biopsies', *Hum Reprod*, 21(8), pp. 1974-80.
- Hyslop, L., Prathalingam, N., Nowak, L., Fenwick, J., Harbottle, S., Byerley, S., Rhodes, J., Watson, B., Henderson, R., Murdoch, A. and Herbert, M. (2012) 'A novel isolator-based system promotes viability of human embryos during laboratory processing', *PLoS One*, 7(2), p. e31010.
- Illingworth, C., Pirmadjid, N., Serhal, P., Howe, K. and Fitzharris, G. (2010) 'MCAK regulates chromosome alignment but is not necessary for preventing aneuploidy in mouse oocyte meiosis I', *Development*, 137(13), pp. 2133-8.
- Jeffrey, P.D., Russo, A.A., Polyak, K., Gibbs, E., Hurwitz, J., Massague, J. and Pavletich, N.P. (1995) 'Mechanism of CDK activation revealed by the structure of a cyclinA-CDK2 complex', *Nature*, 376(6538), pp. 313-20.
- Johnson, J., Bagley, J., Skaznik-Wikiel, M., Lee, H.J., Adams, G.B., Niikura, Y., Tschudy, K.S., Tilly, J.C., Cortes, M.L., Forkert, R., Spitzer, T., Iacomini, J., Scadden, D.T. and Tilly, J.L. (2005) 'Oocyte generation in adult mammalian ovaries by putative germ cells in bone marrow and peripheral blood', *Cell*, 122(2), pp. 303-15.
- Johnson, J., Canning, J., Kaneko, T., Pru, J.K. and Tilly, J.L. (2004) 'Germline stem cells and follicular renewal in the postnatal mammalian ovary', *Nature*, 428(6979), pp. 145-50.
- Kapp, L.D. and Lorsch, J.R. (2004) 'The molecular mechanics of eukaryotic translation', *Annu Rev Biochem*, 73, pp. 657-704.
- Katis, V.L., Lipp, J.J., Imre, R., Bogdanova, A., Okaz, E., Habermann, B., Mechtler, K., Nasmyth, K. and Zachariae, W. (2010) 'Rec8 phosphorylation by casein kinase 1 and Cdc7-Dbf4 kinase regulates cohesin cleavage by separase during meiosis', *Dev Cell*, 18(3), pp. 397-409.
- Katis, V.L., Matos, J., Mori, S., Shirahige, K., Zachariae, W. and Nasmyth, K. (2004) 'Spo13 facilitates monopolin recruitment to kinetochores and regulates maintenance of centromeric cohesion during yeast meiosis', *Curr Biol*, 14(24), pp. 2183-96.
- Kawashima, S.A., Tsukahara, T., Langegger, M., Hauf, S., Kitajima, T.S. and Watanabe, Y. (2007) 'Shugoshin enables tension-generating attachment of kinetochores by loading Aurora to centromeres', *Genes Dev*, 21(4), pp. 420-35.

- Kawashima, S.A., Yamagishi, Y., Honda, T., Ishiguro, K. and Watanabe, Y. (2010) 'Phosphorylation of H2A by Bub1 prevents chromosomal instability through localizing shugoshin', *Science*, 327(5962), pp. 172-7.
- Keeney, S., Giroux, C.N. and Kleckner, N. (1997) 'Meiosis-specific DNA double-strand breaks are catalyzed by Spo11, a member of a widely conserved protein family', *Cell*, 88(3), pp. 375-84.
- Keeney, S. and Neale, M.J. (2006) 'Initiation of meiotic recombination by formation of DNA double-strand breaks: mechanism and regulation', *Biochem Soc Trans*, 34(Pt 4), pp. 523-5.
- Kerrebrock, A.W., Moore, D.P., Wu, J.S. and Orr-Weaver, T.L. (1995) 'Mei-S332, a Drosophila protein required for sister-chromatid cohesion, can localize to meiotic centromere regions', *Cell*, 83(2), pp. 247-56.
- Kingsbury, M.A., Friedman, B., McConnell, M.J., Rehen, S.K., Yang, A.H., Kaushal, D. and Chun, J. (2005) 'Aneuploid neurons are functionally active and integrated into brain circuitry', *Proc Natl Acad Sci U S A*, 102(17), pp. 6143-7.
- Kirschner, M. and Mitchison, T. (1986) 'Beyond self-assembly: from microtubules to morphogenesis', *Cell*, 45(3), pp. 329-42.
- Kitajima, T.S., Hauf, S., Ohsugi, M., Yamamoto, T. and Watanabe, Y. (2005) 'Human Bub1 defines the persistent cohesion site along the mitotic chromosome by affecting Shugoshin localization', *Curr Biol*, 15(4), pp. 353-9.
- Kitajima, T.S., Kawashima, S.A. and Watanabe, Y. (2004) 'The conserved kinetochore protein shugoshin protects centromeric cohesion during meiosis', *Nature*, 427(6974), pp. 510-7.
- Kitajima, T.S., Miyazaki, Y., Yamamoto, M. and Watanabe, Y. (2003a) 'Rec8 cleavage by separase is required for meiotic nuclear divisions in fission yeast', *EMBO J*, 22(20), pp. 5643-53.
- Kitajima, T.S., Ohsugi, M. and Ellenberg, J. (2011) 'Complete kinetochore tracking reveals error-prone homologous chromosome biorientation in mammalian oocytes', *Cell*, 146(4), pp. 568-81.
- Kitajima, T.S., Sakuno, T., Ishiguro, K., Iemura, S., Natsume, T., Kawashima, S.A. and Watanabe, Y. (2006) 'Shugoshin collaborates with protein phosphatase 2A to protect cohesin', *Nature*, 441(7089), pp. 46-52.
- Kitajima, T.S., Yokobayashi, S., Yamamoto, M. and Watanabe, Y. (2003b) 'Distinct cohesin complexes organize meiotic chromosome domains', *Science*, 300(5622), pp. 1152-5.
- Kleckner, N. (1996) 'Meiosis: how could it work?', *Proc Natl Acad Sci U S A*, 93(16), pp. 8167-74.
- Kleckner, N. (2006) 'Chiasma formation: chromatin/axis interplay and the role(s) of the synaptonemal complex', *Chromosoma*, 115(3), pp. 175-94.
- Klein, F., Mahr, P., Galova, M., Buonomo, S.B., Michaelis, C., Nairz, K. and Nasmyth, K. (1999) 'A central role for cohesins in sister chromatid cohesion, formation of axial elements, and recombination during yeast meiosis', *Cell*, 98(1), pp. 91-103.
- Kline-Smith, S.L., Khodjakov, A., Hergert, P. and Walczak, C.E. (2004) 'Depletion of centromeric MCAK leads to chromosome congression and segregation defects due to improper kinetochore attachments', *Mol Biol Cell*, 15(3), pp. 1146-59.
- Knowlton, A.L., Lan, W. and Stukenberg, P.T. (2006) 'Aurora B is enriched at merotelic attachment sites, where it regulates MCAK', *Curr Biol*, 16(17), pp. 1705-10.
- Koshland, D. and Hartwell, L.H. (1987) 'The structure of sister minichromosome DNA before anaphase in *Saccharomyces cerevisiae*', *Science*, 238(4834), pp. 1713-6.
- Kot, M.C. and Handel, M.A. (1990) 'Spermatogenesis in XO,Sxr mice: role of the Y chromosome', *J Exp Zool*, 256(1), pp. 92-105.
-

- Kouznetsova, A., Lister, L., Nordenskjold, M., Herbert, M. and Hoog, C. (2007) 'Bi-orientation of achiasmatic chromosomes in meiosis I oocytes contributes to aneuploidy in mice', *Nat Genet*, 39(8), pp. 966-8.
- Kouznetsova, A., Novak, I., Jessberger, R. and Hoog, C. (2005) 'SYCP2 and SYCP3 are required for cohesin core integrity at diplotene but not for centromere cohesion at the first meiotic division', *J Cell Sci*, 118(Pt 10), pp. 2271-8.
- Kudo, N.R., Anger, M., Peters, A.H., Stemann, O., Theussl, H.C., Helmhart, W., Kudo, H., Heyting, C. and Nasmyth, K. (2009) 'Role of cleavage by separase of the Rec8 kleisin subunit of cohesin during mammalian meiosis I', *J Cell Sci*, 122(Pt 15), pp. 2686-98.
- Kudo, N.R., Wassmann, K., Anger, M., Schuh, M., Wirth, K.G., Xu, H., Helmhart, W., Kudo, H., McKay, M., Maro, B., Ellenberg, J., de Boer, P. and Nasmyth, K. (2006) 'Resolution of chiasmata in oocytes requires separase-mediated proteolysis', *Cell*, 126(1), pp. 135-46.
- Kueng, S., Hegemann, B., Peters, B.H., Lipp, J.J., Schleiffer, A., Mechtler, K. and Peters, J.M. (2006) 'Wapl controls the dynamic association of cohesin with chromatin', *Cell*, 127(5), pp. 955-67.
- Kumada, K., Yao, R., Kawaguchi, T., Karasawa, M., Hoshikawa, Y., Ichikawa, K., Sugitani, Y., Imoto, I., Inazawa, J., Sugawara, M., Yanagida, M. and Noda, T. (2006) 'The selective continued linkage of centromeres from mitosis to interphase in the absence of mammalian separase', *J Cell Biol*, 172(6), pp. 835-46.
- Kumar, T.R., Wang, Y., Lu, N. and Matzuk, M.M. (1997) 'Follicle stimulating hormone is required for ovarian follicle maturation but not male fertility', *Nat Genet*, 15(2), pp. 201-4.
- Lafont, A.L., Song, J. and Rankin, S. (2010) 'Sororin cooperates with the acetyltransferase Eco2 to ensure DNA replication-dependent sister chromatid cohesion', *Proc Natl Acad Sci U S A*, 107(47), pp. 20364-9.
- Lamb, N.E., Feingold, E., Savage, A., Avramopoulos, D., Freeman, S., Gu, Y., Hallberg, A., Hersey, J., Karadima, G., Pettay, D., Saker, D., Shen, J., Taft, L., Mikkelsen, M., Petersen, M.B., Hassold, T. and Sherman, S.L. (1997) 'Characterization of susceptible chiasma configurations that increase the risk for maternal nondisjunction of chromosome 21', *Hum Mol Genet*, 6(9), pp. 1391-9.
- Lamb, N.E., Yu, K., Shaffer, J., Feingold, E. and Sherman, S.L. (2005) 'Association between maternal age and meiotic recombination for trisomy 21', *Am J Hum Genet*, 76(1), pp. 91-9.
- Lan, W., Zhang, X., Kline-Smith, S.L., Rosasco, S.E., Barrett-Wilt, G.A., Shabanowitz, J., Hunt, D.F., Walczak, C.E. and Stukenberg, P.T. (2004) 'Aurora B phosphorylates centromeric MCAK and regulates its localization and microtubule depolymerization activity', *Curr Biol*, 14(4), pp. 273-86.
- Lane, S.I., Yun, Y. and Jones, K.T. (2012) 'Timing of anaphase-promoting complex activation in mouse oocytes is predicted by microtubule-kinetochore attachment but not by bivalent alignment or tension', *Development*, 139(11), pp. 1947-55.
- Lara-Gonzalez, P., Westhorpe, F.G. and Taylor, S.S. (2012) 'The spindle assembly checkpoint', *Curr Biol*, 22(22), pp. R966-80.
- Larsen, U. and Yan, S. (2000) 'The age pattern of fecundability: an analysis of French Canadian and Hutterite birth histories', *Soc Biol*, 47(1-2), pp. 34-50.
- Lee, B.H., Kiburz, B.M. and Amon, A. (2004) 'Spo13 maintains centromeric cohesion and kinetochore coorientation during meiosis I', *Curr Biol*, 14(24), pp. 2168-82.
- Lee, J., Kitajima, T.S., Tanno, Y., Yoshida, K., Morita, T., Miyano, T., Miyake, M. and Watanabe, Y. (2008) 'Unified mode of centromeric protection by shugoshin in mammalian oocytes and somatic cells', *Nat Cell Biol*, 10(1), pp. 42-52.
- Leidy, L.E., Godfrey, L.R. and Sutherland, M.R. (1998) 'Is follicular atresia biphasic?', *Fertil Steril*, 70(5), pp. 851-9.

- LeMaire-Adkins, R. and Hunt, P.A. (2000) 'Nonrandom segregation of the mouse univalent X chromosome: evidence of spindle-mediated meiotic drive', *Genetics*, 156(2), pp. 775-83.
- LeMaire-Adkins, R., Radke, K. and Hunt, P.A. (1997) 'Lack of checkpoint control at the metaphase/anaphase transition: a mechanism of meiotic nondisjunction in mammalian females', *J Cell Biol*, 139(7), pp. 1611-9.
- Lightfoot, D.A., Kouznetsova, A., Mahdy, E., Wilbertz, J. and Hoog, C. (2006) 'The fate of mosaic aneuploid embryos during mouse development', *Dev Biol*, 289(2), pp. 384-94.
- Lin, W., Jin, H., Liu, X., Hampton, K. and Yu, H.G. (2011) 'Scc2 regulates gene expression by recruiting cohesin to the chromosome as a transcriptional activator during yeast meiosis', *Mol Biol Cell*, 22(12), pp. 1985-96.
- Lincoln, A.J., Wickramasinghe, D., Stein, P., Schultz, R.M., Palko, M.E., De Miguel, M.P., Tessarollo, L. and Donovan, P.J. (2002) 'Cdc25b phosphatase is required for resumption of meiosis during oocyte maturation', *Nat Genet*, 30(4), pp. 446-9.
- Lister, L.M., Kouznetsova, A., Hyslop, L.A., Kalleas, D., Pace, S.L., Barel, J.C., Nathan, A., Floros, V., Adelfalk, C., Watanabe, Y., Jessberger, R., Kirkwood, T.B., Hoog, C. and Herbert, M. (2010) 'Age-related meiotic segregation errors in mammalian oocytes are preceded by depletion of cohesin and Sgo2', *Curr Biol*, 20(17), pp. 1511-21.
- Liu, L. and Keefe, D.L. (2002) 'Ageing-associated aberration in meiosis of oocytes from senescence-accelerated mice', *Hum Reprod*, 17(10), pp. 2678-85.
- Liu, L. and Keefe, D.L. (2004) 'Nuclear origin of aging-associated meiotic defects in senescence-accelerated mice', *Biol Reprod*, 71(5), pp. 1724-9.
- Liu, L. and Keefe, D.L. (2008) 'Defective cohesin is associated with age-dependent misaligned chromosomes in oocytes', *Reprod Biomed Online*, 16(1), pp. 103-12.
- Llano, E., Gomez, R., Gutierrez-Caballero, C., Herran, Y., Sanchez-Martin, M., Vazquez-Quinones, L., Hernandez, T., de Alava, E., Cuadrado, A., Barbero, J.L., Suja, J.A. and Pendas, A.M. (2008) 'Shugoshin-2 is essential for the completion of meiosis but not for mitotic cell division in mice', *Genes Dev*, 22(17), pp. 2400-13.
- Longo, F.J. and Chen, D.Y. (1985) 'Development of cortical polarity in mouse eggs: involvement of the meiotic apparatus', *Dev Biol*, 107(2), pp. 382-94.
- Losada, A., Hirano, M. and Hirano, T. (1998) 'Identification of Xenopus SMC protein complexes required for sister chromatid cohesion', *Genes Dev*, 12(13), pp. 1986-97.
- Losada, A., Hirano, M. and Hirano, T. (2002) 'Cohesin release is required for sister chromatid resolution, but not for condensin-mediated compaction, at the onset of mitosis', *Genes Dev*, 16(23), pp. 3004-16.
- Losada, A., Yokochi, T. and Hirano, T. (2005) 'Functional contribution of Pds5 to cohesin-mediated cohesion in human cells and Xenopus egg extracts', *J Cell Sci*, 118(Pt 10), pp. 2133-41.
- Maheshwari, A. and Fowler, P.A. (2008) 'Primordial follicular assembly in humans--revisited', *Zygote*, 16(4), pp. 285-96.
- Maiato, H. and Lince-Faria, M. (2010) 'The perpetual movements of anaphase', *Cell Mol Life Sci*, 67(13), pp. 2251-69.
- Malumbres, M. and Barbacid, M. (2005) 'Mammalian cyclin-dependent kinases', *Trends Biochem Sci*, 30(11), pp. 630-41.
- Marangos, P. and Carroll, J. (2008) 'Securin regulates entry into M-phase by modulating the stability of cyclin B', *Nat Cell Biol*, 10(4), pp. 445-51.
- Maro, B., Johnson, M.H., Pickering, S.J. and Flach, G. (1984) 'Changes in actin distribution during fertilization of the mouse egg', *J Embryol Exp Morphol*, 81, pp. 211-37.
- Maro, B., Johnson, M.H., Webb, M. and Flach, G. (1986) 'Mechanism of polar body formation in the mouse oocyte: an interaction between the chromosomes, the cytoskeleton and the plasma membrane', *J Embryol Exp Morphol*, 92, pp. 11-32.

- Maro, B. and Verlhac, M.H. (2002) 'Polar body formation: new rules for asymmetric divisions', *Nat Cell Biol*, 4(12), pp. E281-3.
- Marston, A.L. and Amon, A. (2004) 'Meiosis: cell-cycle controls shuffle and deal', *Nat Rev Mol Cell Biol*, 5(12), pp. 983-97.
- Martin, R.H., Dill, F.J. and Miller, J.R. (1976) 'Nondisjunction in aging female mice', *Cytogenet Cell Genet*, 17(3), pp. 150-60.
- Matos, J., Lipp, J.J., Bogdanova, A., Guillot, S., Okaz, E., Junqueira, M., Shevchenko, A. and Zachariae, W. (2008) 'Dbf4-dependent CDC7 kinase links DNA replication to the segregation of homologous chromosomes in meiosis I', *Cell*, 135(4), pp. 662-78.
- McGuinness, B.E., Anger, M., Kouznetsova, A., Gil-Bernabe, A.M., Helmhart, W., Kudo, N.R., Wuensche, A., Taylor, S., Hoog, C., Novak, B. and Nasmyth, K. (2009) 'Regulation of APC/C activity in oocytes by a Bub1-dependent spindle assembly checkpoint', *Curr Biol*, 19(5), pp. 369-80.
- McGuinness, B.E., Hirota, T., Kudo, N.R., Peters, J.M. and Nasmyth, K. (2005) 'Shugoshin prevents dissociation of cohesin from centromeres during mitosis in vertebrate cells', *PLoS Biol*, 3(3), p. e86.
- McLaren, A. (2000) 'Germ and somatic cell lineages in the developing gonad', *Mol Cell Endocrinol*, 163(1-2), pp. 3-9.
- Mehlmann, L.M. (2005) 'Stops and starts in mammalian oocytes: recent advances in understanding the regulation of meiotic arrest and oocyte maturation', *Reproduction*, 130(6), pp. 791-9.
- Menken, J., Trussell, J. and Larsen, U. (1986) 'Age and infertility', *Science*, 233(4771), pp. 1389-94.
- Merriman, J.A., Jennings, P.C., McLaughlin, E.A. and Jones, K.T. (2012) 'Effect of aging on superovulation efficiency, aneuploidy rates, and sister chromatid cohesion in mice aged up to 15 months', *Biol Reprod*, 86(2), p. 49.
- Merriman, J.A., Lane, S.I., Holt, J.E., Jennings, P.C., Garcia-Higuera, I., Moreno, S., McLaughlin, E.A. and Jones, K.T. (2013) 'Reduced chromosome cohesion measured by interkinetochore distance is associated with aneuploidy even in oocytes from young mice', *Biol Reprod*, 88(2), p. 31.
- Michaelis, C., Ciosk, R. and Nasmyth, K. (1997) 'Cohesins: chromosomal proteins that prevent premature separation of sister chromatids', *Cell*, 91(1), pp. 35-45.
- Mills, M., Rindfuss, R.R., McDonald, P. and te Velde, E. (2011) 'Why do people postpone parenthood? Reasons and social policy incentives', *Hum Reprod Update*, 17(6), pp. 848-60.
- Minshull, J., Golsteyn, R., Hill, C.S. and Hunt, T. (1990) 'The A- and B-type cyclin associated cdc2 kinases in *Xenopus* turn on and off at different times in the cell cycle', *EMBO J*, 9(9), pp. 2865-75.
- Mitra, J. and Schultz, R.M. (1996) 'Regulation of the acquisition of meiotic competence in the mouse: changes in the subcellular localization of cdc2, cyclin B1, cdc25C and wee1, and in the concentration of these proteins and their transcripts', *J Cell Sci*, 109 (Pt 9), pp. 2407-15.
- Molyneaux, K.A., Stallock, J., Schaible, K. and Wylie, C. (2001) 'Time-lapse analysis of living mouse germ cell migration', *Dev Biol*, 240(2), pp. 488-98.
- Morris, J.K. and Alberman, E. (2009) 'Trends in Down's syndrome live births and antenatal diagnoses in England and Wales from 1989 to 2008: analysis of data from the National Down Syndrome Cytogenetic Register', *BMJ*, 339, p. b3794.
- Musacchio, A. (2011) 'Spindle assembly checkpoint: the third decade', *Philos Trans R Soc Lond B Biol Sci*, 366(1584), pp. 3595-604.
- Musacchio, A. and Salmon, E.D. (2007) 'The spindle-assembly checkpoint in space and time', *Nat Rev Mol Cell Biol*, 8(5), pp. 379-93.
-

- Nagaoka, S.I., Hodges, C.A., Albertini, D.F. and Hunt, P.A. (2011) 'Oocyte-specific differences in cell-cycle control create an innate susceptibility to meiotic errors', *Curr Biol*, 21(8), pp. 651-7.
- Nasmyth, K. (2001) 'Disseminating the genome: joining, resolving, and separating sister chromatids during mitosis and meiosis', *Annu Rev Genet*, 35, pp. 673-745.
- Nasmyth, K. (2011) 'Cohesin: a catenase with separate entry and exit gates?', *Nat Cell Biol*, 13(10), pp. 1170-7.
- Nasmyth, K. and Haering, C.H. (2009) 'Cohesin: Its Roles and Mechanisms', *Annual Review of Genetics*, 43, pp. 525-558.
- Neale, M.J. and Keeney, S. (2006) 'Clarifying the mechanics of DNA strand exchange in meiotic recombination', *Nature*, 442(7099), pp. 153-8.
- Niault, T., Hached, K., Sotillo, R., Sorger, P.K., Maro, B., Benezra, R. and Wassmann, K. (2007) 'Changing Mad2 levels affects chromosome segregation and spindle assembly checkpoint control in female mouse meiosis I', *PLoS One*, 2(11), p. e1165.
- Nishiyama, T., Ladurner, R., Schmitz, J., Kreidl, E., Schleiffer, A., Bhaskara, V., Bando, M., Shirahige, K., Hyman, A.A., Mechtler, K. and Peters, J.M. (2010) 'Sororin mediates sister chromatid cohesion by antagonizing Wapl', *Cell*, 143(5), pp. 737-49.
- Oh, J.S., Han, S.J. and Conti, M. (2010) 'Wee1B, Myt1, and Cdc25 function in distinct compartments of the mouse oocyte to control meiotic resumption', *J Cell Biol*, 188(2), pp. 199-207.
- Oliver, T.R., Feingold, E., Yu, K., Cheung, V., Tinker, S., Yadav-Shah, M., Masse, N. and Sherman, S.L. (2008) 'New insights into human nondisjunction of chromosome 21 in oocytes', *PLoS Genet*, 4(3), p. e1000033.
- Orth, M., Mayer, B., Rehm, K., Rothweiler, U., Heidmann, D., Holak, T.A. and Stemmann, O. (2011) 'Shugoshin is a Mad1/Cdc20-like interactor of Mad2', *EMBO J*, 30(14), pp. 2868-80.
- Östergren, G. (1951) 'The mechanism of co-orientation in bivalents and multivalents', *Hereditas*, 37, pp. 85-156.
- Pacchierotti, F., Adler, I.D., Eichenlaub-Ritter, U. and Mailhes, J.B. (2007) 'Gender effects on the incidence of aneuploidy in mammalian germ cells', *Environ Res*, 104(1), pp. 46-69.
- Paddison, P.J., Caudy, A.A. and Hannon, G.J. (2002) 'Stable suppression of gene expression by RNAi in mammalian cells', *Proc Natl Acad Sci U S A*, 99(3), pp. 1443-8.
- Pagano, M., Pepperkok, R., Verde, F., Ansorge, W. and Draetta, G. (1992) 'Cyclin A is required at two points in the human cell cycle', *EMBO J*, 11(3), pp. 961-71.
- Page, S.L. and Hawley, R.S. (2004) 'The genetics and molecular biology of the synaptonemal complex', *Annu Rev Cell Dev Biol*, 20, pp. 525-58.
- Pahlavan, G., Polanski, Z., Kalab, P., Golsteyn, R., Nigg, E.A. and Maro, B. (2000) 'Characterization of polo-like kinase 1 during meiotic maturation of the mouse oocyte', *Dev Biol*, 220(2), pp. 392-400.
- Panizza, S., Tanaka, T., Hochwagen, A., Eisenhaber, F. and Nasmyth, K. (2000) 'Pds5 cooperates with cohesin in maintaining sister chromatid cohesion', *Curr Biol*, 10(24), pp. 1557-64.
- Pellestor, F., Andreo, B., Arnal, F., Humeau, C. and Demaille, J. (2003) 'Maternal aging and chromosomal abnormalities: new data drawn from in vitro unfertilized human oocytes', *Hum Genet*, 112(2), pp. 195-203.
- Peters, H. (1970) 'Migration of gonocytes into the mammalian gonad and their differentiation', *Philos Trans R Soc Lond B Biol Sci*, 259(828), pp. 91-101.
- Peters, J.M. (2006) 'The anaphase promoting complex/cyclosome: a machine designed to destroy', *Nat Rev Mol Cell Biol*, 7(9), pp. 644-56.
- Peters, J.M., Tedeschi, A. and Schmitz, J. (2008) 'The cohesin complex and its roles in chromosome biology', *Genes Dev*, 22(22), pp. 3089-114.

- Petronczki, M., Matos, J., Mori, S., Gregan, J., Bogdanova, A., Schwickart, M., Mechtler, K., Shirahige, K., Zachariae, W. and Nasmyth, K. (2006) 'Monopolar attachment of sister kinetochores at meiosis I requires casein kinase 1', *Cell*, 126(6), pp. 1049-64.
- Petronczki, M., Siomos, M.F. and Nasmyth, K. (2003) 'Un menage a quatre: the molecular biology of chromosome segregation in meiosis', *Cell*, 112(4), pp. 423-40.
- Pezzi, N., Prieto, I., Kremer, L., Perez Jurado, L.A., Valero, C., Del Mazo, J., Martinez, A.C. and Barbero, J.L. (2000) 'STAG3, a novel gene encoding a protein involved in meiotic chromosome pairing and location of STAG3-related genes flanking the Williams-Beuren syndrome deletion', *FASEB J*, 14(3), pp. 581-92.
- Pfender, S., Kuznetsov, V., Pleiser, S., Kerkhoff, E. and Schuh, M. (2011) 'Spire-type actin nucleators cooperate with Formin-2 to drive asymmetric oocyte division', *Curr Biol*, 21(11), pp. 955-60.
- Picton, H.M. (2001) 'Activation of follicle development: the primordial follicle', *Theriogenology*, 55(6), pp. 1193-210.
- Pidoux, A.L., Uzawa, S., Perry, P.E., Cande, W.Z. and Allshire, R.C. (2000) 'Live analysis of lagging chromosomes during anaphase and their effect on spindle elongation rate in fission yeast', *J Cell Sci*, 113 Pt 23, pp. 4177-91.
- Pinsky, B.A. and Biggins, S. (2005) 'The spindle checkpoint: tension versus attachment', *Trends Cell Biol*, 15(9), pp. 486-93.
- Polani, P.E. and Jagiello, G.M. (1976) 'Chiasmata, meiotic univalents, and age in relation to aneuploid imbalance in mice', *Cytogenet Cell Genet*, 16(6), pp. 505-29.
- Polanski, Z. (1986) 'In-vivo and in-vitro maturation rate of oocytes from two strains of mice', *J Reprod Fertil*, 78(1), pp. 103-9.
- Polanski, Z. (1997) 'Genetic background of the differences in timing of meiotic maturation in mouse oocytes: a study using recombinant inbred strains', *J Reprod Fertil*, 109(1), pp. 109-14.
- Polanski, Z., Homer, H. and Kubiak, J.Z. (2012) 'Cyclin B in mouse oocytes and embryos: importance for human reproduction and aneuploidy', *Results Probl Cell Differ*, 55, pp. 69-91.
- Preiss, T. and Hentze, M.W. (1998) 'Dual function of the messenger RNA cap structure in poly(A)-tail-promoted translation in yeast', *Nature*, 392(6675), pp. 516-20.
- Prieto, I., Suja, J.A., Pezzi, N., Kremer, L., Martinez, A.C., Rufas, J.S. and Barbero, J.L. (2001) 'Mammalian STAG3 is a cohesin specific to sister chromatid arms in meiosis I', *Nat Cell Biol*, 3(8), pp. 761-6.
- Rabitsch, K.P., Gregan, J., Schleiffer, A., Javerzat, J.P., Eisenhaber, F. and Nasmyth, K. (2004) 'Two fission yeast homologs of Drosophila Mei-S332 are required for chromosome segregation during meiosis I and II', *Curr Biol*, 14(4), pp. 287-301.
- Rabitsch, K.P., Petronczki, M., Javerzat, J.P., Genier, S., Chwalla, B., Schleiffer, A., Tanaka, T.U. and Nasmyth, K. (2003) 'Kinetochores recruitment of two nucleolar proteins is required for homolog segregation in meiosis I', *Dev Cell*, 4(4), pp. 535-48.
- Rajkovic, A., Pangas, S.A., Ballow, D., Suzumori, N. and Matzuk, M.M. (2004) 'NOBOX deficiency disrupts early folliculogenesis and oocyte-specific gene expression', *Science*, 305(5687), pp. 1157-9.
- Rankin, S., Ayad, N.G. and Kirschner, M.W. (2005) 'Sororin, a substrate of the anaphase-promoting complex, is required for sister chromatid cohesion in vertebrates', *Mol Cell*, 18(2), pp. 185-200.
- Rape, M. and Kirschner, M.W. (2004) 'Autonomous regulation of the anaphase-promoting complex couples mitosis to S-phase entry', *Nature*, 432(7017), pp. 588-95.
- Reddy, P., Liu, L., Adhikari, D., Jagarlamudi, K., Rajareddy, S., Shen, Y., Du, C., Tang, W., Hamalainen, T., Peng, S.L., Lan, Z.J., Cooney, A.J., Huhtaniemi, I. and Liu, K. (2008) 'Oocyte-specific deletion of Pten causes premature activation of the primordial follicle pool', *Science*, 319(5863), pp. 611-3.

- Rehen, S.K., Yung, Y.C., McCreight, M.P., Kaushal, D., Yang, A.H., Almeida, B.S., Kingsbury, M.A., Cabral, K.M., McConnell, M.J., Anliker, B., Fontanoz, M. and Chun, J. (2005) 'Constitutional aneuploidy in the normal human brain', *J Neurosci*, 25(9), pp. 2176-80.
- Reis, A., Chang, H.Y., Levasseur, M. and Jones, K.T. (2006) 'APCcdh1 activity in mouse oocytes prevents entry into the first meiotic division', *Nat Cell Biol*, 8(5), pp. 539-40.
- Reis, A., Madgwick, S., Chang, H.Y., Nabti, I., Levasseur, M. and Jones, K.T. (2007) 'Prometaphase APCcdh1 activity prevents non-disjunction in mammalian oocytes', *Nat Cell Biol*, 9(10), pp. 1192-8.
- Revenkova, E., Eijpe, M., Heyting, C., Gross, B. and Jessberger, R. (2001) 'Novel meiosis-specific isoform of mammalian SMC1', *Mol Cell Biol*, 21(20), pp. 6984-98.
- Revenkova, E., Eijpe, M., Heyting, C., Hodges, C.A., Hunt, P.A., Liebe, B., Scherthan, H. and Jessberger, R. (2004) 'Cohesin SMC1 beta is required for meiotic chromosome dynamics, sister chromatid cohesion and DNA recombination', *Nat Cell Biol*, 6(6), pp. 555-62.
- Revenkova, E., Herrmann, K., Adelfalk, C. and Jessberger, R. (2010) 'Oocyte cohesin expression restricted to predictyate stages provides full fertility and prevents aneuploidy', *Curr Biol*, 20(17), pp. 1529-33.
- Richardson, S.J., Senikas, V. and Nelson, J.F. (1987) 'Follicular depletion during the menopausal transition: evidence for accelerated loss and ultimate exhaustion', *J Clin Endocrinol Metab*, 65(6), pp. 1231-7.
- Riedel, C.G., Katis, V.L., Katou, Y., Mori, S., Itoh, T., Helmhart, W., Galova, M., Petronczki, M., Gregan, J., Cetin, B., Mudrak, I., Ogris, E., Mechtler, K., Pelletier, L., Buchholz, F., Shirahige, K. and Nasmyth, K. (2006) 'Protein phosphatase 2A protects centromeric sister chromatid cohesion during meiosis I', *Nature*, 441(7089), pp. 53-61.
- Rolef Ben-Shahar, T., Heeger, S., Lehane, C., East, P., Flynn, H., Skehel, M. and Uhlmann, F. (2008) 'Eco1-dependent cohesin acetylation during establishment of sister chromatid cohesion', *Science*, 321(5888), pp. 563-6.
- Rosen, M.P., Johnstone, E., McCulloch, C.E., Schuh-Huerta, S.M., Sternfeld, B., Reijo-Pera, R.A. and Cedars, M.I. (2012) 'A characterization of the relationship of ovarian reserve markers with age', *Fertil Steril*, 97(1), pp. 238-43.
- Rosen, M.P., Sternfeld, B., Schuh-Huerta, S.M., Reijo Pera, R.A., McCulloch, C.E. and Cedars, M.I. (2010) 'Antral follicle count: absence of significant midlife decline', *Fertil Steril*, 94(6), pp. 2182-5.
- Rowland, B.D., Roig, M.B., Nishino, T., Kurze, A., Uluocak, P., Mishra, A., Beckouet, F., Underwood, P., Metson, J., Imre, R., Mechtler, K., Katis, V.L. and Nasmyth, K. (2009) 'Building sister chromatid cohesion: smc3 acetylation counteracts an antiestablishment activity', *Mol Cell*, 33(6), pp. 763-74.
- Rowlatt, C., Chesterman, F.C. and Sheriff, M.U. (1976) 'Lifespan, age changes and tumour incidence in an ageing C57BL mouse colony', *Lab Anim*, 10(10), pp. 419-42.
- Sakuno, T., Tada, K. and Watanabe, Y. (2009) 'Kinetochores geometry defined by cohesion within the centromere', *Nature*, 458(7240), pp. 852-8.
- Sakuno, T., Tanaka, K., Hauf, S. and Watanabe, Y. (2011) 'Repositioning of aurora B promoted by chiasmata ensures sister chromatid mono-orientation in meiosis I', *Dev Cell*, 21(3), pp. 534-45.
- Salah, S.M. and Nasmyth, K. (2000) 'Destruction of the securin Pds1p occurs at the onset of anaphase during both meiotic divisions in yeast', *Chromosoma*, 109(1-2), pp. 27-34.
- Salmon, E.D., Cimini, D., Cameron, L.A. and DeLuca, J.G. (2005) 'Merotelic kinetochores in mammalian tissue cells', *Philos Trans R Soc Lond B Biol Sci*, 360(1455), pp. 553-68.

- Santaguida, S. and Musacchio, A. (2009) 'The life and miracles of kinetochores', *EMBO J*, 28(17), pp. 2511-31.
- Schuh, M. and Ellenberg, J. (2007) 'Self-organization of MTOCs replaces centrosome function during acentrosomal spindle assembly in live mouse oocytes', *Cell*, 130(3), pp. 484-98.
- Schuh, M. and Ellenberg, J. (2008) 'A new model for asymmetric spindle positioning in mouse oocytes', *Curr Biol*, 18(24), pp. 1986-92.
- Shintomi, K. and Hirano, T. (2009) 'Releasing cohesin from chromosome arms in early mitosis: opposing actions of Wapl-Pds5 and Sgo1', *Genes Dev*, 23(18), pp. 2224-36.
- Shirayama, M., Toth, A., Galova, M. and Nasmyth, K. (1999) 'APC(Cdc20) promotes exit from mitosis by destroying the anaphase inhibitor Pds1 and cyclin Clb5', *Nature*, 402(6758), pp. 203-7.
- Siegel, J.J. and Amon, A. (2012) 'New insights into the troubles of aneuploidy', *Annu Rev Cell Dev Biol*, 28, pp. 189-214.
- Sigrist, S., Jacobs, H., Stratmann, R. and Lehner, C.F. (1995) 'Exit from mitosis is regulated by Drosophila fizzy and the sequential destruction of cyclins A, B and B3', *EMBO J*, 14(19), pp. 4827-38.
- Speed, R.M. (1977) 'The effects of ageing on the meiotic chromosomes of male and female mice', *Chromosoma*, 64(3), pp. 241-54.
- Steck, T.R. and Drlica, K. (1984) 'Bacterial chromosome segregation: evidence for DNA gyrase involvement in decatenation', *Cell*, 36(4), pp. 1081-8.
- Stemmann, O., Zou, H., Gerber, S.A., Gygi, S.P. and Kirschner, M.W. (2001) 'Dual inhibition of sister chromatid separation at metaphase', *Cell*, 107(6), pp. 715-26.
- Strong, L.C., and Smith, G. M. (1936) 'Benign hepatomas in mice of the CBA strain.', *Am. J. Cancer*, (27), pp. 279-84.
- Sumara, I., Vorlaufer, E., Gieffers, C., Peters, B.H. and Peters, J.M. (2000) 'Characterization of vertebrate cohesin complexes and their regulation in prophase', *J Cell Biol*, 151(4), pp. 749-62.
- Sumara, I., Vorlaufer, E., Stukenberg, P.T., Kelm, O., Redemann, N., Nigg, E.A. and Peters, J.M. (2002) 'The dissociation of cohesin from chromosomes in prophase is regulated by Polo-like kinase', *Mol Cell*, 9(3), pp. 515-25.
- Sun, S.C. and Kim, N.H. (2012) 'Spindle assembly checkpoint and its regulators in meiosis', *Hum Reprod Update*, 18(1), pp. 60-72.
- Sundin, O. and Varshavsky, A. (1980) 'Terminal stages of SV40 DNA replication proceed via multiply intertwined catenated dimers', *Cell*, 21(1), pp. 103-14.
- Sutani, T., Kawaguchi, T., Kanno, R., Itoh, T. and Shirahige, K. (2009) 'Budding yeast Wpl1(Rad61)-Pds5 complex counteracts sister chromatid cohesion-establishing reaction', *Curr Biol*, 19(6), pp. 492-7.
- Svetlanov, A. and Cohen, P.E. (2004) 'Mismatch repair proteins, meiosis, and mice: understanding the complexities of mammalian meiosis', *Exp Cell Res*, 296(1), pp. 71-9.
- Sweeney, C., Murphy, M., Kubelka, M., Ravnik, S.E., Hawkins, C.F., Wolgemuth, D.J. and Carrington, M. (1996) 'A distinct cyclin A is expressed in germ cells in the mouse', *Development*, 122(1), pp. 53-64.
- Tachibana-Konwalski, K., Godwin, J., van der Weyden, L., Champion, L., Kudo, N.R., Adams, D.J. and Nasmyth, K. (2010) 'Rec8-containing cohesin maintains bivalents without turnover during the growing phase of mouse oocytes', *Genes Dev*, 24(22), pp. 2505-16.
- Tanaka, K. (2013) 'Regulatory mechanisms of kinetochore-microtubule interaction in mitosis', *Cell Mol Life Sci*, 70(4), pp. 559-79.
- Tanaka, K., Hao, Z., Kai, M. and Okayama, H. (2001) 'Establishment and maintenance of sister chromatid cohesion in fission yeast by a unique mechanism', *EMBO J*, 20(20), pp. 5779-90.

- Tang, Z., Shu, H., Qi, W., Mahmood, N.A., Mumby, M.C. and Yu, H. (2006) 'PP2A is required for centromeric localization of Sgo1 and proper chromosome segregation', *Dev Cell*, 10(5), pp. 575-85.
- Thompson, S.L., Bakhoun, S.F. and Compton, D.A. (2010) 'Mechanisms of chromosomal instability', *Curr Biol*, 20(6), pp. R285-95.
- Tingen, C.M., Bristol-Gould, S.K., Kiesewetter, S.E., Wellington, J.T., Shea, L. and Woodruff, T.K. (2009) 'Prepubertal primordial follicle loss in mice is not due to classical apoptotic pathways', *Biol Reprod*, 81(1), pp. 16-25.
- Toth, A., Ciosk, R., Uhlmann, F., Galova, M., Schleiffer, A. and Nasmyth, K. (1999) 'Yeast cohesin complex requires a conserved protein, Eco1p(Ctf7), to establish cohesion between sister chromatids during DNA replication', *Genes Dev*, 13(3), pp. 320-33.
- Toth, A., Rabitsch, K.P., Galova, M., Schleiffer, A., Bonomo, S.B. and Nasmyth, K. (2000) 'Functional genomics identifies monopolin: a kinetochore protein required for segregation of homologs during meiosis', *Cell*, 103(7), pp. 1155-68.
- Touati, S.A., Cladiere, D., Lister, L.M., Leontiou, I., Chambon, J.P., Rattani, A., Bottger, F., Stemmann, O., Nasmyth, K., Herbert, M. and Wassmann, K. (2012) 'Cyclin A2 is required for sister chromatid segregation, but not separate control, in mouse oocyte meiosis', *Cell Rep*, 2(5), pp. 1077-87.
- Tsurumi, C., Hoffmann, S., Geley, S., Graeser, R. and Polanski, Z. (2004) 'The spindle assembly checkpoint is not essential for CSF arrest of mouse oocytes', *J Cell Biol*, 167(6), pp. 1037-50.
- Uhlmann, F., Lottspeich, F. and Nasmyth, K. (1999) 'Sister-chromatid separation at anaphase onset is promoted by cleavage of the cohesin subunit Scc1', *Nature*, 400(6739), pp. 37-42.
- Uhlmann, F. and Nasmyth, K. (1998) 'Cohesion between sister chromatids must be established during DNA replication', *Curr Biol*, 8(20), pp. 1095-101.
- Unal, E., Heidinger-Pauli, J.M., Kim, W., Guacci, V., Onn, I., Gygi, S.P. and Koshland, D.E. (2008) 'A molecular determinant for the establishment of sister chromatid cohesion', *Science*, 321(5888), pp. 566-9.
- van Balen, F., Verdurmen, J.E. and Ketting, E. (1997) 'Age, the desire to have a child and cumulative pregnancy rate', *Hum Reprod*, 12(3), pp. 623-7.
- Vanneste, E., Van der Aa, N., Voet, T. and Vermeesch, J.R. (2012) 'Aneuploidy and copy number variation in early human development', *Semin Reprod Med*, 30(4), pp. 302-8.
- Vanneste, E., Voet, T., Le Caignec, C., Ampe, M., Konings, P., Melotte, C., Debrock, S., Amyere, M., Vikkula, M., Schuit, F., Fryns, J.P., Verbeke, G., D'Hooghe, T., Moreau, Y. and Vermeesch, J.R. (2009) 'Chromosome instability is common in human cleavage-stage embryos', *Nat Med*, 15(5), pp. 577-83.
- Verlhac, M.H., Lefebvre, C., Guillaud, P., Rassinier, P. and Maro, B. (2000) 'Asymmetric division in mouse oocytes: with or without Mos', *Curr Biol*, 10(20), pp. 1303-6.
- Vigier, B., Picard, J.Y., Tran, D., Legeai, L. and Josso, N. (1984) 'Production of anti-Mullerian hormone: another homology between Sertoli and granulosa cells', *Endocrinology*, 114(4), pp. 1315-20.
- Waizenegger, I.C., Hauf, S., Meinke, A. and Peters, J.M. (2000) 'Two distinct pathways remove mammalian cohesin from chromosome arms in prophase and from centromeres in anaphase', *Cell*, 103(3), pp. 399-410.
- Wang, F., Yoder, J., Antoshechkin, I. and Han, M. (2003) 'Caenorhabditis elegans EVL-14/PDS-5 and SCC-3 are essential for sister chromatid cohesion in meiosis and mitosis', *Mol Cell Biol*, 23(21), pp. 7698-707.
- Wang, L., Wang, Z.B., Zhang, X., FitzHarris, G., Baltz, J.M., Sun, Q.Y. and Liu, X.J. (2008) 'Brefeldin A disrupts asymmetric spindle positioning in mouse oocytes', *Dev Biol*, 313(1), pp. 155-66.

- Wassmann, K., Niaux, T. and Maro, B. (2003) 'Metaphase I arrest upon activation of the Mad2-dependent spindle checkpoint in mouse oocytes', *Curr Biol*, 13(18), pp. 1596-608.
- Watanabe, Y. (2012) 'Geometry and force behind kinetochore orientation: lessons from meiosis', *Nat Rev Mol Cell Biol*, 13(6), pp. 370-82.
- Watanabe, Y. and Nurse, P. (1999) 'Cohesin Rec8 is required for reductional chromosome segregation at meiosis', *Nature*, 400(6743), pp. 461-4.
- Watanabe, Y., Yokobayashi, S., Yamamoto, M. and Nurse, P. (2001) 'Pre-meiotic S phase is linked to reductional chromosome segregation and recombination', *Nature*, 409(6818), pp. 359-63.
- White, Y.A., Woods, D.C., Takai, Y., Ishihara, O., Seki, H. and Tilly, J.L. (2012) 'Oocyte formation by mitotically active germ cells purified from ovaries of reproductive-age women', *Nat Med*, 18(3), pp. 413-21.
- Wickramasinghe, D., Ebert, K.M. and Albertini, D.F. (1991) 'Meiotic competence acquisition is associated with the appearance of M-phase characteristics in growing mouse oocytes', *Dev Biol*, 143(1), pp. 162-72.
- Wirth, K.G., Wutz, G., Kudo, N.R., Desdouets, C., Zetterberg, A., Taghybeeglu, S., Seznec, J., Ducos, G.M., Ricci, R., Firnberg, N., Peters, J.M. and Nasmyth, K. (2006) 'Separase: a universal trigger for sister chromatid disjunction but not chromosome cycle progression', *J Cell Biol*, 172(6), pp. 847-60.
- Woods, L.M., Hodges, C.A., Baart, E., Baker, S.M., Liskay, M. and Hunt, P.A. (1999) 'Chromosomal influence on meiotic spindle assembly: abnormal meiosis I in female Mlh1 mutant mice', *J Cell Biol*, 145(7), pp. 1395-406.
- Wu, X., Chen, L., Brown, C.A., Yan, C. and Matzuk, M.M. (2004) 'Interrelationship of growth differentiation factor 9 and inhibin in early folliculogenesis and ovarian tumorigenesis in mice', *Mol Endocrinol*, 18(6), pp. 1509-19.
- Yang, R., Morosetti, R. and Koeffler, H.P. (1997) 'Characterization of a second human cyclin A that is highly expressed in testis and in several leukemic cell lines', *Cancer Res*, 57(5), pp. 913-20.
- Yokobayashi, S. and Watanabe, Y. (2005) 'The kinetochore protein Moa1 enables cohesion-mediated monopolar attachment at meiosis I', *Cell*, 123(5), pp. 803-17.
- Yuan, L., Liu, J.G., Hoja, M.R., Wilbertz, J., Nordqvist, K. and Hoog, C. (2002) 'Female germ cell aneuploidy and embryo death in mice lacking the meiosis-specific protein SCP3', *Science*, 296(5570), pp. 1115-8.
- Zachariae, W. and Nasmyth, K. (1999) 'Whose end is destruction: cell division and the anaphase-promoting complex', *Genes Dev*, 13(16), pp. 2039-58.
- Zamore, P.D., Tuschl, T., Sharp, P.A. and Bartel, D.P. (2000) 'RNAi: double-stranded RNA directs the ATP-dependent cleavage of mRNA at 21 to 23 nucleotide intervals', *Cell*, 101(1), pp. 25-33.
- Zhang, B., Jain, S., Song, H., Fu, M., Heuckeroth, R.O., Erlich, J.M., Jay, P.Y. and Milbrandt, J. (2007) 'Mice lacking sister chromatid cohesion protein PDS5B exhibit developmental abnormalities reminiscent of Cornelia de Lange syndrome', *Development*, 134(17), pp. 3191-201.
- Zhang, J., Shi, X., Li, Y., Kim, B.J., Jia, J., Huang, Z., Yang, T., Fu, X., Jung, S.Y., Wang, Y., Zhang, P., Kim, S.T., Pan, X. and Qin, J. (2008) 'Acetylation of Smc3 by Eco1 is required for S phase sister chromatid cohesion in both human and yeast', *Mol Cell*, 31(1), pp. 143-51.
- Zou, K., Yuan, Z., Yang, Z., Luo, H., Sun, K., Zhou, L., Xiang, J., Shi, L., Yu, Q., Zhang, Y., Hou, R. and Wu, J. (2009) 'Production of offspring from a germline stem cell line derived from neonatal ovaries', *Nat Cell Biol*, 11(5), pp. 631-6.
- Zuckerman, S. (1951) 'The number of oocytes in the mature ovary.', *Recent Progress in Hormone Research* 6, pp. 63-108.